Sources of moisture for Central America and transport based on a Lagrangian approach: variability, contributions to precipitation and transport mechanisms

UNIVERSIDADE DE VIGO

Ana María Durán Quesada

Applied Physics Department

Universidade de Vigo

Thesis submitted for the degree of

Doctor of Philosophy in Applied Physics with International mention

July 2012

This dissertation entitled *Sources of moisture for Central America and transport based on a Lagrangian approach: variability, contributions to precipitation and transport mechanisms* by Ana María Durán Quesada is accepted as satisfying the dissertation requirement for the degree of Doctor of Philosophy.

Date Dr. Luis Gimeno Presa, Advisor

Date Dr. Jorge A. Amador, Co-advisor

Dissertation Committee

Date Dr. David Enfield

Date Dr. Margarida Liberato

Date Dr. Pedro Ribera

Date Dr. Juan Añel

Date Dr. Ramón Gómez-Gesteira

To my parents

Taing son an sàmhchair ri linn dhith
son aotrom ri linn gruamach.
Mòran taing son bad ri linn easbhaidh sanas
son an sil ri linn tha mi anns deur.
A chum son beatha nuir tha mi marbh,
ceud mìle taing.

A.M

Acknowledgements

I would like to thank my advisors Dr. Luis Gimeno Presa (UVigo) and Dr. Jorge A. Amador (UCR) as they encouraged the development of this work. I want to thank the EPhysLab members for hosting me during these years. To colleague Alex Ramos for the support and discussions on analysis methods. To colleague and friend Michelle Reboita with whom I learn in every discussion. I also want to thank the patience and hard work of the EphysLab IT group: José Company and Julio Figueiras who helped with the data retrieval process, Diego Pérez who has been keen to make 'megatron' work, Orlando García-Feal who provided great support with coding, data and optimisation. I want to thank the support provided by the colleagues of the Center for Geophysical Research and the School of Physics of the University of Costa Rica. To the ATMOS group at the Norwegian Institute for Air Research (NILU), Dr. Andreas Stohl, Dr. Harald Sodemann (now at ETH, Zurich) and Dr. Sabine Eckhardt who guided me during a short term scientific mission in their group. To the Energy and Environmental Modeling unit of the Italian National Agency for New Technologies, Energy and Sustainable Economic Development (ENEA) who hosted me during long term internship. I would like to thank Dr. Paolo Ruti, as well as UTMEA group members Dr. Sandro Calmanti, Dr. Alessandro dell' Aquila, Dr. Vincenzo Artale, Dr. Salvatore Marullo, Dr. Emanuele Lombardi and Ms. Ivana Berdini. The financial support through a PhD grant provided by the Fundación Carolina (Agencia Espanola de Cooperación Internacional) and the University of Costa Rica that made possible the work developed during the PhD Programme in Applied Physics at the University of Vigo and that allowed the preparation of the thesis herein presented is greatly acknowledged. Additional financial support from the European Science Foundation, The National Research Council (UK) and the University of Vigo for attending conferences and summer schools during the four years of my PhD Programme is also acknowledged. Finally I want to thank the support of the nice persons I have met in these years, to my family, Isa, Tames, Caro, Fede, Niko, Link, Bianca, Rod and my beloved Eilean Bharraigh.

Abstract

The present work presents a long term analysis of the sources of moisture for precipitation over Central America based on a Lagrangian analysis method. The importance of the water vapour in the climate system is presented in order to introduce the importance of the sources and sinks of moisture for understanding climate. The main global sources of moisture are presented to highlight the importance of studying regions like the Intra Americas Sea (IAS). The state of the art of the regional climate system is presented through a summary of the main features of regional climate, their importance and the sensitivity to the forcing of selected signals. The advantage of using Lagrangian approaches is ipresented followed by an introduction to the problem of the transport of moisture in the IAS region is presented with the main works that have been done. The objectives of this study and the main research activities are also given as a closure to the introductory part. The second part of this work is composed by the description of the methodology and datasets used for the study, followed by the long term analysis of the sources of moisture for Central America and their variability and information on the contributions to precipitation from the individual sources. The three dimensional structure of the moisture transport is explored, jointly with further discussions on the mechanisms that lead the moisture transport process. The role of the Caribbean Low Level Jet (CLLJ) as a moisture conveyor is analysed as well as its response to the vain variability modes affecting the IAS. A third and final part contains the summary of the main conclusions and results of this work closed by the proposal of the future research lines derived from the work herein presented.

Preface

This work presents a detailed analysis on the sources that provide moisture to Central America based on a backward Lagrangian trajectories approach. As it is known many other regions in tropical America have been extensively analysed (e.g Amazon), Central America has been left aside in terms of extensive studies on climate processes in regard to moisture transport. Central America is a region well known for its vulnerability to natural hazards from which extreme precipitation episodes and drought can be mentioned to affect severely both socio-economics and biodiversity. In order to improve the knowledge on the regional processes that control precipitation, the study of the sources that provide moisture for that precipitation is necessary. Under this motivation, an exploratory analysis of the sources of moisture was performed and results obtained encouraged the proposal of a more detailed analysis on the issue.

The aim of this work is to provide a comprehensive study of the regional component of the hydrological cycle that may improve the knowledge on the regional climate processes. To study how different structures merge together to build up regional climate and to which extent processes ongoing in this region may exert an influence on remote locations. The problem proposed was the identification of the sources of moisture for continental Central America using a Lagrangian framework, the analysis of the mean state of the sources and its time and space variability. To understand how important sources of moisture are for precipitation, the quantitative estimation of the contributions from the sources of moisture needed to be considered. To finally obtain an integral picture of the relation between the sources of moisture and precipitation over Central America, the analysis of the moisture transport process completes the mainframe of the work with a focus on the mechanisms that relate the components of the regional hydrological cycle.

Contents

The development of this work is divided in three main parts. A first introductory part in which the state of the art of the water vapour distribution and its role in the climate system is presented. The structure of atmospheric water vapour and the generalities of the components of the hydrological cycle are introduced. The main concepts on global sources of moisture, which are those regions and how are they related to continental precipitation aims to put a global background to the regional problem. The main features of regional climate climate is presented in chapter 2: Climate and Variability in the Intra Americas Seas. The problem of moisture availability and transport in the IAS is presented in chapter 3 which also contains a brief discussion on previous studies. The generalities on the use of Lagrangian methodologies is presented before introducing the formal proposal on the work that has been carried out. This first part closes with the description of the work proposed to solve the problem described. The main motivation and objectives of this work are indicated there. Chapter 4 presents the data and analysis methodologies used. First, the FLEXPART model is introduced and the details on how the backward trajectories simulations were performed. The description of the method used for the identification of the sources of moisture is presented. Then the clustering methodology applied is introduced as well as the used datasets and indices. The general description of the main statistical methodologies used in this study is included, so that the reader may know how computations were made. The results and discussions of the Lagrangian identification of sources of moisture for continental Central America are presented in chapter 5. The mean state of the sources of moisture as well as the seasonal cycle is presented. The variability of the sources under the influence of selected variability modes is presented by describing the patterns of anomalies. At the end of the chapter, an introduction to the role that the transport of moisture from the sources of moisture may have is presented as a link with the following chapter.

Chapter 6 presents the analysis of the relative contributions from the identified source to precipitation. Through chapter 6, the results of the quantitative estimates of the contributions of the sources to precipitation are presented. In the absence of a proper complete dataset on observed precipitation, the response of the contributions from the sources of moisture is carried out using observational data from few selected stations as explained in chapter 4. A comparison between the estimates of the relative contributions to precipitation and observed precipitation in selected regions is performed. Then, the interannual variability of the contributions to precipitation is

analysed. The dynamics of the transport of moisture in presented in chapter 7, starting by the simplistic description of the origin of the air masses, following with the description of the three dimensional structure of the transport. Finally, the processes and structures involved in the transport of moisture through a conceptual model that describes the main features of the transport of moisture that precipitates over Central America are explained. At the end of this part of results and analysis, in chapter 8 the special case of the CLLJ is analysed with detail along with the influence this structure exerts on regional climate and how this low level jet modulates the distribution and variability of regional precipitation. This part closes with the proposal of a simplified method for describing the structure of the sources of moisture as well as transport of moisture modulation and associated precipitation over Central America. The presentation of this work closes with a third section in which the conclusions of the work are presented, the main results remarked and the problems found advertised in chapter 9. The last chapter 10 presents a list of scientific questions that merged from the work herein presented as future research lines that will be followed based on the results of this work and motivated by the useful concepts developed and described. Further information on the FLEXPART model and a brief description of the transport of moisture to another location of interest in the IAS to be the North American Monsoon System are included in separated appendices.

This work has been performed with the financial support of Fundacion Carolina from the Agencia Espanola de Cooperacion Internacional, Universidad de Costa Rica and Universidade de Vigo. Additional support for attending workshops and summer schools was provided by Universidade de Vigo, National Research Council (UK) and the WAVACS. A scientific mission held at the Norwegian Institute for Air Research (NILU) was supported by the SSTM program of the European Cooperation in Science and Technology (COST). A long terms was done at the ENEA with the support of the Universidade de Vigo. Support for attending different conferences where some of the results were presented was provided by the Universidade de Vigo and Ttorch (Founded by the European Science Foundation).

Contents

List of Figures

List of Tables

Part I

Introduction

1

Water Vapour in the climate system

The water vapour is a main element of the climate system that plays a direct role via radiative effects and indirectly through cloud, aerosols and chemical feedbacks *(Gaffen et al., 1991)*. It has a relatively large heat capacity and is related with the storage of large amounts of energy. Moisture is key for driving the circulation in the atmosphere. The availability of water vapour is part of the closed cycle that links the radiative transfer and the circulation. The distribution of moisture in the atmosphere depends on temperature, evaporation and precipitation. The general known features of the distribution of moisture in the atmosphere are a) its decrease with height and b) the excess of water vapour in the tropics compared to higher latitudes *(Peixóto and Oort, 1984)*. A brief description of the distribution of atmospheric moisture is presented followed by a review of the main details of the key components of the hydrological cycle. Since the hydrological cycle can be understood in terms of the balance between evaporation and precipitation with the transport of moisture and it can be associated with sources and sinks of moisture. The general picture of the global moisture sources and sinks is presented.

1.1 The structure of the distribution of moisture and moisture availability

The mean distribution of moisture in the atmosphere is depicted in figure 1.1, specific humidity is maxima in the tropics (figure 1.1.a) and the major part of the moisture content is trapped in the lower levels (figure 1.1.a and 1.1.b). The sharp difference between the moisture content in the tropics and the poles is due to the fact that cold air can only hold very little water vapour *(Pierrehumbert et al., 2008)*. This particular distribution highlights the importance of the tropical regions, where most of the global moisture is contained. The monitoring of the distribution of atmospheric water vapour is complex and has been favoured by the satellite era and recently with the use of Global Positioning Satellite (GPS) networks [1].

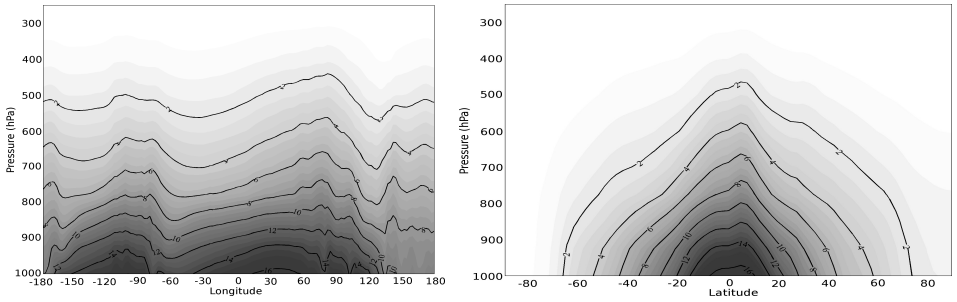

(a) Zonal average (b) Meridional average

Figure 1.1: Average profiles of specific humidity in g/Kg from ERA-40 Reanalysis data for the 1980-2000 period

From the meridional average of specific humidity shown in figure 1.1.b two regions are highlighted. First, the region extending from the easternmost portion of the tropical Atlantic to the region enclosed by the China Sea. North Africa, the Mediterranean Sea, Middle East and China (and surrounding water bodies) are the components of this region. Processes involving large amounts of moisture and important convection are known to occur in these locations. The global distribution of water vapour has a strong relation with the regions associated as large sources of moisture for determined regions. Consider for example the case of the Mediterranean Sea, which is known to be an important source of moisture for weather systems affecting Europe and North Africa. Meanwhile, the Red and Arabian Seas have been also found

[1] satellites are of particular importance for estimating water vapour (among other parameters) in the upper levels, where measuring is complex and very expensive

to be important moisture suppliers to Middle East and from the region formed by central to eastern Eurasia (*Gimeno et al., 2011,* see their figure 1.b). The second region that exhibits a maxima in specific humidity is the one comprised between the Caribbean Sea and the Eastern Tropical Pacific (ETPac). This region is extremely important since it includes the elements of the IAS, the Western Hemisphere Warm Pool (WHWP) and a portion of the tropical Pacific featured to be a region of important evaporation.

1.2 Water vapour and the water cycle

The relationship between the distribution of moisture and the surface energy balance implies a link between moisture and temperature. As any other substance, phase changes of water are strongly related with the temperature. In fact, for water vapour, the saturation vapour pressure can be approximated as an exponential function of the temperature (Clausius-Clapeyron relationship). The Sun provides the energy required to evaporate water from the ocean surface, which is transported in all directions and approximately one third of this evaporated water precipitates over land areas *(Hartmann, 1994)*. In agreement with the distribution of water vapour, the convergence of meridional flux of water vapour peaks at the tropics. Within the water cycle, evaporation and recycling provide the moisture that precipitates over the globe and is redistributed by transport processes. The diagram of figure 1.2 shows an adaptation of figure 1 from *Eltahir and Bras (1996)* in which the global and local water cycles are represented. Several studies on the global and regional water cycle have been carried out in terms of the atmospheric water budget. From diagram in figure 1.2, the balance between evaporation, precipitation, recycling and transport of moisture is important at different spatial scales.

Components of the water cycle

Evaporation

The evaporation simply said, is the conversion of water into vapour. In the air-water interface it can be estimated in terms of a turbulent exchange coefficient c_e, wind speed U, the saturation specific humidity at the sea surface q_s, near surface atmospheric specific humidity q_a (function of air temperature T_{air} and relative humidity RH) and $dq = q_s - q_a$ as described by *Fairall et al. (2003)* (see equation 1.2). As part of the hydrological cycle, evaporation from the ocean surface is of main interest since it provides approximately an 80% of the total evaporated

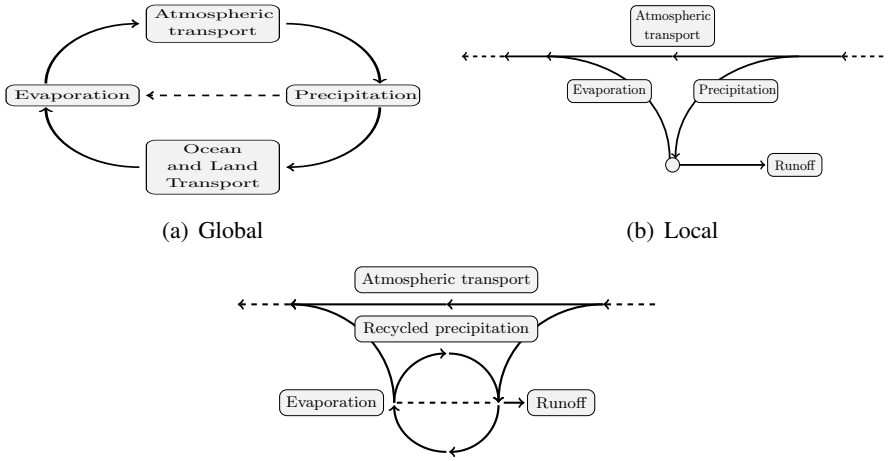

(a) Global (b) Local

(c) Regional

Figure 1.2: Sketch showing a representation of the components of the hydrological cycle (a) Global, (b) local, and (c) regional based on an adaption from *Eltahir and Bras (1996)*.

water from the globe (*Trenberth, 2007*). *Yu and Weller (2007)* indicate heat energy, air-sea humidity differences and wind as main requirements for evaporation to occur. The first to break the hydrogen bonds, the second to set up a threshold for which evaporation may undergo or not and the third to maintain the vertical air-sea humidity gradient. From the dependence of evaporation on temperature it follows the role of SST patterns in the distribution of evaporation. Therefore, evaporation is also a function of the radiative energy balance and present a similar pattern to those of incoming solar radiation and SST distribution. Estimation of evaporation is quite complex and biases are large since calculations require surface fluxes that are not easy to measure systematically for the entire globe. Traditional bulk parameterizations *(Liu et al., 1979)* and current satellite facilities *Schlosser and Houser (2007)* enable the computation of global datasets of reasonable accuracy. The OAFlux[2] products *(Yu and Weller, 2007)* are widely used for different applications requiring surface fluxes and evaporation data. Figure 1.3 shows the climatological mean of evaporation for a) February and b) July, showing the most important regions of oceanic evaporation to be the tropical regions and the western boundary currents.

$$E = c_e U(q_s(SST) - q_a(T_{air}, RH)) \tag{1.1}$$

$$E = c_e U dq \tag{1.2}$$

[2]http://oaflux.whoi.edu/

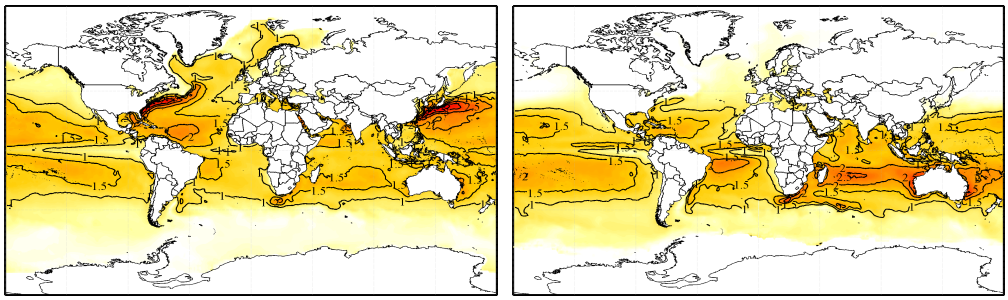

(a) February (b) July

Figure 1.3: Climatological monthly mean of evaporation based on OAFLUX data for the 1980-1999 period in m for (a) February and (b) July, the magnitude of the field is shown by the line contours every 0.5 m . Data was retrieved from the OAFLUX website.

Recycling

Recycling is the contribution of local evaporation to local precipitation *(Trenberth, 1998)*. Over land, this is basically the contribution of evaporation from the land surface. Recycling helps to understand the land-atmosphere coupling and supply of water vapour and latent energy to the atmosphere, leading variables in the formation of precipitation. Recycling has a significant contribution to the heat and moisture budgets of the clouds *(Worden et al., 2007)*. Precipitation recycling is an important moisture supplier for large regions such as the Amazon basin and Europe *(Bisselink and Dolman, 2008)*. Determinant factors for the modulation of precipitation recycling are winds, topography and land cover. The theoretical framework for its quantification was set after *Budyko and Drosdov (1953)* and later in English by *Budyko (1974)*. The analytical model of Budyko to estimate recycling assumes: a) a well mixed atmosphere and b) that the change in storage of water vapor is smaller compared to the fluxes of atmospheric water vapour at long timescales. Thus, the Budyko model has been extended to two dimensional models. *Dominguez et al. (2008)* and *Trenberth (1999)* present a recycling formulation in terms of the intensity of the hydrological cycle, from which large recycling is noticed over the main river basins and transport of moisture shows a determinant role. Additional methods for estimating recycling consider the scales at which recycling is important as presented by *van der Ent et al. (2010)*.

Precipitation

The global picture of precipitation follows a similar distribution to that of humidity in the air, with larger values over the tropical belt where low level convergence is a maximum. As the distribution of raingauges is not homogeneous[3] over the globe, measuring precipitation over the oceans is not straightforward. As with water vapour content and estimation of evaporation, satellites become very useful to overcome the issue of observing precipitation at a global scale. Merging observations with satellite retrievals provides a reasonable reanalysis of global precipitation (even when biases are large). *Trenberth et al. (2011)* present in their figure 4 a comparison between different global precipitation datasets. Despite the differences among them, the pattern is similar, with a marked intensification of precipitation over some regions during summer. Figure 1.4 shows the climatological mean of precipitation from CMAP data *(Xie and Arkin, 1997)*. There are regions in which precipitation is more intense as a result of monsoon circulations. These regions are West Africa *(Janicot et al ., 2009)*, Asia *(Kang et al.,1999)*, Australia *(Taschetto et al., 2010)* and the Americas *(Vera et al., 2006)*.
It is also important to mention that moisture is a requirement for precipitation to occur in terms of microphysical processes. *Houze and Betts (1981)* point out that the upper level clouds in the tropics, enhanced by deep convection, generate precipitation that falls through a subsaturated environment. Therefore, the importance of water vapour associated to precipitation is also related with stability, convection and the transport of moist air. The latter is important in the case of deep convection since it enhances the transport of saturated air into the upper troposphere acting as a source of moisture (*Salathé and Hartmann, 1997*).

Transport of moisture

The role played by the transport of moisture is a fundamental element of the water cycle as shown in figure 1.2. Moisture is transported by winds, mainly from the oceans to continental regions but also from other continental areas. Seasonality of precipitation is strongly associated with the circulation by means of the winds. Consider e.g. the case of the monsoon circulation associated with heavy rainfall as mentioned previously. Moisture can be transported at different scales, the most efficient is the regional transport, in which most of the moist content of the air can be transferred between nearby locations. However, transport at larger scales has been

[3] historically, the observing systems have been located in the northern hemisphere

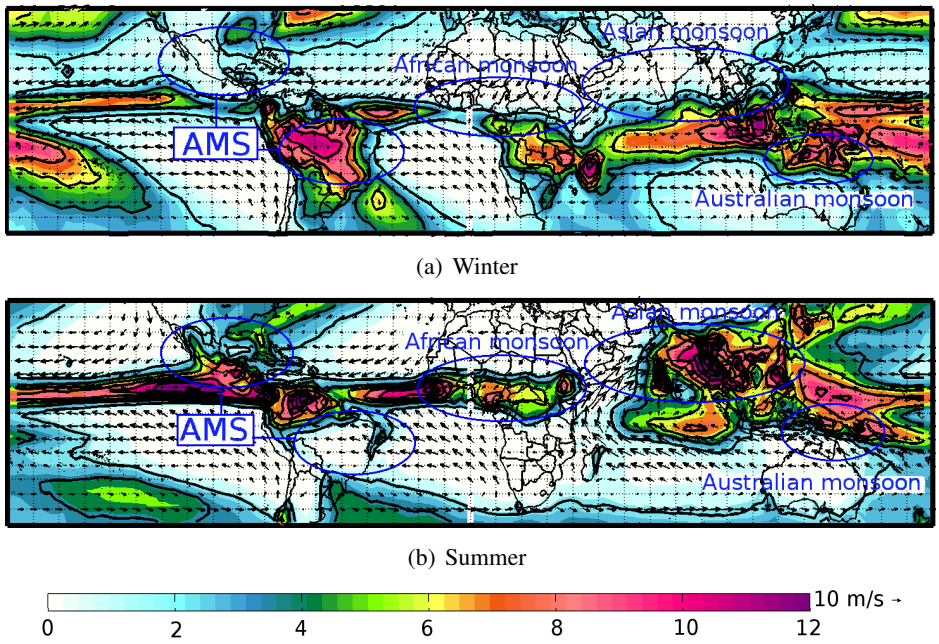

Figure 1.4: Climatological monthly mean of precipitation based on CMAP data for the 1980-1999 period in mm/day and wind vector at 850 hPa from ERA-40 Reanalysis for (a)Winter and (b) Summer. Worth is to notice the largest intensity of precipitation over the tropical belt, from which the ITCZ and the monsoon circulation regions are noticeable as the main large scale features of global precipitation

found to be important, as is the case of the transport between tropics and extratropics. In this, moisture can be transported long distances, providing a connection between processes in the tropics with extratropical precipitation as the case of the 'pineapple express' (*Knippertz and Wernli, 2010*). Since moisture availability is larger in the lower troposphere, low level winds are expected to carry most of the moisture. Nevertheless, the vertical transport of moisture is also important in terms of convection. The vertically integrated total horizontal flux of water vapour provides an approximation to the transport of moisture in the atmosphere. Let Θ be the transport of moisture, P the pressure, q the specific humidity, $V_{x,y}$ the horizontal wind field and g the acceleration of gravity, the transport can be estimated as:

$$\Theta = \frac{1}{g} \int_{sfc}^{top} q V_{x,y} dp \tag{1.3}$$

The principle of conservation of mass states that the rate of change of water storage W must be balanced by the vertically integrated moisture flux divergence $\nabla \cdot \Theta$ and the difference between

evaporation "E" and precipitation "P" when the balance water residual is small, so that equation 1.3 becomes.

$$\frac{dW}{dt} = (E - P) - \nabla \cdot \Theta \tag{1.4}$$

when the averaging time period is large (several years), the water vapour storage term becomes small and can be neglected so that the vertically integrated moisture flux divergence balances the difference between evaporation and precipitation.

$$\nabla \cdot \Theta = E - P \tag{1.5}$$

This expression is very useful in the interpretation of the presence of sources and sinks of moisture, since it provides an estimate of the fresh water flux balance at the surface from the divergence of the moisture transport flux.

1.3 Sources of moisture and precipitation around the globe

If water evaporated from the oceans is transported to the continents where it accounts for precipitation, the oceans are a determinant moisture supply for continental precipitation. Figure 1.5 shows the mean divergence of the vertically integrated moisture flux. According to the balance equation, regions in which evaporation exceeds precipitation can be considered sources of moisture. Therefore, those regions in which the divergence of moisture flux is negative are sinks of moisture. The conditions of these sources and sinks of moisture are sensitive to the seasonal variations of the moisture availability in the atmosphere as well as to circulation. As is natural, from the figure 1.5 it can be followed that the oceanic regions represent important sources of moisture whereas the regions associated with strong convergence are large moisture sinks (as is the case of the ITCZ). To determine which source contributes with moisture for precipitation over determined regions, the source-sink relationship is extremely useful. Several studies focus on the study of the sources of moisture associated with precipitation in regions of specific interest.

Main global sources of moisture

From figure 1.5, the large evaporation regions correspond to the oceans, which are the main sources of moisture for continental precipitation *(Gimeno et al., 2010)*. One of the most important oceanic sources of moisture is the Atlantic ocean (AO). The tropical AO is known to

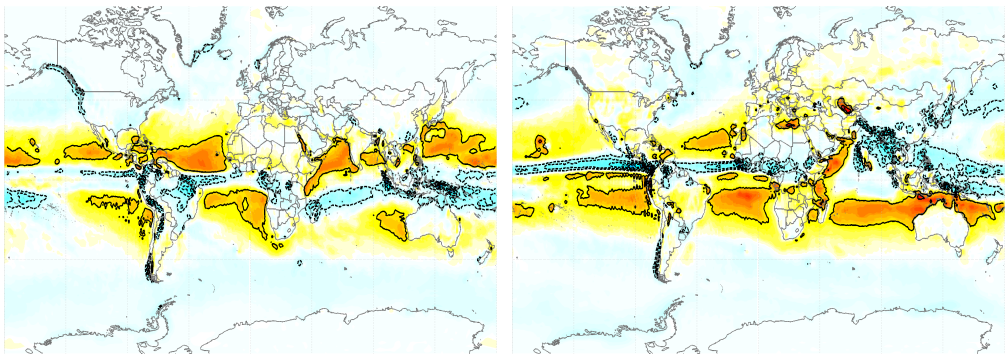

(a) February (b) July

Figure 1.5: Climatological monthly mean of vertically integrated divergence of moisture flux computed from ERA-40 data for the 1980-1999 period in $Kgm^{-2}s^{-1}$ for (a) February and (b) July. Note the regions where divergence is in average positive (yellow and orange) compared with the regions with more intense evaporation in figure 1.3. Those regions are featured to be importance sources of moisture, conversely to those regions featured by convergence (light blue shaded) where precipitation is known to be more intense, in agreement with the patterns of figure 1.4)

be a source of moisture for the IAS system and the Amazon region *(Marengo,1992)*. The North-Atlantic Ocean is able to provide moisture for several regions as Mexico, USA, British Isles, Mediterranean and Central Europe *(Gimeno et al., 2010)*. The South Atlantic Ocean is well known to contribute to the northeastern part of Brazil *(Yoon and Zeng, 2010)*, as well as for providing moisture for the development and maintenance of major cyclones in South America *(Reboita et al., 2010)*.The Caribbean Sea has been determined to be the main source of moisture for Central America*(Durán-Quesada et al., 2010)*, the Gulf of Mexico *(Mestas-Núñez et al., 2005)* and even the extratropics *(Knippertz and Wernli, 2010)*. The Pacific Ocean, characterised by the presence of the largest warm pool contributes to Eurasia, west coast of North America. The Indian Ocean (IO) is also an important source despite is not active all year round as is the Atlantic. The IO is a key source of moisture for the development of the Indian monsoon and it also contributes to Africa, Australia and southern Asia *(Hoskins and Rodwell, 1995)*. Seas and rivers account also as important sources of moisture (see e.g *Stohl and James, 2005*).

Evaporation also occurs over land, so that the continental regions themselves are also sources of moisture due to recycling. The Amazon has been shown to be an important source of moisture due to this process as well as the NAM region *(van der Ent et al., 2010)*. Table 1.1 provides a

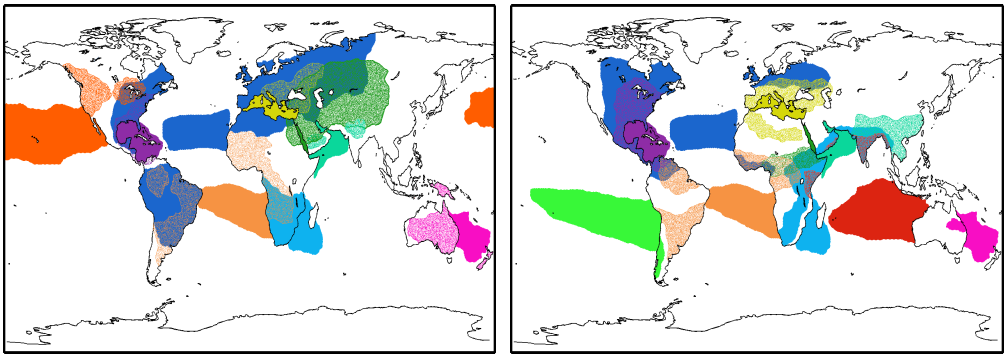

(a) February (b) July

Figure 1.6: Schematical representation of the main sources of moisture and associated sink locations for (a) February and (b) July, adapted from figure 1 of *Gimeno et al. (2011)*. Colours indicate the related regions, pattern shaded is used for the sources that overlap other regions in order to avoid confusion.

summary of the mean global sources of moisture and figure 1.6 shows a summary of the main sources of moisture and the associated continental region to which they contribute to show the seasonal behaviour of the sources os moisture and their sinks.

SOURCE	INFLUENCE REGION	REFERENCES
	CONTINENTAL SOURCES	
EEEV	China	*van der Ent et al., 2010*
	Siberia	*Kurita et al., 2004*
USEV	Northeastern USA, Europe	*van der Ent et al., 2010*
NAM	North America	*Dominguez et al., 2010*
SA	South America	*Dirmeyer and Brubaker, 2007*
WAf	West Africa	*Savenije, 1995*; *Eltahir and Gong, 1996*
SAf	West Africa	*Savenije, 1995*; *Eltahir and Gong, 1996*
EAf	West Africa	*Savenije, 1995*; *Eltahir and Gong, 1996*
	Congo	*van der Ent et al., 2010*
Congo	Sahel	*van der Ent et al., 2010*
	OCEANIC SOURCES	
NAtl	Continental and ECNA	*Gimeno et al., 2010*
	Western Europe, British Isles	*Gimeno et al., 2010*
CS	Caribbean Islands, Central America	*Durán-Quesada et al., 2010*
	Gulf of Mexico	*Durán-Quesada et al., 2010*
SA	South American east coast	*Yoon and Zeng, 2010*; *Reboita et al., 2010*
SA	Antartica	*Sodemann and Stohl, 2009*
NP	Eurasia, North America west coast	*Rosen et al., 1979*
SP	South America west coast	*Rosen et al., 1979*
	Australia, Indonesia and Antartica	*Krishnamurty and Shukla, 2000*
IO	East Africa, Australia and Southern Asia	*Krishnamurty and Shukla, 2000*
	South Africa	*Stohl and James, 2005*
MS	Iberian Peninsula, North Africa	*Knippertz and Martin, 2005*
RS	Gulf of Guinea, Indochina	*Knippertz an Martin, 2005*
	African Great Lakes and Asia	*Stohl and James, 2005*

Table 1.1: A summary with the main sources of moisture with their correspondent sink regions is provided, note that the list aims to provide a general idea and is not an exhaustive list of source/sink regions and related works

2

Climate and variability in the IAS

The Intra Americas Sea, comprised of the Gulf of Mexico and the Caribbean Sea, is fundamental for the regional climate system. Its particular location makes it sensitive to the effect of both regional and large scale dynamical systems acting in its vicinity. A belt of large latent heat fluxes, strong easterly winds, a developed pressure system defined as the NASH (North Atlantic Subtropical High), warm SSTs and intense precipitation build up the general picture of regional climate and variability *(Wang et al., 2008)*. The Caribbean Sea as a component of the IAS is significant due to its importance as a cyclonesis region. The region overlaps with the Inter Tropical Convergence Zone (ITCZ), enhancing its importance for precipitation regimes jointly with the Mid Summer Drought (MSD) which is another feature of regional precipitation *(Magaña et al., 1999)*. Local intensification of the easterly winds is a remarkable feature of the region associated with the Caribbean Low Level Jet, CLLJ, *(Amador, 1998; Wang, 2007)*. The wide variety of processes and structures of climate and its variability in the IAS is of importance for the region but also for the mid latitudes. To provide the basis of the general processes that take place in the analysis region, a brief introduction to the main features of climate in the IAS and the major modes leading variability are described in this chapter.

2.1 Climate in the IAS region

The location of the IAS enables the entrance of large amounts of net radiant flux of energy into surface, while the heat capacity of regional water bodies favours the energy storage. The main features of the IAS climate include pressure systems, precipitation patterns over Central America, the Caribbean Sea and the Gulf of Mexico and the hurricane season. The presence of a warm water body and the particular distribution of precipitation are of importance for the discussions provided through this document.

Western Hemisphere Warm Pool

As already mentioned, the tropical belt is known for a maximum of incoming solar radiation (of the order of $240\ Wm^{-2}$) and SST is particularly warm in the vicinity of the Caribbean Sea and the Gulf of Mexico. The WHWP has been defined as enclosed by the 28.5 C isotherm *(Wang and Enfield (2001)*. It corresponds to the second largest warm water body after the Indo-Pacific Warm Pool *(Wang and Enfield, 2001, 2002, 2003)*. The WHWP has a marked seasonal cycle in which warmer temperatures are phased sequentially from the Eastern North Pacific (ENP) and west of Central America to the IAS. The structure extends along the western Tropical North Atlantic (TNA) following the description by *Wang and Enfield, 2001* (see details in figure 2.1). According to *Wang and Enfield (2002)*, *Wang and Enfield (2003)*, there is an important link between seasonal variations in tropospheric heat and moisture over tropical Americas and the development of the WHWP. Moreover, the WHWP anomalies have a significant impact on the development of tropical convection *(Wang et al., 2006*).

The east component of the WHWP defined as the Atlantic Warm Pool (AWP) has been shown to be important for the IAS at both seasonal and inter-annual scales *(Wang et al., 2006)*. The importance of the AWP relies on its potential role to influence local winds, precipitation and hurricanes *(Wang and Sang-Ki, 2007)*. SST gradients enhanced by the AWP may be partially responsible to force low level winds and convergence in the region, through mechanisms as the one proposed by *Lindzen and Nigam (1984)*. A similar reasoning involving the influence of the NASH is followed by *Wang et al. (2007)*, to study the role of the AWP in the forcing of the CLLJ and associated zonal moisture transport.

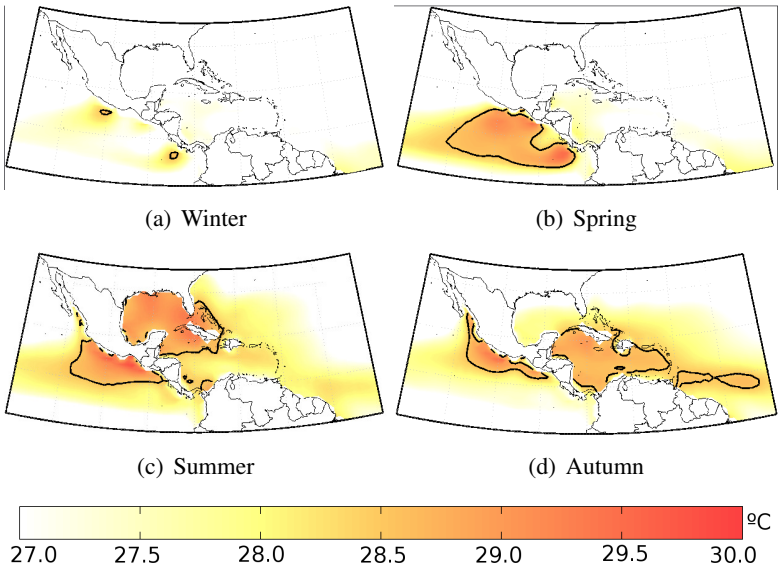

Figure 2.1: Seasonal climatological SST for the analysis region based on ERA-40 Reanalysis monthly data for the 1980-1999 period. SST larger than 28.5 C is contoured from orange to reddish colors in order to highlight the area comprised by the WHWP as defined by *Wang and Enfield, 2001*. Data were retrieved from the ECMWF MARS server.

Based on observations, *Wang et al. (2006)*, showed a relationship between variations in the AWP and the vertical wind shear that may affect the Atlantic hurricane activity. The period between summer and autumn is of particular importance since the AWP is fully developed. The influence exerted by the AWP on the vertical wind shear seems to be restricted to the transition between summer and autumn. In this period, the AWP moves southward and extends into the Atlantic sector (see figure 2.1) as highlighted by *Wang et al. (2007)*. Variability of the AWP is influenced by remote modes such as ENSO and NAO which exert their influence through their impact on the NASH. The importance of the AWP for climate in the IAS as well as interactions with the CLLJ and convective systems have been extensively studied. The role of the AWP for the climate system goes beyond regional interactions since atmospheric circulation cells have been proposed to be affected by Atlantic variability *(Wang and Enfield, 2002)*. It is important to point out that the WHWP is of importance regarding moisture availability due to the enhancement of evaporation as well. At the same time that the relation between warmer SSTs and regional winds is key for moisture transport processes.

Distribution of precipitation

The distribution of precipitation in the IAS is determined by convective processes over the Caribbean, the seasonal migration of the ITCZ, the hurricane season and the MSD among other systems such as cold fronts. The IAS is sensitive to intense rainfall events and severe floods which affect mainly the Caribbean Isles and Central America. In general terms the distribution of precipitation over this region is bimodal. A significant reduction of precipitation during July-August is the main feature of the dry spell that affects Central America, specially the Pacific slope and most of the Caribbean, there are remarkable differences among different locations (see figure 2.2 for details on monthly precipitation patterns in the IAS). Precipitation in Central America is the result of the junction of various systems. The ITCZ, local winds and topography play a major role leading the observed precipitation distribution.

The climatologies of precipitation show the presence of the ITCZ as a well determined band. Precipitation in the Pacific slope is partly under the influence of the seasonal migration of the ITCZ. The Caribbean slope is mainly triggered by the transport of moisture from the Caribbean Sea, local topography and cyclonic systems developing in the Atlantic *(Amador et al., 2003)*. Early descriptions of precipitation distribution in Central America have been given by *Portig (1965)*, and *Hastenrath (1966)*. A general overview is provided by figures 1 and 9 of *Portig (1965)*, and *Hastenrath (1966)*, respectively, where both authors remark the presence of a dry spell during mid-Summer. *Hastenrath (1966)*, discusses the main features of the precipitation distribution in terms of the dynamics and focuses on the importance of regional climate variability, pointing out the role of the easterly waves for the regional distribution of precipitation. Precipitation in Central America is described by two rainfall maxima in May-June and September-October with a marked dry spell in July-August. Winter and early Spring are normally dry periods with even drier conditions in the Pacific slope on average, as described by *Alfaro (2002)*. The dry period between the two rainfall maxima is known as the MSD *(Magaña et al., 1999)* and will be discussed later on. Precipitation distribution over Central America has been also found to be of importance related to storm activity in the eastern Pacific as pointed out by *Curtis and Gamble (2008)*. Other studies are based on reanalysis and supported by observations on some Caribbean Isles to analyse the annual cycle of precipitation in the Caribbean as well as its variability *(Gamble et al., 2008; Giannini et al., 2000)*. The use of statistical and numerical modelling has been also an alternative to study different aspects related to precipitation and variability in the Caribbean for forecasting *(Ashby et al., 2005; Curtis and Gamble,*

2007; Martinez-Castro et al., 2006). However, some important biases are caused primarily by physical parametrizations. Great efforts have been put in ongoing research to overcome this difficulty *(Biasutti et al., 2006)*. The assimilation of observations has been found to solve significantly the biases, see for example recent NCEP Climate Forecast System Reanalysis dataset *(Saha et al., 2010)*. Dynamically, Caribbean rainfall is influenced also by the Pacific ocean because of the location of the Central American Isthmus. The influence of these two water bodies determine some of the fluctuations observed in the rainfall rates *(Chen and Taylor, 2002; Taylor et al., 2002)*. A dry season in the Caribbean occurs during winter, followed by a sharp increase in precipitation after March. The mean climatological distribution of precipitation can be observed in figure 2.2, from which similarities and differences with respect to precipitation in Central America can be noticed. It is also important to remark that precipitation in the Caribbean has been shown to be related with large-scale disturbances as ENSO and the North Atlantic Oscillation (NAO) which also tend to affect the NASH *(Giannini et al., 2000; Mapes et al., 2005; Amador and Magaña, 1999)*.

The Mid-Summer Drought

This feature of Central American and Caribbean distribution of precipitation refers to a decrease in precipitation from July to August. There is a dry period during winter and early spring, followed by a peak in precipitation during the rest of spring and autumn with a dry period in-between. This dry period is popularly known as 'canícula' or 'veranillo' and has been used by local farmers to determine the crop season for some agricultural crops. This MSD is a permanent feature of regional precipitation and is extremely related with low level winds and the NASH *(Magaña et al., 1999; Wang, 2007)*. The link between the MSD and SST anomalies over warm water bodies is explained by variations in convective activity *(Magaña et al., 1999)*. The SST is not the only field involved, note that both the MSD and the intensification of the CLLJ are related to an intraseasonal strengthening and westward expansion of the NASH *(Wang, 2007)*. The MSD is then, associated with changes in convective activity linked to SST distribution , incoming solar radiation and the seasonal cycle of the easterly wind flow *(Magaña et al., 1999)*. According to *Wang (2007)*, the MSD is a large-scale phenomenon associated with both the NASH and the strength of the CLLJ.

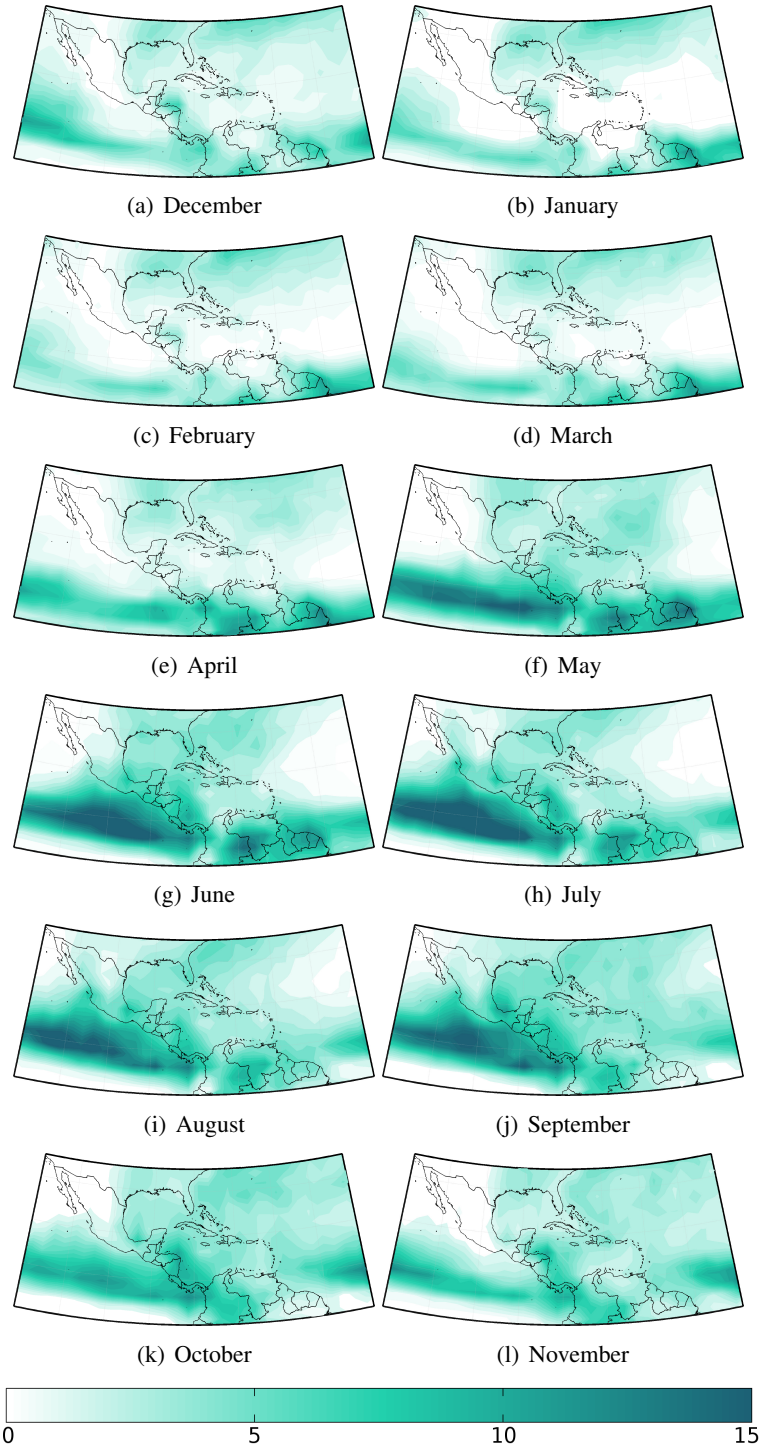

Figure 2.2: Climatological monthly mean precipitation for the 1980-1999 period from the Climate Prediction Center Merged Analysis of Precipitation (CMAP) dataset, units are in $mmday^{-1}$. Data was retrieved from the CMAP website http://www.esrl.noaa.gov/psd/data/gridded/data.cmap.html.

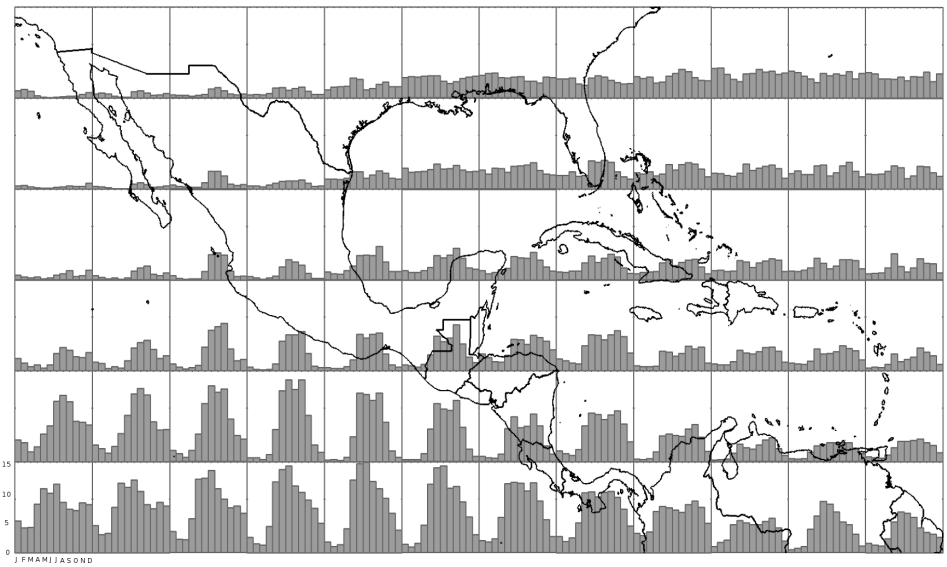

Figure 2.3: Climatological distribution of monthly mean precipitation ($mmday^{-1}$) for contiguous 5 x 5 area boxes. Dataset and analysis period as in figure 1.3. Bars show the value of precipitation for each month, the scale is from zero to 15 $mmday^{-1}$

2.2 The American Monsoon System

The IAS has been found to be important for climate processes in Central America and the Caribbean. However, the configuration of the IAS is of remarkable importance for climate in the surrounding extra-tropics. As an example, the distribution of precipitation in southern North America and central South America is modulated by processes that take place within the IAS with influence of moisture recycled over the Amazon (see e.g *Dirmeyer and Brubaker, 2006*). The large amounts of energy stored in the IAS and the ocean-land distribution enable monsoon-like circulations to be fed by local moisture transport processes *(Amador, 2006)*. Seasonal surface pressure distribution and low-level inflow of oceanic moisture in the Americas exhibit a monsoon-type pattern *(Mechoso et al., 2004)*. Precipitation distribution with significant maxima over some locations in the Americas is also an indicator of such monsoon-like circulations in the region *(Vera et al., 2005)*. Those circulations and precipitation distributions have been identified as a regional monsoon system known as the American Monsoon System (AMS) *(Maddox et al., 1995; Adams and Comrie, 1997)*.

The AMS is comprised of two individual systems located in the northern and southern hemispheres of the Americas. The North American Monsoon System (NAMS) features intense precipitation over some locations in Mexico and south-west United States. Meanwhile, the South American Monsoon System (SAMS) is featured by intense precipitation over Central Brazil and Bolivia *(Mechoso et al., 2004)*. The AMS is influenced by the continental distribution and alignment, topography and meteorological fields (e.g SST, SLP and winds). The presence of low level jets that transport moisture to favour the development of the monsoon circulation and enhance the intensification of precipitation is a common feature of both systems (SAMS and NAMS). The dynamics underlying the onset of the NAMS and the SAMS has been an important subject of study and field campaigns have been implemented to improve the knowledge of these structures. A brief description of both NAMS and SAMS is provided, focused on the main features of the structures, their seasonal cycle and mechanisms involved in it.

North American Monsoon System

The NAMS accounts for approximately over 40 % of the summer rainfall for western Mexico and southern United States. *Douglas et al. (1993)*, point out that in some regions of Mexico, rainfall associated with the NAMS can contribute up to the 70% of annual rainfall (see figure 2.4 for an overview of precipitation distribution over North America during Summer). There is a relationship between the rainfall observed during the monsoon and the ITCZ movement. The meridional thermal contrast also accounts for an important component of the monsoon over water *(Ropelewski et al., 2004)*. The Gulf of Mexico, Pacific Ocean and the Gulf of California are the major oceanic components playing a role for the NAMS onset.Complex orography over the region is the counterpart over land (Rocky Mountains and Sierra Madre) which indeed influences the evolution of the circulation patterns of the NAMS in the upper levels.

Low level circulation during the pre-development of the NAMS, is characterised by the importance of easterly and south-easterly flow in the Gulf of Mexico and linked to the Great Plains Low Level Jet (GPLLJ) *(Higgins et al., 1997)*. Due to the rainfall amount associated with the NAMS and in order to understand the dynamics and variability of the NAMS it is helpful to know the sources that provide moisture to the NAMS. Previous studies have suggested that the

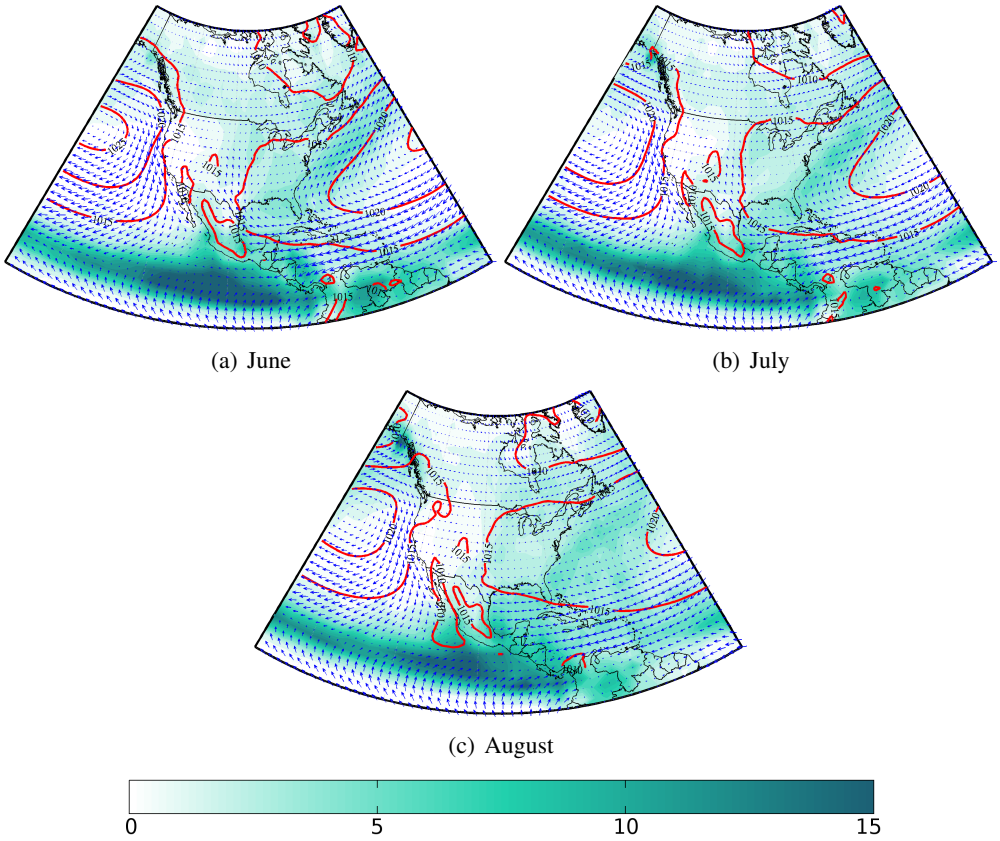

(a) June (b) July

(c) August

Figure 2.4: Climatological values for mean precipitation (green shaded contours in mm/day) from CMAP dataset, SLP (red line contours in mb) and surface wind (blue vectors in m/s) from ERA-40 Reanalysis dataset for the period of active NAMS for the months of a) June, b) July and c) August.

moisture source for the NAMS is located eastward, particularly the Gulf of Mexico as indicated by *Higgins et al. (1997)*. Observations, reanalyses and and modelling studies have been used to determine the origin of the moisture of the NAMS *(Castro et al., 2001)*. According with those studies, the dominant sources of monsoon precipitation associated with the NAMS are the result of local continental evaporation and transport from adjacent oceanic regions. The North American Monsoon Experiment (NAME) *(Higgins et al., 2006)* provided a large dataset of observations to study specific components of the NAMS. The modelling strategy has been useful in the improvement of the ability in the simulation and prediction of the monsoon precipitation.

The importance of moisture transport from the Gulf of Mexico and the Caribbean Sea *(Wang,*

2007; MestasNuñez et al., 2007) has been highlighted. Moisture transport from the Caribbean Sea and the related transport mechanisms are then crucial to understand the evolution of the NAMS. This evidences the importance of studying the interactions between regional systems that may trigger the transport of moisture. The relation of the GPLLJ and the NAMS regarding moisture transport from the Gulf of Mexico and the Caribbean Sea has been indicated in some of the above mentioned works. Furthermore, it has been proposed a connexion between the GPLLJ, the transport of moisture and the CLLJ. The general picture acquires complexity while trying to have an integral overview of the climate system in the IAS. Different scientific questions merge regarding mechanisms and processes. In this framework, a key element must be highlighted: moisture. Questions of remarkable interest to understand one of the components of the NAMS are where does the moisture come from? and, how does the moisture is transported to the NAMS?

South American Monsoon System

The precipitation regime in South America is lead by the Andes, the Bolivian High , the Chaco Low and the South America Convergence Zone (SACZ) *(Y., 1992)*. This region is well known for the variations from extreme rainfall to severe droughts. Intense rainfall has been documented to be a permanent feature of the seasonal cycle in some locations, i.e the Amazon *(Houze and Betts, 1981; Czikowsky and Fitzjarrad, 2009; Petersen et al., 2002)*. Conversely, there are some periods marked by severe droughts in North-east Brazil *(Hastenrath, 2006)*. The transition between dry and wet seasons has been explored in terms of thermodynamic and dynamical variations of the troposphere *(Marengo et al., 2001)*. The seasonal distribution of precipitation and the sharp contrast between dry and rainy seasons are what defines the SAMS as the counterpart of the NAMS in South America (*Vera et al., 2006*, and references therein). Figure 2.5 shows the distribution of precipitation during austral Summer, period in which a monsoon-like precipitation pattern is identified.

The intensification of precipitation is related to the presence of strong low level winds and intense moisture convergence. This latter is related to the interaction between the Chaco Low (note pressure contours in figure 2.5) and the trade winds from the north-east (vectors in figure 2.5) as indicated by *Lenters and Cook (1998)*. Despite the enhancement of the development of the wet season in South America by synoptic systems, the vertical thermodynamic structure is fundamental. Variations in this structure are linked to the moistening of the lower levels

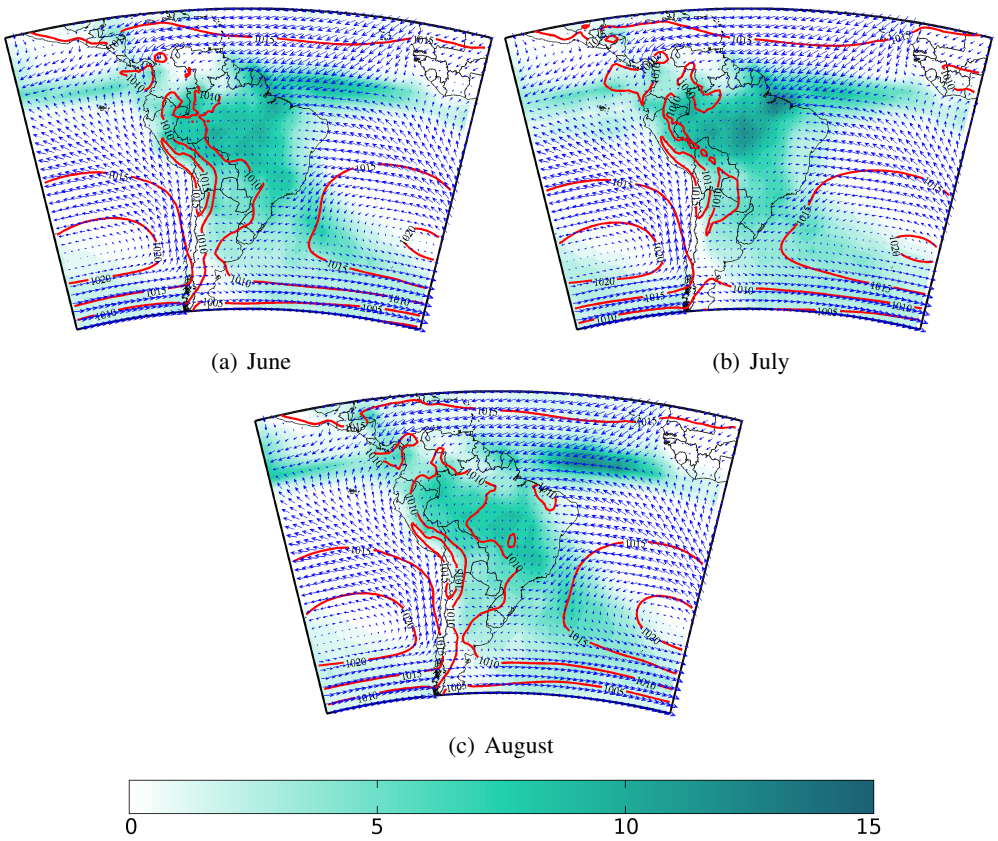

Figure 2.5: Climatological values for mean precipitation (green shaded contours in mm/day) from CMAP dataset, SLP (red line contours in mb) and surface wind (blue vectors in m/s) from ERA-40 Reanalysis dataset for the period of active SAMS: a) December, b) January and c) February.

as highlighted by *Marengo et al. (2001)*. The temporal evolution of the SAMS has been indicated to start with an increase of the westerly wind flow of the upper troposphere in late austral Spring *(Zhou and Lau, 1998)*. The following development of a vortex to the south-east of the Altiplano is associated with an increase in precipitation over subtropical eastern Brazil. According to *Zhou and Lau (1998)*, during the mature phase of the SAMS, there is a displacement of the intense rainfall core to the southernmost Brazilian highlands. Finally, during late austral summer the withdrawal of the SAMS is related to the decrease of the moisture supply by the low level north-westerly flow. This moisture supply from low levels corresponds to the moisture transport due to the South American Low Level Jet (SALLJ). Significant moisture variations have been determined to occur in the austral Summer based on observations during

the South American Low Level Jet Experiment (SALLJEX) as indicated by *Falvey and Garreaud (2005)*. *Grimm (2003)* has found evidence of the presence of atmospheric disturbances remotely produced during warm phases of ENSO in the early monsoon season.

2.3 The Caribbean Low Level Jet

Amador (1998) reported the presence of a structure featured by intensified easterlies with a core located approximately at 75W between 12 and 15N at the 925hPa level. He suggested the structure to be barotropically unstable and related with local SST gradients. *Magaña et al. (1999)*, propose this low level jet-like structure to be implicated in the seasonal distribution of moisture over Central America and Mexico. Recent publications have been focused on the structure and importance of the CLLJ for regional climate as will be discussed. The presence of intensified easterlies over the Caribbean region have also been documented by *Stensrud (1996)* in the context of the importance of low level jets to climate.

Structure

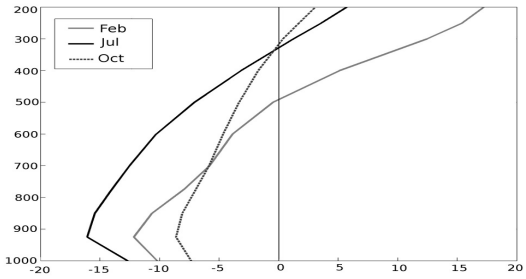

Figure 2.6: Climatological mean vertical profile of the zonal wind at $75W$ for the two maximum intensity in July (black line), and February (gray line) and minimum in October (dashed line) of the CLLJ based on ERA-40 Reanalysis data for the 1980-1999 period. Height in pressure units (mb) in the y-axis and zonal wind intensity in m/s in the x-axis.

The climatological zonal wind speed is evaluated from ERA-40 Reanalysis data. The lower levels are found to present the strongest westward winds over the Caribbean. The zonal wind field in figure 2.6 shows the presence of this low level jet structure as intensified easterlies as described by *Amador (1998)*. Following the criteria for identification of a low level jet structure by *Bonner (1968)*, the vertical profile of zonal wind speed is represented in the vicinity of

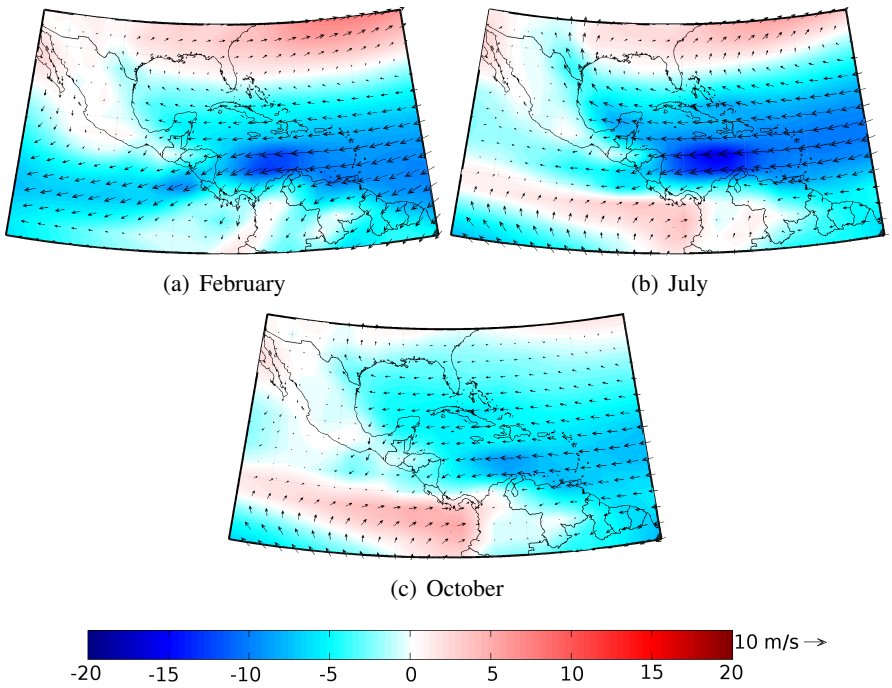

Figure 2.7: Contours of mean zonal wind in m/s (shaded) and wind vectors at 925hPa for the months of a) February, b) July and c) October for the analysis region based on data from the ERA-40 Reanalysis dataset for the period 1980-1999. The reference vector is 10 m/s.

the region where the CLLJ core is located. The peak shown below the $900hPa$ level conforms to the structure of intensified winds that the criteria to be considered as a low level jet. As pointed out by different authors, the CLLJ is real and not an artifact of reanalysis data. The CLLJ does not have a single peak but two, it reaches the highest wind speeds in July but a secondary peak of intensity occurs by February *(Wang, 2007)*. Figure 2.7 shows the monthly mean of the structure of the wind during July and February (when maximum occurs) and October (minimum intensity of the zonal wind). The seasonality of the CLLJ makes it particularly interesting for the discussion of the distribution of precipitation as will be briefly commented. In recent years various groups have focused attention on the study of this structure, mainly because of its importance as a regional climate modulator which is clear despite the dynamics of the CLLJ is still an open problem.

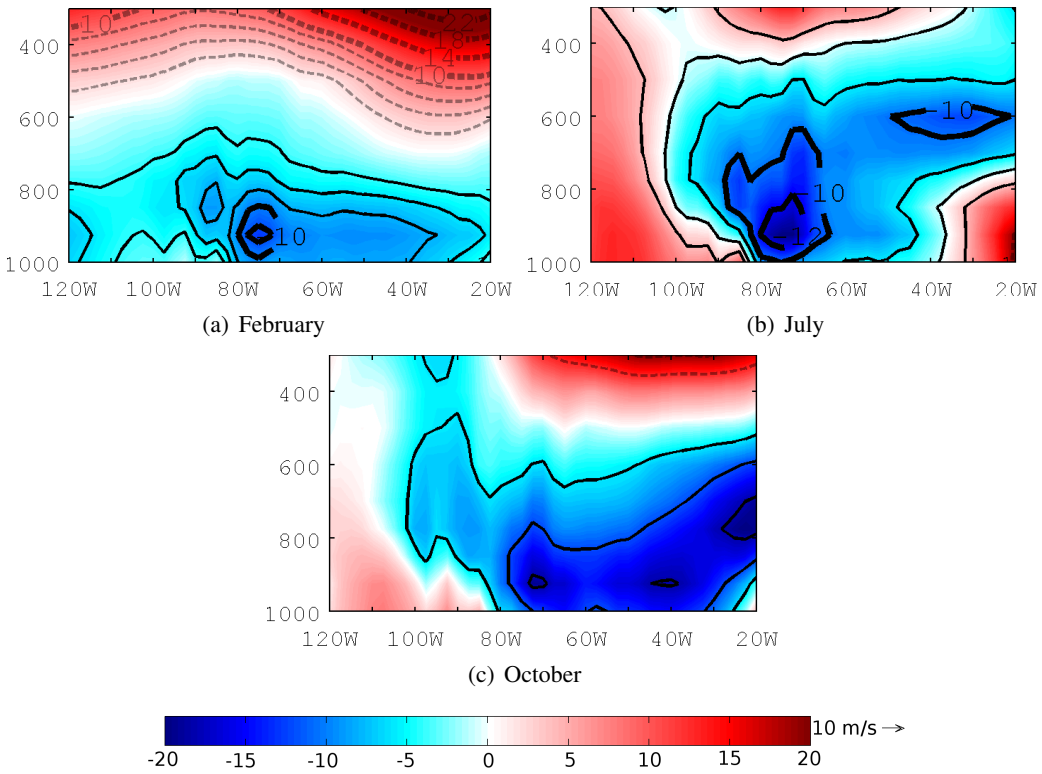

Figure 2.8: Mean meridional cross section of the vertical profile of the zonal wind at $12N$ a) February, b) July and c) October from ERA-40 Reanalysis dataset for the period 1980-1999. The plots show the vertical structure of the wind field in the CLLJ core.

Importance for regional climate

Wang (2007), finds an association between the maximum intensity of the CLLJ during summer, a maximum of SLP, the MSD and a minimum of cyclone-genesis in the Caribbean Sea. Using an index to measure the intensity of the CLLJ, he studies the relation of the CLLJ with the SST and SLP fields. According to his results, during winter the CLLJ is related to the strengthening of the NASH and the weakening of the wintertime Auletian Low. Meanwhile during summer the increased (decreased) intensity of the CLLJ is due to positive (negative) SLP anomalies near the NAM region. This result implies that a strong (weak) CLLJ is associated with a weak (strong) summer monsoon. The mechanism for this to occur finds an explanation in the role of the WHWP modulating the CLLJ as a result of a Gill type response *(Wang et al., 2008; Magaña et al., 1999)*. Regarding SST, the results of *Wang (2007)*, indicate that warm (cool)

anomalies of the Caribbean SST are related to weak (strong) CLLJ.

Whyte et al. (2008), present a study on the features of the CLLJ with a characterization of the structure. They indicate the CLLJ to be the first EOF mode of the zonal wind during July (40% of the variability). The authors focus the study on the SST gradients and propose the intensification of the CLLJ to be modulated by a Pacific (warm) an Atlantic (cool) SST gradient (see their figure 5). They also suggest that the El Niño triggers the CLLJ, which may be used to assess forecasting since strong CLLJ is associated with wet conditions. *Muñoz et al. (2007)*, analyse the structure of the CLLJ during its peaks and describe the CLLJ as an extension of the Bermuda High with an intensity modulated by temperature and orographic influences. They suggest that the strengthening of the CLLJ during late Spring is a result of the of the east-west gradient of diabatic heating between Central America and the Caribbean. A detailed study on the hydrodynamics of the CLLJ was published by *Cook and Vizy (2010)*, in which the authors consider the geopotential gradient to explain the seasonal cycle of the CLLJ. They point out that this gradient tightens in July due to the presence of the NASH and in February due to the heating of northern South America, as has been proposed by *Amador (2008)*. They suggest that the minimum of the CLLJ during October is a result of the increase of SST and a well developed planetary boundary layer (PBL) that debilitates the geopotential gradient. The role of Central American topography is also proposed as an element that may modulate the intensity of the CLLJ. *Wang (2007)*, analyses its variability and relation to climate and finds (as suggested by *Magaña et al., 1999*) a relation between the CLLJ and the MSD. *Wang (2007)*, proposes the increase of the moisture flux divergence over the Caribbean due to the presence of the CLLJ as a mechanism to suppress convection, reduce precipitation and suppress the formation of cyclones. Moreover, *Wang (2007)*, mentions that the vertical wind shear during the intense phase of the CLLJ during summer may be related with the inhibition of the organisation of deep convection and as a result, the reduction of rainfall. *Muñoz et al. (2008), Amador et al. (2003), Amador (2008), and Cook and Vizy (2010)*, conclude that the CLLJ contributes to the generation of orographic precipitation at the same time that enhances the eastward divergence of the moisture flux, causing a minimum of precipitation over the Caribbean. The role of this vertical wind shear associated with the CLLJ is also analysed by *Wang and Lee (2007)*, regarding its potential impact on the Atlantic hurricanes activity.

2.4 Principal modes of variability

The ENSO is known to affect inter-annual climate variability in the IAS but it is not the only mode exerting an influence on regional climate. In addition the Pacific Decadal Oscillation (PDO) is quite important for desribing the variability of climate in the tropical Pacific. The NAO has been found to be associated with the variability of the WHWP while the Madden-Julian Oscillation MJO (MJO) is the most important intraseasonal global signal. Both, ENSO and NAO are related with modifications in the easterly winds and for instance play a role leading variability of the transport of moisture and regional precipitation patterns. The Atlantic Multidecadal Oscillation (AMO), Atlantic Meridional Mode (AMM) and the Amazon convection complete the list of important variability modes (note that AMM is not herein described).

EL Niño-Southern Oscillation

The ENSO is a two-component physical mechanism that describes the coupling of SST anomalies in the tropical Pacific Ocean (El Niño) and a pressure gradient in the southern Pacific (Southern Oscillation). Pioneering work on the ENSO was carried out mainly by *Walker (1932, 1937)* and *Bjerknes (1966, 1969)*. These works set the fundamentals for the recognition of the link between the two components *(Cane et al., 1986)*. A decrease in the intensity of the Atlantic hurricane season has been identified during warm ENSO events *(Goldenberg and Shapiro, 1996)*. Inter-annual variability of the cyclone-genetic activity in the tropical Atlantic has been widely studied *(Bell and Chelliah, 2006; Chen and Taylor, 2002)*. These studies suggest that ENSO forces variations in the SST field and vertical wind shear triggers this variability. Moreover, the ENSO effect on precipitation has been globally documented. Cold ENSO phases are characterised by a rainfall increase while the warm phase by a reduction in observed precipitation *(Dai and Wigley, 2000)*. *Giannini et al. (2000)*, highlight the intense inter-annual variability of precipitation over the Caribbean. An increase (decrease) of precipitation has been associated with cold (warm) ENSO phases. Variability of the surface winds has been also observed related to ENSO. The flow over surface has been found to increase during El Niño events while a reduction occurs in the opposite phase. These variations in the wind field influence the vertical wind shear and cyclone-genetic processes. It can be followed that ENSO is able to affect precipitation distribution by modulating two different mechanisms: a)

evaporation variability linked to SST and surface drag variations and b) transport of moisture due to wind flow modulation.

North Atlantic Oscillation

The NAO is the main variability mode in the SLP field, it is defined as the pressure difference between the Azores High and the Icelandic Low *(Rogers, 1984)*. Interesting features linked to the NAO are the regions characterised by SST anomalies in the East/South-east of Greenland. Negative anomalies during the NAO positive phase and vice-versa with contrasting SST anomalies in North America. The main aspect of the NAO is its relationship with the strengthen of the NASH and the North Eastern trade winds, affecting thus the circulation in the IAS. The impact of the NAO is therefore associated with the climate features of the IAS, SST in the TNA, the size of the WHWP and the CLLJ. According to *Barnston and Salstein (2006)*, the seasonal variations of the NAO may be reflected in its influence on the IAS easterly winds and precipitation patterns. *Malmgren et al. (1998)* found that during boreal Summer the NAO index has an inverse relation with the observed precipitation patterns over Puerto Rico.

Madden-Julian Oscillation

In 1971 Roland Madden and Paul Julian found a 40-50 days oscillation in zonal wind anomalies in the tropical Pacific, after them named as the Madden-Julian Oscillation (MJO) *(Madden and Julian, 1994)*. A detailed review on the MJO basics can be found in *Zhang (2005)*. An interesting analysis of the ocean-MJO relationship is provided by a recent study by *Webber et al. (2010)*. This oscillation is known for its effects on the tropical troposphere and strong impact on tropical convection. A significant interaction between the MJO and ENSO has been also found *(Tang and Yu, 2008; Moon et al., 2011)*. The importance of the MJO for the monsoon systems is well documented. According to *Lorenz and Hartmann (2005)*, the MJO-related zonal wind anomalies in the ETPac region might be associated with the increase of rainfall in the NAM region. The authors point to the amplification of easterly waves as a trigger of gulf surges development that may be related with the variability of the moisture sources that feed the NAMS. Moreover, they also suggest the westerly phase of the MJO to be associated with the enhancement of favourable conditions for MCS (Mesoscale Convective System) development in the region. *Maloney and Esbensen (2003)*, studied the strength of the MJO during Autumn in terms of the MJO signal in the ETPac. *Barlow and Salstein (2006)*,

analyse the impact of the MJO on precipitation over Mesoamerica based on stations data. A positive (negative) phases of the MJO is found to be associated with the increase (decrease) of precipitation in the region. Recently, *Martin and Schumacher (2010)*, published their analysis on the role of the MJO as a modulator of Caribbean precipitation. From their results, a link between the intensity of the CLLJ and the MJO is suggested to lead changes in precipitation. Both studies of *Barlow and Salstein (2006)*, and *Martin and Schumacher (2010)*, find some relation between the occurrence of extreme events and the MJO phase.

Pacific Decadal Oscillation

According to *Zhang et al. (1997)*, the Pacific Decadal Oscillation (PDO) is a long-lived El Niño-like pattern of the variability of the Pacific climate. The PDO was determined through independent studies by *Mantua et al. (1997)*, to be the dominant pattern of Pacific Decadal Variability (PDV). Even when the PDO is referred as an El Niño-like pattern, it differs from ENSO in a) the time scale of the persistence of events and b) its fingerprint is more noticeable in the extratopics rather than the tropics *(Mantua and Hare, 2002)*. These authors point out that the pattern of a warm PDO phase is featured by cooler than normal SSTs in the central North Pacific and warmer than normal SSTs along the west coast of the Americas. Symmetry in SSTAs patterns between northern and southern hemispheres exhibited by the PDO has been determined by *Evans et al. (2001)*. The mechanisms of the PDO are complex and still and open issue, however some studies suggest the importance of the tropical coupling for the existence of the PDO *Feng et al., 2010). Schneider and Cornuelle (2005)*, propose the PDO to evolve from a composition between the forcing due to El Niño 3.4, and the changes of the Aleutian low (in terannual frequencies) and the Kuroshio-Oyashio Extension (decadal time scales). The importance that the PDO may have for global climate is related to a correlation between the PDO index *(Mantua et al., 1997)* and precipitation anomalies. Warm PDO phases have been found associated with anomalously dry periods in the eastern coasts of Eurasia, Northwest Pacific of USA, Central America and northern South America. While the same phase seems to be related to wetter than normal conditions in the Gulf of Alaska, South-west USA and Mexico, South-east Brazil, South central South America and western Australia.

Atlantic Multi-Decadal Oscillation

Folland et al. (1986), detected the presence of a multidecadal mode in SST and later *Schlesinger and Ramankutty (1994)*, isolated this mode and suggested it has a 70-yr cycle. This cycle has been confirmed by a significant peak around 70 years found through spectral analyses of climate time series by *Delworth and Mann (2000)*. The low frequency variability signal has been found in different modelling analysis *(Delworth et al., 1993; Latif et al., 2004; Delworth and Greatbatch, 2000)*. The multidecadal pattern was identified as the first rotated North Atlantic SST EOF by *Mestas-Nuñez & Enfield (1999)*. The low frequency mode featured by changes in the SST of the North Atlantic Ocean was named as Atlantic Multidecadal Oscillation (AMO) *(Kerr, 2000)*. An index of SSTs in the North Atlantic (0 and 70N) is used to define the AMO *(Enfield et al., 2001)*. The AMO signal has been found to be important as it modulates precipitation variations in different regions such as Africa *(Fontaine and Janicot, 1996)*, Europe *(Rodwell et al., 1999)*, the Caribbean *(Giannini et al., 2003)* and South America *(Carton et al., 1996)*. In the IAS region, the signal of AMO has been found to be related to precipitation *(Gianinni et al., 2003)*. *Curtis and Gamble (2008)*, reported positive AMO to be linked with a reduction of the transport of moisture from the Gulf of Mexico to northwestern Mexico which may be related with a decrease in precipitation. Meanwhile wetter (drier) conditions over Central America (north-east Brazil) during JJA (DJF) were found by *Zhang and Delworth (2006)*. AMO has been also determined to be of importance modulating the impact of ENSO on drought. Connection between AMO and other regional features such as the AWP has been also studied. *Wang et al. (2008)*, show that warm (cool) phases of the AMO are associated with repeated large (small) AWPs, suggesting the relationship between the AMO and Atlantic tropical cyclones. The latter in agreement with results that indicate the presence of multidecadal variations in hurricane activity due to the Atlantic SST (see e.g. *Gray, 1990; Landsea et al., 1999; Goldenberg et al., 2001*). AMO is then of importance related to the low frequency variability of precipitation as it modulates the distribution of moisture and extreme rainfall events.

Convection in the Amazon

Despite the convection in the Amazon has been mainly studied in relationship with the release of latent heat associated with the development of the Bolivian high (see e.g *Hastenrath, 1990;*

Lenters and Cook, 1997) its potential influence over the IAS is of importance. In a modelling study of remote tropical climate to ENSO, *Lintner and Chiang (2007)* have explained the changes in convection over the Amazon as a response to the stabilization of the upper troposphere as well as subsidence. Even when the effect of the Amazon convection over the IAS has been fully explored, it is known to have an impact on the NE trade winds as it affects the Hadley circulation that is connected with the NASH in different time scales (see e.g *Wang et al., 2006; Mestas-Nuñez and Enfield, 2001*). More recently, *Muñoz et al. (2010)* show that the changes of convection over the Amazon have a strong connection with changes in the IAS during winter and spring. It is important to remark that the combination of changes of convection in the Amazon and other variability modes may trigger SST on the TNA and therefore have a strong impact in the development of tropical cyclones and the regional transport of moisture.

3

Moisture availability and transport in the IAS

Despite the richness of processes in which moisture is involved in the IAS region, the study of transport of moisture has been mainly addressed for those regions in which a monsoon like circulation has been found to develop. Therefore, regions like Central America, with such important precipitation patterns have been poorly studied. Few published studies have being focused in the transport of moisture over this region. Most of the studies have as an objective the development of the AMS and its regional influence. Therefore, those specific studies are particularly focused on the north.There are very few direct studies on the identification of the sources of moisture for Central America, their variability and how they impact regional precipitation until the publication of *Durán-Quesada et al. (2010)*. Here we aim to introduce the importance of the problem of moisture availability and transport for the region with the a proposal of the study of the sources of moisture, transport, associated precipitation, variability and mechanisms using a Lagrangian approach.

3.1 Importance and previous studies

The atmospheric moisture is transported by several mechanisms and plays an important role jointly with evaporation to provide moisture to moist- convective regions. The processes involved in the transport of moisture have been traditionally studied using water vapour fluxes.

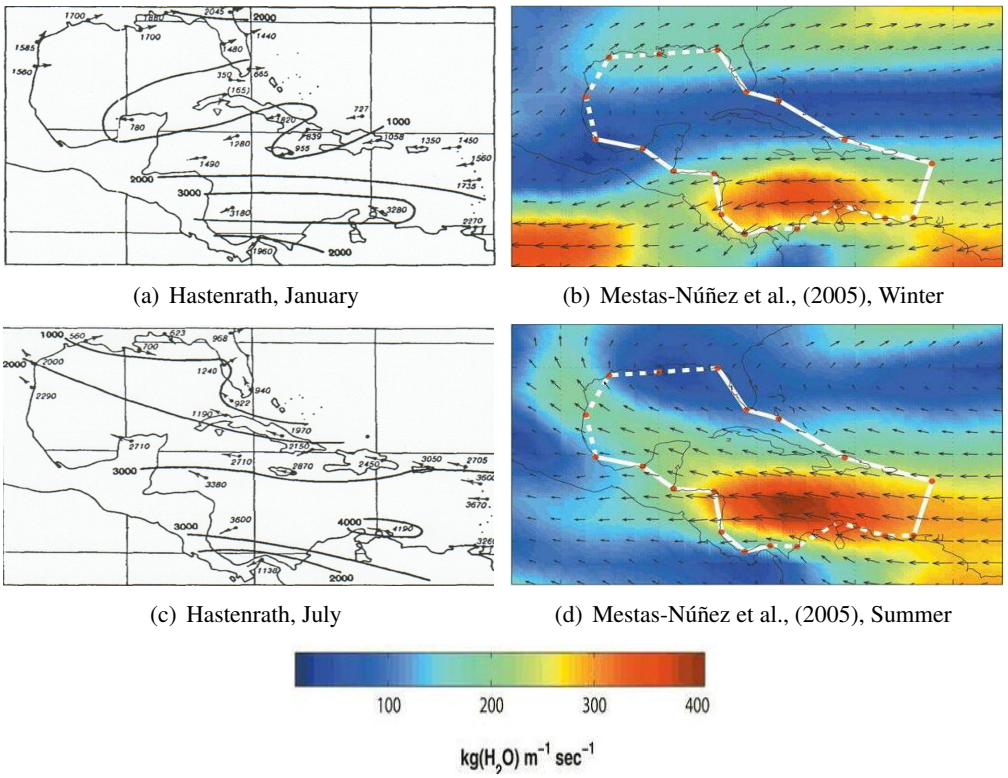

(a) Hastenrath, January

(b) Mestas-Núñez et al., (2005), Winter

(c) Hastenrath, July

(d) Mestas-Núñez et al., (2005), Summer

Figure 3.1: (a) Vertically integrated total flux of water vapour January (figure 4 from Hastenrath 1966), (b) December-March average of monthly vertically integrated water vapour flux (figure 3.a of *Mestas-Núñez et al., 2005*), c) As a but for July (figure 8) and d) as b but for June-September (figure 3.b)

The study of the water vapour fluxes facilitates the understanding of the processes involved in the transport of moisture, interaction of transport with other structures and their role on precipitation. The classification of air fluxes into the contributions from mean flows, stationary eddies and transient perturbations are the traditional way to study the transport of moisture *(Rosen et al., 1979; Peixoto and Oort, 1984)*. On the basis that the transport of water vapour in the troposphere has a filamentary structure *(Zhu and Newell, 1994; Zhu and Newell, 1998)* the atmospheric rivers approach was proposed by *Newell et al. (1992)*. This approach is useful in the analysis of the transport of moisture that undergo determined weather events such as cyclones and cold fronts.

Studies of Lagrangian transport yield a relatively accurate representation of the transport of air moisture *(Galewski et al., 2005)*. *Schneider et al. (1999)* provide a climatological analysis

based on isentropic coordinates from which suggest the balance between the drying into the extratropics with the moistening from the tropics into regions of relative humidity minima by eddy transport (in both directions). These two studies set up a good background for the role of transport of moisture between the tropics and the extra-tropics. Recently, *Knippertz and Wernli (2010)* have also addressed this relation and the importance of associated transport of moisture. Regional studies of the transport of moisture Considering the importance of moisture for enhancing the occurrence of precipitation in (and outside) the tropics, the transport of moisture is key to understand the patterns of precipitation over determined locations. Transport of moisture occurs at different scales, large scale transport, for example, is more associated with stronger low level winds and the modulation of the distribution of water vapour . Large scale moisture transport is of particular importance since it is involved with the triggering of convection *(Sherwood, 1996; Sherwood et al., 2010)*.

Several studies of the transport of moisture and the main sources of moisture are mostly focused in the Amazon region *(Rao et al., 1996; Marengo, 1992)* and North America *(Douglas et al., 1993; Schmitz and Mullen, 1996; Bosilovich et al., 2001; Hu and Feng, 2001; among many others)*. In the Americas, there is a variety of studies on regions such as the Great Plains of North America and the Amazon whereas Central America can be considered as poorly studied. Among the few direct works on the transport of moisture for central America, pioneering papers by *Hastenrath (1966)* can be found. The role of the transport of moisture from the Caribbean Sea and the Gulf of Mexico in association with local winds and the regional distribution of precipitation is highlighted in those works. Hastenrath discusses that 'the westward direction of transport has its maximum below the 900 hPa level, and its core is clearly situated over the southern Caribbean Sea'. Hastenrath addresses the presence of 'a northward transport of moisture across the 20N latitude circle' and also remarks the southward shift of the minimal transport of moisture during boreal autumn. In this paper and a companion work on the analysis of rainfall in Central America *(Hastenrath, 1967)* the author focused on the main details of the transport of moisture and the distribution of precipitation that are still being studied.

Forty years later, *Mestas-Núñez et al. (2005)* published an analysis on the water vapour fluxes over the Intra Americas Seas. Their results reveal a zonal structure of the moisture flux balance over the IAS and the balance between moisture exports from the tropical North Atlantic and evaporated locally and the transport toward the Pacific over Mexico and Central America. This result of the mostly zonal conditions of transport can be interpreted as an analogue to what

Hastenrath (1966a) called as westward direct transport. The increase of the meridional transport found by *Mestas-Núñez et al. (2005)* which they suggest as consistent with the seasonal cycle of the CLLJ is no more than the northward transport mentioned in Hastenrath works of 1966. Despite the lack of obervations, Hastenrath identifies with good accuracy that the transport conditions over the Caribbean must be related with the winds as he uses a calculation of the water vapour transfer in terms of a wind vector. A comparison of the results found by *Hastenrath (1966)* and *Mestas-Núñez et al. (2005)* is presented in figure 3.1, in which both works are interested in the analysis of the water vapour fluxes over the region formed by the Caribbean Sea and the Gulf of Mexico (IAS) . To contrast these two studies is very helpful to illustrate how slow has been the advance in the understanding of the regional hydrological cycle over Central America and the scarcity of specific studies on this issue for the region. Fortunately the interest of studying the IAS region has increased as a result of interest in the analysis of the North American Monsoon system. Therefore the number of studies focused on the distribution of precipitation over the Caribbean and Central America has grown and the scientific community is little by little turning into the importance of studying this region not only for its specific features but also for its importance for climate in other scales.

3.2 The problem of analising moisture sources and transport in the IAS region

Within the IAS system, there are tow cases: a) the sources of moisture that may be of importance for feeding the NAMS and thus maintaining the summer monsoon over North America and b) the moisture sources for Central America and correspondent transport. The nature of precipitation over both regions differs, however, as part of a system being influenced by the IAS, it is important to understand the common elements they have. The general picture described in the previous section may suggest that the system is under the influence of the moisture transported by the wind regime. This statement may sound quite simplistic, however it has a complex meaning due to the richness of the regional dynamics.

Studying the sources of moisture and transport in the IAS region is a problem as information available for Central America differs enormously from that for North America. There are few

[2]Note that units in figures from *Hastenrath (1966)* are $g\ H_2O\ cm^{-1}s^{-1}$ while for those from *Mestas-Núñez et al. (2007)* are $Kg\ H_2O\ m^{-1}s^{-1}$ so that a factor of 10 must be taken into account for direct comparisons

complete records of precipitation observations over Central America so that long term observations of the main variables required for such studies is limited. Resolution is another problem, since Central America is a small continental region surrounded by large water bodies. The resolution of analysis products was not enough to appropriately resolve key processes and only few grid points represented the complete continental region. Higher resolution datasets are often not global and in some cases do not cover Central America and even if so, the access is not always public (even for research purposes[1]). In the absence of a complete analytical solution and long term and high resolution observations, recent higher resolution reanalyses and numerical models are the most suitable solution to asses the problem of moisture sources and transport in the IAS, particularly over regions that deserve special attention as Central America.

3.3 Lagrangian methodologies as an alternative

The study of the sources of moisture can be treated as a source-receptor relationship problem, and reanalyses products can be used in two different ways to establish such relationship. One of the alternatives to these studies is the use of numerical water vapour tracers (WVT) which offer a good tool for tracking the origin of precipitable water vapour. This method can be divided in two different groups which are Eulerian and Lagrangian. For the present analysis the Lagrangian methodology was selected. First, it is important to remember that the Lagrangian formulation follows an element of fluid along its trajectory. The atmosphere can be considered as a finite number of homogeneous elements of fluid from which position and other properties are known at every time (see diagram in figure 3.2). Lagrangian methods allow the study of the source-receptor relationship using a coordinate system in which the three dimensional position of a particle (air mass) is considered at any time. Conditions at every time are given by meteorological fields so that the movement of the particles is represented by relatively accurate atmospheric conditions. In such models, turbulent fluxes play a key role in the processes in which sources and sinks are involved.The importance of these models is that they provide valuable information for the complete transport history of the air parcels *(Sodemann et al., 2008)*. The accuracy of the results obtained with these models depends on how proper is the representation of the meteorological conditions and the chemistry involved[2].

[1] Fortunately, several research centers are improving the resolution of the datasets they made public for research purposes

[2] particularly important depending on the tracers used

Better parametrisation schemes, higher resolution datasets and the assimilation of observations improve significantly the performance of the models. Lagrangian dispersion models are used to study the source-receptor relationship under different methodologies. In particular, back trajectories are used to determine potential source regions and associated contributions to receptor locations through different approaches such as flow climatologies *(Katsoulis and Whelpdale, 1993*), classification of trajectories by cluster analysis *(Stohl et al., 1996)* and source-receptor matrix calculation *(Seibert and Frank, 2003)*.

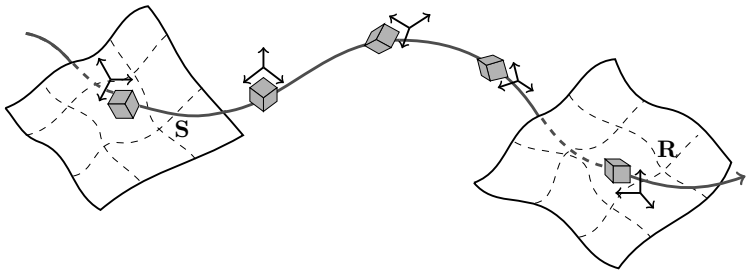

Figure 3.2: Schematic representation of the Lagrangian interpretation of a finite element of fluid. S indicates the source region and R the receptor, the gray cubes represent the finite element of fluid that in this case corresponds to an air parcel (particle).

Lagrangian models can be used both in forward and backward modes to determine concentration fields. Alternative methods have been recently addressed in the literature such as the determination of sources through Bayesian inference *(Andrew et al., 2007)*. Since Lagrangian approaches offer important information on the composition, content and history of air parcels, their use for moisture sources studies has increased. A wide variety of studies using Lagrangian approaches for assessment of the source-receptor relationship related to moisture sources can be found in the literature *(e.g Stohl and James, 2004; Sodemann et al., 2008; Durán-Quesada et al., 2010; Gimeno et al., 2010)*. The use of Lagrangian analysis methods has become very useful for studying the hydrological cycle *(Stohl and James, 2004, 2005)*. Lagrangian methods have been also used in the study of moisture sources and transport during monsoonal circulations *(Joseph and Moustaoui, 2000)*. Other studies present a Lagrangian diagnosis of the variability of moisture sources associated with precipitation under forcing of atmosphere signals *(Sodemann et al., 2008)*. Tables 3.1 and 3.2 present a comparison among Eulerian and Lagrangian methods for the analysis of the source-receptor relationship.

Type	Advantages	Disadvantages
Analytical Box Models	-Simple as few parameters are required and they consider grid based spatial variability	-Neglet in-boundary processes -Some are based on the well mixed assumption (the local source of water in the whole vertical column) -Requires knowledge on the ratios of recycled to total precipitation and precipitable water
	References: Budyko (1974), Brubaker et al. (1993), Eltahir and Bras (1994) Burde and Zangvil (2001)	
Physical water vapour traces	-Simplicity -Global coverage -Include vertical processes -Reanalysis input data (high spatio-temporal resolution) -Enable the combination of GC Ms and Langrangian Rayleigh models	-Sensitivity of the isotopic signal -Calculation time -Availability of data for validation -Do not account for convection and and rainwater evaporation/equilibration
	References: Gat and Carmi (1970), Salati et al. (1979), Rozanski et al. (1982) Koplen et al. (2008)	

Table 3.1: Comparative table of the advantages and disadvantages of the methods used for the analysis of the source-receptor relationship. Part 1, analytical box models and physical water vapour tracers

Back trajectory analysis in the region as part of the WCR Programme of the NSF

A quasi-isentropic backward trajectory analysis was applied for the 'Characterizing Land Surface Memory to Advance Climate Prediction' collaborative research developed as part of the Water Cycle Research Programme (WCR) of the National Science Foundation (NSF) at the Center for Ocean-Land-Atmosphere Studies (COLA) *(Dirmeyer and Brubaker, 2006a, 2006b* or the WCR for details [3]). The identification os the sources of moisture by *Dirmeyer and Brubaker (2006.a, 2006.b)* for the nations of Central America are shown in figure 3.3. Their results suggest the main source of moisture associated to precipitations event to be the Caribbean Sea, with an extension over northern South America and the ETPac region. The results by *Durán-Quesada et al. (2010)* are in good agreement with the spatial structure of the sources of vapour as identified by *Dirmeyer and Brubaker (2006a,b)*, however, important differences arise when comparing the seasonal climatologies shown by them and the seasonal results of

[3] available at http://www.iges.org/wcr/

Type		Advantages	Disadvantages
Numerical water vapour tracers	Eulerian	-Detailed atmospheric processes -Realistic moisture circulation	-Dependent on the model bias -Global forcing is required -Poor representation of short time scale hydrological cycle parameters -Do not include the remote sources of water for a region
		References: Benton and Estoque (1954), Starr and Peixoto (1968), Peixoto and Oort (1983) Jousame et al. (1984), Koster et al. (1986), Bosilovich and Schubert (2002)	
	Langrangian	-High spatial resolution moisture sources diagnostics -Quantitative interpretation of moisture origin allowed -No limited by a specific RCM domain and spin-up -Source-receptor relationship establishment can be easily assessed as budgets can be traced along suitably defined trajectory ensembles -Net freshwater flux can be tracked from a region both forward and back ward in time -Realistic trails of air parcel -Computationally efficient compared to perfoming multiyear GCM simulations -More information provided than a purely Eulerian description of velocity fields -Parallel use of information from Eulerian tagging methods allowed	-Moisture fluxes computations sensitivity to data noise increases for shorter time periods or smaller regions -Simple method do not provide diagnostics of surface fluxes of moisture -Surface fluxes under (over) estimation if dry (cold) air masses tracking as the budget is not closed -Evaporation rates are based on calculations rather than observations in some methods -Evaporation and precipitation are not crearly separable (in some methods) -Movement and extraction of water do not depend on the physical tendencies included in the reanalysis data
		References: dAbreton and Tyson (1995), Wernli (1997), Massacan et al. (1998) Dirmeyer and Brubaker (1999), Brubaker et al. (2001), Dirmeyer and Brubaker (2006) Stohl and James (2004; 2005)	

Table 3.2: Comparative table of the advantages and disadvantages of the methods used for the analysis of the source-receptor relationship. Part 2, numerical water vapour tracers

the Lagrangian analysis. This because the quasi-isentropic methodology used do not fully represent the losses of moisture along the trajectories. The latter results in the interpretation of the origin of the air masses and not strictly the origin of moisture, as air is identified to come from a region even when moisture may be lost before precipitating over a target location.

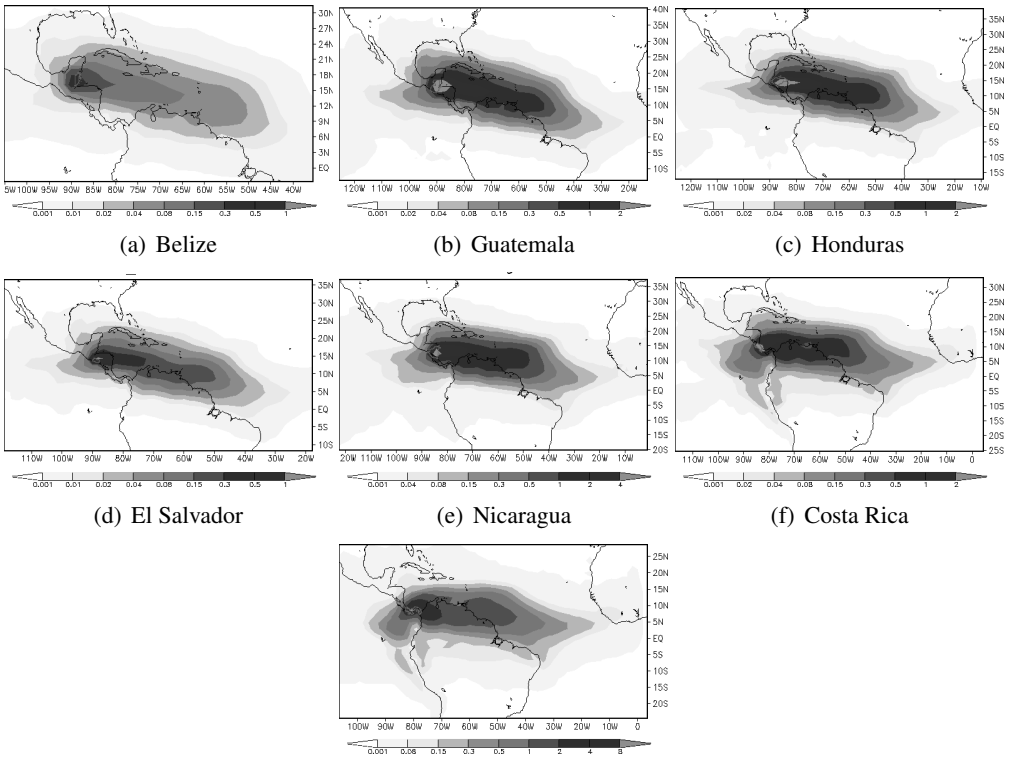

(a) Belize (b) Guatemala (c) Honduras

(d) El Salvador (e) Nicaragua (f) Costa Rica

(g) Panama

Figure 3.3: The results of the climatological evaporative sources of vapour for precipitation events for the countries of Central America are shown as retrieved from the WCR database through their webpage. Units are in Kg/m2/month. The results of *Dirmeyer and Brubaker (2006 a, b)* highlight the importance of the Caribbean Sea as main source of moisture.

The database of *Dirmeyer and Brubaker (2006a, b)* offer a good global dataset with the identification of the origin of air masses associated with precipitation events but not directly of moisture, as the complete history of the air parcels is missed. The main differences found between results from *Durán-Quesada et al. (2010)* and *Dirmeyer and Brubaker (2006a,b)* are more important for the source over the ETPac region, as the quasi-isentropic method does not account for moisture losses due to the presence of the ITCZ which modulates the moisture transport from the ETPac to Central America. Moreover, the method applied by *Durán-Quesada et al. (2010)* uses the one degree resolution ERA-40 dataset as input for the generation of the backward trajectories whereas *Dirmeyer and Brubaker (2006a)* use 1.875 by 1.9 degrees

resolution NCEP NCAR reanalysis for the lowest 16 sigma levels while *Durán-Quesada et al. (2010)* use the full 61 vertical levels of the ERA40 Reanalysis. Here we aim to provide a complete inter-annual variability study of the sources of moisture associated with precipitation over Central America under similar conditions as those used by *Durán-Quesada et al. (2010)*.

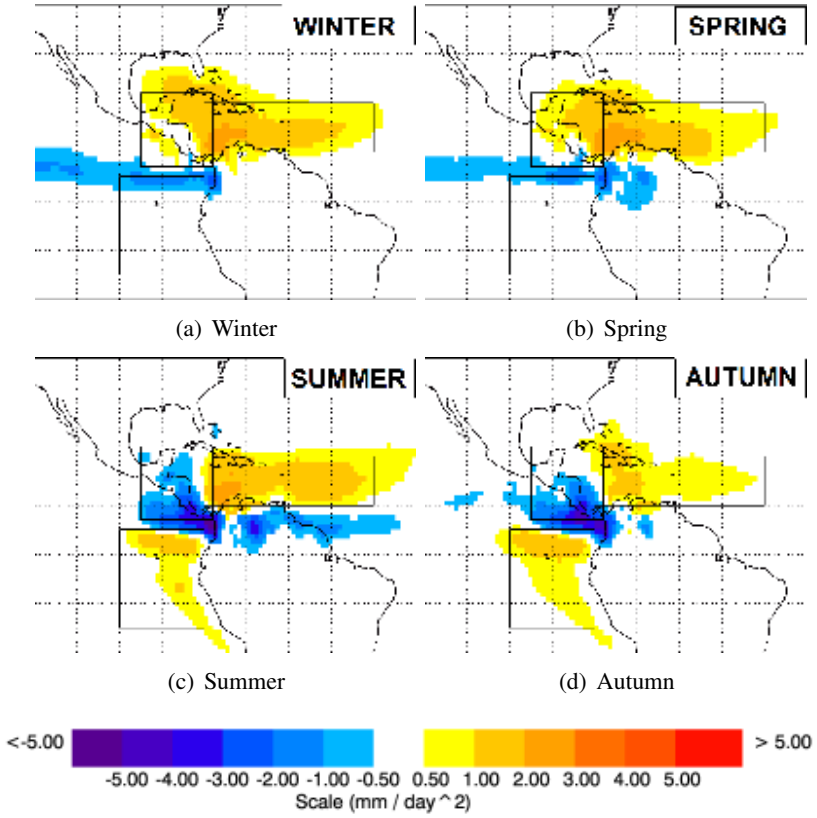

(a) Winter (b) Spring

(c) Summer (d) Autumn

Figure 3.4: Results for the sources of moisture identification from *Durán-Quesada et al. (2010)* , $(E - P)^{-6}$ field, the positive colours represent the excess of evaporation over precipitation which is associated with an evaporative sources of moisture while the negative values represent the sinks of moisture . Note that the box domain used for Central America contains important parts of water compared to that of land

3.4 The proposal

Motivation

In a previous work *(Durán-Quesada et al., 2010)*, an exploratory analysis of the sources of moisture for Central America was performed using a Lagrangian backward trajectories dataset for the five years period 2000-2004. The skills of a Lagrangian approach to analyse the region were evaluated and the main findings of that work can be summarised as:

1. Two sources of moisture of oceanic origin for Central America were identified to be the Caribbean Sea (CS) and the Eastern tropical Pacific (ETPS).

2. The CS was determined to be the most important in terms of intensity in comparison the the ETPS.

3. The horizontal extent and intensity of the sources of moisture has a marked seasonal cycle. The CS is important all year with a slight displacement towards the Gulf of Mexico during winter. In contrast, the ETPS shows significant variation throughout the year, as it disappears during winter and spring.

4. The transport of moisture was attributed to the effect of regional low level winds and the seasonal displacement of the ITCZ (however a complete discussion on the mechanisms was not provided). Further associations between the sources of moisture and relative contributions to precipitation were established between the seasonality of the sources and regional climate features.

The importance of the CS as the main source of moisture is a natural result of the regional climate and the presence of the ETPS required more attention. Even when the ETPS is supported by the findings of *Lachiet et al. (2007)* using isotope analysis, the intensity of the ETPS is small and since little evidence exists, a longer time span was required in order to be conclusive. The need of using longer datasets is also justified to allow the assessment of the impact of variability modes, which are well known to affect the region. To identify the sources of moisture for Central America and provide more details on the ETPS it is necessary to provide a long term analysis of the mean state of the sources of moisture for Central America. This analysis may only accounting for the continental region, since the exploratory analysis defined Central

America as a box that contained an important portion of water. Beyond the identification of the sources of moisture, information is required that may answer the next questions:

1. Which are the main sources that provide moisture to continental Central America?
2. Which is the response of the sources of moisture to the forcing of the signals that influence the IAS region?
3. What are the contributions from the sources to precipitation over Central America?
4. How the variability of the sources of moisture impact the regional precipitation through modulation of the contributions from the sources?
5. Which are the mean trajectories followed by the air parcels in their transit from the sources to continental Central America?
6. Which are the main circulation patterns associated with the regional transport of moisture and how do they respond to the local variability.
7. Based on the importance of the CLLJ as a regional climate feature, what it its role in the dynamics of transport and which is its effect on the modulation of precipitation over Central America.

Objectives

Motivated by these questions from the exploratory analysis of the sources of moisture, a complete study of the sources of moisture within the IAS region is proposed. A set of main objectives was proposed:

1. Generate a new backward trajectories dataset that allow the study of the sources of moisture to Central America for a longer time period.
   (a) The 1980-1999 time period was selected for the analysis due to availability of ERA-40 data with one degree of resolution to be used as input for the LDM FLEXPART to generate the trajectories dataset.
   (b) Using a domain centred in Central America, the trajectories dataset was generated with output every three hours (further details can be found in chapter 4).

2. Present a complete study of the sources of moisture for Central America.

   (a) Obtain a new climatology of the sources of moisture for continental Central America using a longer time span.

   (b) Determine accurately the seasonal behaviour of the sources of moisture

   (c) Analyse the interannual variability of the sources of moisture (intensity and horizontal extent) and evaluate the impact of the major modes of variability.

3. Study the relationship between the contributions from the identified sources of moisture and precipitation falling over continental Central America.

   (a) Determine the relative contributions to precipitation from the sources and analyse their seasonal cycle in comparison with the known seasonal cycle of precipitation over Central America

   (b) Evaluate the estimation of contributions to precipitation using available observations of precipitation.

   (c) Evaluate the behaviour of the contributions from the sources of moisture during the presence of the MSD

   (d) Study the inter annual variability of the contributions from the sources and associated precipitation to identify which modes force the major variations in precipitation.

4. Study the transport of moisture.

   (a) Determine the preferred path followed by the air parcels in their transit from the sources to Central America. Provide a complete analysis of the mean air streams from the sources to Central America by considering the differences between different locations within Central America.

   (b) Identify regions of significant variations in the air moisture content along the trajectories.

   (c) Analyse the correspondence between the mean air streams and regional climate structures that may act as moisture conveyors.

   (d) Establish a conceptual model of the regional transport of moisture.

5. Analyse the role of the CLLJ in the process of regional transport of moisture

   (a) Identify from the trajectories the mean structure of the CLLJ.

   (b) Determine how much of the moisture that contributes to precipitation over Central America is transported by the CLLJ.

   (c) Propose a mechanism by which the CLLJ may be able to modulate precipitation over Central America and the Caribbean.

Part II

Lagrangian analysis of sources of moisture and transport processes in the IAS

4
Data and Methods

The analysis of the sources of moisture, precipitation and transport iss proposed based on the skills of a Lagrangian approach developed by *Stohl and James (2004)*, and that was applied for Central America in the preliminar study of *Durán-Quesada et al. (2010)*. A dataset of Lagrangian backward trajectories was generated as explained in this chapter. The key details of the method used for the identification of the sources of moisture is presented as well as the assumptions made to estimate the relative contributions of the sources to precipitation. A clustering algorithm based on *Dorling and Davies (1992)*, was implemented to reduce the huge dataset of trajectories into representative air plumes. It was based on a non-hierarchical clustering method that is herein describe, the clustering algorithm was modified to be used to create composites of clusters as well. In order to study the transport due to the CLLJ, trajectories under the influence of this structure were isolated for an specific analysis. Additional datasets used for this study are indicated. A brief description of the observations dataset used for the evaluation of the estimations of the relative contributions to precipitation is included. Finally, some details on how the computations were made for processing the data are indicated.

4.1 The backward Lagrangian trajectories dataset

The aim of this work is to improve the comprehension of the processes involved in the transport of moisture in the IAS region and their relationship with the local precipitation. An accurate knowledge of the history of the air masses is required to accomplish the proposed study. For this reason, a Lagrangian approach is proposed instead of Eulerian methods. As mentioned, this work is based on a backward Lagrangian trajectories dataset generated with a Lagrangian Dispersion Particle Model (LDPM). A LPDM is a three-dimensional model that includes both three-dimensional wind and turbulence *(Seibert and Frank, 2003)*. In this section, a very brief introduction of the FLEXPART model is presented, followed by a description of the input data used and an explanation of some details of the performed simulations along with a description of the generated dataset.

The FLEXPART model

Some details of the FLEXPART[1] model are highlighted, it is not to present a complete description of the model which can be found in the FLEXPART technical note by *Stohl et al. (2005)*. FLEXPART is a LPDM developed originally for air pollutant dispersion calculations and is now used as a tool for atmospheric transport modelling and analysis in a wide variety of applications *(Stohl et al., 2005)*. The main reason for using FLEXPART instead of other available Lagrangian models is its robustness, supported with a large list of peer-reviewed publications in which the model is applied as well as validated. Since the interest region of the present work is located in the tropics, convective processes are of importance and most LPDM do not take into account the effects of convective processes while FLEXPART does. The structure of the model and implemented parametrisations allows its use for receptor-oriented transport studies. Those are of particular importance for determining the contribution from identified sources of moisture to precipitation over a receptor region.

The physics of the FLEXPART model is described by the zero acceleration scheme and a set of parametrisations. *Hanna (1982)*, parametrisation scheme is used for wind fluctuations. Frictional velocity computed using surface stresses and sensible heat fluxes considered in the boundary layer parametrisation. Meanwhile the profile method *(Berkowickz and Prahm, 1982)*

[1] available at http://transport.nilu.no/flexpart

is applied in absence of frictional velocity information. Turbulent motion is parametrised considering a Markov process based on the Langevin equation *(Thomson, 1987)*. *Emanuel and Zivkovic-Rothman (1999)*, one-dimensional convection model is used as convection scheme. Radioactive decay as well as dry and wet deposition are also considered in the physics of the model.

Input data and simulations

Input data

FLEXPART model can be initialised with different datasets. In the case of the present work, ERA-40 Reanalysis *(Uppala et al., 2005)* data have been used with one degree of horizontal resolution in 61 vertical levels. Analyses were used every 6 hours (0000, 0600, 1200 and 1800) and three hours forecasts for the intermediate times (0300, 0900, 1500, 2100). This due to the importance of temporal resolution for accuracy of the trajectories as is pointed out by Stohl *et al.*, 2005. ERA-40 was used instead of ERA-INTERIM because of high resolution data availability for the twenty-year analysis period [2]. FLEXPART requires five three-dimensional fields: horizontal and vertical wind components, temperature and specific humidity. Additional two-dimensional fields are also required: surface pressure, total cloud cover, 10 m horizontal wind components, 2 m temperature and dew point temperature, large scale and convective precipitation, sensible air heatflux, east/west and north/south surface stress, topography, land-sea-mask and subgrid standard deviation of topography. ERA-40 data with three hours temporal resolution have been retrieved in GRIB format through the MARS server. A landuse inventory in which categories are related with Leaf Area Index and roughness length is used. Similarly, an inventory that contains some characteristics of different chemical species/radionuclides is used.

Model configuration

Version 8.1 of the FLEXPART model was installed on a NUMALink Blade System with 16 Itanium 2 core processors with a performance of 106 GFLOPS. Due to the relatively large time span of the simulations and in order to optimise the usage of computational resources, it was decided to use a limited domain instead of a global domain for the simulations. In the case

[2]No attempts were made to use MM5 or WRF models to generate higher resolution datasets through dynamic downscaling as input for FLEXPART

of limited domain runs: a) the domain set up is based on the coordinates specified for the first release, b) mass fluxes are determined in small grid boxes at the boundary of the domain, c) mass fluxes are accumulated over time and new particles are released at random positions at the boundaries of the domain whenever the accumulated mass exceeds the mass of a particle and d) particles are terminated at the outflowing boundaries. A total of 250000 particles were uniformly distributed in the domain with each receiving the same mass. Notice that the number of particles can vary throughout the simulation as a result of the variations of the mass of the atmosphere and numerical effects. A numeric label is assigned to each particle so that it is unique and when new particles are released they do not replace any existing particle. The selection of the domain (see figure 4.1) for the simulations considered the horizontal extension of the main structures involved in the regional climate processes. The domain includes the ETPac region, the IAS (Gulf of Mexico and the Caribbean Sea). The longitude of a typical African Easterly Wave (AEW) was used as criteria for the selection of the easternmost boundary. Since we were interested in the analysis of moisture, tracer used was water vapour and the simulations were performed for the complete analysis period in backward mode using the convection and subgrid terrain effect parametrisations.

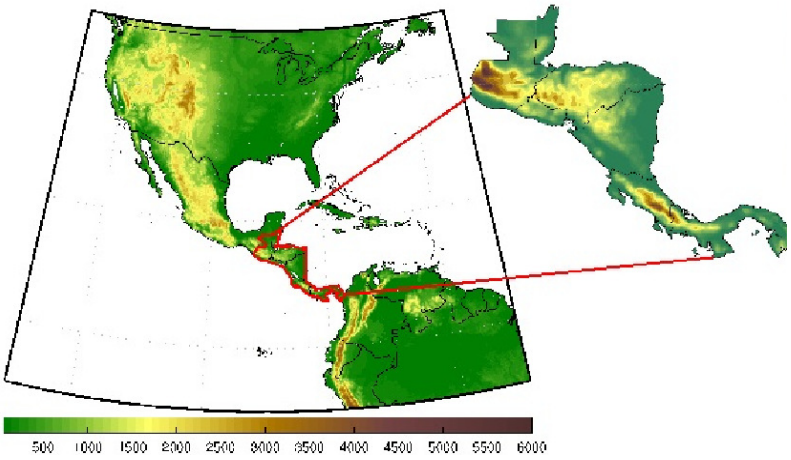

Figure 4.1: Domain used to generate the backward trajectories dataset with the FLEXPART model. A zoom view of the analysis region (Central America) indicated by the red lines is detailed in the right side. The topography height in m is shaded (information of the topography height was retrieved from the USGS).

Output data

Output for a set of twenty-years backward Lagrangian trajectories every three hours (00, 03, 06, 09, 12, 15, 18 and 21) was obtained from the simulations performed with FLEXPART. For every one of approximately 250000 particles, 13 variables were stored at every output time step (see table 4.1).

Variable	Symbol	Units
Latitude	lat	
Longitude	lon	
Height	H	m
Topography height	TH	m
Potential Vorticity	PV	10^{-6} (m^2K/sKg)
Specific Humidity	q	g/Kg
Air density	ρ_{air}	Kg/m^3
Mixing height	Hmixi	m
Temperature	T	K

Table 4.1: Output variables of the LPD M FLEXPART

Identification of sources of moisture

As known from the Lagrangian point of view, a fluid can be represented by a discrete number of finite elements of volume, for which position and several properties are known every time step. The FLEXPART model divides the atmosphere in a discrete number of N homogenous 'air particles' of mass m. This representation is very useful since, as from *Stohl and James (2004)*, the net rate of change of water vapour of an air particle can be expressed as

$$e - p = m\frac{dq}{dt} \tag{4.1}$$

so that over an area A, the surface freshwater flux results from the sum of the changes in moisture for all the particles and then can be written as

$$E - P \approx \frac{\sum_{i=1}^{N}(e-p)}{A} \tag{4.2}$$

where changes of moisture along the trajectory are related to evaporation and precipitation, as indicated in the following diagram:

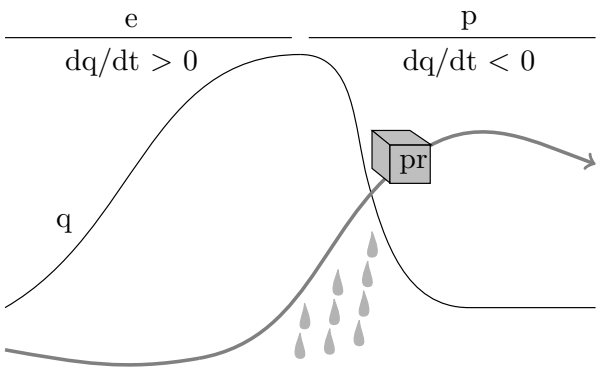

Figure 4.2: Schematic representation of the evaporation-precipitation cycle for a finite element of fluid, adapted from figure 1 of Stohl and James (2004). Decreases of the specific humidity (q) content of the air parcel (ap) correspon to precipitation and increases to evaporation. The integration of those 'e' and 'p' over an area (A) in a vertical column are used to compute the estimates of the $(E - P)^{-n}$ field.

$$\begin{array}{llll} e & if & \frac{dq}{dt} > 0 \\ p & if & \frac{dq}{dt} < 0 \end{array} \tag{4.3}$$

This can be used as a Lagrangian approximation of the balance equation (equation 1.4). Those particles arriving to a target location (Central America) that are featured by a loss of moisture during the last time step are then traced backward a determined number of days and then integrated over the atmospheric column (equation 4.2). (see figure 4.3).

Estimation of contributions to precipitation

Estimating precipitation is complex, numerical models are under constant improvements in order to reduce the biases associated with this variable. In a simplistic model, precipitation can be assumed to be approximated by projection onto the receptor region of the decrease of specific humidity at the last time step before arriving at the receptor region *(Stohl and James, 2004)*. For those air particles for which $dq/dt < 0$ for the last time step it is assumed that the moisture decrease is due to precipitation that falls immediately on the surface. The estimation of precipitation over the receptor region due to the contribution from air parcels coming from

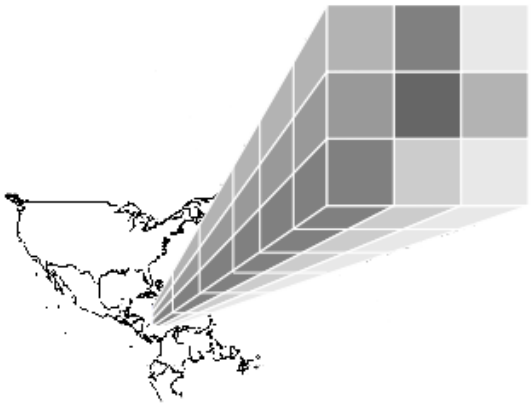

Figure 4.3: Schematic representation of vertical integrate of the changes of specific humidity of the contributing particles used to compute the conditional $E - P$ field following equation 4.2. In the case of the generated dataset, the vertical column is comprised by all the 61 vertical levels of the ERA-40 dataset.

a source is computed by integrating those decreases in specific humidity. Let g be the acceleration of gravity , Δq_k^0 the change of specific humidity for the last time step to the arrival to the receptor, Δh the vertical extent of the air column. Precipitation P can be approximated, for a determine time interval, by integrating the change of specific humidity for those particles for which $dq/dt < 0$ for the last time step (see figure 4.5) as:

$$P \approx -\frac{1}{g}\sum_{i=1}^{N} \Delta q_k^0 \cdot \Delta h \tag{4.4}$$

This approximation may be considered bold since it does not consider all processes in which air particles can be involved (e.g microphysical processes). However as a first guess approximation it is considered acceptable. More detailed estimates use the evaluation of the moisture content of the air particles along the trajectory (see e.g. *Sodemann et al., 2008*).

4.2 Clustering method applied

Clustering is a multivariate statistical technique that aims to explore structures in a given dataset *(Everitt, 1980)*. In atmospheric science studies, the result of clustering is analogous to a flow climatology and allows the grouping of trajectories that have similar characteristics (e.g length and curvature) *(Harris and Kahl, 1990)*. Due to the large amount of trajectories obtained, to

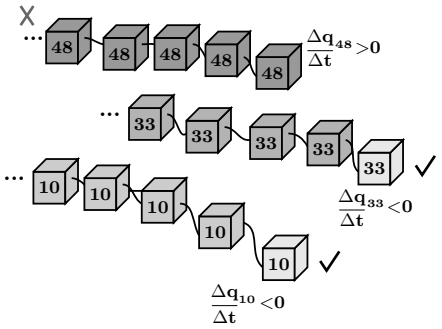

Figure 4.4: Representation of the criteria used for selecting the air particles that contribute to precipitation over a receptor location.

explore the structure of the air flow, using mean air streams from the backward trajectories dataset instead of the total of trajectories is better for climatological purposes. One of the non hierarchical clustering methods is known as the Centroid method, in which clusters with the smallest distance between the centroids are fused and the measure of similarity is then defined as the squared Euclidean distance (equation 4.5) *(Everitt, 1980)*. Herein, we used a clustering algorithm applied based on the Dorling method *(Dorling et al., 1992)*. The clustering process consist of : a) selection of the particles reaching a target regions, b) the application of an iterative clustering procedure based on *Dorling et al. (1992)*, c) once the set of trajectories was reduced into a number of representative clusters, the identification of the clusters is performed.

$$D = \sqrt{\sum_{i=1}^{N}(x_i - y_i)^2} \tag{4.5}$$

Selection of the particles of interest

From the complete dataset not all the particles circulated over the analysis regions and not all of them precipitated over the target. For this reason the first step was to select only those particles in order to speed up the calculations. From each selected analysis receptor region, all the particles that have circulated over the region and that lost moisture in the last time step previous to the arrival were selected and then tracked ten days backwards. This first classification reduces significantly the volume of trajectories and creates a new dataset in which

only the particles of interest and their trajectories are stored. Since the objective is the analysis of moisture transport in the lower levels of the troposphere, those particles that along their trajectories were above the tropopause level were discarded. Criteria for the height of the tropopause was based on the monthly means of tropopause height from the ERA-40 Analysis.

The clustering

A non-hierarchical clustering algorithm following *Dorling et al., 1992* was applied, the algorithm consisted of a set of steps described as follows.

1. In order to avoid introducing a subjective bias in the selection of the structure of the clusters and to make sure that all the possible directions are considered in the determination of the initial trajectories, a set of 'seed' trajectories were defined in a Cartesian plane as rays pointing out of the origin[3] with a separation of 6 degrees among them. This distribution gives a total of 60 'seed trajectories' covering the totality of horizontal space (see figure 4.5) to initialise the clustering.

2. The squared Euclidean distance (equation 4.5) is used as the similarity measure between each 'real trajectory' from the dataset and the 'seed trajectories', each 'real trajectory' is assigned its nearest neighbor 'seed trajectory'.

3. Once each 'real trajectory' is paired with a 'seed', a new set of 'seed trajectories' is calculated as the centroid of a set of 'real trajectories' paired with each initial 'seed'. Each new 'seed trajectory' is the equivalent average trajectory between the elements assigned to the initial seeds.

4. Finally a set of clusters is obtained and the particles trajectories are classified into groups sharing a common basic spatial structure.

With this procedure we are able to reduce large amounts of trajectories to more manageable smaller sets which represent the mean structure of the complete datasets. This is very useful to determine the regions from which air parcels that precipitate over a receptor region come [4]. However, apart from the problem of transport we are interested in the problem of transport due

[3] the origin is considered as the centroid of the target area

[4] note that this procedure is quite flexible to be used for reducing datasets and obtaining information on more processes rather than precipitation

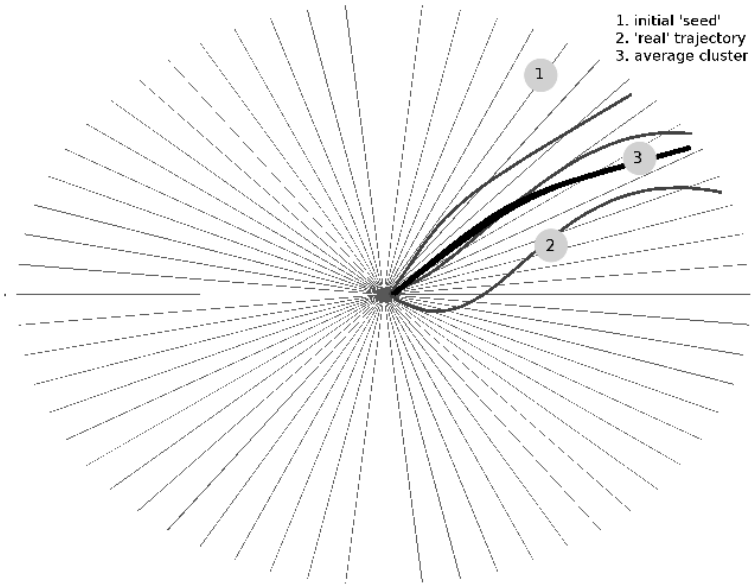

Figure 4.5: Schematic representation of the clustering algorithm used based on the algorithm developed by *Dorling et al., (1992)*. The thinner gray lines represented the initial seed trajectories, thick gray lines the 'real trajectories' and thicker black the cluster generated as the average of the real trajectories belonging to a seed trajectory.

to dynamical processes. To accomplish the identification of atmospheric moisture transported by the CLLJ, additional selections and assumptions were made.

To select those particles that were moved within the CLLJ, two main conditions were imposed. The first was that the air particles must remain along the trajectory below the 3000m and second that they must flow inside the area of influence of the CLLJ. To determine this area of influence the effect of the pressure gradient was considered. Under the assumption that a boundary layer separates the airflow in two parts inside and outside the influence area of a pressure gradient, a separation between the jet current and the mean flow was stablished as the point in which the pressure gradient tend to zero. All those particles that circulated under the influence of the jet, were then separated from the rest of particles.

4.3 Indices for CLLJ intensity and the SST and geopotential gradients

To have a measure of the intensity of the CLLJ and of SST gradients that are of importance for further analysis, three indices related to low level winds, SST and geopotential height gradients

were defined in this study. An index to quantify the intensity of CLLJ zonal wind defined similar to a previous work by *Wang (2007)*, and *Amador et al. (2010)*, by averaging the zonal wind speed at 850hPa over a box defined between $(12-18)N$ and $(80-70)W$ (see box in figure 4.3), anomalies for the $CLLJ_{index}$ were computed in order to be used as a measure of the variability of the intensity of the CLLJ.

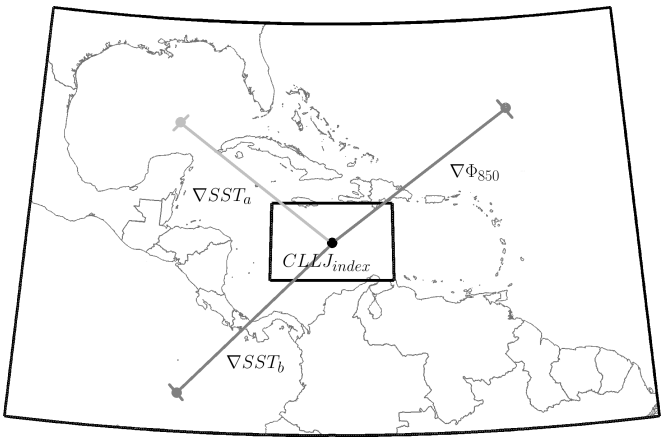

Figure 4.6: Representation of selected points for computing additional indices. The box is the area selected to compute the average of the zonal wind to define the CLLJ intensity index, black spot marks the CLLJ core location, dark and light gray the points selected to compute the SST difference between the CLLJ core and the ETPac and Gulf of Mexico respectively while dark gray on the right shows the point selected to compute the geopotential difference between a point of the NASH and the CLLJ

$$CLLJ_{index=} - (\overline{U_{x,y}}) \tag{4.6}$$

A geopotential height difference was estimated as the difference between the centre of the CLLJ core and a point nearby the mean centre of a developed NASH.

$$\Delta\Phi_{850} = \Phi_{850}(15N, 75W) - \Phi_{850}(25N, 60W) \tag{4.7}$$

Analogously, SST difference between the centre of the CLLJ core and the Gulf of Mexico and the ETPac region were computed.

$$\Delta SST_a = SST(15N, 75W) - SST(24N, 88W) \tag{4.8}$$

$$\Delta SST_b = SST(15N, 75W) - SST(3N, 87W) \tag{4.9}$$

A representation of the locations at which the values of $U_{x,y}$, $\Delta\Phi_{850}$ and SST were taken for computing the indices is shown in figure 4.6.

4.4 Additional Reanalysis variables, climate indices and precipitation data

In order to support the Lagrangian trajectories dataset and provide a proper interpretation of the results, additional datasets have been used in the development of this work. Reanalysis data for variables of interest regarding the content of moisture as well as transport and energy were used. Since studying the relation between the transport of moisture and precipitation was part of the objectives of this work, CMAP precipitation data was also used.

ERA-40 data

As mentioned, information of additional variables was required to provide a robust analysis of the results and improve their interpretation. This extra information was basically related to winds, atmospheric content of moisture and transport. A set of variables from the high resolution ERA-40 Reanalysis both in surface and vertical levels depending on availability were retrieved. These variables were used to analyse the mean fields and variability, perform composite analysis to study the effect of determined atmospheric signals among other applications that will be indicated through the document. All data was retrieved for a global domain in a monthly basis with one degree of horizontal resolution and vertical resolution determined depending on the specific required application of the data. Table 4.2 presents a summary of the retrieved variables, corresponding units and resolution.

Precipitation

CMAP data

Precipitation is fundamental for the analysis, in particular regarding the analysis of the source-receptor relationship and extreme events. In the case of this work, the use of precipitation information is particularly complex since the representation of regions like Central America in the global datasets is poor due to the coarse resolution of the General Circulation Models (GCM) that perform the reanalysis. In addition, the availability of observational data in these

[5] data from ERA40 Reanalysis was used for computing these indices

Variable	**Symbol**	**Units**
Pressure levels: 500, 600, 700, 775, 850, 925, 1000		
Divergence	DIV	s^{-1}
Potential Vorticity	PV	K m^2 kg^{-1} s^{-1}
U component of wind	U	m s^{-1}
V component of wind	V	m s^{-1}
vertical pressure velocity	OMEGA	Pa s^{-1}
Geopotential height	Φ	m
Pressure levels: 100, 150, 200, 250, 300, 400, 500, 600, 700, 775, 850, 925, 1000		
Specific Humidity	Q	kg kg^{-1}
Temperature	T	K
Surface		
Mean Sea Level Pressure	MSLP	Pa
Total column water vapour	TCWV	kg m^{-2}
Sea Surface Temperature	SST	C
Vertical integrals		
Vertical integral of divergence of moisture flux	VIDMF	kg m^{-2} s^{-1}
Vertical integral of eastward water vapour flux	VIEWVF	kg m^{-1} s^{-1}
Vertical integral of northward water vapour flux	VINWVF	kg m^{-1} s^{-1}
Vertical integral of total column water vapour	VITCWV	kg m^{-2}

Table 4.2: Additional variables retrieved from ERA-40 dataset (monthly means) for the analysis performed in this study. The resolution of the datasets is one degree. Retrieve of data was done using the MARS server.

regions is scarce. So it was decided to use CMAP dataset. Monthly data for the 1980-1999 time period was extracted from the global CPC Merged Analysis of Precipitation (CMAP) which has a resolution of 2.5 degrees. The CMAP data are produced using information from raingauges and satellite-based estimations (which are not constant in time due to the availability of information). The merging technique used to generate the CMAP consists of a reduction of random errors based on the maximum likelihood method used to obtain linear combinations of the satellites estimates and further use of *Reynolds (1988)*, blending technique. Raingauge

information for surrounding areas is used to determine the errors over global land areas while information over the Pacific atolls is used to estimate the random error over oceans. A complete description of the datasets and computation methodology can be found in *Xie and Arkin (1997)*.

Observations

Due to the nature of this study and the contribution it may represent for further studies on precipitation, moisture transport and the hydrological cycle in general over Central America, the possibility of evaluating the results using long term observations is of importance. However, the availability of long term complete datasets that meet the criteria of good quality data is poor, since most of the observations are distributed along the different regional institutions (and particular companies and owners) and the effort of merging these data is a recently ongoing process [5]. Due to the importance of evaluating at some point the results, an additional effort was made in the attempt of using observations. Data for a total of 386 stations were provided by the Center for Geophysical Research (of the UCR) with daily and monthly mean values ranging from the late forties to 2004 (see distribution of stations in figure 4.7.a). Those stations for which data for the 1980-1999 period was not available at all were discarded. Unfortunately, due to the political conflict in Central America during the 80s and 90s most of the stations have more than 75% of missing data for those years. For a reduced number of stations, listed in table 4.3, a basic quality control procedure was applied the data based on the identification of outliers and homogeneity test. The Standard Normal Homogeneity Test *(Alexandersson, 1986)* was applied using as reference station a weighted average of the regional time series. After neglecting those stations that did not meet the homogeneity criteria, 42 stations located over Belize, El Salvador, Costa Rica and Panama were found to be usable (see distribution in figure 4.7.b). The criteria can be considered as very restrictive. However, it was decided that it was better to use assured quality data for a minor number of stations than using more stations and increase the biases since the objective was to use averaged values (so homogeneity was fundamental). Missing data were filled using the sample mean method which consists of simply filling in the gaps using the sample mean of the series due to its simplicity. Because of the availability of observations, a simple sort of evaluation was performed but only for those locations for which reliable quality observations data were available.

[5] as part of the projects of the Comité Regional de Recursos Hidráulicos (CRRH)

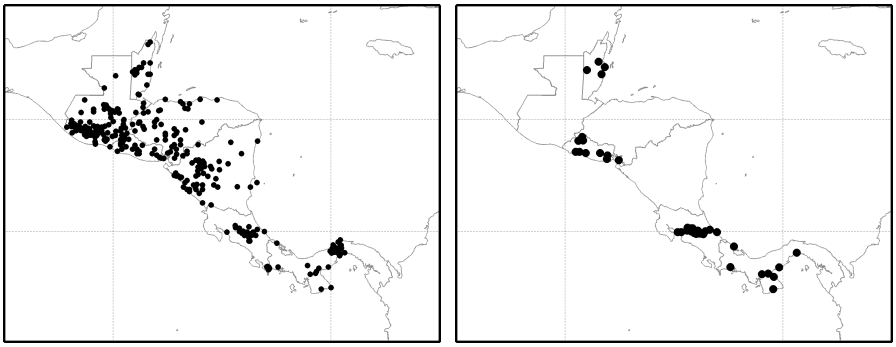

(a) Complete set of stations (b) Stations that passed the quality control

Figure 4.7: Location of a) complete set of raingauges considered for the quality control analysis and b) raingauges that met the quality criteria for the analysis and for which the imputation method was applied to fill the gaps of missing data to be used for the analysis.

Climate Indices

As part of the analysis, different indices were used to identify the presence of strong signals during 1980-1999 period, in particular ENSO, NAO, PDO and MJO. All climate indices used were retrieved from the Climate Prediction Center (CPC) from the website of the Earth System Research Laboratory http://www.esrl.noaa.gov/psd/data/climateindices.

ENSO An El Niño 3.4 index defined as the SST anomalies for the Niño region 3.4 which is bounded by $(120 - 170)W$ and $5S - 5N$ *(Trenberth, 1997)* was used since the analysis region is mainly influenced by the Niño region 3.4 to which is closer.

NAO NAO index *(Hurrell, 1995; Jones et al., 1997)* index from the UK Climate Research Unit (CRU) was retrieved through its website [6]. The NAO index available from the CRU Pressure and Circulation Indices is calculated using the normalized pressure difference between one station on Gibraltar and one on Iceland. Information available from the CRU site includes data for SW Iceland (Reykjavik), Gibraltar and Ponta Delgada (Azores).

PDO PDO index from Mantua dataset *(Mantua et al., 1997)* was extracted for the 1980-1999 period. This PDO index is derived as the leading principal component of monthly SST anomalies in the North Pacific Ocean (poleward of 20 N). SST data used to compute

[6] http://www.cru.uea.ac.uk/cru/data/

Station	**%**	**Station**	**%**	**Station**	**%**
Belmopan	77.08	Sesuntepeque	97.50	Rosemont	99.58
Central Farm	93.33	Juan Santamaria	100.00	San Josesito Heredia	100.00
Melinda	90.83	San Jose	80.00	San Vicente	100.00
Pswgia	98.75	Avance 3 Rios	100.00	Zarcero	95.00
Ahuanchapan	99.17	Barrio Mexico	98.33	Cerro Prec	100.00
Candelaria de la Frontera	99.17	CATIE	95.42	Linda Vista	100.00
Guija	99.17	Guadalupe Esparza	100.00	Aton	100.00
La Hachadura	98.33	Diamantes	95.42	David	100.00
La Union	100.00	Laguna Fraijanes	98.33	Divisa	100.00
Nueva Concepcion	100.00	La Lola	95.00	Los Santos	100.00
Planes de Montecristo	96.25	Limon	100.00	Santiago	100.00
San Francisco Gotera	99.17	Pacayas	100.00	Tocumen	100.00
El Papalon	99.17	Puntarenas	100.00	Tonosi	100.00
Santa Ana El Palmar	99.17	Rancho Redondo	100.00	Bocas del Toro	100.00

Table 4.3: List of the stations used for the evaluation of the estimations of precipitation from the Lagrangian approach, the percentage of available data for the 1980-1999 period is indicated. Data was facilitated by the Center for Geophysical Research of the University of Costa Rica.

the anomalies is from UKMO Historical SST data set, version 1 of Reynold's Optimally Interpolated SST.

MJO Using daily MJO index 7 ($40W$) from CPC (interpolated from pentads to daily values), two annual cycles were computed monthly anomalies were computed with respect to the annual cycle to compute an estimated monthly MJO index.

WHWP The WHWP index defined by *Wang and Enfield (2001)*, as the monthly anomaly of the ocean surface area Ocean region enclosed by the 28.5 isotherm in the Atlantic and eastern North Pacific was used for evaluate the influence the presence of the WHWP may have in the regional moisture availability and transport.

4.5 Analysis tools

Empirical Orthogonal Functions

Introduced in fluid dynamics by Edward Lorenz in 1956, this is a technique that provides information of the spatial and temporal variability of time series in terms of orthogonal functions often referred as statistical modes. So it is an useful tool for the identification of patterns *(von-Storch and Zwiers, 2003)*. An EOF corresponds to a spatial pattern that is used to represent the statistical modes associated with the signals detected in a dataset. The computation of the EOFs uses a covariance matrix of the timeseries and its decomposition into eigenvalues and eigenvectors. For computing EOFs for a Field F, a spatial covariance matrix X_F must be derived

$$X_F = F * F^T \tag{4.10}$$

$$X_F * E = E\Lambda \tag{4.11}$$

where λ_m are the corresponding eigenvalues

$$\Lambda = \begin{vmatrix} \lambda_1 & 0 & \cdots & 0 \\ 0 & \lambda_2 & \cdots & 0 \\ \cdots & \cdots & \cdots & \cdots \\ 0 & 0 & \cdots & \lambda_m \end{vmatrix} \tag{4.12}$$

$$E = \begin{vmatrix} E_1^1 & E_1^2 & \cdots & E_1^m \\ E_2^1 & E_2^2 & \cdots & E_2^m \\ \cdots & \cdots & \cdots & \cdots \\ E_m^1 & E_m^2 & \cdots & E_m^m \end{vmatrix} \tag{4.13}$$

Here the E_m^k are the eigenvectors associated with each λ_m eigenvalue since the matrix E meeting the orthogonality criteria $E * E^T = E^T * E = I$ (I is the identity matrix).

The temporal evolution of the k^{th} EOF is given by a series G obtained by projecting the original series F onto E_m^k such that

$$G_k(t) = \sum E_m^k F_m(t) \tag{4.14}$$

so that

$$G = E^T * F \tag{4.15}$$

Note that each eigenvalue λ_m is proportional to the percentage o variance of F that accounts for the k^{th} mode, used to indicate the variability explained by each mode .

Composites

Despite the simplicity of composite analysis, it is a powerful tool to be used in the construction of an estimate of the mean state of a given variable conditioned by the value of an external index. Composites were constructed for positive and negative phases of the main variability modes (ENSO, NAO, PDO and MJO). To select the basis for compositing, the climate indices for each mode were used. The categories were set to be positive, negative and neutral condition depending if the negative and positives values of each index were larger or smaller than a threshold defined as $+/-0.75STD$ from the mean series. Values relying in between were classified as neutral, all in a monthly basis, following *vonStorch and Zwiers (2003)*, as in equation 4.16, where the sets (composites) Γ of a field $\mathbf{X}$ conditioned by an index $\mathbf{n}$ for a number of observations i are given as:

$$\hat{\mathbf{X}}_{\Gamma} = \frac{1}{i}\sum_{j=i}^{i} \mathbf{x}_{ti} \tag{4.16}$$

A non parametric test *(Mann and Whitney, 1947)* was used to determine the evaluate the statistical significance at the 95% of confidence. Depending on the specific purpose of the analysis, the difference between the values of the fields for the positive/negative phase and the values for the neutral conditions was also computed to express the results in terms of the anomalies.

Wavelet analysis

The analysis of time series sometimes finds a problem in their non-stationary nature and wavelet analysis solves this issue by estimating the spectral characteristics of a given time series as a function of time *(Torrence and Compo, 1998)*. Wavelet can be used as a method to detect climate-induced patterns. An advantage on the usage of wavelet analysis is that the wavelet transform decomposes a signal over functions. One of the advantages of this analysis tool is that it allows a good localisation in both time and frequency *(Lau and Weng, 1995)*. A complete description of the wavelet analysis and the correspondent mathematical treatment can be found in *Daubechies (1992)*. For the present work, the analysis was performed following

the guide of *Torrence and Compo (1997)* from which follows that using a mother wavelet Ψ, the continuous wavelet transform of a time series x_n is given by

$$W_n(s) = \sum x_{n'} \Psi^* \left[\frac{(n' - n)\delta t}{s} \right] \tag{4.17}$$

which by means of the convolution theorem $F[fg] = F[f] * F[g]$ can be expressed as

$$W_n(s) = \sum \hat{x}_k \hat{\Psi}^*(s\omega_k) e^{i\omega_k n \delta t} \tag{4.18}$$

where the discrete Fourier transform of x_n is $\hat{x}_k$ such that

$$\hat{x}_k = \frac{1}{N} \sum x_n e^{-2\pi i k n / N} \tag{4.19}$$

with the angular frequency ω defined as

$$\omega_k = \begin{cases} \frac{2\pi k}{N\delta t} & \text{if } k < \frac{N}{2} \\ \frac{-2\pi k}{N\delta t} & \text{if } k > \frac{N}{2} \end{cases} \tag{4.20}$$

The global wavelet spectrum was computed as

$$\overline{W^2}(s) = \frac{1}{N} \sum |W_n(s)|^2 \tag{4.21}$$

and the scale averaged wavelet power used to analyse the fluctuations within a range of scales was computed as

$$\overline{W_n^2}(s) = \frac{\delta_j \delta_t}{C_\delta} \sum |\frac{W_n(s_j)}{s_j}|^2 \tag{4.22}$$

Due to its characteristics, for this study, the selected mother wavelet was Morlet which is defined as:

$$\Psi_0(\eta) = \pi^{1/4} e^{i\omega_0 \eta} e^{-\eta^2/2} \tag{4.23}$$

5

Lagrangian identification of sources of moisture for continental Central America

In chapter 3 the problem of the availability of moisture in the IAS was introduced. From the studies that have analysed this problem, few have had among their main objectives the study of moisture availability and transport to Central America. This is one of the issues that is aimed to be accomplished with this work. The identification of the sources of moisture for Central America is carried out following a Lagrangian approach based on a backward trajectories dataset generated with the LDPM FLEXPART. A mean state of the main sources of moisture for the twenty years analysis period and the seasonality of the sources are presented. The variability of the sources of moisture and their response to the effect of the main climate modes that affect the region are studied using composites. The aim of this chapter is to provide a detailed study of the horizontal structure of the sources of moisture for continental Central America.

5.1 Identification of moisture sources

As mentioned in chapter 1, the use of vertically integrated divergence of moisture flux provides information on the regions that may act as moisture suppliers. From figure 1.5, the presence of a strong divergence region in the vicinity of the tropical Atlantic, the IAS and the ETPac can be observed. From figure 1.6, the role of the IAS as a moisture supplier for Central America,

the Gulf of Mexico and northern South America can be observed. The seasonal averages of vertically integrated divergence of moisture flux and the vertically integrated water vapour flux are shown in figure 5.1. A strong convergence region over the equator shows the presence of the ITCZ. Larger positive divergence values are observed in the South American west coast and the IAS region, similar to the global pattern of figure 1.5. The field of vertically integrated divergence of moisture flux (VIDMF) in figure 5.1 shows a marked seasonality. These plots are a good starting point of the origin of air parcels that contribute to precipitation but do not give an immediate estimate of how much of that moisture is actually being transported to Central America.

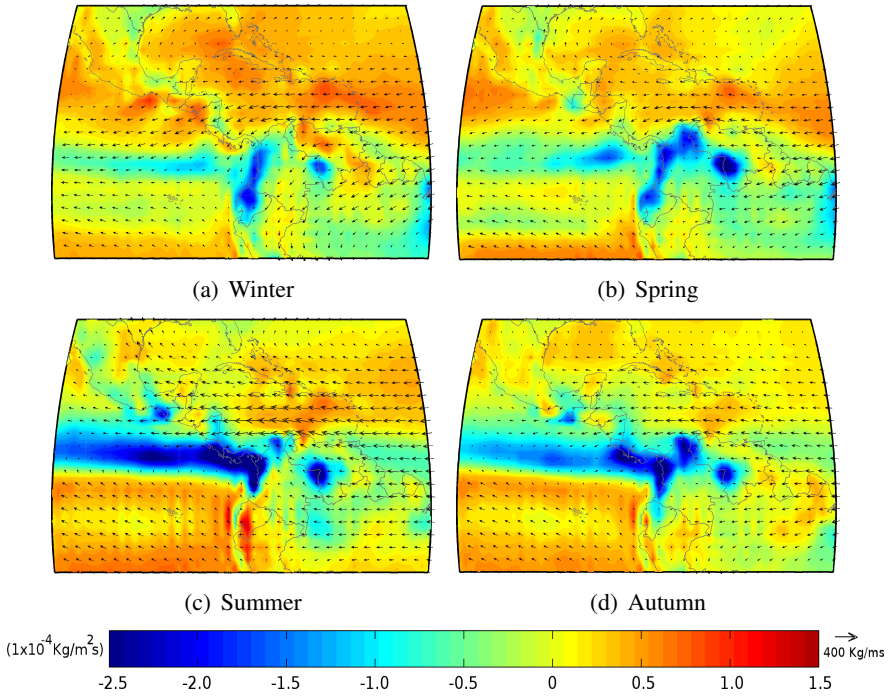

Figure 5.1: Seasonal mean vertically integrated divergence of moisture flux (VIDMF) field (shaded contours) and vertically integrated water vapour flux vector. Contour shades from $-2.5x10^{-4}$ to $1.5x10^{-4}$ in Kg/ms. Vector reference is $400Kg/ms$. Positive values are associated with sources of moisture and negative sinks of moisture.

Using the dataset of backward trajectories generated with FLEXPART and ERA-40 data, the method developed by *Stohl and James (2004)* is used to identify the sources of moisture for Central America.

The mean climatology and seasonal cycle

Tracking the air particles that arrive to Central America and computing their changes of moisture backward in time, $E - P$ can be estimated from equation 4.2. The residence time of water vapour in the atmosphere is of the order of ten days *(Numaguti, 1999)* as well as the moisture-convection feedback time scale in the tropics *(Grabowski and Moncrieff, 2004)*. Integrates of $(E - P)$ were computed for those ten days and it was found that for Central America, they tend to converge at 6 days so for present analysis 6 days integrates of $(E - P)$ were used.

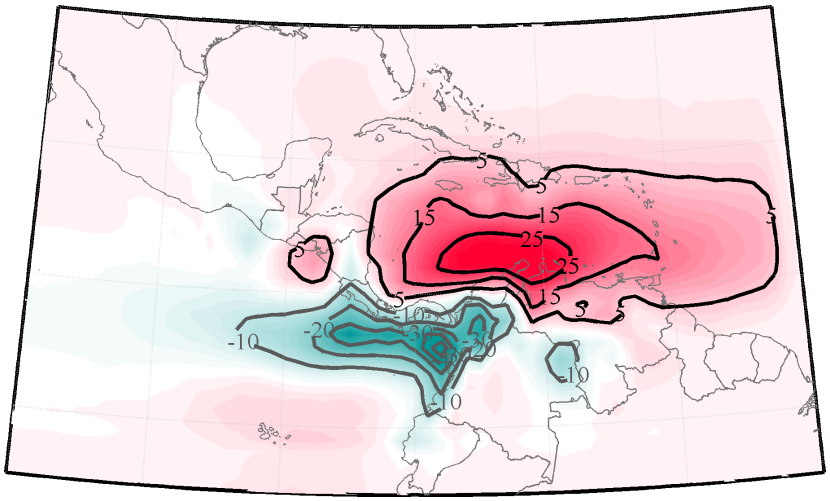

Figure 5.2: Long term mean of the six backward days integrated conditional net fresh water flux $(E - P)^{-6}$ field in mm/day. Positive contours (in red) every $10mm/day$ starting in $5mm/day$ and negative contours every $10mm/day$ starting in $-10mm/day$. Sources of moisture for precipitation over Central America are indicated by the positive contours. The main climatological source of moisture associate with precipitation over Central America is the Caribbean Sea.

Dominance of positive $(E-P)^{-6}$ values is useful to determine evaporative sources of moisture associated with precipitation over a receptor region. This means that positive values of the (E-P) field computed for the trajectories backward from a receptor region provide a map of the source of moisture for that region. This is the way the source-receptor relationship can be established. The excess of evaporation observed over the Caribbean Sea is evident from figure 5.2, while evaporation is observed in the Pacific Nicaraguan coast and west of Ecuador and NW of the Galapagos (just below the maximum of precipitation shown in green as a sink). Both sources of moisture are in agreement with the results of *Durán-Quesada et al. (2010)*. The

climatological mean of $(E-P)^{-6}$ shown in figure 5.2 provides a good picture of the sources of interest but may be neglecting important aspects linked to the seasonality of the sources. The seasonal overview of the $(E-P)^{-6}$ field is provided in figure 5.3, which highlights the role of the Caribbean Sea (CS) as the major source of moisture for the region as in figure 5.2. Both intensity and horizontal extent of the CS presents a marked seasonal pattern. So does the source of moisture identified in the ETPac (ETPS), which is characterised for being active only during summer and autumn. Here again, in good agreement with the work by *Lachniet et al. (2007)*. Recycling over northern South America is observed from patterns on figure 5.3 (particularly Venezuela Plains and the Magdalena River basin [1]). This region is a source of moisture for Central America was not a direct result of the study of *Durán-Quesada et al. (2010)* and is an important finding of this work.

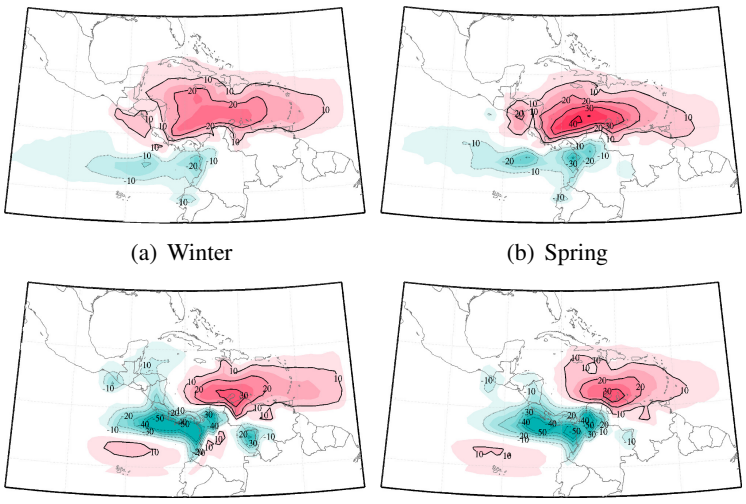

(a) Winter (b) Spring

(c) Summer (d) Autumn

Figure 5.3: Long term seasonal means of the the conditional $(E-P)^{-6}$ field in mm/day. Positive(red) and negative(green) contours indicated every $10mm/day$ starting in $10mm/day$ and $-10mm/day$ respectively. Sources of moisture for precipitation over Central America are indicated by the positive contours. The seasonal cycle of the sources of moisture can be extracted from the figure. The Caribbean Sea is a permanent source of moisture with intensity fluctuations while on average a source is identified over the ETPac region.

The Caribbean is a permanent source of moisture for the region while the ETPS is active only during summer and autumn. Note that during winter and spring the CS source is located in the proximity of the Central American coast and moves to the east for the rest of the year

[1] one of the rainiest locations on Earth, as indicated in *Poveda and Mesa, 2000*

with associated intensity variations. The maximum intensity is found (on average) at the end of spring. This is also the period when the core of the contributions has a zonally elongated structure that extends along the Caribbean Sea. As the summer approaches, the core of the CS moves eastward. A decrease in the magnitude of the CS occurs in association with the intensification of the easterly winds. This reflects that stronger easterlies are able to transport moisture from the Caribbean longer distances. Therefore, the Caribbean moisture is able to reach the Pacific whereas contributions to continental Central America decrease. The easterly winds are able to modulate precipitation over Central America by modulating the availability of moisture. This supports the proposal of the MSD being a result of the summer intensification of the easterlies as pointed out by *Magaña et al. (1999)*.

The ETPS starts to developed at the end of spring and reaches a noticeable intensity until August. The presence of a source of moisture in the ETPac is a result of a region of strong evaporation (as noticed from figure 1.3 chapter 1). The southwesterly flow intensifies in the same period, allowing moisture to reach the southern part of Central America. The efficiency of the ETPS is constrained to both the northwesterly flow and the movement of the ITCZ. The inactivity of the ETPS during winter and spring may be associated with the southernmost position of the ITCZ. The rate of moisture loss is by far larger than the rate of evaporation, therefore evaporated moisture precipitates over the ocean and air parcels arrive drier to Central America. On the contrary, as the ITCZ moves northward, moisture from the ETPS is allowed to go north and eventually reach Central America until the ITCZ moves south.The ITCZ represents a blocking mechanism for the influence of the ETPac moisture for Central America.

An even less observed source in the mean patterns is the Gulf of Mexico (GoM). The monthly means of $(E-P)^{-6}$ show that at the end of autumn and winter, the CS extends to the entrance of the GoM. These small influences may be neglected, but in the mean the sum of the contributions from the source of the Gulf of Mexico (GoMS) may account (particularly for northern Central America). Moreover, the importance of the Gulf of Mexico may be magnified by the regional wind conditions, as during winter and early spring, when there is an important wind component pointed southerly to Central America over the Caribbean.

Continental sources of moisture are also important. Recycling of moisture over Central America is expected as a result of a) known precipitation cycle and b) vegetation coverage. Central America is a source of moisture (hereafter CAS) for itself mainly during winter and spring,

as follows from the seasonal patterns shown in figures 5.3.a and 5.3.b, that is when evaporation exceeds precipitation over the region. The role of northern South America is identified with particular intensity over the Magdalena river basin and the Venezuela plains region. This northern South America source (NSAS) is of importance during summer and early autumn. However, the seasonal patterns do not provide a proper image of what is actually happening and look the monthly means is necessary. The NSAS is of importance from July to October with the Magdalena river basin exhibiting a maxima of its intensity during September (see Appendix D for the monthly march of the $(E - P)^{-6}$ field). This excess of evaporation over northern South America is in good agreement with the annual cycle of precipitation in the region featured by a dry season between June and September *(Restrepo et al., 2006)*.
It is important to consider the horizontal structure of the evaporative sources of moisture provide some information on the conditions of transport and the processes that the air parcels may experience along their trajectories. Figure 5.4 shows the $(E-P)^{-n}$ for the first, second, fourth and seventh backward days. The major $(E - P)^{-n}$ positive values occur to the first backward day ($n = 1$), which implies a strong local contrast between divergence and convergence prior to the arrival of the air parcels. Moreover, the source is much more confined previous to the major moisture loss over the receptor region. The pattern suggests that evaporation is strongly increased over central and western Caribbean. Even when air parcels acquire moisture from the eastern Caribbean, the most relevant uptakes occur in the first four backward days. In the case of the ETPS, the result is different, since the larger intensity occurs for the second and third days prior to the arrival while few or no source is noticed for the day before the arrival. Seven and/or eight days before the air arrives to Central America, the air parcels do not contribute significantly to precipitation since the major moisture changes occur over the western Caribbean. This as a result of the regional structures involved in the process of evaporation, SST distribution and zonal winds.

5.2 Variability of the sources of moisture

Part of the motivation of the present study was to present an analysis of the interannual variability. That is why after presenting the identification of the main sources of moisture for Central America, the influence of the main variability modes is considered. An overview of the sensitivity of the field $(E - P)^{-6}$ to the main variability modes that affect the region is

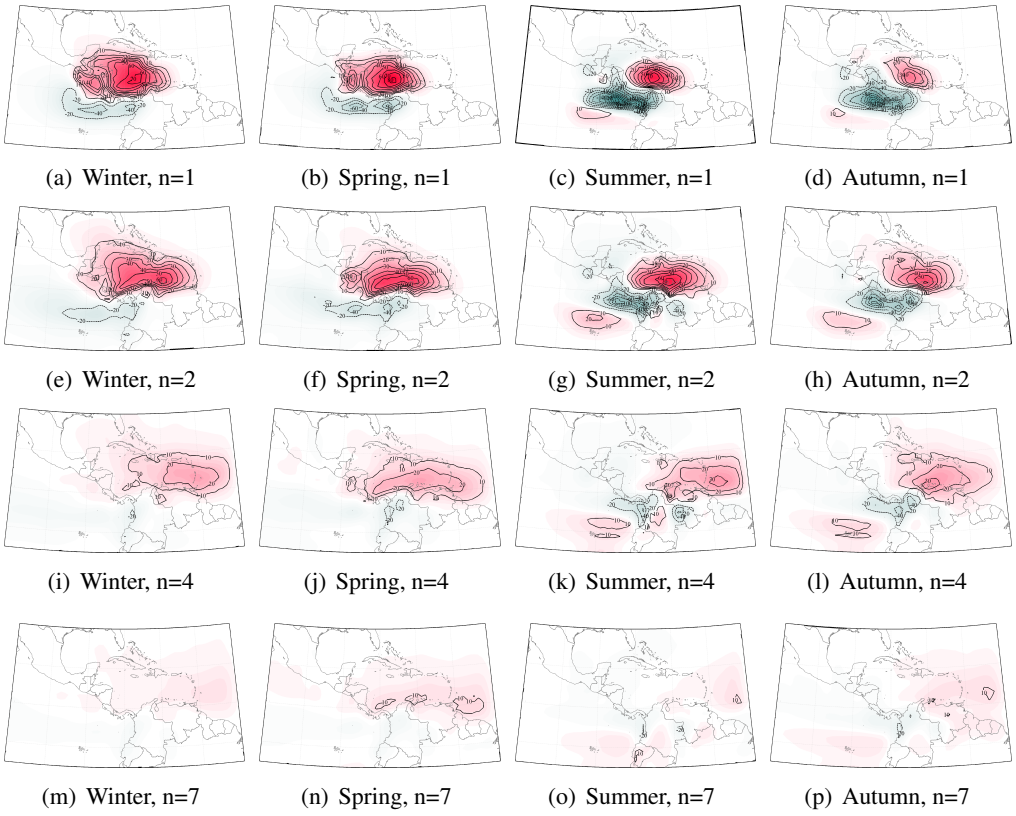

(a) Winter, n=1 (b) Spring, n=1 (c) Summer, n=1 (d) Autumn, n=1

(e) Winter, n=2 (f) Spring, n=2 (g) Summer, n=2 (h) Autumn, n=2

(i) Winter, n=4 (j) Spring, n=4 (k) Summer, n=4 (l) Autumn, n=4

(m) Winter, n=7 (n) Spring, n=7 (o) Summer, n=7 (p) Autumn, n=7

Figure 5.4: Long term seasonal means of the $(E-P)^{-n}$ field in mm/day. Positive(red) and negative(green) contours indicated every $10mm/day$ starting in $10mm/day$ and $-10mm/day$ respectively. Sources of moisture for precipitation over Central America are indicated by the positive contours. After day 7 the net freshwater flux is almost nil and after day, for this reason integrates are used for the first 6 backward days.

provided by the spatial pattern of the EOFs depicted in figure 5.5. Figure 5.5.a suggests the high sensitivity of the two remote oceanic sources to variability (Note EOFs were computed using the $(E-P)^{-6}$ anomalies).

First EOF (fig 5.5.a) explains 16.2% of the variability, the negative patch that covers the entire Caribbean contrasts with the positive patches in the northernmost Caribbean region that extends toward the GoM and the region which coincides with the maximum of evaporation that feeds the ETPS. The negative structure shows larger variability associated with the periods of 83-84 and 97-98 while for the positive 88-89, 95-96 and 99 (see the PC series shown in fig 5.5.d). The negative values of the first PC associated with periods in which the first

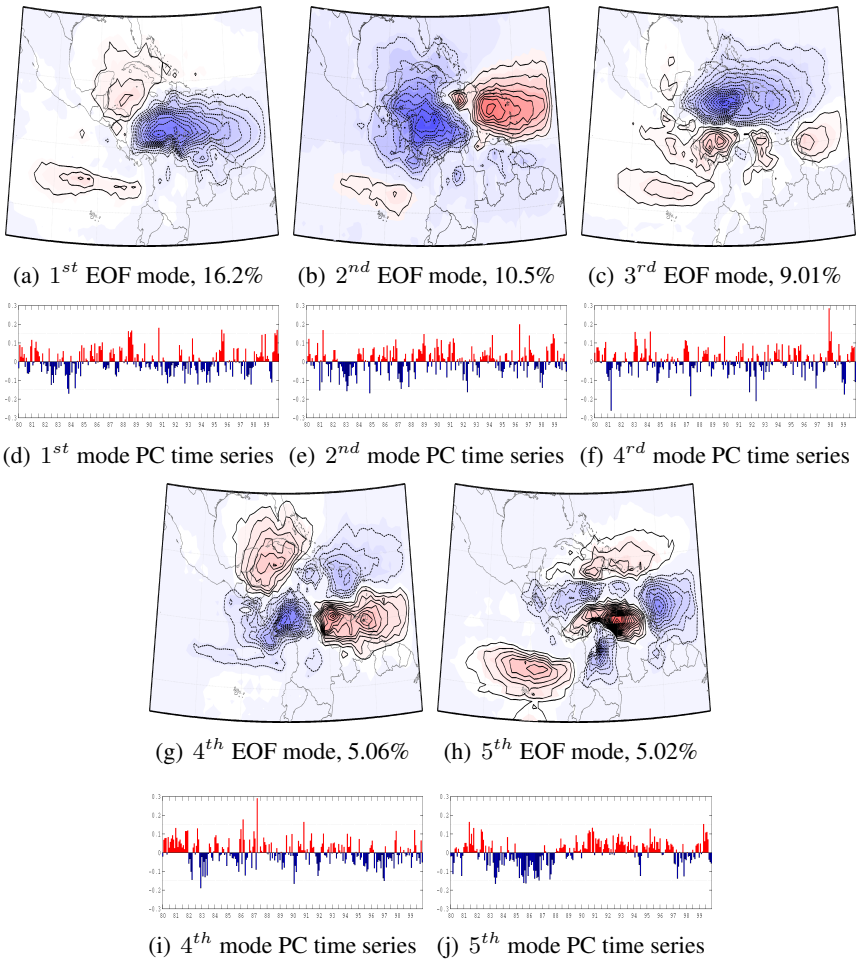

(a) 1^{st} EOF mode, 16.2% (b) 2^{nd} EOF mode, 10.5% (c) 3^{rd} EOF mode, 9.01%

(d) 1^{st} mode PC time series (e) 2^{nd} mode PC time series (f) 4^{rd} mode PC time series

(g) 4^{th} EOF mode, 5.06% (h) 5^{th} EOF mode, 5.02%

(i) 4^{th} mode PC time series (j) 5^{th} mode PC time series

Figure 5.5: First 5 modes of the non rotated EOF spatial pattern for the of conditional $(E - P)^{-6}$ field computed from the backward trajectories from continental Central America with their principal component time series and explained variance. EOF (a) shows the largest variability related to the easterly wind flow and evaporation over the ETPS. EOF (b) suggests variability of intensity of the CS, EOF (c) shows a relationship with the fluctuation of the zonal wind, suggesting variability associated with the CLLJ The fifth EOF (h) shows variability of the NSAS source, with a different behaviour between the Venezuela plains and the Magdalena river basin.

PC of the zonal wind over the IAS domain presents the same tendency to negative values. The second mode (fig 5.5.b) which accounts for a 10.5% of the variability is related with the horizontal extent of the CS. The difference between the inner and outer Caribbean patterns suggests that when the outer Caribbean provides a larger contribution, contributions from the inner Caribbean are reduced and viceversa. The pattern described by the third mode (9% of the variability, fig 5.5.c) is more related to the variability of the meridional position of the source. As the first mode may be associated with the mean easterly flow, the third mode seems to be more related with the fluctuations of the zonal wind. This mode can be associated with the CLLJ as it seems to modulate the contributions from the Caribbean, ETPS, local recycling and transport from the Venezuelan plains. Important peaks in the PC (fig 5.5.f) are found at the end of spring for 81, 87, 92 and 98. This suggests a marked sensitivity of this mode to ENSO. The fourth (fig 5.5.g) and fifth (fig 5.5.h) EOFs account approximately 5% each, being particularly interesting the pattern of the fifth mode. This describes the variability of the southernmost ETPS as well as the contrast between the components of the NSAS with the PC (fig 5.5.j) showing a low frequency variability which seems to range from five to ten years. The latter remarks the importance low frequency variability modes as the PDO may have.

To obtain a more complete picture of the role of the variability modes, composites for positive and negative phases of ENSO, NAO, MJO and PDO were computed for positive $(E - P)^{-6}$ values that are associated with evaporative sources. Differences between the composites of each phase and neutral conditions were computed in order to provide a direct comparison of the deviations from the neutral conditions when each phase is active. The discussion of the results will be presented individually for each variability mode. Table 5.1 summarises the relationship between the sources of moisture and the climate indices (monthly basis) as the correlation coefficients between the time series significant at the 95%. Note that only correlation coefficients larger than 0.4 are shown.

		Jan	Feb	Mar	Apr	May	Jun	Jul	Aug	Sep	Oct	Nov	Dec
ENSO	CS	-	-0.47	-	-	-	-	0.80	0.71	0.66	-	-	-
	CAS	0.52	0.75	-	-	-	-	-	-	-	0.47	-	-
	ETPS	0.58	0.79	0.64	-	-	-	-	-0.56	-0.70	-	-	-
	GoMS	-	-	-	0.43	-	-	-	-	-	-	-	-
	NSAS	-	0.40	0.50	-	-	-	-	-	0.56	-	-	0.53
NAO	CS	-	-	-	-	0.65	-	-	-	-	-	-	-
	CAS	-	-0.58	-	-	0.53	-	-	-	-	-	-	-
	ETPS	-	-	-	-	-	-	-	-	-	-	-	-
	GoMS	-	-	-	-	0.56	-	-	-	-	-	-	-
	NSAS	-	-	-	-	-	-	-	-	-	-0.58	-	-
PDO	CS	-	-	-	-	-	-0.48	-	-	0.42	0.49	-	-
	CAS	-	-	-	-	-	-	-	-	-	-	-	-
	ETPS	-	-	-	-	-	-	-	-0.41	-0.64	-0.43	-0.67	-
	GoMS	0.61	-	-	0.59	-	-	-	-	-0.46	-	-	-
	NSAS	-0.41	-	-	-	-0.66	-0.49	-	0.43	0.48	0.43	-	-
MJO	CS	-	-	-	-	-	-	-	-	-	-	-	-
	CAS	-0.63	-0.58	-0.47	-	-	-	-	-	-	-	-	-
	ETPS	-0.60	-0.51	-0.67	-0.55	-	-	-	-	-	-	-	-
	GoMS	-	-	-	-0.61	-	-	-	-	-	-	-	-
	NSAS	-	-	-	-	-	-	-0.51	-	-	-	-	-

Table 5.1: Correlations coefficients between the conditional positive $(E-P)^{-6}$ integrated in each source location and weighted by the area of the source and the selected climate indices. Coefficients are shown only for significant correlations at the 95% and largest correlation values are gray shaded.

ENSO

In general terms the warm and cold phases of ENSO have an opposite effect on the sources of moisture for Central America. For warm ENSO, the CS is strongly intensified, in agreement with results by *Enfield and Alfaro (1999)* in which increasing CLLJ was found for warm ENSO, thereby increasing E-P. Note that the positive SST anomalies associated with the onset of El Nino lead to an increase in the CLLJ and CS evaporation over precipitation (red contours in the CS region) in panels b, c, and d. The structure of the CS is confined to the southwestern portion of the Caribbean with an intensified band over northern Venezuela for warm ENSO. In January, a westward displacement of the CS starts (as shown by the increase in the magnitude of the CS over the western Caribbean and Central America) while the intensity of the CS decreases significantly over the eastern Caribbean. This displacement peaks in February, when the source region is located crossing Central America and reaching the Pacific side. At this moment the CS has been strongly decreased over the Greater Antilles (figure 5.6.a). The pattern is similar for the following months with decreasing anomalies. During July, the CS is centred over the Caribbean Sea with an intensified branch over Venezuela (figure 5.6.b). Note that for this month, the conditions of the NSAS indicate a decrease in the intensity of the source region over the Magdalena river basin in contrast with the intensification of the Venezuelan component of the NSAS. During August, the intensification of the CS drops at the same time that the ETPS starts a significant reduction of intensity until November. The end of autumn is featured by a pattern, that besides the reduction of the ETPS, shows the intensification of the CS with an extension at the east of the Lesser Antilles. This is linked to the decrease of the northern part of the CS with respect to its neutral conditions (figures 5.6.c and 5.6.d). It is important to point that during the onset of warm ENSO the positive SST anomalies lead to an increase in the CLLJ, therefore in the intensity of the evaporation over the Caribbean which result in the intensification of the CS as observed from the red contours over the Caribbean in figures 5.6.a, b and c.

In the case of the cold phase of ENSO, the eastward displacement of the CS starts during December with an intensified core at the east of the Greater Antilles (figure 5.7.a). In January, the December core is displaced to the south while the CS over the Central Caribbean decreases strongly. The structure of the CS is modified, its intensity increases to the west (centred over the southern Central American Caribbean region) and reduces over the Antilles (figure 5.7.b).

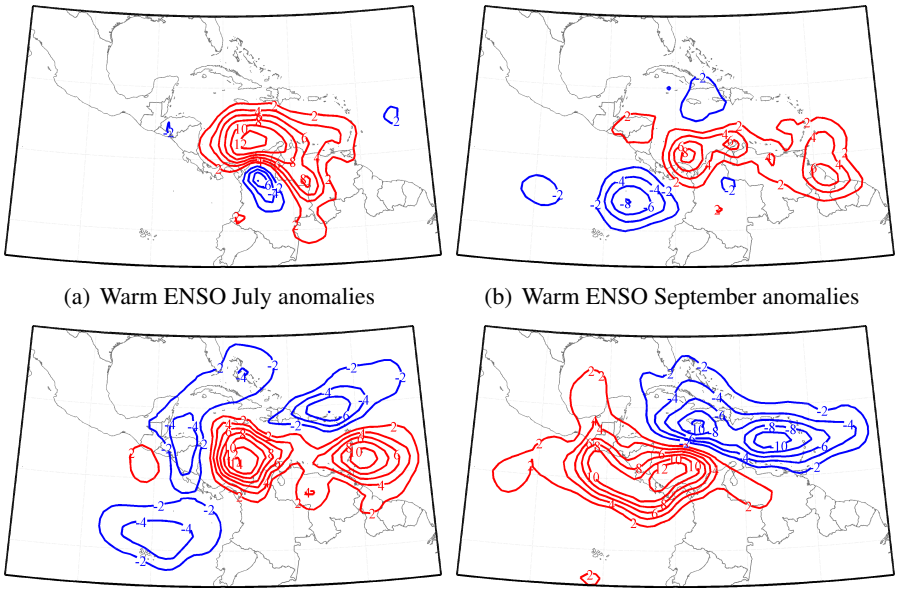

(a) Warm ENSO July anomalies (b) Warm ENSO September anomalies

(c) Warm ENSO November anomalies (d) Warm ENSO February anomalies

Figure 5.6: Differences between the positive $(E - P)^{-6}$ field for warm ENSO and neutral conditions composites. Contours every 2 mm/day, red for positive anomalies and blue for negative.

The peak of this intensification is reached in May, followed by a drastic reversal of the pattern in June. A strong intensification of a evaporative source west off Costa Rica is accompanied by a marked decrease of the potential source directly over the Caribbean Sea and NSAS (figure 5.7.c). The anomalies that determine these patterns decrease slightly to be reinforced at the beginning of autumn. This occurs when the reduction of the CS is observed over the region of the Gulf of Mexico. In this period, increases of the ETPS are elongated to the west (figure 5.7.d). At the end of autumn, the intensification of the CS over the central Caribbean is marked. From the contrast noticed for autumn between the warm and the cold ENSO phases it can be observed that warm ENSO is featured by the increase of evaporation over NSA and a decrease of evaporation over the easternmost ETPac whereas for cold ENSO evaporation is noticed to drop importantly over NSAS and the CS with the intensification over the ETPac region. This result is in good agreement with the previous findings by *Hastenrath (1976)*, *Giannini et al. (2000)* and *Taylor et al. (2002)* that suggest a drier (wetter) second rainy season for warm (cold) ENSO. The difference observed by the mentioned authors is supported by the observed decrease (increase) of the intensity of the ETPS for warm (cold) ENSO, from which transport

is very efficient during autumn as will be later on discussed in chapter 7.

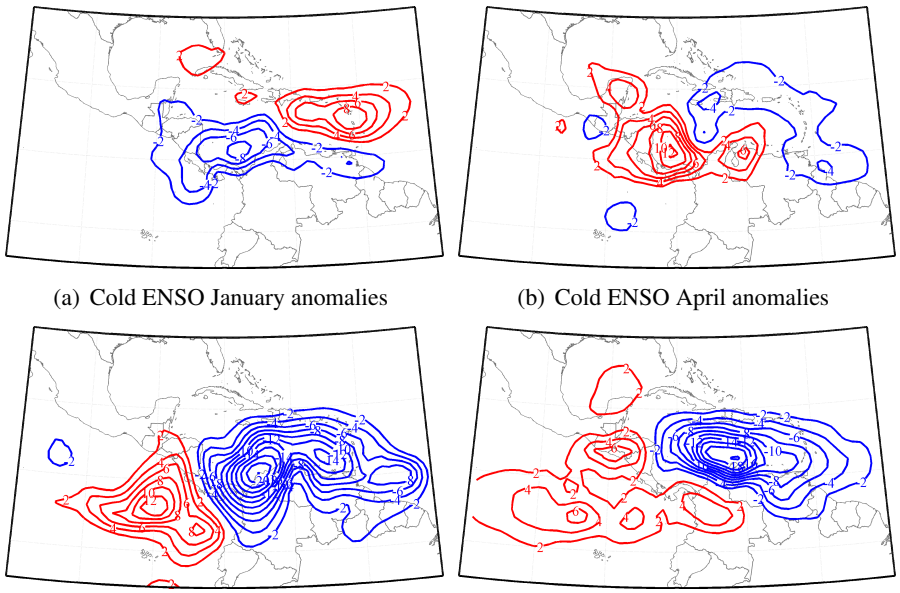

(a) Cold ENSO January anomalies (b) Cold ENSO April anomalies

(c) Cold ENSO June anomalies (d) Cold ENSO September anomalies

Figure 5.7: Differences between the positive $(E-P)^{-6}$ field for cold ENSO and neutral conditions composites. Contours every 2 mm/day, red for positive anomalies and blue for negative..

The $(E-P)^{-6}$ field and the zonal wind speed at 850mb are regressed onto the Nino 34 index. From the regression coefficients shown in figure 5.8, it shows that during winter (5.8.a) the positive coefficients are centred at the southernmost portion of Central America with larger values west of Panama. As spring approaches (5.8.b) those positive values extend all over the Pacific coast. For summer and autumn, those positive values moves to the Caribbean (5.8.c, 5.8.d) with an important component over the Venezuela plains (5.8.c) (which is maximum during summer). Negative regression coefficients can be noticed over the region occupied by the ITCZ and the Lesser Antilles during winter (5.8.a) and only over the ETPac ITCZ region during spring (5.8.b). During summer, strong negative regression coefficients over the ETPac region contrast with the positive pattern observed over the Caribbean (5.8.c). Moreover, there is a difference in the evapotranspiration pattern over continental Central America, as suggested by the positive (negative) values for southern (northern) Central America. The regression of the zonal component of the wind shows an important shift between the Caribbean and the Pacific. The regression over the Caribbean exhibits negative (positive) regression coefficients

during summer and autumn (winter and spring). Meanwhile, over the ETPac positive values are observed all year round. Note that the easterlies and the structure of the negative regression of the zonal wind becomes more intense and extended to the ETPac. However, during winter (when the CLLJ has the secondary maximum), the structure of the regression coefficients, even when extended through the ETPac, is positive (5.8.a). Following the results shown in table 5.1, the most direct relationship between the sources of moisture and ENSO occurs during summer and winter. The CS is anticorrelated with ENSO during winter (r=-0.47) whereas a high correlation is observed for summer (r= 0.80). Local recycling is sensitive to ENSO as noticed from the positive correlation during winter (r=0.75) and the ETPS presents the opposite behaviour compared to the CS, this is, highly correlated with ENSO during winter (r= 0.79) and anticorrelated during summer (r=-0.70).

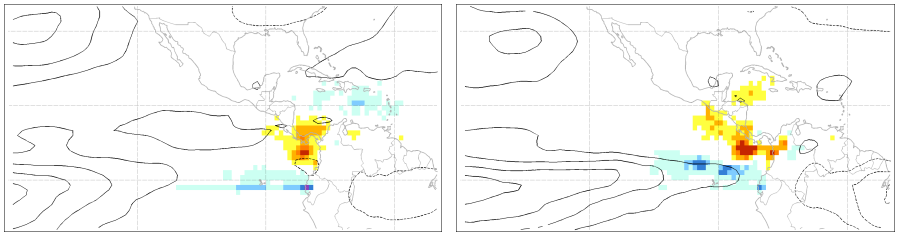

(a) Winter (b) Spring

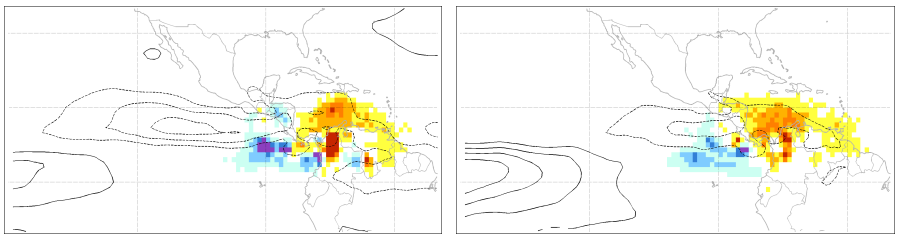

(c) Summer (d) Autumn

Figure 5.8: Regression coefficients maps for conditional $(E-P)^{-6}$ and zonal component of the wind at 850 hPa regressions onto the Nino34 index.

The contrast between the regression coefficients for the main oceanic sources of moisture highlights the opposite response the sources have to ENSO. This is important as it is related to the variability of precipitation, which is also associated with to the forcing of this mode as will be discussed in the following chapter.

NAO

The influence of the NAO starts to be of importance in spring, with the reduction of the magnitude of the CS (figure 5.9.a) during the positive phase. The intensification of evaporation over the northernmost Caribbean is observed during April, while the magnitude and extension of the ETPS are reduced (figure 5.9.b). A pattern of strong intensification of the source over the northern Caribbean and the reduction of the ETPS feature the end of spring. In early summer, evaporation over continental Central America has decreased in comparison to the neutral years and the CS exhibits a different pattern. In June, the region of larger evaporation is located to the east of the Lesser Antilles (figure 5.9.c). During July, the excess of evaporation over the central Caribbean Sea is intensified for NSAS while decreased in the Pacific coast of northern South America. In August the intensity of NSAS is significantly enhanced. The pattern for September presents a well defined intensification of the CS along the horizontal extension of the Caribbean Sea. A band of negative anomalies over continental Central America and the ETPac shows a marked decrease of evaporation that implies a reduction of the intensity of CAS and ETPS (figure 5.9.d). Local recycling of moisture is found to be anti-correlated with the NAO index during winter, meanwhile the CAS and the sources located in the IAS (CS and GoMS) are correlated with NAO index for May. The NSAS is on the contrary anti-correlated with NAO during October. Regarding the increase of recycling for negative NAO suggested by the anti-correlation observed for February it can be argued that it has do do with the modifications of the instability, if so, an interesting question may be are there subsidence anomalies produced by the influence of the NASH associated with the NAO?.

Negative NAO presents the opposite pattern for March compared to the positive phase. The CS is intensified over the central Caribbean while reduced over the easternmost part (figure 5.10.a). During April, the position of the CS is limited to the westernmost portion of the Caribbean and has a latitudinal extension that reaches the Gulf of Mexico. The CAS is also intensified while the pattern shows a decrease of the evaporation from the middle to the east Caribbean as well as for the ETPS (figure 5.10.b). In July, the evaporation over the westernmost Caribbean and Venezuela decreases, while the ETPS is strongly reduced. Small intensifications of evaporation over different parts of the Caribbean take place until November. When the evaporative source extends from northern Central America to the Greater Antilles with a strong intensification that peaks in front of Honduras Caribbean coast. During the same month, the NSAS as well as evaporation over the Lesser Antilles and a latitudinal band in the Pacific

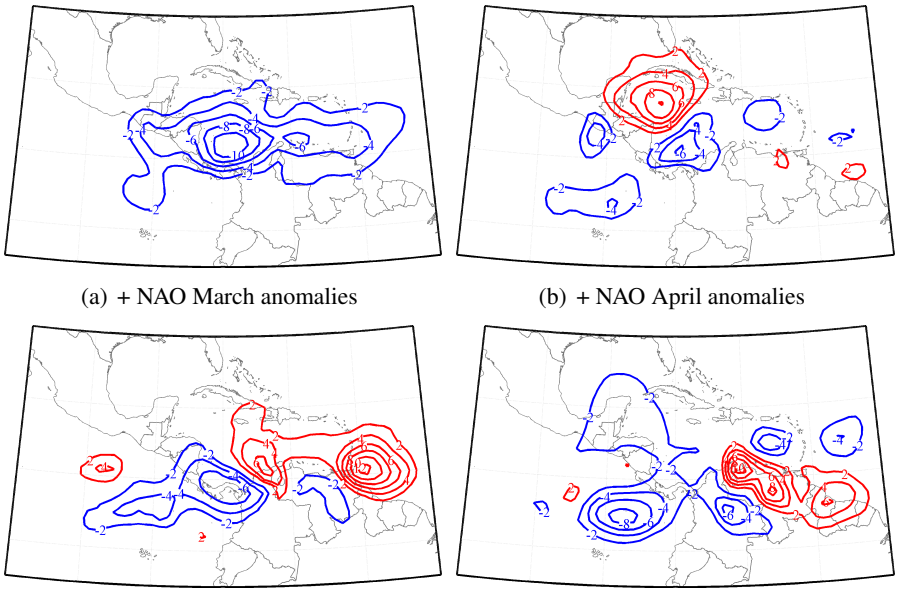

(a) + NAO March anomalies (b) + NAO April anomalies

(c) + NAO June anomalies (d) + NAO September anomalies

Figure 5.9: Differences between the positive $(E-P)^{-6}$ field for positive NAO and neutral conditions composites. Contours every 2 mm/day, red for positive anomalies and blue for negative.

that extends from 13 N to 3S is decreased (figure 5.10.d). Moreover, the band-like pattern observed for the anomalies of positive $(E-P)^{-6}$ field for the negative NAO composites during November (sig 5.10.d) may suggest an intensified ITCZ located over NSA and the easternmost ETPac which is interesting as may imply an anomalous migration of the ITCZ for this NAO phase. The increase of the contributions of moisture from the central Caribbean during negative NAO, which are more intense for spring and November, coincide with the rainy seasons. Note that in these cases the availability of moisture over the Caribbean is increased, therefore convective activity is enhanced and an associated pattern of enhanced precipitation over the Caribbean is suggested. In contrast, negative anomalies for spring during positive NAO suggest the reduction of moisture over the Caribbean region.

The regression of the $(E-P)^{-6}$ field and zonal wind over the NAO index (5.11) shows the effect that this mode has on the sources of moisture (therefore on precipitation) during spring . As the NAO signal is more intense during winter, its effect becomes more noticeable in spring when precipitation is more intense (compared to the minimum of precipitation during winter). Positive regression coefficients are noticed in the northern Caribbean and southern

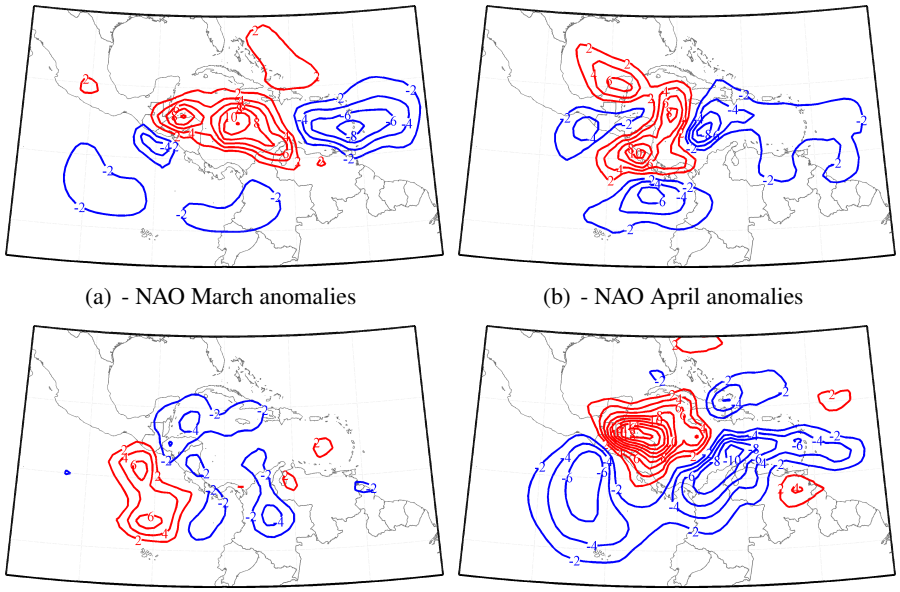

(a) - NAO March anomalies (b) - NAO April anomalies

(c) - NAO May anomalies (d) - NAO November anomalies

Figure 5.10: Differences between the positive $(E-P)^{-6}$ field for negative NAOand neutral conditions composites. Contours every 2 mm/day, red for positive anomalies and blue for negative.

Central American Pacific coast. Marked negative values can be observed over the region located in the vicinity of the topographic gap of the Sierra Madre in southern Nicaragua through which winds pass to the ETPac. In spring the fingerprint of the NAO is very important for the northern Caribbean, its effect shows a tendency to enhance the variations in evapotranspiration over Central America. Therefore, this mode may be related with important variations in the continental precipitation patterns. The previous considerations suggest the increase (decrease) of moisture availability in the Caribbean during negative (positive) NAO. Moreover, the negative anomalies observed for March during positive NAO (fig 5.9.a) is well explained by the strengthen of the easterly winds documented by *Giannini et al. (2001)* in spring. The differences of composite anomalies of potential velocity at 200mb, divergent wind and precipitation are shown in figure 5.11. The green contours encircled by a low level convergence wind field suggest negative (positive) NAO to be related with an increase (decrease) of precipitation over the Caribbean. In agreement with *Malgrem et al. (1998)* and *Giannini et al. (2001)* that suggest the anti-correlation relationship between precipitation over the Caribbean and the NAO index. This opposite relation between precipitation over the Caribbean and the NAO can be in

our terms interpreted as the correlation observed for May (r=0.65) between the NAO and the intensity of the CS associated with precipitation over Central America.

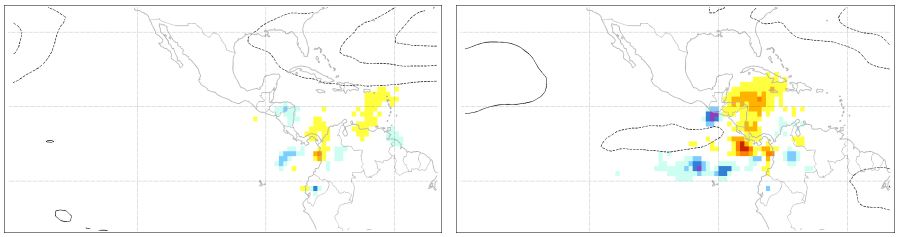

(a) Winter (b) Spring

Figure 5.11: Regression coefficients maps for conditional $(E-P)^{-6}$ and zonal component of the wind at 850 hPa regressed onto the NAO index.

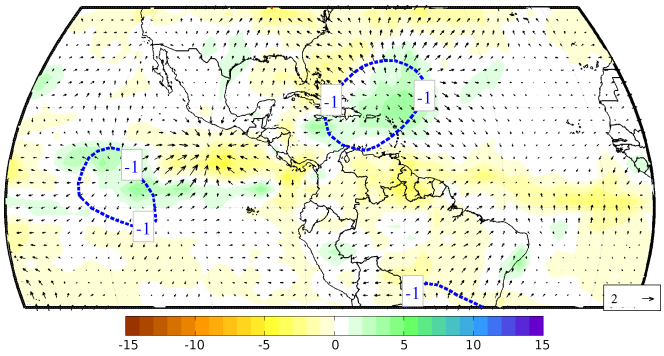

Figure 5.12: differences of composite anomalies of potential velocity at 200mb and precipitation. Units in $10^6 m^2 s^{-1}$, m/s and mm/day.

PDO

The influence of the PDO is more complex to describe in terms of the observed anomalies patterns. For the positive phase, the decrease of the intensity of the CS occurs for December and January (figure 5.13.a). A short intensification of evaporation over continental Central America during February is accompanied by the decrease of evaporation over the Lesser Antilles (figure 5.13.b). The further decrease of evaporation over the complete Caribbean basin during March is followed by similar conditions in the NSAS and a reduction of the ETPS during April. In May, the ETPS presents a small intensification as well as a region of the Caribbean

enclosed between northern Central America and Cuba. Evaporation increases over the ETPac, southern Central America and the border between Colombia and Venezuela during June. Then, the importance of these regions as sources of moisture increases too. Meanwhile, a small decrease of the CS is noticed (figure 5.13.c). During August the evaporative source over central Caribbean increases altogether with evaporation over Colombia. Small positive anomalies over the Caribbean and ETPac are followed by reductions of evaporation between Nicaraguan east coast and the Greater Antilles for the remaining months. This occurs until November, when evaporation is enhanced over Central America and to the east of the Lesser Antilles while reduced over the Caribbean and the ETPac (figure 5.13.d).

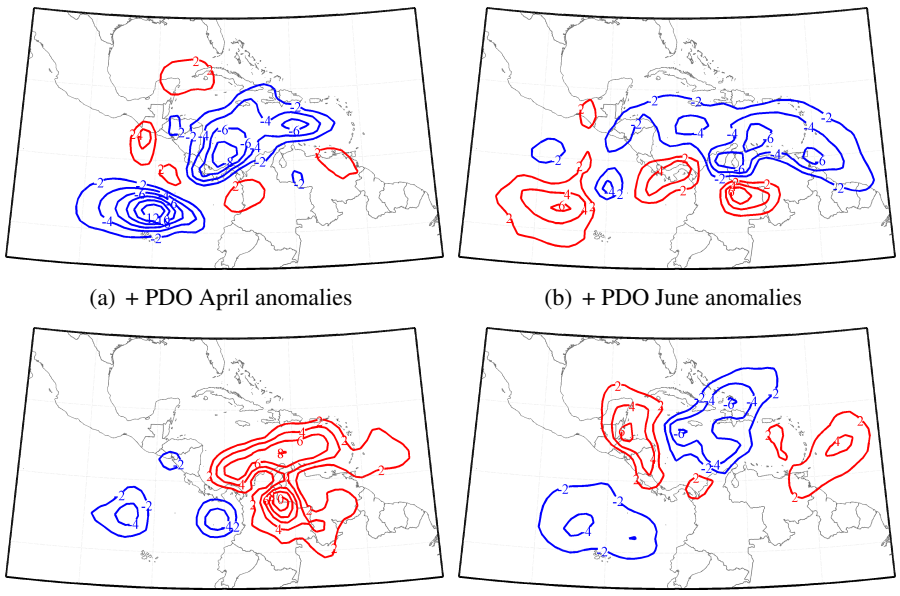

(a) + PDO April anomalies

(b) + PDO June anomalies

(c) + PDO August anomalies

(d) + PDO November anomalies

Figure 5.13: Differences between the positive $(E-P)^{-6}$ field for positive PDO and neutral conditions composites. Contours every 2 mm/day, red for positive anomalies and blue for negative.

For negative PDO, the evaporative source is intensified over the Lesser Antilles and decreased from the middle Caribbean to the east coast of Central America, with a reduction over the Gulf of Mexico during January (figure 5.14.a). Small decreases of evaporation occur over the Caribbean and west coast of southern Central America for February and March. In April the evaporative source over the ETPac decreases jointly with evaporation over Central Amer-

ica and the transect between northern Central America and Cuba. This at the same time that increases over easternmost Caribbean. In May, the reduction of evaporation over southern Central American west coast decreases its intensity and a small increase of the ETPS takes place (figure 5.14.b). The latter, accompanied by the intensification of evaporation for a zonal band extended over southern Caribbean and northern South America. This zonal band of increases of the evaporative source moves northwestern while a reduction of evaporation takes place over the ETPac and Colombia(figure 5.14.c). The following months are featured by the reduction of NSAS and evaporation over southern Central America as well as the intensification of CS and ETPS. During September evaporation over Venezuela exhibits a decrease of intensity while an increase is noticed over northern Central America, Panama and the ETPac. For October the increase of evaporation over the ETPac and southern Panama east coast persists while the intensity of evaporative sources decreases over central Caribbean. In November, the evaporative source present a generalised decrease over central and south Caribbean while is intensified over the northern Caribbean, the Gulf of Mexico and the ETPac (figure 5.14.d).

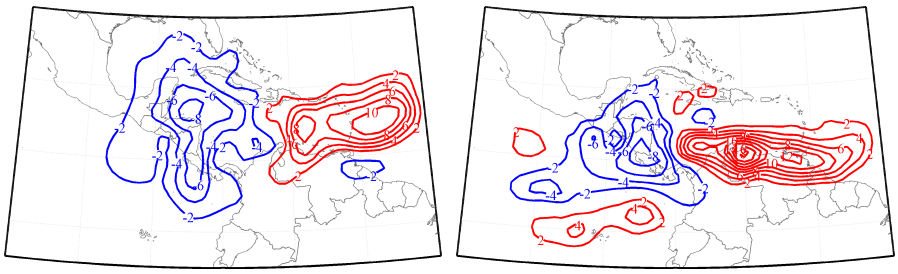

(a) - PDO January anomalies

(b) - PDO May anomalies

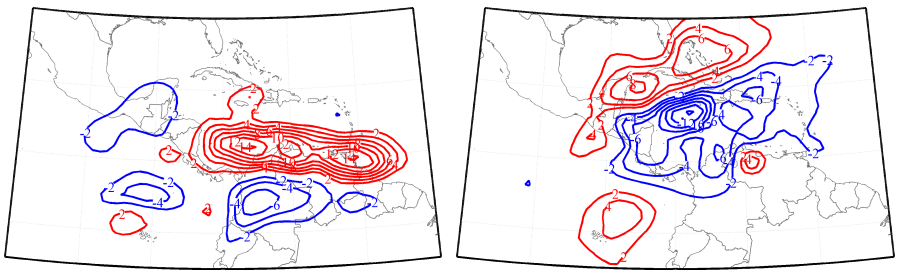

(c) - PDO June anomalies

(d) - PDO November anomalies

Figure 5.14: Differences between the positive $(E-P)^{-6}$ field for negative PDO and neutral conditions composites. Contours every 2 mm/day, red for positive anomalies and blue for negative.

The regression maps (5.15) show positive coefficients during winter all over Central America

during winter and negatives in the outern Caribbean (5.15.a). In spring, negative regression coefficients over Panama and the Venezuela Plains can be noticed. The regression map for spring is also featured by positive values over Costa Rica, Nicaragua, northern Caribbean and Costa Rican Pacific coast (5.15.b). The contrast between maximum positive regression values over NSAS and Costa Rica and the negative pattern observed over Central America can be noticed during summer (5.15.c). In autumn, the contrast more noticeable, intense positive regression coefficients for the Caribbean and NSAS while negative for the ETPac region (5.15.d). Positive coefficients for the regression of the zonal component of wind onto the PDO index is observed extending from the TNA to the Gulf of Mexico during winter (5.15.a) and over the Caribbean during spring (5.15.b). Negative coefficients for the zonal wind regression extends from the Caribbean through the ETPac in autumn (5.15.d). It is important to remark that the regression maps show the importance the PDO has particularly for NSAS. The signal of the PDO is noticed to have a remarkable effect on the distribution and intensity of the sources of moisture mainly during summer and autumn. The strong relation between the PDO and the variations of local recycling implies quite a large response of local precipitation to this mode. Moreover, the impact for the CS is observed during autumn with a very important signal over NSAS. The latter result will be more exploited in the following chapter where the contributions to precipitation are analysed. It is important to highlight that the intensification of the CS during negative PDO (see fig 5.14) is strongly related the variations in the transport of moisture through the forcing that the PDO exerts on the easterly wind flow. According to *Méndez and Magaña (2010)*, the negative PDO is associated with the weakening of the CLLJ, as the intensity of the easterly flow decreases, moisture from the CS is transported to Mesoamerica rather than to the northern region. This imply an increase in the moisture export from the CS to Central America for negative PDO during summer as shown by the moisture sources anomalies. The case of NSAS is of particular interest, from table 5.1 we follow that the CS is anti-correlated with the PDO for late spring and early summer while correlated for late summer and autumn. This contrast may be explained by variations induced by convection anomalies over the NSAS. The differences of the anomalies composites of potential velocity at 200mb, divergence wind and precipitation are shown in figures 5.16.a and 5.16.b for June and August respectively. From figure 5.16 we can observe the contrast over northern South America that may explain the effect observed in the activity of the NSAS under the influence of the PDO.

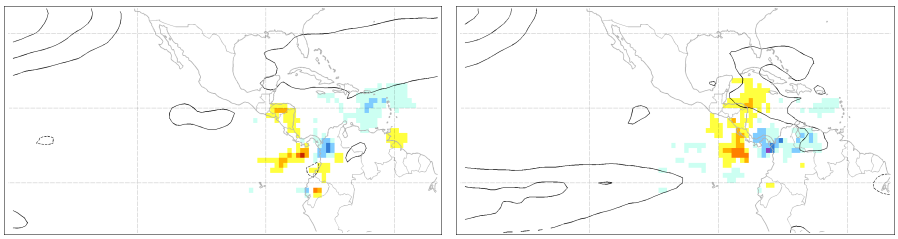

(a) Winter (b) Spring

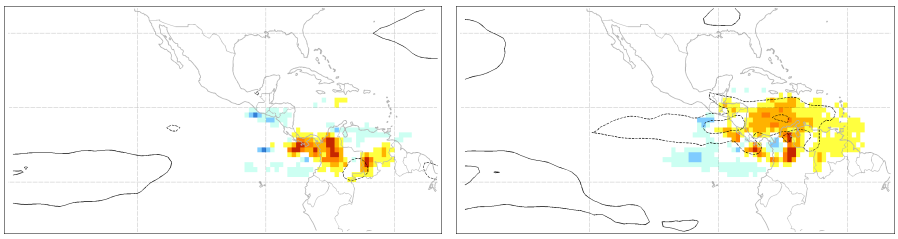

(c) Summer (d) Autumn

Figure 5.15: Regression coefficients maps for the conditional positive $(E-P)^{-6}$ field and the zonal component of the wind at 850 hPa regressed onto the PDO index.

MJO

For the defined positive MJO phase (active phase propagating over the tropical Atlantic determined using OLR), a generalised decrease of evaporation over the Caribbean takes place during winter. Increases to the east of the Lesser Antilles are more intense in February (figure 5.17.a). The decrease of evaporation is strong over Central America during March. From April to May a new intensification of the evaporative sources CAS and CS while the ETPS shows significant reductions of intensity compared to the neutral years (figure 5.17.c). In June a positive-negative pattern shows evaporation to be increased over the tropical Atlantic coast of northern South America and Colombia while decreased over the Venezuela plains (figure 5.17.e). A reduction of evaporation over the ETPS and CAS west coast is also present during June. A moderate decrease of evaporation over the Caribbean and northern Colombia occurs for July (figure 5.17.g). This with an intensification of evaporation in the Colombia-Venezuela border in August. Variations for the remainder months are very small. A marked intensification of the evaporative source over the north-westernmost Caribbean is noticed accompanied by a decrease of NSAS, the easternmost CS and the ETPS (figure 5.17.i).

In November, for the negative phase of the MJO, the confinement of the CS and the presence

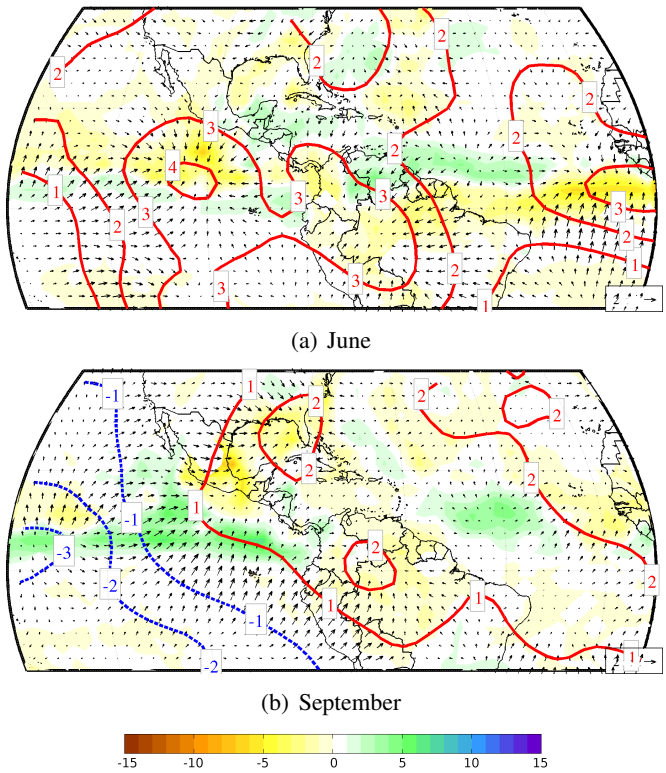

(a) June

(b) September

Figure 5.16: differences of composite anomalies of potential velocity at 200mb and precipitation. Units in $10^6 m^2 s^{-1}$ and mm/day.

of an intensified GoMS with decreases of evaporation on the borders are noticeable for December. A pattern of small negative(positive) anomalies over the Caribbean (CAS and ETPS) is observed from January to March (figure 5.17.b). The decrease of the easternmost ETPS during April is compensated by the increase of CAS, northern CS and GoMS. For May, an the western ETPS is intensified and decreased to the east. A zonal band of intensified evaporative source is visible along the southern Caribbean with a band of decreased intensity of evaporation just below in June (figure 5.17.f). During July, the band of negative anomalies is vanished and the positive band is transformed into a well defined region of intensified CS and NSAS (figure 5.17.h). Small deviations from the neutral conditions for Autumn are followed by intensified (decreased) evaporation over the Lesser (Greater) Antilles, central-southern Caribbean and ET-Pac (figure 5.17.j).

The influence of the MJO is relatively small during winter as it increases after spring, being

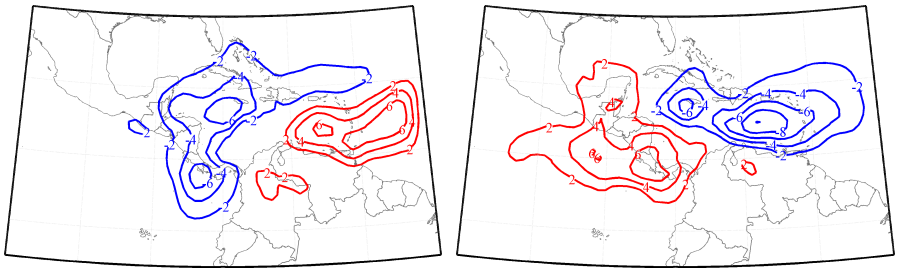

(a) + MJO February anomalies

(b) - MJO February anomalies

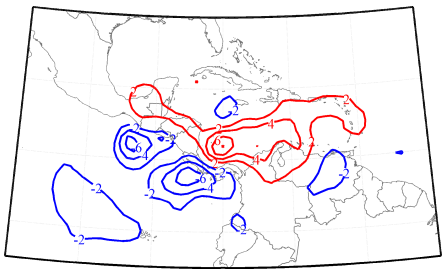

(c) + MJO May anomalies

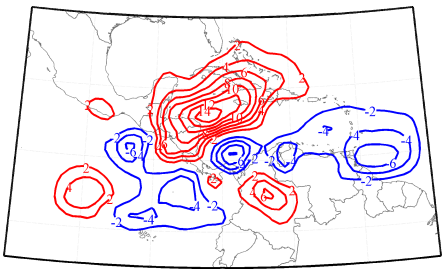

(d) - MJO May anomalies

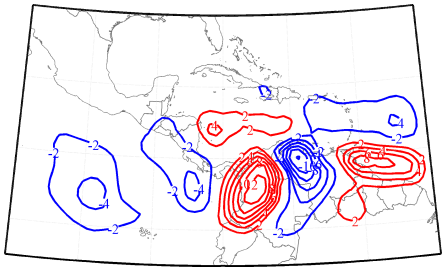

(e) + MJO June anomalies

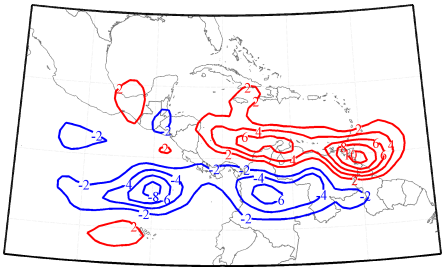

(f) - MJO June anomalies

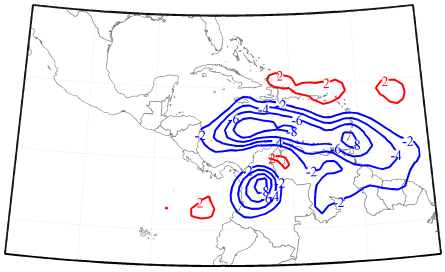

(g) + MJO July anomalies

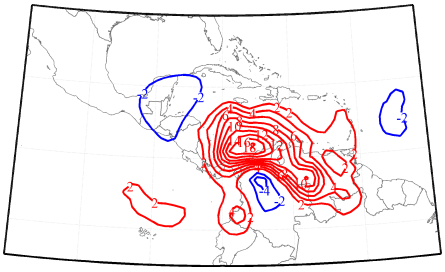

(h) - MJO July anomalies

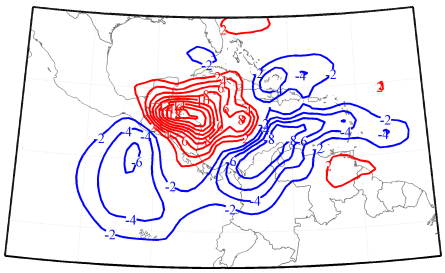

(i) + MJO November anomalies

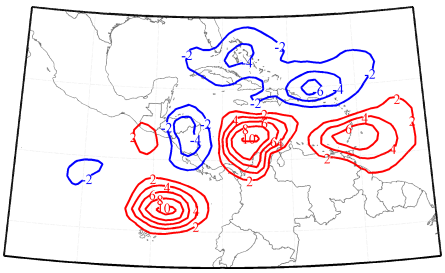

(j) - MJO November anomalies

Figure 5.17: Differences between the $(E-P)^{-6}$ field for positive MJO and neutral conditions composites (a,c,e,g,i). Contours every 2 mm/day, red for positive anomalies and blue for negative and differences between the $(E-P)^{-6}$ field for warm ENSO and neutral conditions composites. Contours every 2 mm/day, red for positive anomalies and blue for negative MJO (b,d,f,h,j). Positive MJO composites at the left and negative to the right hand side.

more intense during summer and autumn, in agreement with results by *Martin and Schumacher (2011)*. The $(E-P)^{-6}$ and zonal wind fields were regressed onto the MJO index defined in chapter 4. From the regression maps shown in figure 5.18 the positive regression coefficients are noticed to be important over the southern ETPac during spring (5.18.a) with a dislocation to the north and maximum of positive values during summer (5.18.b). Note the positive values over the Venezuela plains and northern Central America. Negative values are observed over the Pacific coast of Central America during spring (5.18.a) and over the Caribbean during summer (5.18.b) in contrast with the positive observed over the ETPac for the same season. Negative regression coefficients are also well defined over the Caribbean during autumn with the largest negative values over the Caribbean coast of Panama and northernmost part of NSAS (5.18.c) in contrast with the positive values extending from the Costa Rican Pacific coast to the west.

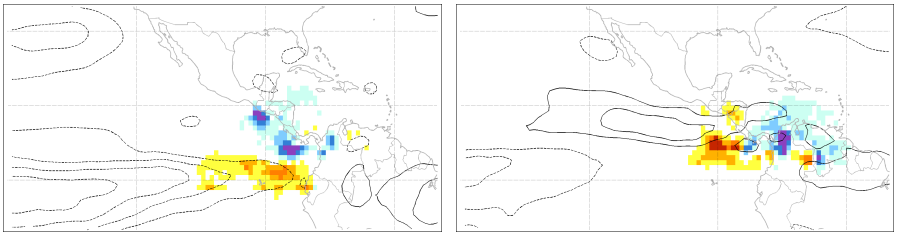

(a) Spring (b) Summer

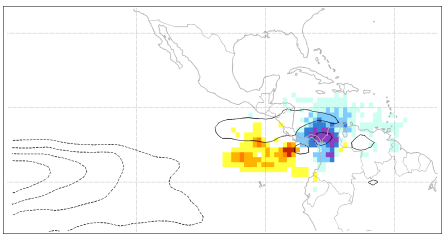

(c) Autumn

Figure 5.18: Regression coefficients maps for conditional positive $(E-P)^{-6}$ and zonal component of the wind at 850 hPa regressed onto the MJO index.

5.3 Chapter highlights

In the present chapter, the sources of moisture for precipitation over Central America were identified using the Lagrangian methodology described in chapter 4. In good agreement with previous studies, the Caribbean Sea was determined to be the main source of moisture for

Central America. Further evidence of the importance of a source over the ETPac region, as provided as in *Durán-Quesada et al. (2010)* and in agreement with findings using isotopes *(Lachniet et al., 2007)* was shown but now for a longer time span. The role of northern South America for providing moisture to Central America was determined to be of importance, as well as recycling over Central America. More detailed information on the regional hydrological cycle in comparison to previous studies was provided. The identification of a remote continental source of moisture over Northern South America that has been mentioned by *Dirmeyer and Brubaker (2006 a, b)* but in this work more detailed information abou this source was given and its importance was discussed (see also *Durán-Quesada et al., 2012*). The identified sources were found to have a well marked seasonal cycle, where month to month variations are of importance for analysing features that are lost in the averaging, as is the case of the Gulf of Mexico acting as a moisture sources. Up to almost a 70% of the variability of the sources of moisture is explained by the first 5 EOFs modes which suggests that the CS undergoes the most significant variability, both in intensity as in movement of the location of the main source region in the inner/outer Caribbean. An interesting pattern of variability of the NSAS suggests that this source has two components which are modulated in the Venezuelan by low level winds over the plains and by the convergence over the Colombian counterpart. The response to the reviewed variability modes was found to be basically the modulation of intensity but more importantly for the CS the horizontal structure of the source. The low frequency variability of the fifth EOF associated to the ETPS and NSAS is quite interesting and it would be a ideal to study the remote continental source in detail for longer time periods since for this purpose the 20 years series may be too short. Moreover, information about the response of the horizontal patterns of the composites of anomalies of positive $(E-P)^{-6}$ (used to study the sources of moisture) was provided for the analysed climate modes. The increasing $(E-P)^{-6}$ observed for warm ENSO is in good agreement with previous findings that report an association between the increasing intensity of the CLLJ and the activity of the CS for positive ENSO. Negative NAO was found to reduce the export of moisture westward, this result was hypothesized to be caused by the effect of NAO over the local instability triggered by variations in the influence of the NASH, in this regards further detailed analysis of the instabilities under NAO are still needed. The PDO was determined to be strongly linked to variations in the activity of the NSAS as a response of convection anomalies over South America, this result opens an interesting problem that may be studies with detail.

6 Relative contributions to precipitation

The identification of the sources of moisture in the previous chapter allows to determine the regions that play a role as sources of moisture for Central America. The pattern of the annual cycle describes the variations of the evaporative sources of moisture as a result of the seasonal mean conditions. This is a good approximation to identify the origin of moisture that arrives to a region. Moreover, the Lagrangian trajectories allow a more specific analysis of the relationship between the moisture available from any source and precipitation. Here we provide an estimation of the contribution from the sources to precipitation on Central America. This chapter presents the seasonal mean $(E - P)^6$ fields from tracking for the identified sources of moisture. The contributions to precipitation over Central America are analysed. Finally, variability of the contributions is analysed along section and the response of the contributions to the influence of the main variability modes is explained.

6.1 Estimation of moisture lost over Central America

From the identification of sources of moisture, five main source regions were found to provide moisture that precipitates over continental Central America. The Caribbean Sea (CS), the Gulf of Mexico (GoMS), Eastern Tropical Pacific (ETPS), Northern South America (NSAS) and local recycling over Central America (CAS), see figure 6.1. Note from figure 6.1 that the

region assigned to the ETPS does not exactly match the extension of the evaporative source observed in figures 5.2 and 5.3. However, this selection for the ETPS was made in order to consider not only the climatological mean horizontal extension of the source but to account for the monthly variations of this source as well as its internannual variability, as detailed in section 5.2 chapter 5. The selection made for the ETPS allows the consideration of all possible meridional dislocations of the source that may be lost in the averaging of the fields.

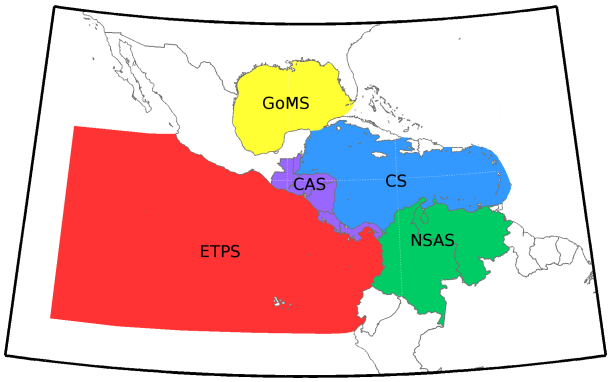

Figure 6.1: Representation of the sources of moisture for continental Central America identified in the previous chapter. Note that the area comprised by the ETPS is more extended in comparison with the regions where the positive values of the conditional $(E-P)^{-6}$ field were found, this in order to account for the meridional movements of the source of moisture over this location which varies month to month.

When the air particles are allowed to move forward in time from a source region, the (E-P) estimation provide further information on the destination where moisture is lost. Integrates of $(E-P)^6$ were computed from the sources (as we are interested only in precipitation associated term, only negative values are shown and the sign was inverted to represent precipitation as a positive term). From the seasonal means of the $(E-P)^6$ field for the Caribbean Sea it can be observed that most of its moisture precipitates remotely over CA. During winter, the major contributions from the Caribbean Sea are to precipitation over the Gulf of Mexico and the ETPac region, under the precipitation regime of the ITCZ (figure 6.2.a). During spring, precipitation originated from Caribbean air masses falls over Central America, the contributions do not go further 100W (figure 6.2.b). This increases precipitation over Central America and western Colombia, in agreement with the observed peak of precipitation over Central America. In the same figure, enhancement of precipitation due to Caribbean moisture can be noticed

over northern Central America (mainly Guatemala). The intensification of precipitation associated with moisture from the Caribbean is larger in summer. It increases over eastern Mexico and southern Central America and larger $(E - P)^6$ values are found west of Costa Rica and south-westernmost Mexico (figure 6.2.c). The decrease of precipitation is associated with the contributions from the CS over northern Central America and western Mexico. This pattern is similar to that of zonal winds, with the locations in which $(E - P)^6$ is larger being almost the same that the regions where the wind enhanced by the presence of topographic gaps. During this period, contributions from the CS to precipitation over the Pacific side of the topographic gaps is larger than 35 mm/day while contributions to precipitation over the Caribbean Sea roughly reach 5 mm/day. This in good agreement with the suppression of precipitation over the Caribbean during summer, as known from previous works (see e.g. *Magaña et al., 1999*). Contributions to precipitation over Central America are limited to the south, however it can be observed how the major part of moisture is lost over the ETPac. In autumn, the intensity of the negative values of $(E - P)^6$ has decreased in the north, but it is strongly intensified over southernmost Central America (figure 6.2.d). The export of moisture from the Caribbean Sea that precipitates over Central America explains a good part of the differences observed in the precipitation regime of Central America. Up to 40 mm/day are lost over southern Central America while a maximum of 15 mm/day are lost over the northern part of Central America, in agreement with a drier northern Central America compared to the south. It is also important to highlight that the ITCZ is located farther south, which is an important factor to determine the distribution of precipitation.

As for the Caribbean Sea, the $(E - P)^6$ fields were computed for the other component of the IAS, the Gulf of Mexico. Most of the moisture from this source is lost over the Great Plains and northeastern Mexico. The pattern observed for autumn, winter and spring is quite similar, with larger $(E - P)^6$ values (up to 15 mm/day) for spring. It is important to notice that during autumn, some moisture is lost over southern Mexico, crossing along Tehuantepec and reaching the Pacific side (figure 6.3.a). Moisture from this source lost over Central America is basically limited to the north. In summer the negative values of the $(E - P)^6$ field present an extended horizontal structure with a strong presence over Mexico in comparison to the other seasons (figure 6.3.b). These contributions from moisture of the Gulf of Mexico that precipitates over Mexico is important since moisture lost over this region account later to feed the NAM that is

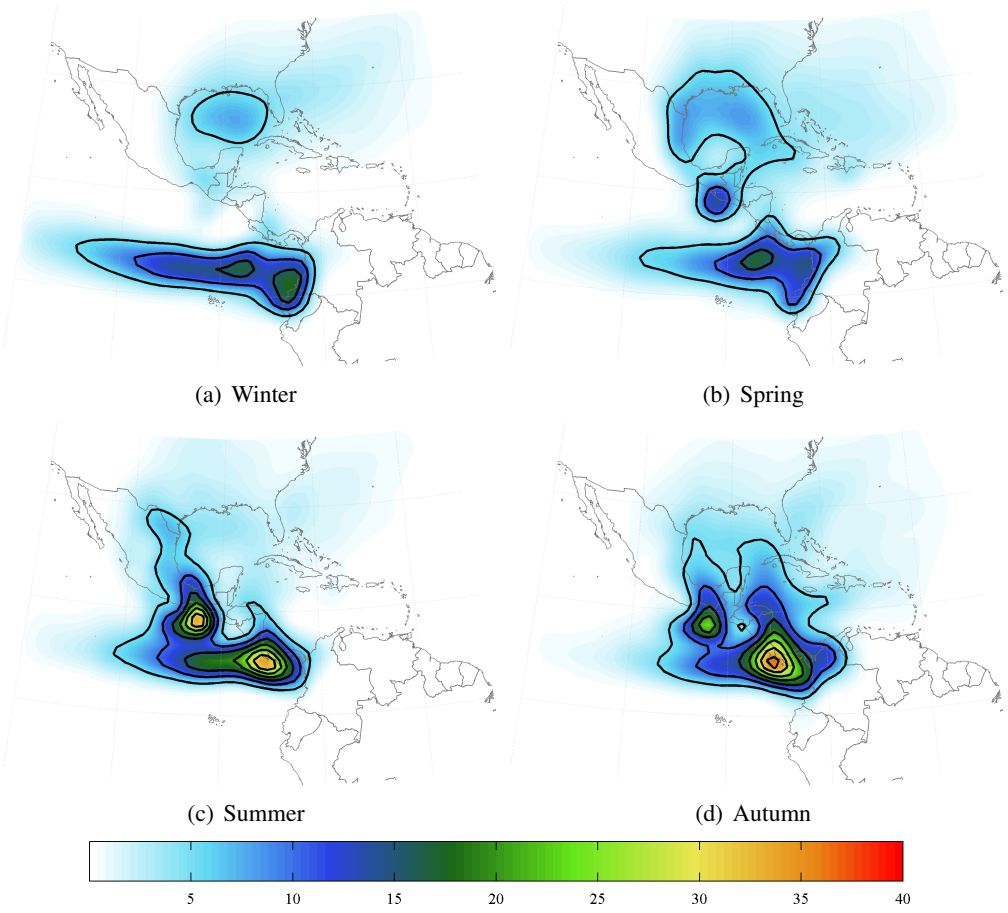

Figure 6.2: Average six days integrates of the conditional $(E - P)$ field computed forward from the Caribbean Sea for a) Winter, b) Spring, c) Summer and d) Autumn. Larger positive values in yellow and orange show the regions where precipitation associated with moisture from the CS is larger. Values in mm/day and contours every 5 mm/day starting at 5 mm/day.

active during this period[6].

Similar to the CS and GoM, seasonal $(E - P)$[6] field for ETPS is shown in figure 6.4. There is no moisture from the ETPS being lost on average over Central America during winter, moisture is mainly lost along a narrow band of the ITCZ west of 120W. In spring the pattern is similar to that of winter, with larger moisture losses near the coastal region and over north-easternmost Central America (Guatemala) (figure 6.4.a). During summer a strong increase in the losses of moisture west of Central is maximum near 95W. Moisture from the ETPS is lost in considerably important amounts over southern and northernmost Central America while little or no moisture

[6]see further details for the sources of moisture for the NAM in Appendix E

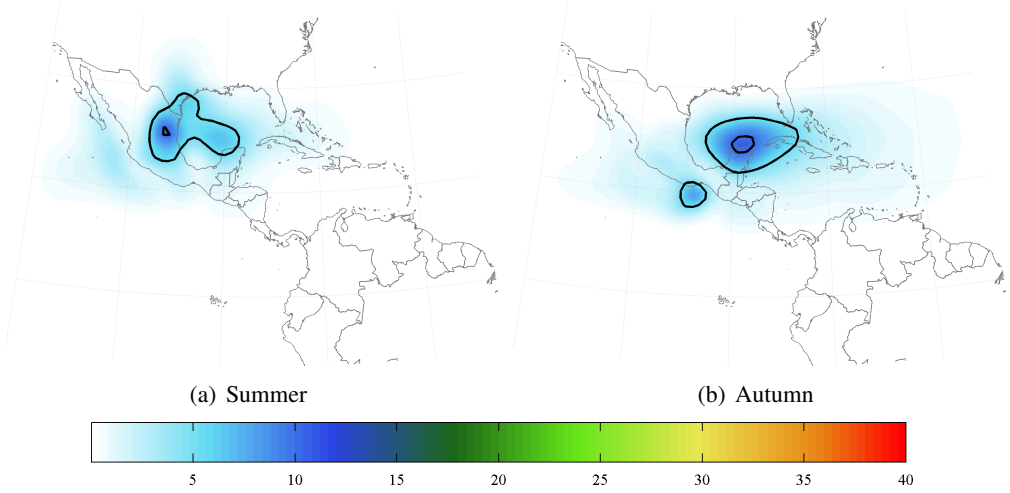

Figure 6.3: Average six days integrates of the conditional $(E - P)$ field computed forward from the Gulf of Mexico for a) Summer and b) Autumn. Larger positive values are smaller than those found for the CS, most of the moisture from the Gulf of Mexico contributes to precipitation over the same Gulf, however during Summer an important component of precipitation associated with moisture inflow from this source can be noticed to be maxima over eastern Mexico, which is of importance and may enhance the transport of moisture during the active period of the NAMS. Values in mm/day and contours every 5 mm/day starting at 5 mm/day.

is lost over Honduras and Nicaragua. A similar pattern but much more intensified in magnitude is observed for autumn and with more influence over Nicaragua than in the previous months (figure 6.4.b).

In the case of the results for the $(E - P)^6$ fields for the continental regions, results for CAS suggests that precipitation is reduced during winter. Few moisture is available due to recycling because of a minimum of precipitation. In spring, moisture from CAS is lost over the Pacific and in major amounts over the west coasts of Guatemala and El Salvador. A similar pattern is found for summer, but with the amounts of precipitation lost over these regions larger and some moisture is also lost over southernmost Central America (figure 6.5.a)[1]. Contributions are reduced during autumn. Moisture from NSAS is significantly larger than from local recycling. However, large amounts of moisture from NSAS are lost over the Magdalena and Orinoco river basins. These two basins are the main sink of moisture from the north of South America and only the remaining moisture is able to be transported and precipitate over Central America. The pattern of $(E - P)^6$ field for NSAS shows the smallest contributions to precipitation over Central America during winter and the largest during summer (6.5.b) and autumn. Note

[1] remember the heterogeneous precipitation pattern over Central America that allows the MSD to co-exist with intense precipitation in southernmost CA

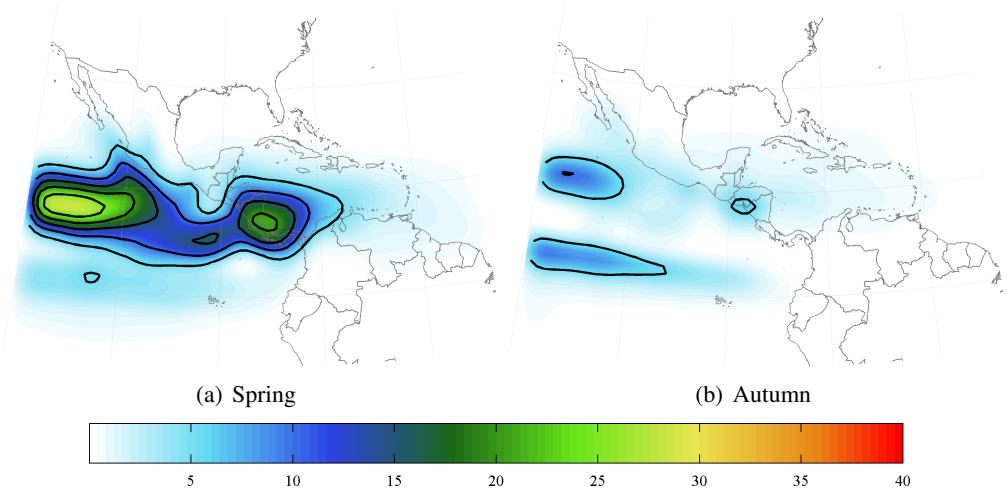

Figure 6.4: Average six days integrates of the conditional $(E-P)$ field computed forward from the ETPac region for a) Spring and b) SUmmer . Values in mm/day and contours every 5 mm/day starting at 5 mm/day. Precipitation associated with moisture transported from the ETPS is considerably reduced during Autumn (b) in the vicinity of Central America. However, during Spring (a) strong precipitation due to the presence of the ITCZ is noticed with a significant core of precipitation over Central America. During Autumn, this core is small and constrained to the Pacific coast of northern Central America.

however, that during summer most of the moisture (up to 30 mm/day) from NSAS is lost over the northernmost part of Colombia and southern Panama.

6.2 Relative contributions to precipitation from the moisture sources

By studying the changes of moisture of the air particles from the source to the receptor region, an estimation of the contribution from the source to precipitation over the target region can be obtained, following the reasoning of *Wernli (1997)* and *Stohl and James (2004)*, despite the disadvantages of this approximation such as simplicity as pointed out by *Sodemann et al. (2008)*. Contributions to precipitation were computed using equation 4.4 after identifying the air particles that left precipitation over continental Central America and classifying their origin. The mean annual cycle of the contributions is plotted in figure 6.6.a as well as their sum and as a reference quantity, the mean precipitation from CMAP. It must be noted that even when the sum of the contributions follow the pattern of CMAP precipitation, interpretation must be cautious. From figure 6.6.a, differences among the sources contributions suggest that the importance of each source to precipitation depends on its activity. Contributions from the CS are the largest, contributions from the ETPS are quite uniform after april with a small maximum

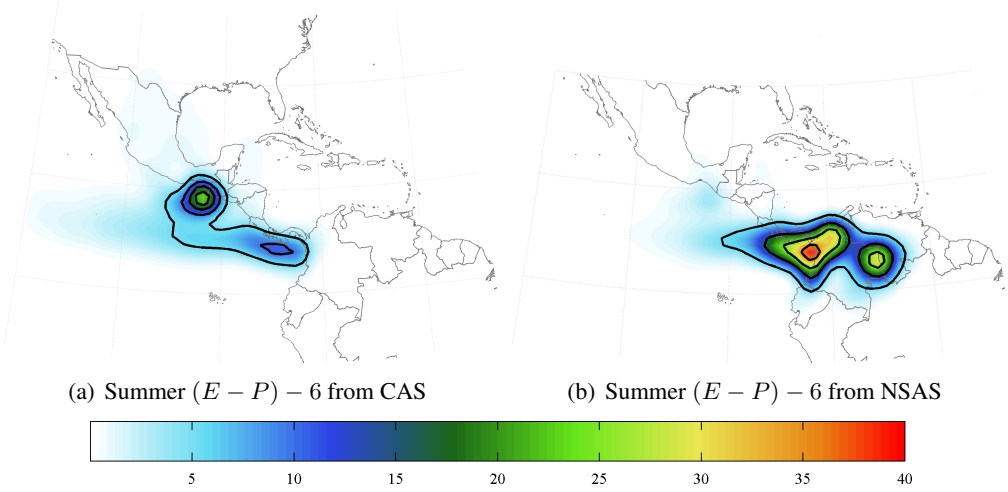

(a) Summer $(E - P) - 6$ from CAS (b) Summer $(E - P) - 6$ from NSAS

Figure 6.5: Average six days integrates of the conditional $(E - P)$ field computed forward for Summer from a) continental Central America and b) Northern of South America. Values in mm/day and contours every 5 mm/day starting at 5 mm/day. Moisture from CAS contributes to regional precipitation due to recycling with the largest contributions over southern Central America and the Pacific coast of Northern Central America and Mexico. Moisture from NSAS is very large during Summer with the largest contributions over the Venezuelan Plains and Northern Colombia as recycling of moisture and with an important contribution over Southernmost Central America.

in summer. Recycling has a large contribution, following the pattern of precipitation while the contributions from NSAS exhibit a single peak during summer. This implies that this remote source is of a great importance to conserve the bimodal pattern of precipitation over Central America. When the source is not active, precipitation may be reduced unless the other sources experience an intensification. The percentage distribution of the contributions is summarised in figure 6.6.b, from which the relevance of the sources can be noticed. This percentage of total relative contributions attributed to each source shows clearly the dominance of moisture coming from the IAS (GoM + Caribbean) all year round. The pattern of the contributions from NSAS represents quite well the pattern of precipitation over northern SA. The increase of the contributions to precipitation during summer are a result of the reduction of precipitation over northern South America. Therefore evaporation and associated availability of moisture transported by local winds increases too.

The increase in the contributions from the CS source during autumn is in good agreement with the rainiest season in the Caribbean side of Central America *(Magaña et al., 1999)*. Moreover, the result reflects the importance of cyclonic systems development in the tropical Atlantic and Caribbean for regional precipitation during this part of the year. Relative contributions from

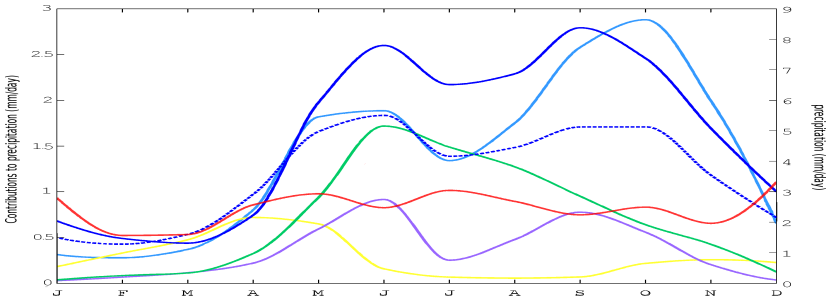

(a) Annual cycle of contributions to precipitation

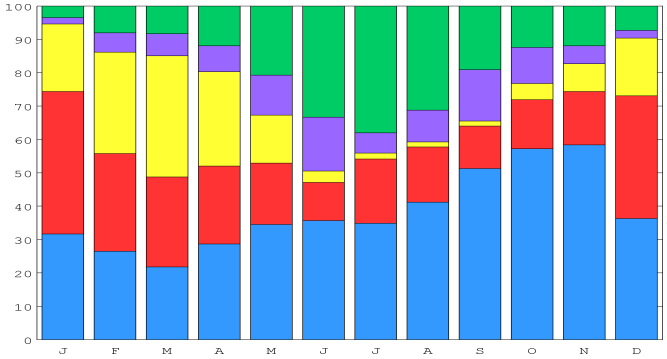

(b) Distribution of contributions to precipitation

Figure 6.6: a) Mean annual cycle of CMAP precipitation averaged over Central America (dark blue) and sum of the contributions from the individual sources (light blue) (right axis) and relative contributions of the sources of moisture to precipitation (in mm/day) from each source of moisture following the color code of figure 6.1 b) Distribution of the composition of the total estimated of contributions to precipitation from the identified sources of moisture. Note the bimodal distribution of the sum of the relative contributions to precipitation in good agreement with the annual cycle of precipitation from CMAP. The distribution of the contributions to precipitation show the dominance of the oceanic sources of moisture with an important component of the contribution of the NSAS that is developed during Summer.

NSAS can account as a secondary source of moisture during summer due to its intensity, result that until now has not been addressed.

6.3 Response of the contributions from the moisture sources using observational data

Due the features of the analysis region, a quantification of the precipitation is not straightforward and results must be interpreted with caution. The heterogeneity of precipitation patterns over Central America suggests that any evaluation or validation of precipitation must consider this distribution. For that reason, to evaluate the estimations of precipitation, selected subregions of the analysis domain are presented in order to a) deal with the heterogeneous

distribution of precipitation and b) to avoid comparing results with observations over regions from which there is no information (Guatemala, Honduras and Nicaragua). Estimates of 'relative' contributions to precipitation over Belize, El Salvador and the region formed by Costa Rica and Panama are computed for each source. The individual contributions were added to obtain a total of relative contributions to precipitation for each subregion. Figure 6.7 shows the correlation between the estimated contributions to precipitation and observed precipitation for a) Belize, b) Honduras and c) Costa Rica and Panama.

Estimated precipitation from the Lagrangian approach is biased compared to observations in the indicated regions by 23-46% which may be considered to be a high bias. However it is important to remember that the value of the estimated contributions to precipitation accounts for precipitation due to moisture transport from the remote sources and local recycling and not to total observed precipitation. Note that larger bias is that for the location with less number of stations to the northern part of Central America. In addition, a comparison made between estimates from the approach of precipitation over Central America and precipitation from CMAP results in a bias of 29% which could be considered as a reasonably good agreement between estimated and observed precipitation taking into account the difficulties of estimating with more accuracy precipitation in this particular tropical location. Anyway, in order to be more correct in terms of the discussions, we will not refer the estimates as of precipitation but as to relative contributions to precipitation since we are aware that the approximation does not consider further processes that may be of importance for precipitation as microphysical processes.

6.4 Long term time series of contributions to precipitation and associated variability

Once the mean annual cycle is determined, the variations that occur in time are important. Figure 6.8 shows the time series for monthly mean of a) CMAP precipitation and contributions from the b) CS, c) ETPS, d) GoM, e) CAS and f) NSAS. The CS was found to be the most important of the sources in terms of contribution to precipitation. By comparing a and b, one can find how some of the peaks of variations correspond for both time series (end of 1988 and 1998). However there are some cases in which variations do not present any immediate correspondence (1982, 1997). Conversely, correspondence is found between precipitation and

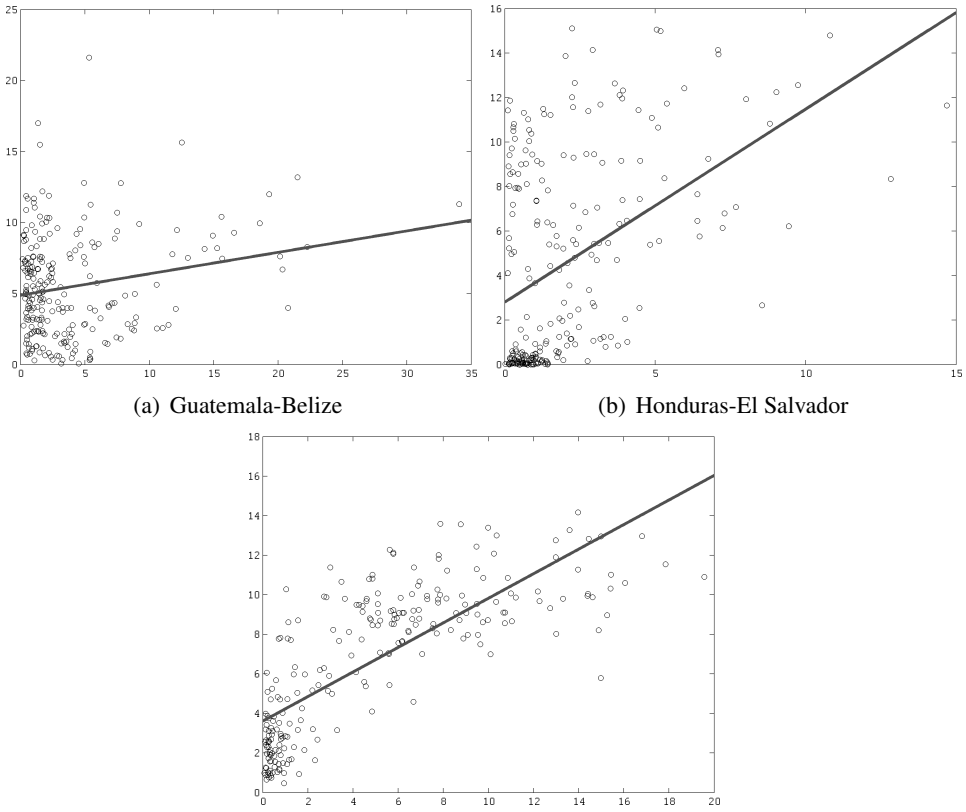

(a) Guatemala-Belize (b) Honduras-El Salvador

(c) Costa Rica-Panama

Figure 6.7: Correlations between observed precipitation estimated as the average of the selected rain gauges for different locations of Central America and the relative contributions to precipitation estimated from the identified sources of moisture for a) Belize, b) El Salvador and c) Costa Rica and Panama. The corresponding linear fits are shown by the lines, the largest r value is found for the region of CRP, notice this result is biased by the amount of rain gauges as their distribution over northern Central America is poorly homogeneous. Observed precipitation in the y-axis and sum of the estimated contributions to precipitation from the sources in the x-axis.

contributions from other sources. Strong variations for the twenty year time series is found for years 1987-1988, 1995, 1997-1999 that are identified as strong ENSO events.

The mean picture of the variability

The EOF patterns in previous chapter present a strong relation between the zonal wind with the well defined structure of the CS. Variations in the spatial patterns of the evaporative sources over northern South America and the ETPac region were observed to be important. From the variations of the evaporative sources of moisture, variations in the contributions from those sources to precipitation is expected. In the previous section, an evaluation of the relative con-

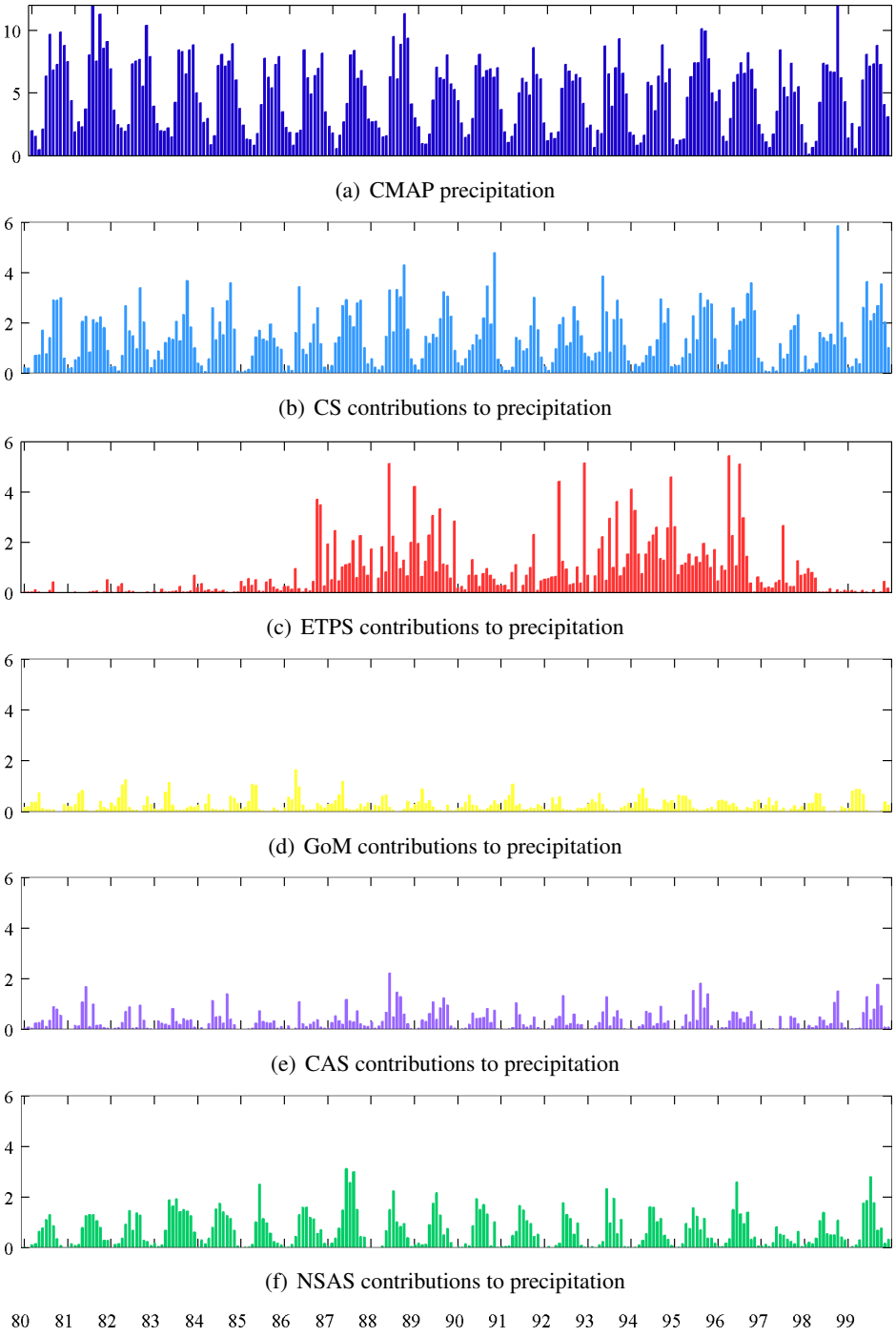

Figure 6.8: a) Time series of monthly CMAP precipitation averaged over Central America for the 1980-1999 period, estimates of relative contributions to precipitation over Central America from a) CS, b) ETPS, c) GoMS, d) CAS and d) NSAS as estimated from the Lagrangian approach, units in mm/day.

tributions to precipitation estimated in contrast with observed data was presented. In order to find the temporal band of larger variations of the contributions to precipitation from the sources, wavelet analysis is applied for the time series once the annual cycle was removed. Wavelet analysis was used on the basis that it enables the reconstruction of the time evolution of the main oscillating components of the time series. Modulus of the wavelet transform are shown in figures 6.9 (a,d,g,j,m). The average wavelet power spectrum for the contributions from the individual sources, similar to the Fourier spectrum, is shown in figures 6.9 (b,e,h,k,n). From the wavelet power spectrum, large variability is found for all the sources except for the GoMS (not significant at the 95% confidence level). The average wavelet power spectrum (significance marked by the dashed line) shows that for contributions from the CS the dominance of variability is on the two years band and that important shifts occur for the one and four years band too. In the case of the ETPS, the dominant period is the 4-8 years band and significant shifts are noticed for the 2-4 and 8-16 years bands. The same pattern of periodicity of variability for the contributions from the CS is found for the contributions from CAS. For NSAS, dominant periods of variability are found for the 2 and 8 years band with further important shifts for 6 and 1.5 years. It is also important to note the irregular pattern of the ETPS, which presents a marked minimum 1980 and 1986 and reduces again 1991 and 1998.

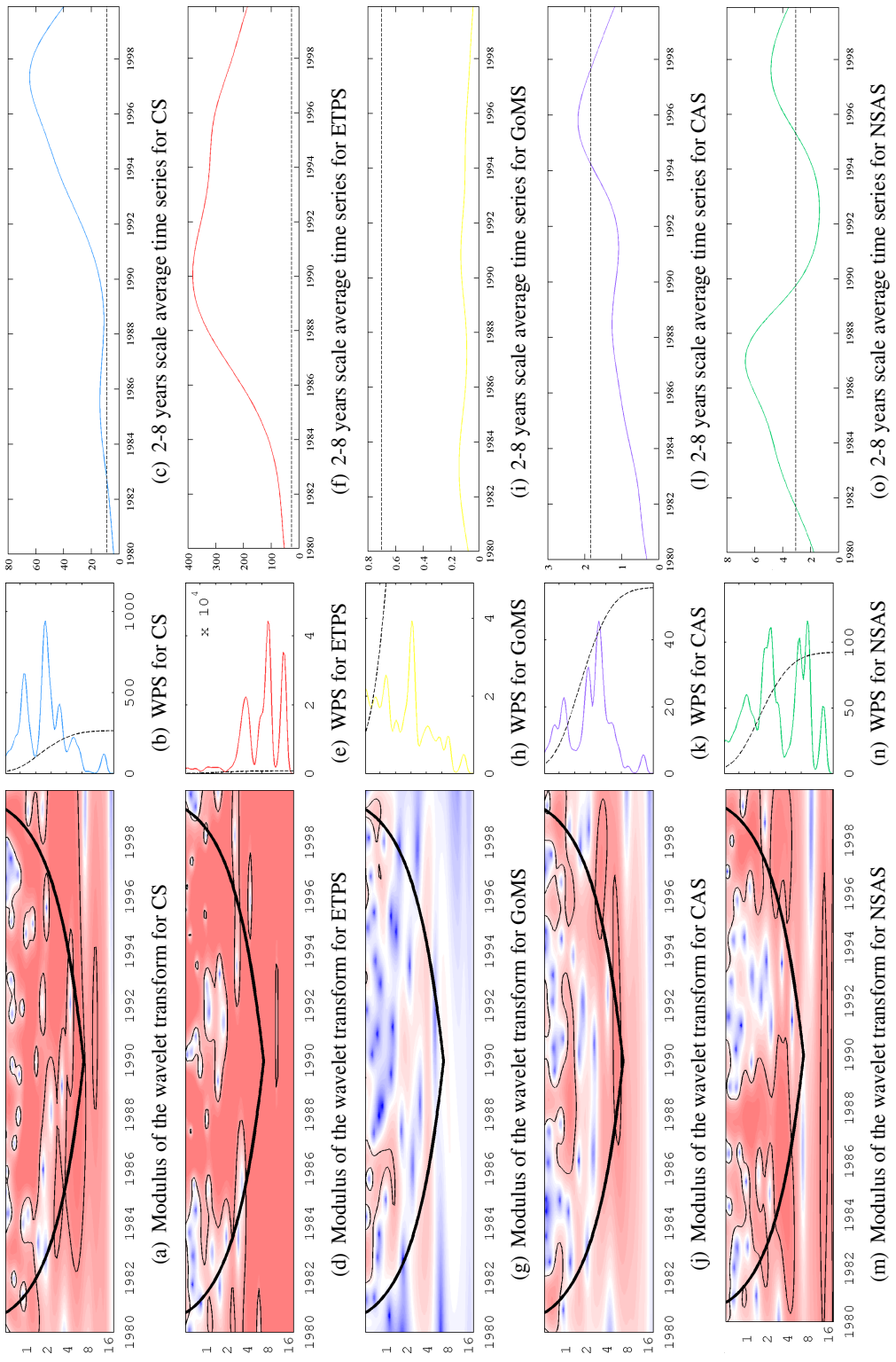

Figure 6.9: Modulus of the wavelet power spectrum for the time series the relative contributions to precipitation over Central America from a) CS, d) ETPS, g) GoMS, j) CAS and m) NSAS, the cone of influence is marked by a thick black line and the contours significant at 95% percent are enclosed by a black contour is indicated for the modulus of the wavelet transform. Average wavelet power spectrum for the same time series: b) CS, e) ETPS, h) GoMS, k) CAS and n) NSAS. Two- eight years average time series (variance) for the same time series: c) CS, f) ETPS, i) GoMS, l) CAS and o) NSAS, 95% significance level is indicated with black dotted line for the average wavelet power spectrum and 2-8 years scale average time series.

In general, the 2-8 years band was found to be the one in which the largest variations occurred, so the 2-8 years scale average time series (variance) were computed. Results from figures 6.8 (c,f,i,l,o) indicate the years at which variance of the anomalies of the contributions to precipitation peak. The CS exhibits a large peak centred in 1990 and 1996. Variance is below the significance level for the GoM and a peak centred in 1996 is noticed for the contributions from CAS. The contributions from northern South America peak with larger intensity centred in 1987 and a secondary maximum by 1997. These results remark the result obtained for the spatial structure of the sources shown in previous chapter, which presented an important variability mainly associated to ENSO. It is also important to notice the suggestion of a low frequency band of variability for the contributions from ETPS and NSAS. Even when the time series may be not long enough, the results present what can be considered as evidence of a strong forcing of the PDO in the contributions to precipitation from these two sources.

Evolution of the anomalies of the contributions to precipitation

From the wavelet analysis, the major variability is centred in the 2-8 years band, in which ENSO is the leading mode. However, we can not determine directly which seasons are more sensitive to interannual variability. The Hovmoller plot for the anomalies of contributions to precipitation for each source (fig 6.10) provides further details of temporal variability. The CS, with larger variability patterns show increases for the first half of the year during 1983, 1990 and 1993 with marked decreases for 1984-1988, 1992 and 1997-2000. Even more interesting is the anomalous increase of the contributions during summer for 1982 and 1998-2000. Negative anomalies are observed in 1987 for the contributions from the ETPS, and the patterns of strong positive anomalies is similar to that of the CS but much more intense. Contributions experience a marked strengthening in autumn 1986, summer 1989, summer 1993, winter 1995 and spring-summer 1997. Few variations of importance were noticed for the GoMS (not plotted).
In the case of CAS, important increases are highlighted for 1987-1989 and summer 1999, in agreement with an increase of precipitation that may enhance the recycling over the region. Notice however, that for the other sources any increase is found for this period. This implies that the increments of contributions to precipitation and precipitation itself were probably, for this period, locally induced. A more complex pattern is described by the anomalies of the contributions from NSAS. An increase in the contributions to precipitation starts in summer 1983 and extends through summer 1984. A similar increase does occur two years earlier with

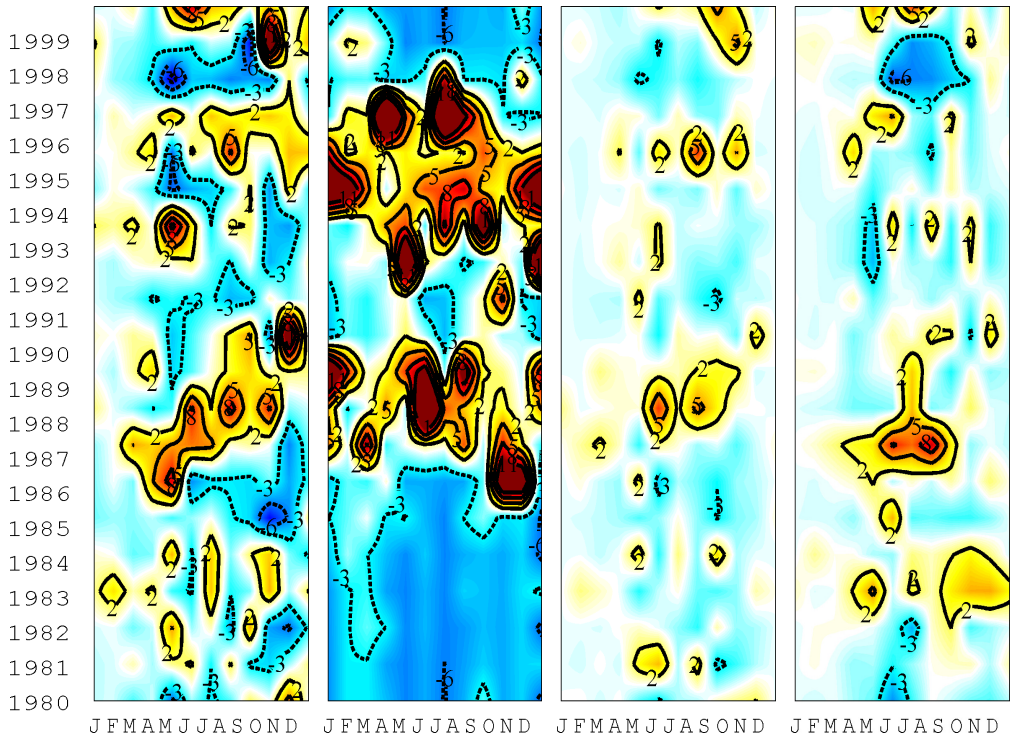

(a) CS (b) ETPS (c) CAS (d) NSAS

Figure 6.10: Hovmoller plot for the anomalies of the relative contributions to precipitation from the identified sources: a) CS, b) ETPS, c) CAS and d) NSAS Positive contours every 3 mm/day starting in 2 mm/day and for negative every 3 mm/day starting in 3 mm/day. Values for the contributions from the GoMS are not shown as are considerably small compared to the contributions from the other sources and variability was found to be under the confidence level.

an intensification at the beginning of summer but not for the following year. For winter, the contributions from this source experience a decrease during 1993 and for 1998-1999 a marked intensification occurs for winter while a decrease for summer. Note the intense variability for the contributions from the ETPS, which present a tendency to occur before the onset of a warm El Niño event.

6.5 Variations under the influence of main variability modes

The Hovmoller plot shown in figure 6.10 evidences the structure of the time variability of the intensity of the contributions to precipitation from the sources of moisture. The patterns described for determined years suggest the influence of determined modes of variability, as described previously for the spatial patterns of the sources of moisture in chapter 5. To evaluate

to which extent the variability modes trigger the variability of the contributions to precipitation, the percent composition of the total of contributions was estimated. Monthly composites for each mode for positive, neutral and negative conditions were computed. The months for which a significant relation was found between the climate indices and the activity of the moisture sources (see chapter 5) are shown.

Warm ENSO is associated with the increase in the contributions from the CS, and the intensification of local recycling at the end of winter (see fig 6.11.a). During spring, the ETPS shows a pattern that is reversed if compared to winter. In summer, warm (cold) ENSO is related to the increase (decrease) of the intensity of the contributions from the ETPS. Note that the contributions from the GoMS tend to compensante those of the CS. This result suggests that variations in precipitation respond to modifications of the transport patterns, probably due to the response of the CLLJ to ENSO (a more detailed discussion will be provided in chapter 8). The opposite pattern is observed for the contributions from NSAS (6.11.b). During summer, the difference observed between ENSO phases in the variations of the distribution of contributions to precipitation compared to the neutral condition, reflects the known distribution of precipitation. The increase of local recycling during cold ENSO is in very good agreement with the intensification of precipitation for this phase and the contrast with the drier conditions known to occur for warm ENSO.

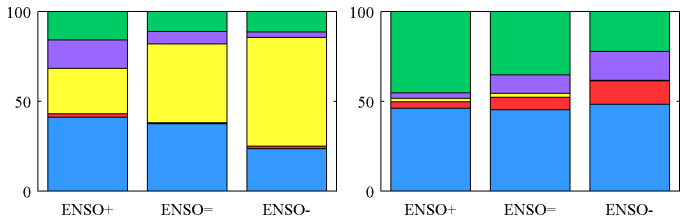

(a) February (b) August

Figure 6.11: Distribution (percentage) of the monthly mean composites of the relative contributions to precipitation from the sources based on composites for positive, negative and neutral ENSO. Sky blue for the CS, red for the ETPS, yellow for the GoMS, purple for the CAS (local recycling) and green for the NSAS.

Under the influence of NAO, the CS experiences decreases for the negative phase during winter (6.12.a) and part of summer (6.12.c) while increases during spring (6.12.b). The magnitude of the contributions from GoMS is reduced for this phase during winter (6.12.a). Large variations in the intensity of the contributions from the ETPS are noticed for this mode. A marked increases in the contributions from this sources during is linked to the negative phase. The

other sources experiences small variations, most of them associated to the negative phase. The increase of the CLLJ associated with positive NAO suggests an intensification of the CS, this may result in a pattern of decrease in the contributions from the CS from positive to negative NAO as shown in figures 6.12.a and 6.12.c. However during April (6.12.b) we do not observed the same pattern and one may explore which mechanisms may be responsible for that. The contributions from the ETPS is larger for negative NAO, this result is explained by the increase in the occurrences of South West monsoon flows from the Pacific allowed by a decreased CLLJ.

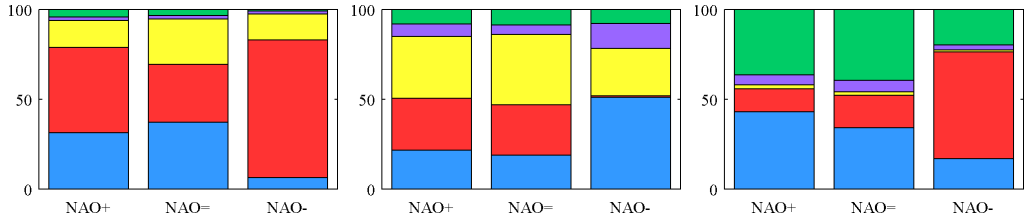

(a) February (b) April (c) August

Figure 6.12: Distribution of the monthly mean composites of the relative contributions to precipitation from the sources based on composites for positive, negative and neutral NAO. Sky blue for the CS, red for the ETPS, yellow for the GoMS, purple for the CAS (local recycling) and green for the NSAS.

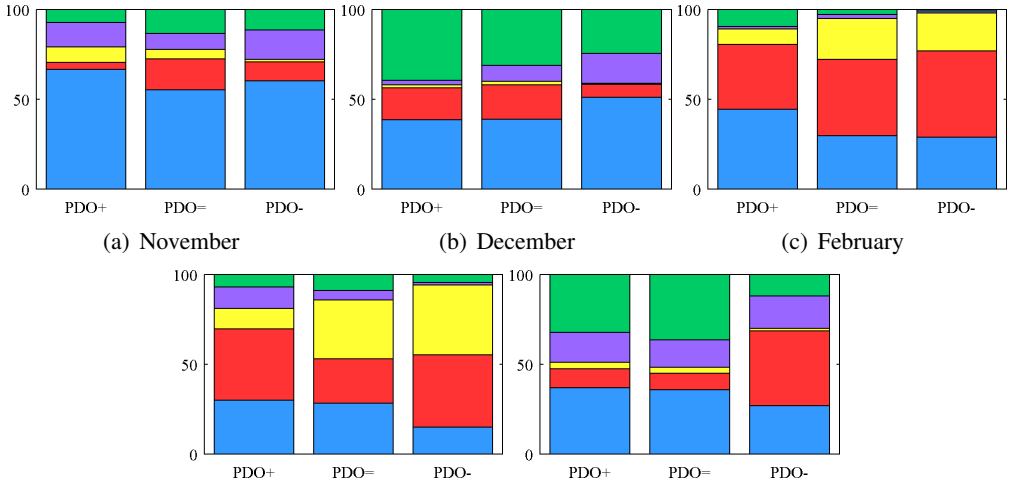

(a) November (b) December (c) February

(d) March (e) July

Figure 6.13: Distribution of the monthly mean composites of the relative contributions to precipitation from the sources based on composites for positive, negative and neutral PDO conditions. Sky blue for the CS, red for the ETPS, yellow for the GoMS, purple for the CAS (local recycling) and green for the NSAS.

In the case of the PDO, variations tend to be more noticeable for winter and spring. For

November, positive PDO enhances the intensification of the contributions from NSAS with the further reduction of the contributions from local recycling over Central America, then a reduction of CAS (6.13.a). During December, a decrease of the contributions from the CS and ETPS is compensated by the increase of the contributions from the GoMS (6.13.b).The contributions from CS (ETPS) increases in positive (negative) PDO for late winter (6.13.c). At the beginning of spring, positive PDO seems to favour the increase of contributions from the Gulf of Mexico (6.13.d). Few variations are found for the remaining months and is also important to remark that negative PDO favours a more active ETPS in terms of contributions during July (6.13.e).

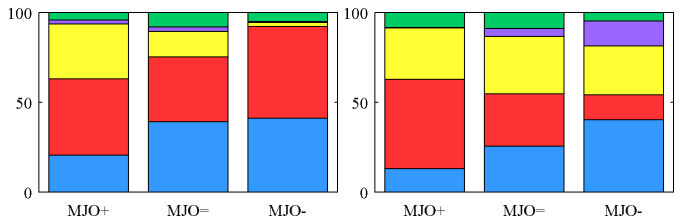

(a) January (b) March

Figure 6.14: Distribution of the monthly mean composites of the relative contributions to precipitation from the sources based on composites for positive, negative and neutral MJO. Sky blue for the CS, red for the ETPS, yellow for the GoMS, purple for the CAS (local recycling) and green for the NSAS.

Under the influence of the MJO, a similar case as for NAO occurs, with the main variations being more noticeable during winter. In general, MJO negative (positive) phase is related with the decrease (increase) of contributions from the Gulf of Mexico during winter (fig 6.14.a). The reduction of the contributions from the GoMS is compensated by the intensification of the contributions from the ETPS and CS. At the end of winter, the negative phase of MJO seems to favour the increase of local recycling compared to the neutral conditions and the positive phase, for which recycling is reduced. Notice that the CS is reduced (increased) for positive (negative) MJO, in contrast with the opposite behaviour of ETPS (fig 6.14.b). Some less significant variations are found for spring time and the remaining months. Variations in the contributions attributed to the presence of the MJO have to do with the enhancement of convection in the region as well as with the tropical cyclone activity.

The analysis of the response to the variability modes of the estimates of precipitation due to transport and recycling with the Lagrangian approach show a good agreement with previous

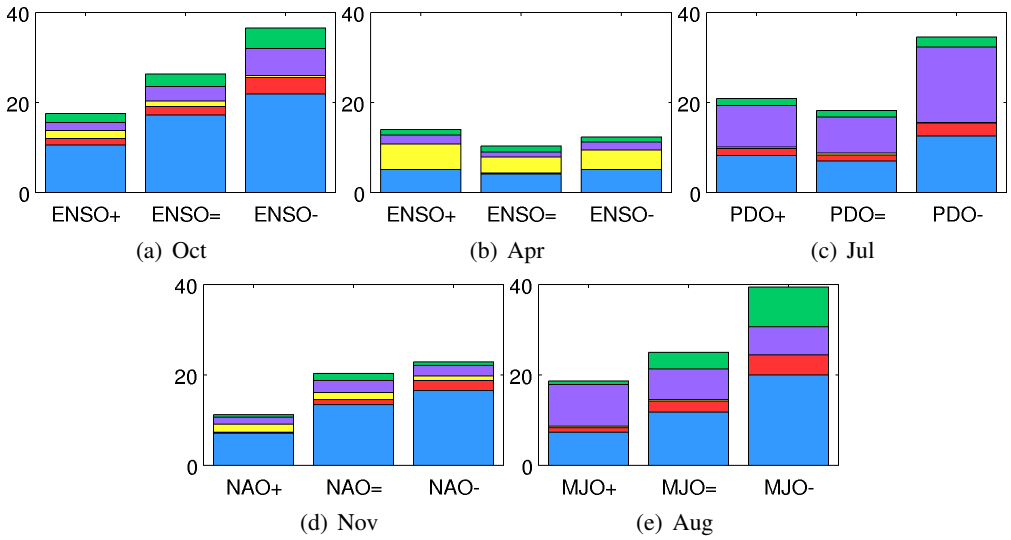

Figure 6.15: Estimated relative contributions to precipitation from the sources based on composites for positive, negative and neutral phases conditions of the indicates variability modes. Sky blue for the CS, red for the ETPS, yellow for the GoMS, purple for the CAS (local recycling) and green for the NSAS.

results. Some authors *(Hastenrath, 1976; Giannini et al., 2000; Taylor et al., 2002)* have indicated for the analysis region and the Caribbean a trend to a drier second rainfall season for warm ENSO. It can be noticed from figure 6.15.a that for October estimated relative precipitation doubles its intensity for cold ENSO compared to the warm phase. This result implies that during the second rainy season the modulation of precipitation through changes in the transport of moisture is of great importance to define the regional distribution of precipitation. Meanwhile wetter first rainy season for warm ENSO is also noticed (fig 6.15.b) but with less differences compared to the second rainy season. The anticorrelation between precipitation in the vicinity of the Caribbean and the NAO suggested by *Malgrem et al. (1998)*, and *Giannini et al. (2001)* is also found with largest signal for late Autumn (fig 6.15.c). Regarding the importance of the PDO, a strong signal is noticed starting at the end of spring through summer (fig 6.15.d). Negative PDO is featured by the increase of relative contributions to precipitation from moisture transport from the CS but also from local recycling (fig 6.15.e). This in agreement with the mechanism proposed by *Mendez and Magaña (2010)*, which remarks an increase of tropical convection over Mesoamerica and a weakened CLLJ during the negative phase of the PDO. This result is also related with the reduction in the transport of moisture from the Caribbean Sea which is associated with drier conditions in northwestern Mexico as

indicated by *Brito et al. (2002)*. From mid summer to mid autumn, the effect of the MJO (as computed from the Lagrangian estimates) suggests a reduction of precipitation for our defined positive MJO phase with the contrasting increase for the negative phase that for August (fig 6.15.e) shows differences of the 100%. This result is confirmed by the work of *Barlow and Salstein (2006)*, which reports for summer differences from 25% to 100% in observed precipitation depending on the MJO phase. According to their results, precipitation is larger when convection is enhanced as it occurs for the negative MJO phase (note their positive phase is the negative phase in this work). A recent work by Martin and Schumacher also shows influence of the MJO to be of importance during late summer and fall.

6.6 Chapter highlights

A simple evaluation of the performance of the approximation for estimating precipitation due to the contribution of the sources of moisture was carried out using available observations of precipitation for Costa Rica and Panama. The results indicate relatively acceptable biases of the estimations of precipitation over the region suing the Lagrangian approach. This in the basis that the estimations of precipitation do not account as total precipitation but for a relative contribution to the total. This result is encouraging and suggests that the Lagrangian methodology applied reproduces not only the seasonal cycle of precipitation but also enables the study of the variability of observed precipitation in terms of the variability of the sources that provide moisture for Central America. One of the advantages of the used approach is that as the analysis of individual sources can be done, information on which sources may be responsible for certain patterns can be gathered. The importance of the remote continental sources, in this case NSAS, to maintain the seasonal cycle of precipitation over Central America is quite important as it has not been considered before. The role of the contributions from the ETPS may be more related with precipitation in the Pacific regime. From this analysis, the variability of precipitation was found to be strongly bounded to the effect of ENSO, despite the influence of other modes is also important. The pattern described by the contributions from the ETPS resembles not only the pattern of the PDO but also that of drier than normal conditions over some locations of Central America (mainly Nicaragua). The case of PDO result interesing as the time series of contributions to precipitation seemed weird as a first view for the ETPS, further relations between the influence of the PDO during the positive phase can be argued to explain

the observed pattern, however a more rigurous analysis must be done. More detailed analysis of the variability of this source may provide valuable knowledge in terms of the dynamics of drought associated with the variability of the evaporation, the ITCZ and transport of moisture over the ETPac region. The analysis of local recycling allowed us to show the differences observed for each subregion of Central America, which are in good agreement with the climatological differences observed in precipitation. The local response to the forcing of the main variability modes describes a different response to the modes depending on the location of the subregion. This highlights the importance of considering the subregions for climate analysis in order to provide a more accurate picture of the regional water cycle. Moreover, taking into account Central America as a single region provides good information on local precipitation, moisture transport and recycling, however a more proper analysis requires considering Central America as a complex region in which small regions despite near may present a complete opposite behaviour. The recycling of moisture was found to present a more uniform response to the forcing of the MJO, or at least at the effect it seems to have for Autumn, as the four subregions into which Central America was divided present a decrease (increase) in the recycling of moisture for positive (negative) MJO. Meanwhile for the PDO and NAO modes, the direct relationship between the variability modes and local recycling were found to be small compared to those observed for the estimated recycling for MJO. Here, the most important result is that the variations in the contributions to precipitation over Central America, which also affects the recycling require a better understanding of the transport of moisture, that will be treated in detail in the following chapter. It is important to mention that even when the estimation of contributions to precipitation was computed and analysed, the method used for the computation can be improved and up to this stage the analysis of which mechanisms are responsible for the remainging of observed precipitation needs also to be considered.

7
Dynamics of transport

In the previous chapter, a quantitative estimation of the relative contribution to precipitation from the identified sources of moisture was provided. These relative contributions to precipitation are an estimation of how much moisture is transported from the sources to the correspondent target region. One of the advantages of using a Lagrangian formulation, is that for the trajectory followed by a particle from one point to another, the given properties of the particle are known. In the case of backward trajectories, this formulation is important since it enables us to reconstruct the history of air particles before they reach a receptor source with knowledge of the changes that the properties of the air parcel experienced previous to the arrival. In the previous chapters 5 and 6, the results provided information on the final conditions of the air parcels, since the ultimate interest is precipitation. However, the information of the variations of the air parcels properties we can obtain from the Lagrangian trajectories allows a more detailed study on what has happened prior to precipitation. In order to extend our framework and investigate the processes of during the transport of moisture, the analysis of the trajectories before their arrival and further precipitation over Central America is presented in this chapter.

7.1 Origin of air masses

Air masses arriving at Central America may provide part of the moisture that accounts for precipitation. In chapter 5, the identification of the main sources of moisture for Central America determined the presence of sources over the Caribbean Sea, the ETPac region, a remote source over northern South America and Central America itself with small influence from the Gulf of Mexico. Once a general idea on where moisture may come from is obtained, a good question may be where does the air that contains (and transports the moisture) come from? This question must be considered carefully as the origin of air parcels and the origin of moisture may be similar but are not the same. In order to answer this question, the trajectories followed by the air parcels arriving at Central America must be reviewed. One way to do so is to follow the air parcels backward in time and assess their origin at different time steps. Since we are interested in a 6 days time scale, air parcels were tracked backwards in time a total of 48 time steps (remember the time step used is three hours) to identify their positions and classify the trajectories according to them.

For each of the subregions into which Central America was divided (same as shown in figure 6.19) [1], the air parcels were found to come for three main remote sources (Caribbean, Gulf of Mexico and ETPac) for Guatemala-Belize (GB), Honduras-El Salvador (HS) and Nicaragua (NIC). For Costa Rica-Panama (CRP), the northern South America region is added to the list of origin locations mentioned for the rest of subregions. From the total of air parcels arriving to each subregion, the percentage of the particles with origin in each source region was estimated in a monthly basis to give an idea of the regions from which the air parcels come from. Figure 7.1 shows these estimated percentages, from which can be noticed the large difference between particles from the Caribbean and from the other sources. For the northern most part of Central America (GB and HS), the amount of air parcels from the Caribbean is quite uniform except for summer when an increase of a 20% is observed. At the same time that the amount of air particles from the Gulf of Mexico has decreased almost to zero for that season. These summer variations are a bit larger for GB than for HS. This suggest an increase in the efficiency of moisture transport from the Caribbean. During winter, a decrease of the air particles from the ETPS is compensated by the increase of air particles from the GoMS. The case of Nicaragua has a similar pattern to that of northern Central America in the seasonal variations of the source

[1] criteria for dividing the region was based on the heterogeneity of precipitation patterns as indicated in previous chapter

distribution. However, variations are not as large for summer compared to those for northern Central America, a decrease in the amount of air parcels with Caribbean origin and by the increase of air parcels from the Pacific during Autumn. Southernmost Central America, (CRP), presents a distribution well differentiated from the rest, where air parcels also originate over northern South America. For winter and spring, the origin of air parcels is distributed between the Caribbean and northern South America. A sharp decrease of Caribbean air parcels is noticed while a strong increment of air parcels originates from northern SA and the ETPS. The amount of air parcels originating at the GoM is very small. For autumn the pattern is also modified, air parcels come from the Caribbean, northern SA and in a major amount from the ETPS. It can be seen that precipitation due to transport from remote sources is controlled by the contributions from the ocean, except for CRP which has an important component of moisture being transported from NSAS. The case of CRP and even Nicaragua is interesting since it shows a sharp seasonality in the transport. For CRP, during July a significative decrease in the amount of air particles from the Caribbean Sea occurs, which is compensated by the increase in the transport from NSAS. This may be caused by the intensification and configuration of the low level winds over the Caribbean. The easterly flow provides a mechanism through which the moisture from NSAS increases over the coast and enters a convergence region that develops in the Caribbean coast of Central America. For the northern subregions (GB, HS) during July, the influence of air from NSAS also increases. The mechanism is the same as mentioned for CRP, the presence of the maximum of the CLLJ couples with the wind flow from NSAS. It strengthens the flow from NSAS to travel longer distances. The curvature of the CLLJ is also fundamental in providing the conditions that favour the effective transport to GB and HS. It is important to highlight that the amount of air parcels transported from the Caribbean to CRP has the largest amplitude. Meanwhile the rest of subregions present a relatively similar distribution, with the importance of the GOMS increasing for the higher latitudes. The bimodal distribution of air transported associated with precipitation from the Caribbean to CRP and NIC contrasts with the observed distribution for the north as air transported increases during summer, which is a result of the development of the northward branch of the CLLJ during summer.

The 'amount of air particles' travelling to the different locations of Central America and leaving precipitation present a large year to year variability. Tables in appendix F show the percent distribution of air parcels that precipitate over the subregions of Central America according to their origin for the months of February, May, July and October respectively (peaks of the

CLLJ intensity and peaks of rainy seasons). The variability of the amount of air particles associated with precipitation over continental Central America is present in similar bands as for the relative contributions to precipitation estimated from the Lagrangian approach as presented in chapter 6. Largest year to year variability is noticed for the CS and ETPS as the amount of particles is much larger. Anomalies of the daily mean number of particles associated with precipitation in each subregion for selected months are depicted in figure 7.2. It is worth noticing that in most of the cases the largest anomalies are related with extreme ENSO events. Notice also the interesting eight years cycle of the anomalies of the particles that transport moisture from the ETPS to precipitate over HS during August (7.2.k).

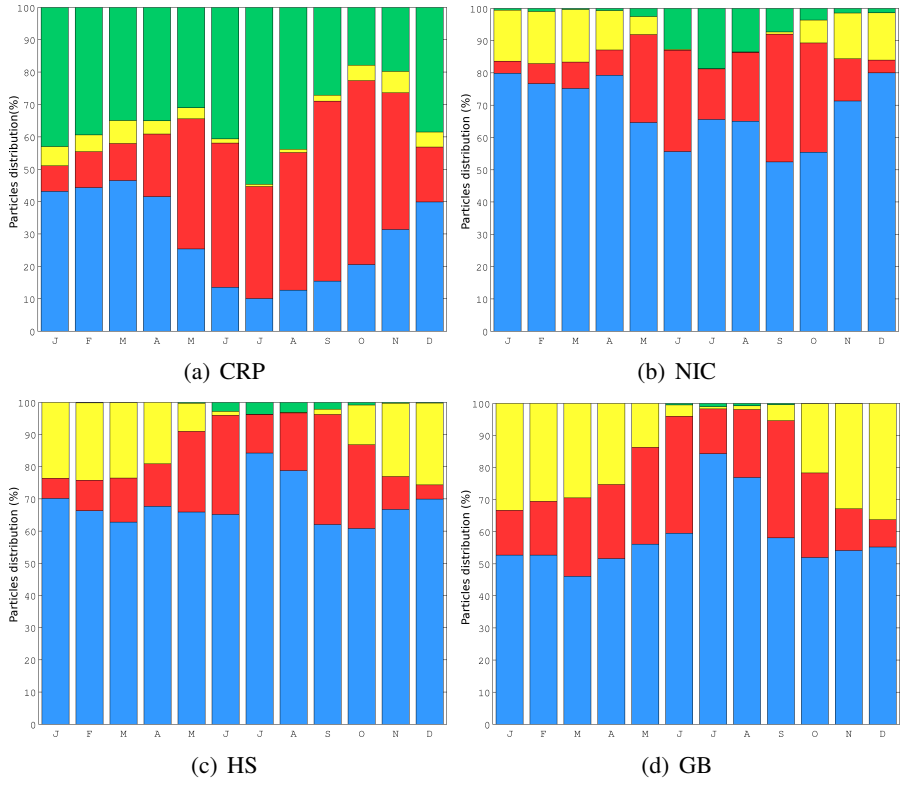

(a) CRP (b) NIC

(c) HS (d) GB

Figure 7.1: Annual cycle of the distribution of particles (%) for each of the analysed subregions. Sky blue for the CS, red for the ETPS, yellow for the GoMS, purple for the CAS (local recycling) and green for the NSAS.

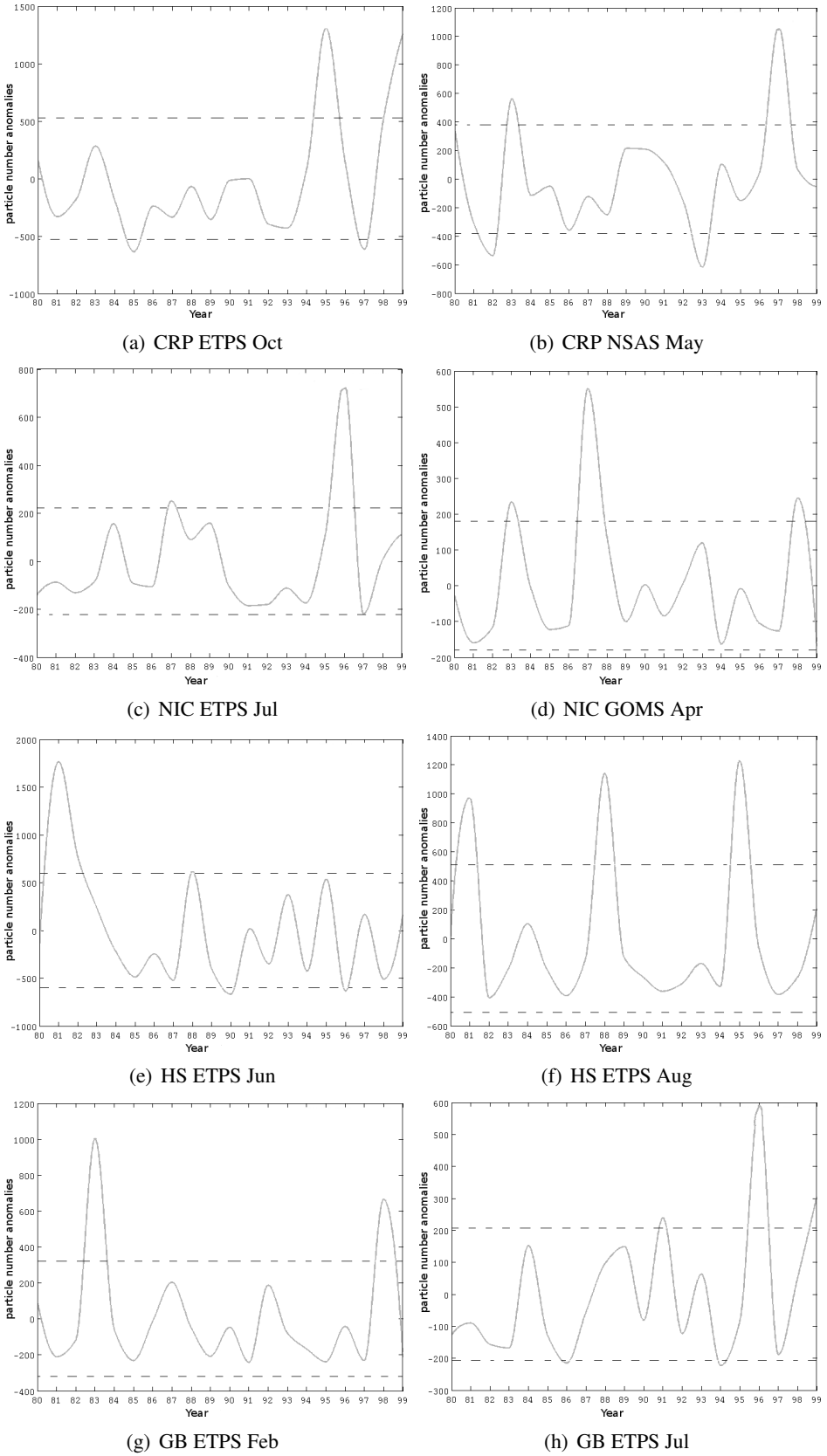

(a) CRP ETPS Oct

(b) CRP NSAS May

(c) NIC ETPS Jul

(d) NIC GOMS Apr

(e) HS ETPS Jun

(f) HS ETPS Aug

(g) GB ETPS Feb

(h) GB ETPS Jul

Figure 7.2: Time series of monthly means of the anomalies of daily number of particles associated with precipitation for selected subregions (for the indicated months).

7.2 The horizontal structure of transport

To establish how the transport process occurs it is necessary to know how air moves. With such a large amount of air parcels, to obtain a mean picture a clustering technique was used to reduce a large set of backward trajectories into a smaller set of trajectories. A first separation of the trajectories aimed to retain those that contributed to precipitation. As we are interested in the air particles that account for precipitation in the subregions, we are mainly concerned to those particles that always circulated along their trajectories below the tropopause level and where precipitation occurrs below the PBL. Those particles which at any moment circulated upper the tropopause were neglected, then those that were found to contribute to precipitation in the particular regions were retained for analysis. Note that the height of the tropopause and PBL were considered as given by the ERA-40 Reanalysis data. For each of the subregions in which Central America was divided, air particles arriving to them were identified in order to obtain the climatological mean air streams. The general picture of these air streams looks quite alike for the different regions, despite the differences related mainly due to the position of the target region. The mean air streams for May are shown in figure 7.2 for each region to highlight this condition. As can be followed from this figure, air moves to the different locations of Central America mainly from the following regions: a) CS b) ETPS, c) GoMS and d) NSAS for southernmost Central America (7.3.d). Air moves from the Caribbean permanently while the movement of air from the Gulf of Mexico and ETPac is seasonally constrained. For GB, HS and NIC air moves from the Gulf of Mexico (ETPac), while in the case of CRP, less air moves from the Gulf of Mexico during October.

7.3 The content of air moisture along the trajectories

Moisture content of an air parcel varies along its trajectory depending on different conditions (vertical movements, evaporation, precipitation). An air parcel can be dry at one point of the trajectory and later on the moisture content can be increased (known as uptake) or the inverse process can occur. These points for which the major moisture uptakes take place are of importance since they give a more accurate idea on the location of a point source of moisture associated with the trajectory of individual air parcels. To ensure this, it is first important to identify the variations of moisture that air parcels undergo along their trajectories. Then, we can determine the regions over which the moisture of the air parcels is increased. In the

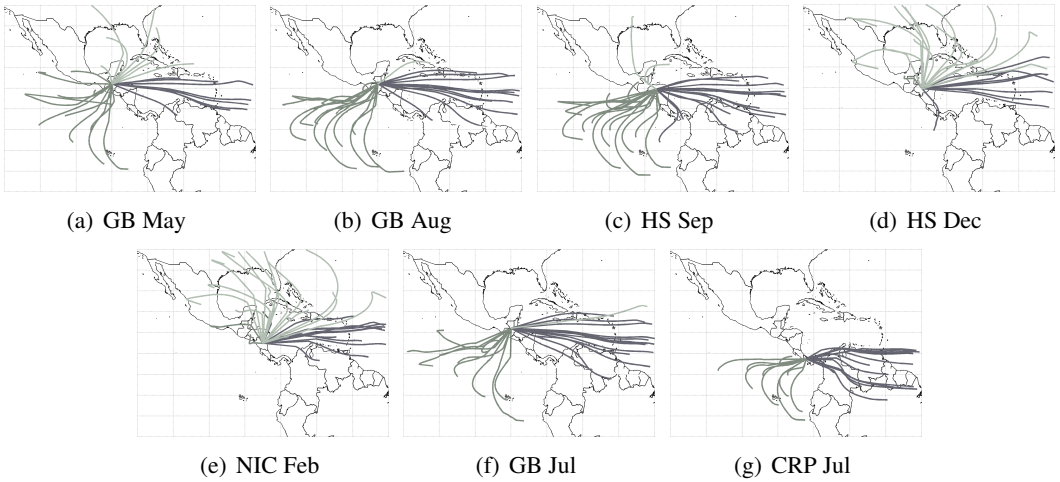

(a) GB May (b) GB Aug (c) HS Sep (d) HS Dec

(e) NIC Feb (f) GB Jul (g) CRP Jul

Figure 7.3: Mean climatological air streams for the trajectories losing moisture over different locations of Central America.

computation of the mean air streams using the clustering algorithm, the specific humidity was averaged at each time step for all the particles belonging to the same cluster. This allows us to obtain an estimate of the mean moisture content of the air streams along the trajectories (backward in time). Figures 7.4 to 7.7 present the results of the climatological monthly mean air streams and their associated moisture content for GB, HS, NIC and CRP respectively.

The four regions have in common the low moisture content of the air flowing from GoMS. This result is reflected in the small contributions to precipitation from this region, as shown in chapter 6 (see figure 6.2.d). Also, for the four regions, the major moisture content of the particles' trajectories is located over the oceanic regions (CS and ETPS). Moreover, we note that the largest values of mean specific humidity are those from the trajectories circulating over the ETPac. A question here might be why the contributions to Central America from the ETPS are smaller than for CS? By examining the temporal evolution of the moisture content of the trajectories we observe how the major changes in specific humidity occur over the ocean before the trajectories reach the target region. This implies that even when the largest moisture uptakes occur for the ETPS, they contribute to precipitation over the ocean (ITCZ) rather than continental Central America, which then receives smaller contributions from these regions (see diagram in figure 7.8).

From figure 7.4 and 7.5, regarding air parcels travelling from the Caribbean, we note that for winter and early spring the moisture content is low and it contributes less to precipitation.

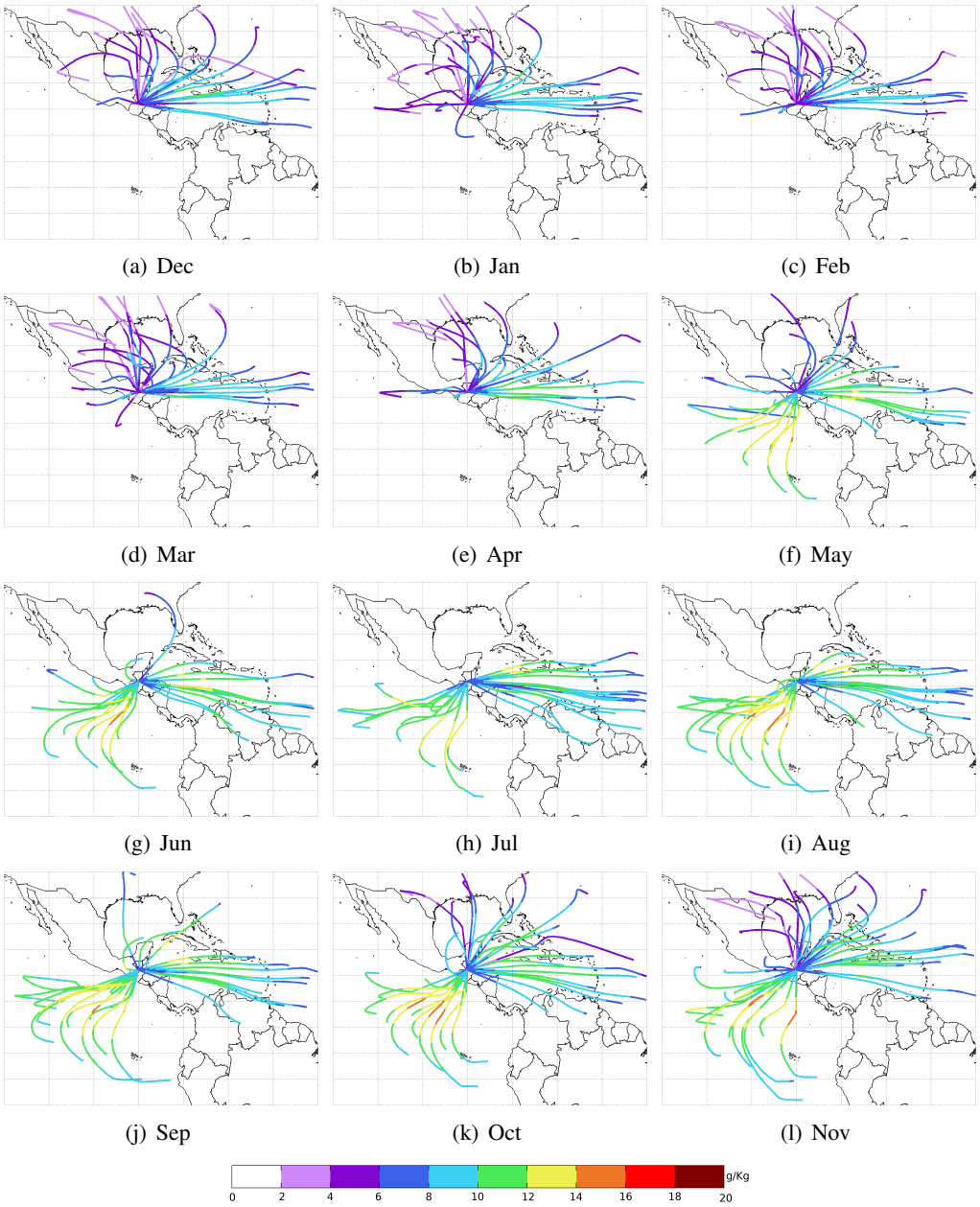

Figure 7.4: Monthly climatological average air streams for the trajectories losing moisture over Guatemala and Belize (GB). The moisture content (in units of g/Kg) along the trajectories is shown. Average clusters were computed based on the method by *Dorling et al (1992)* for the 1980-1999 period.

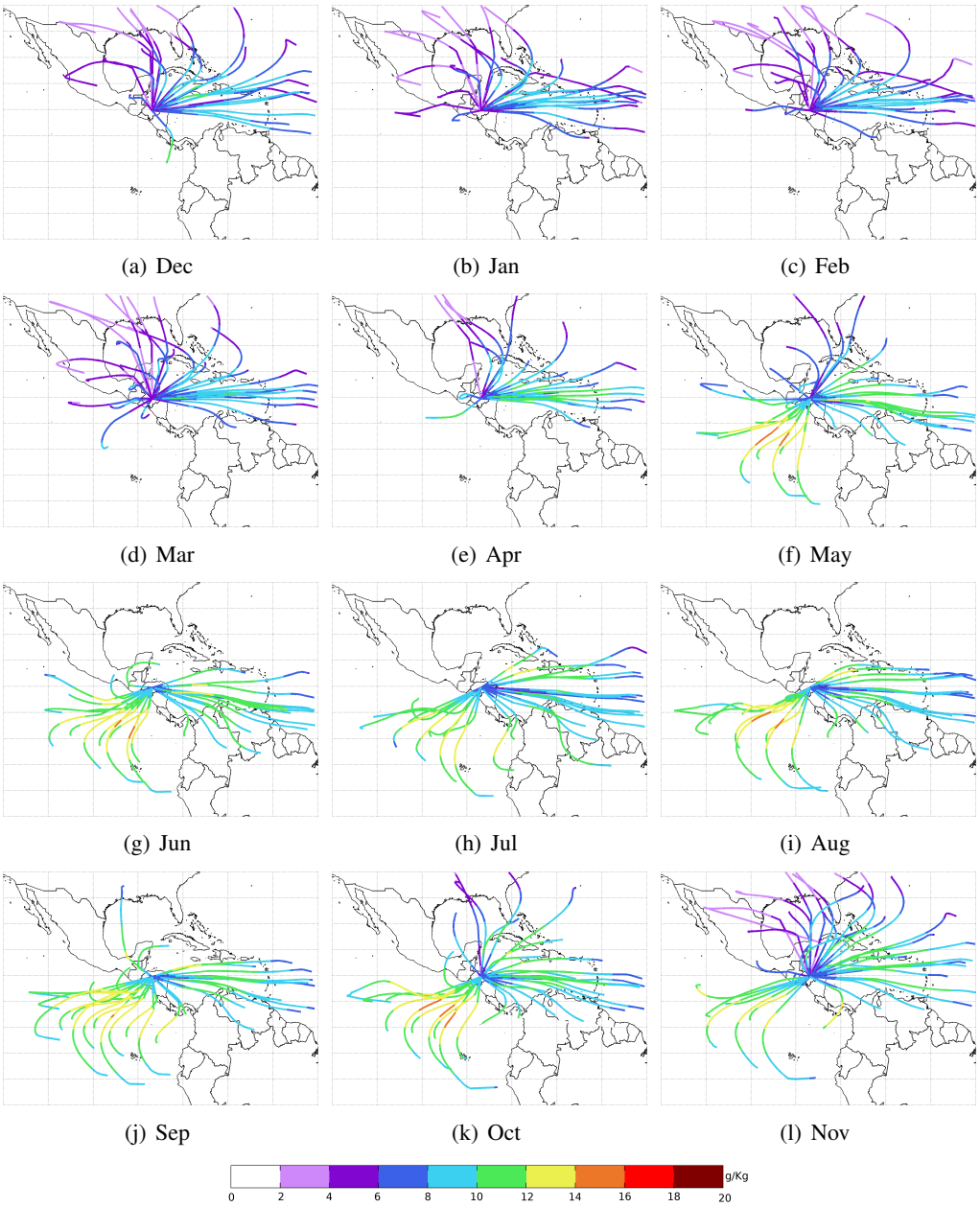

Figure 7.5: Monthly climatological average air streams for the trajectories losing moisture over Honduras and El Salvador (HS). The moisture content (in units of g/Kg) along the trajectories is shown. Average clusters were computed based on the method by *Dorling et al (1992)* for the 1980-1999 period.

For the remainder of spring and early summer, particles are moister and the specific humidity at the arrival point quite small, which implies larger contributions to precipitation along the trajectory. Notice that between June and August the differences in the moisture content is reduced compared to the previous months. This implies that less moisture is being left over the target at the arrival so contributions to precipitation are reduced. Moreover, the moisture content of the trajectories itself is on average lower compared to other periods, suggesting drier trajectories during summer leaving even less moisture over Guatemala, Belize, Honduras and Salvador. During Autumn, differences become larger and also the moisture content of the trajectories, so contributions to precipitation rise. This reduction in the moisture content of air parcels reaching GB, HS from the Caribbean causes a decrease in the contributions to precipitation, in good agreement with the presence of the MSD as pointed out by *Magaña et al. (1999)*, and *Small et al. (2008)*.

The situation of the air parcels from the ETPac region is a little different since even when the differences are similar to those from the Caribbean, the moisture content of the air parcels is larger. Therefore, over the northernmost portion of Central America, the moisture transported from the Pacific is key for determining the summer precipitation. The case of the trajectories arriving to Nicaragua (figure 7.6) is similar, but with the difference that moisture lost over the continental region becomes larger in October and not September as for the northern regions. The latter result is of importance as it may help to understand the processes that drive severe droughts in these regions. This result suggests that the dry season present during summer may be more extended in Nicaragua than in the neighboring region to the north. In the case of southernmost Central America (fig 7.7) the arrival of particles from the ETPS occurs all year round except for March. A strong increase of the amount of particles occurs after the end of spring. During winter, the content of moisture of the air parcels increases modestly over the Caribbean. During summer, trajectories from the central Caribbean are significantly reduced and air masses coming from the east have an increase of moisture content over the northernmost region of Venezuela. This intensification of the moisture content is sustained over the Caribbean until it reaches the region of Costa Rica and Panama, where the strong decrease in the moisture content indicates precipitation has occurred. This pattern is also present during autumn, but air parcels from the east travel a little bit farther north, so the uptake locations reside in the Caribbean Sea rather than NSAS.

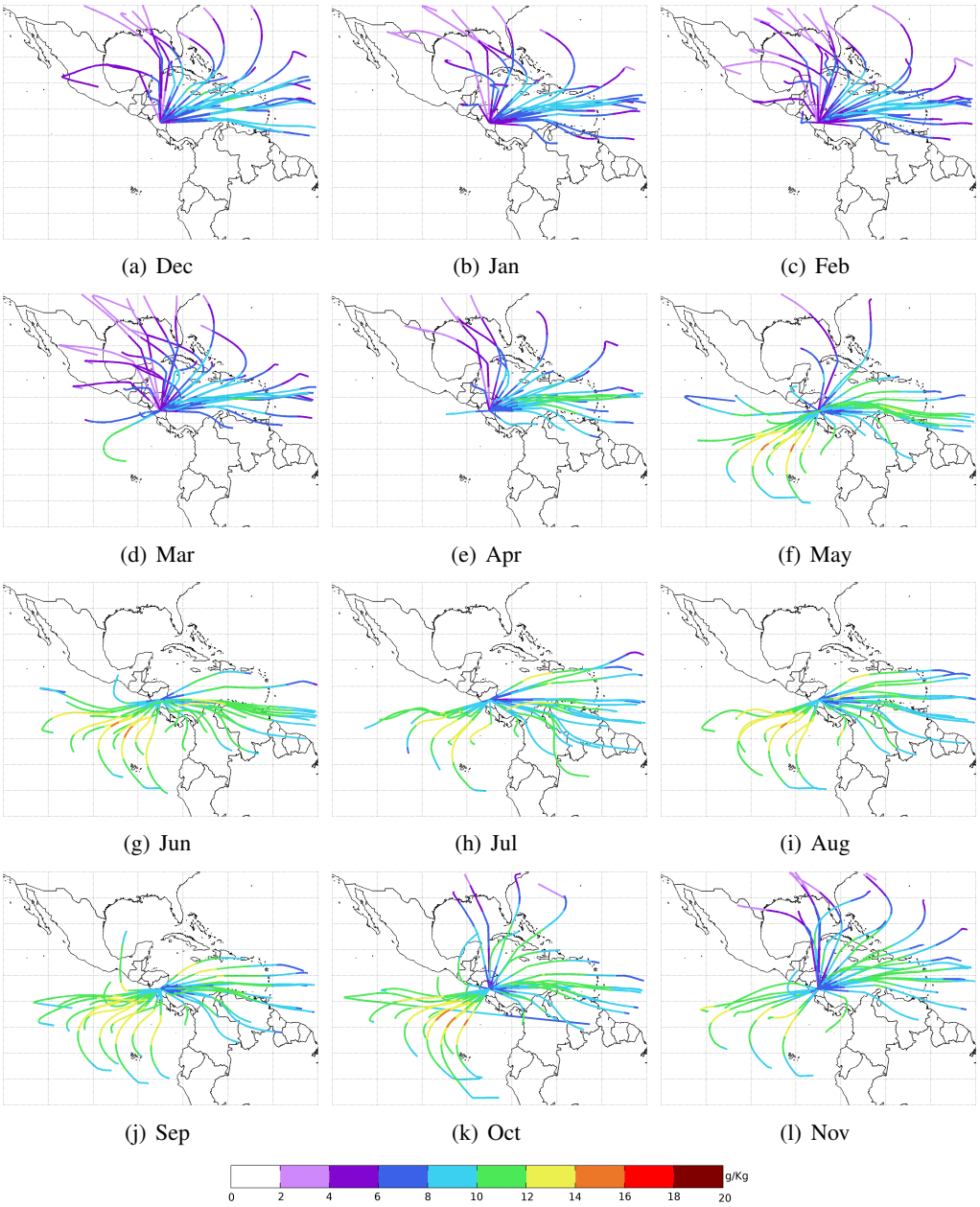

Figure 7.6: Monthly climatological average air streams for the trajectories losing moisture over Nicaragua. The moisture content (in units of g/Kg) along the trajectories is shown. Average clusters were computed based on the method by *Dorling et al. (1992)* for the 1980-1999 period.

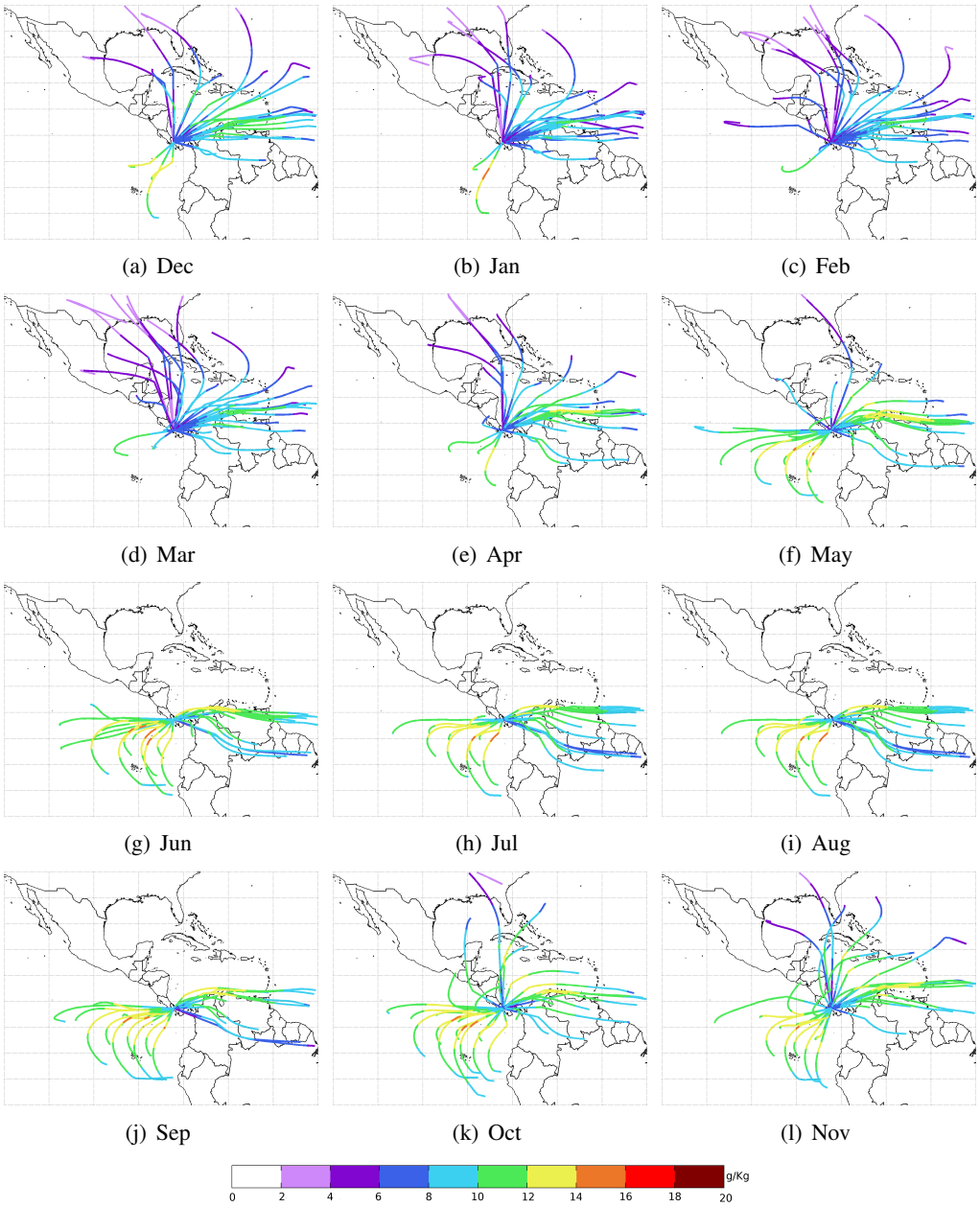

Figure 7.7: Monthly climatological average air streams for the trajectories losing moisture over CRP and associated moisture content in g/Kg. The moisture content (in units of g/Kg) along the trajectories is shown. Average clusters were computed based on the method by *Dorling et al (1992)* for the 1980-1999 period.

The location of the main uptake regions can be also identified as shown by the variations in the moisture content. Two locations are featured by the increase of the mean moisture content of air particles along the trajectories: the regions over the ETPac and the Caribbean Sea. For the different arrival locations defined, we note that despite the origin of the air parcels, they are relatively dry and moisture increases occur for very specific locations. Uptake over the ETPac is well constrained to the region of intense evaporation (see figure 1.3, chapter 1) which implies that evaporation is the process that triggers the moisture history of the air parcels under the Pacific regime. Few or no intense uptake occurs when the ITCZ is located over this region as is known to happen during (mid-end) winter and part of spring, rather these are periods of moisture loss due to oceanic precipitation in the ITCZ. These periods correspond to weak contribution from the ETPS and moreover, with the decrease in the contributions to precipitation, in agreement with results shown in chapter 6. The NAMS is of importance to explain the seasonal cycle of the distribution of the transport of moisture. It can be followed that the GoMS becomes more important for the northern part of Central America and it was shown in figure 7.1 that during summer there is a sharp reduction in the amount of air parcels travelling from the GoMS to the different locations of Central America. During winter, the presence of Arctic air masses is associated with a cooler GoM troposphere that can not hold much moisture, for this reason the contribution of the air masses from GoM to precipitation over Central America is small, note that this dry air from the GoM is noticeable from the figures that show the moisture content along the trajectories (figs 7.4 to 7.7). In summer the moisture content increases as the GoM becomes warmer, however, during this period the flow is mostly southerly monsoonal flow which is directed toward the North American heartland. This reasoning is also useful to explain the distribution of the air parcels from the CS. Back in figure 7.1 we observe that during summer the air masses from the CS are strongly reduced for CRP and that increase as northern the target region is located. The southerly monsoonal flow during summer (associated with what has been called a northern branch of the CLLJ) transport moist to the north and part of the air masses can contribute to precipitation over northern Central America in their transit to southern North America. This is the reason we observe a decrease in the distribution of the air particles carrying moisture to CRP while an increase for the case of NIC, HS and GB during summer.

Vertical structure of the air streams

The climatological averaged air streams described in the previous section show in detail the mean path followed by the air parcels between the sources and the arrival locations, that is, the mean history of horizontal transport, and the regions of major uptake or loss. The air flow from the Gulf of Mexico was mentioned to be particularly dry, and it was speculated to be related with the height of the flow and the drier winter air. Note that the lower the level of the air parcels greater is the content of moisture. However, it is also important to know with accuracy the vertical structure of air, since it provides information about the mixing processes and vertical variations associated with particular systems.[2] As for the horizontal structure, the climatological averages of the vertical structure of the air streams are presented for the defined subregions. Figure 7.8 to 7.11 show the average vertical structure of the climatological clusters for each subregion of Central America coming from each source region. After the classification of the tropopause air particles was done, it was found that more than 87% of the air particles that contributed to precipitation circulated below approximately 4Km height. Moreover, most of the retained air particles that have the largest moisture content circulate below 3Km and for that reason the results presented in the following plots use this height limit in order to present with more detail the vertical structure of the average clusters.

[2] this is of great importance for case analysis because the vertical structure provides information on several atmospheric processes.

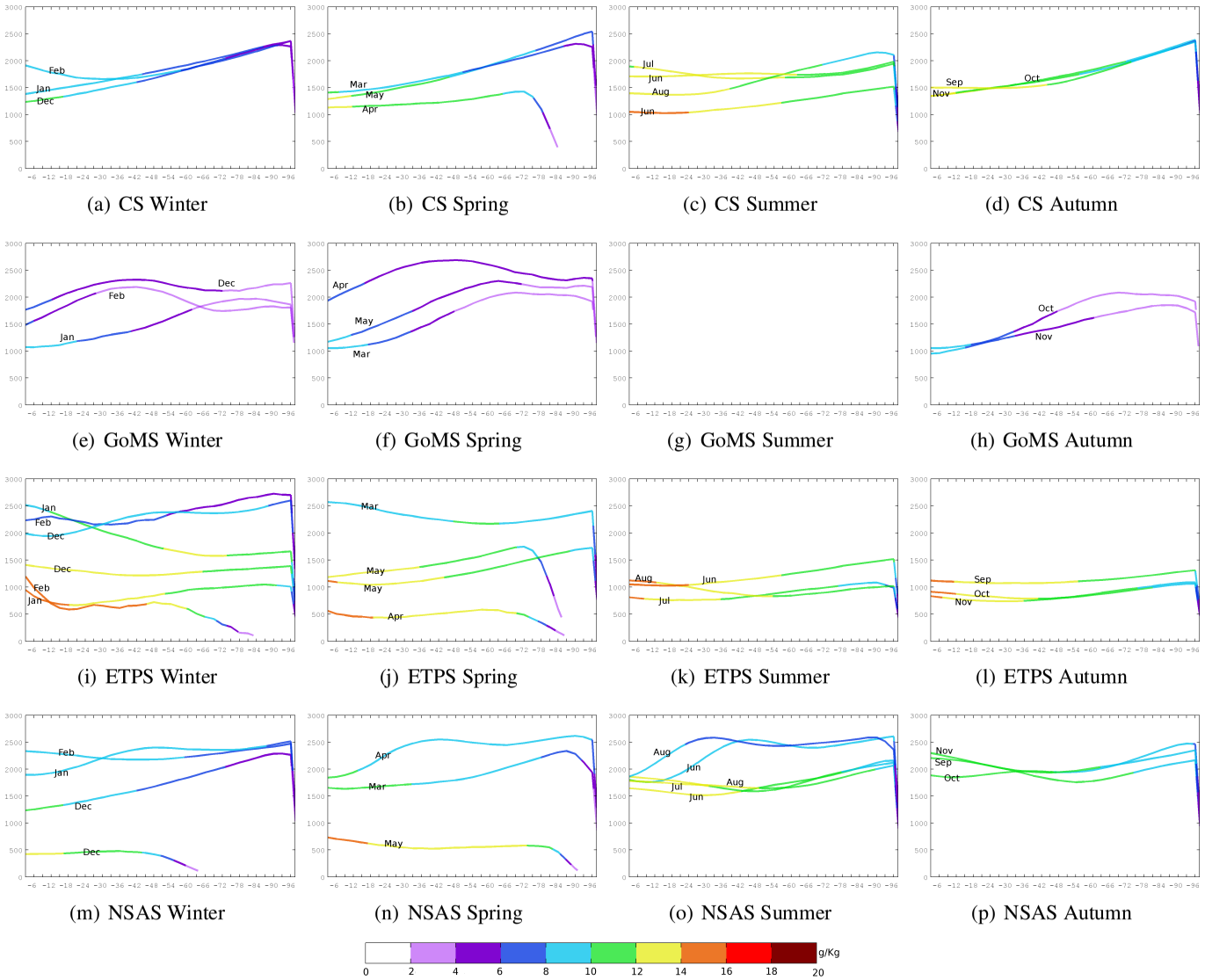

Figure 7.8: Mean climatological air streams for the trajectories losing moisture over CRP and associated moisture content in g/Kg. Height in m in the y-axis and backward hours in the x-axis, the hour zero (not indicated) was taken as the instantaneous moment of precipitation over Central America.

For southernmost Central America, namely the CRP region, the larger contributions are from CS, ETPS and NSAS as shown in previous chapters. The vertical structure of the transport shows a good coherence with the wind flow, which is well known to be low-level on average. For the air travelling from the CS, a significant increase in the moisture uptake is found during summer (fig 7.8.h). This uptake takes place up to 3 days before the arrival of the air masses into CRP when precipitation occurs. We notice that during late spring (fig 7.8.e) and early Summer (fig 7.8.f), a strong increase in the moisture content of the air particles occurs (June, fig 7.8.g). Moist air that contributes to precipitation over CRP from the CS is on average below the 2Km and its height decreases substantially as moisture increases. During Summer and early Autumn, the moisture uptake occurs over the inner Caribbean, where the easterly flow is known to peak (as noticed from the horizontal structure in previous section). Air travelling from the GoMS is very dry in comparison and presents a variable vertical structure, with a reduced amount of air particles that contribute to precipitation during summer, as the wind flow from the Caribbean moves northward due to the increased intensity of the CLLJ. The case of the transport of air particles from the ETPS is particularly interesting as two well differenced air flows can be noticed. During winter (fig 7.8.a) and spring (fig 7.8.k) the presence of a very moist and very low level flow is remarkable at the same time that a drier air flow layer is noticed at higher altitudes. The latter flow is associated with the westerly wind regime whereas the lower level moist flow is found to be related with the more near surface air flow from the southwest. As summer approaches, the upper dry flow vanishes (fig 7.8.g) and during autumn, the vertical structure of the air flow from the ETPS is basically the same as for summer. Note that the largest uptake of moisture occurs for the low level air flow as it is directly related with the region where evaporation is larger. Moreover, the uptake linked to precipitation is remarkably intensified during February and it is maintained during a larger time period. This suggests that the southwesterly flow plays a primary role for triggering evaporation from the ocean surface. Furthermore, moisture increase that results from it contributes directly to precipitation over CRP. On the other hand, moisture transport from the NSAS is not as low- level as that coming from the oceanic regions. Air from this source is very dry, as is that from the GoMS, except after May (fig 7.8.f) when moisture uptake increases. This marks the start of the contributions from this source that was found to be active during the summer period. As summer ends, the airflow from this source returns to its dry conditions.

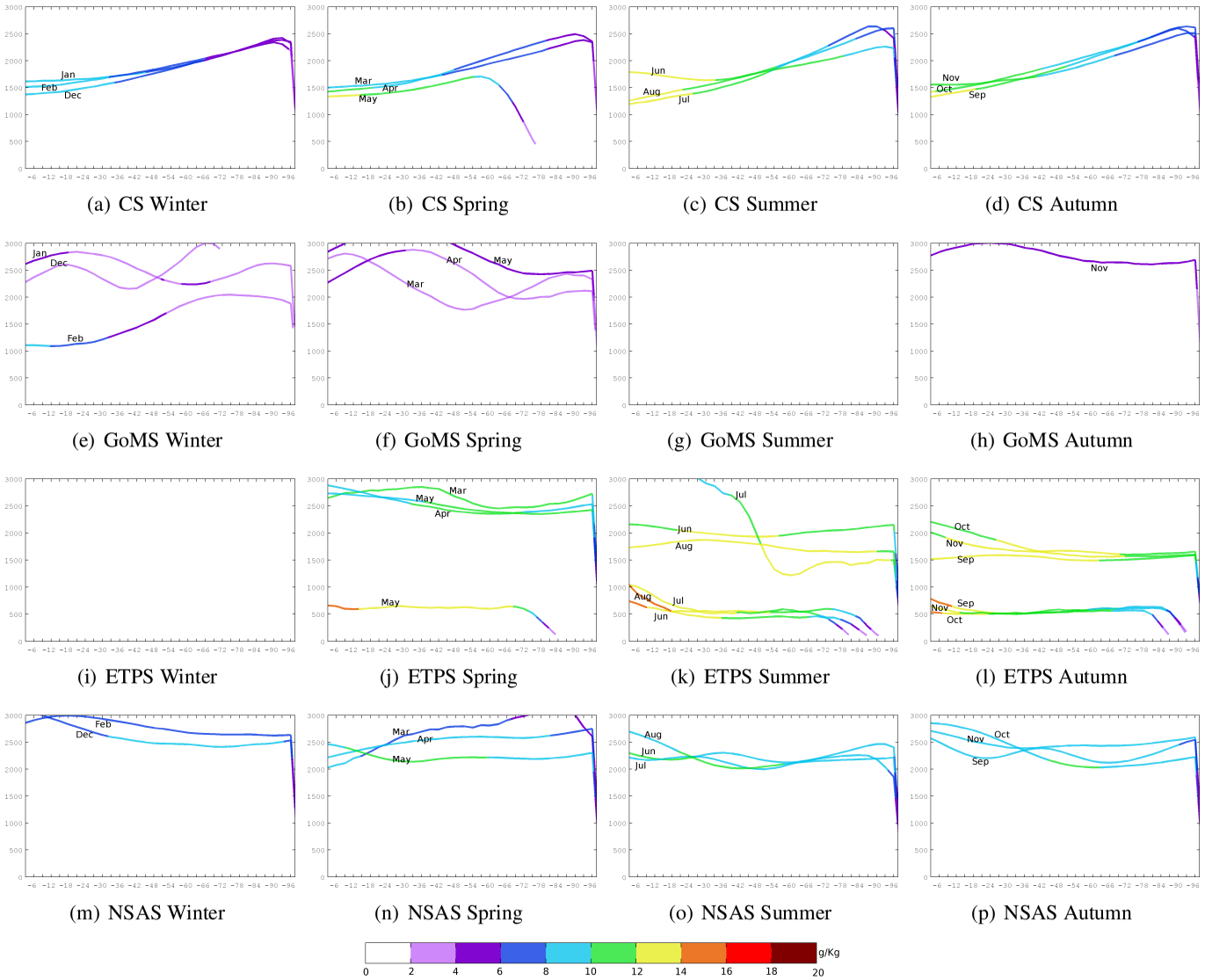

Figure 7.9: Mean climatological air streams for the trajectories losing moisture over NIC and associated moisture content in g/Kg. Height in m in the y-axis and backward hours in the x-axis, the hour zero (not indicated) was taken as the instantaneous moment of precipitation over Central America

For Nicaragua, the vertical structure of the air flow from the CS looks similar to that for CRP but with uptake being less intense and occurring in the first 24 hours before arrival (figures 7.9.a to 7.9.d). Air from the GoMS is even drier than for CRP and flows at higher altitudes as it travels above 3 Km (fig 7.9.e to fig 7.9.h). There is no airflow below the 3Km height from ETPS on average as air that contributes to precipitation during this period is upper level and even drier. During May, flow separation in the vertical also occurs as found for CRP, with the separation being even more marked for the air travelling to NIC (fig 7.9.j). This air flow separation, different from what happened for CRP, is found to persist for the rest of the year with a peak of uptake during summer (fig 7.9.k). It is also worth noticing that the moisture content of the air particles travelling at upper levels from the west have an important moisture content as moisture uptake is intense even 96 hours prior to the moment at which precipitation occurs. The fact that the moist content of the air is conserved for longer time periods implies that less rainout occurs along the trajectory of the air parcels. In the case of the lower level flow, the moisture gains are constrained to the day previous to the arrival, except for May as for CRP. Air flow from NSAS is on average found to circulate at upper levels, it is very dry and no significant moisture uptake is found as for CRP. This result suggests that the transport of moist air from NSAS to the North is very well constrained by precipitation (and the mountain range) over CRP. Therefore, a decreasing influence of the transport from NSAS is expected as we move North, as was shown in the previous chapter.

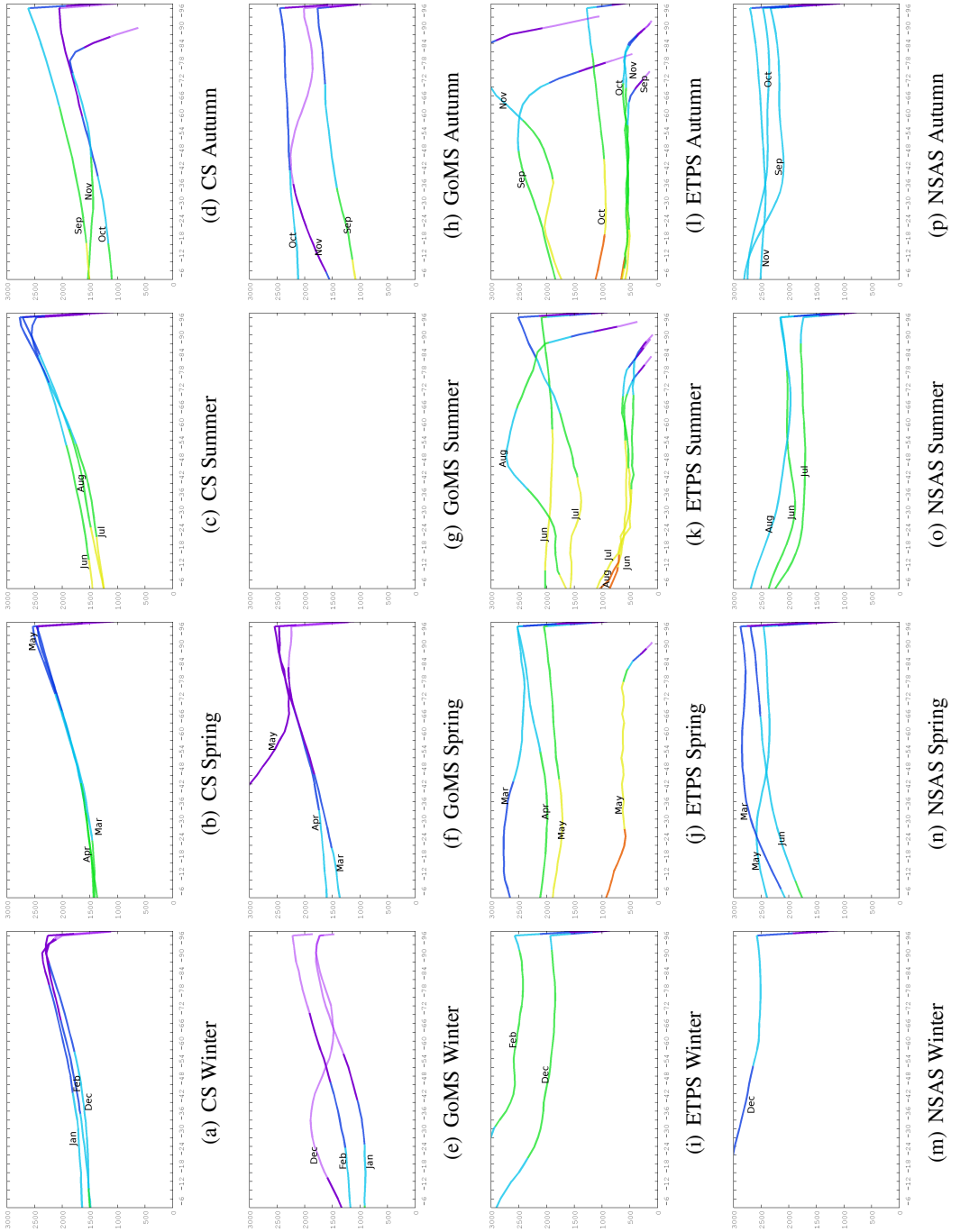

Figure 7.10: Mean climatological air streams for the trajectories losing moisture over HS and associated moisture content in g/Kg. Height in m in the y-axis and backward hours in the x-axis, the hour zero (not indicated) was taken as the instantaneous moment of precipitation over Central America

Similar to what was found for CRP and NIC, moist air transport from the CS to HS shows a coherent structure with increasing moisture uptake during winter (fig 7.10.a) with the flow level below the 1.5 Km. Transport from the GoMS is drier and it was found to circulate at lower levels, particularly in September (fig 7.10.g). During this period, it is found to flow below one kilometer height with the largest moisture uptake in the first 24 hours prior to precipitation. The flow separation for the air flow travelling from the ETPS is also noticed, during winter the solely presence of the upper level flow is noticed (fig 7.10.i) which is also found to be higher in altitude compared for the same period for NIC. The development of the moist inflow from the lower levels is noticed with intense moisture uptake for May as for the other subregions analysed (fig 7.10.j). It is important to remark that for Summer (fig 7.10.k) and Autumn (fig 7.10.l) the height of the upper level flow has decreased compared to the other subregions. Moreover, a significant in the moisture uptake is noticed, being very important during the previous 48 hours before the arrival of the air parcels to the target location for both upper and low level air flow. Air travelling from NSAS (fig 7.10.m to fig 7.10.p) is found to circulate at higher levels. Moist air transport from the sources of moisture for GB presents a vertical structure very similar to that described for HS, with the upper level air flow having the largest moisture uptake during spring (fig 7.9.j) and summer (fig 7.9.k) going back up to 4 days before the arrival of the air particles to the target.

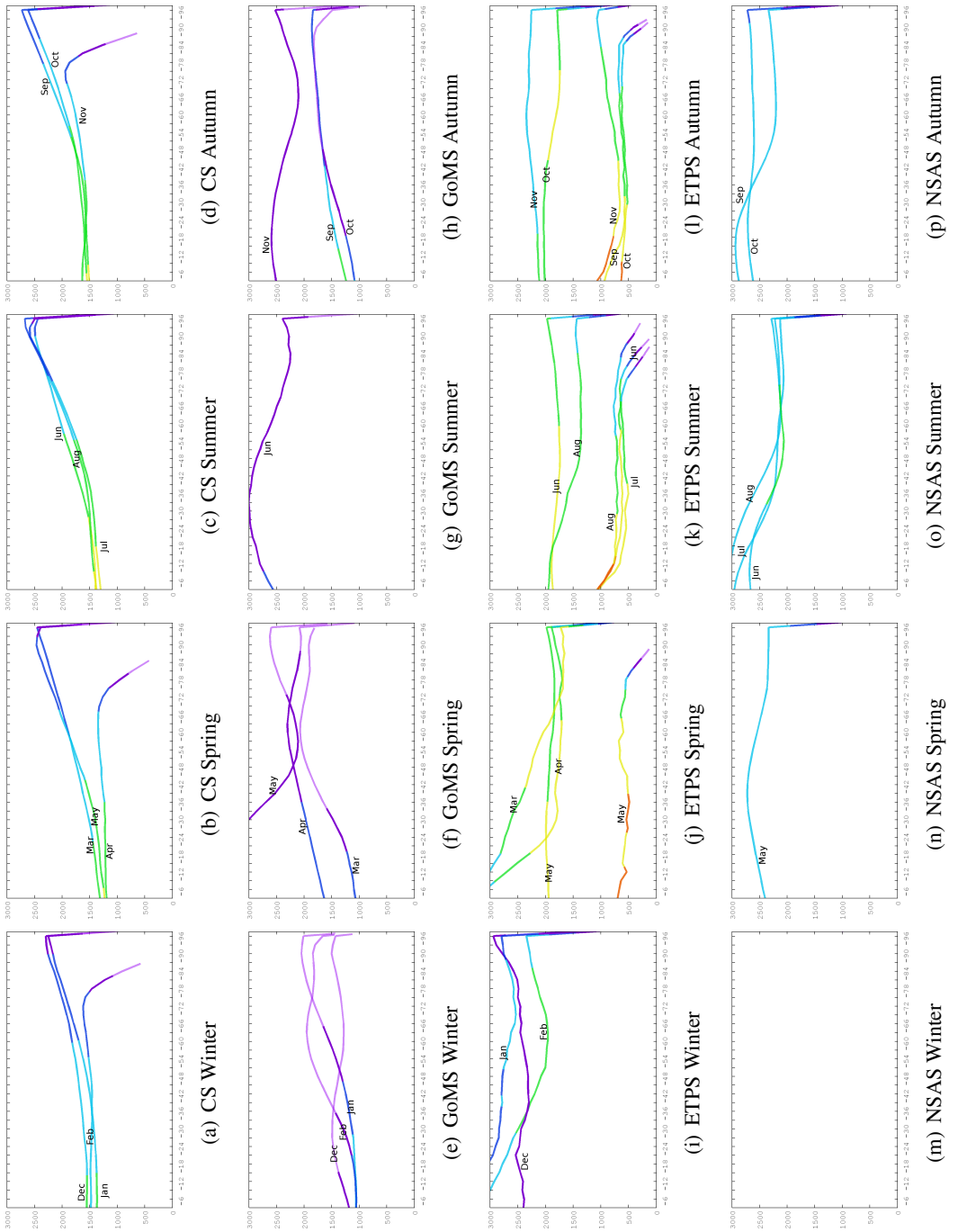

Figure 7.11: Mean climatological air streams for the trajectories losing moisture over GB and associated moisture content in g/Kg. Height in m in the y-axis and backward hours in the x-axis, the hour zero (not indicated) was taken as the instantaneous moment of precipitation over Central America

7.4 Dynamics of transport

There is a strong relationship between the wind fields, sources of moisture and associated contributions to precipitation. The horizontal structure of the mean water vapour transport is consistent with the low level wind vector. The link between wind and precipitation is not surprising since this relationship is known for several regions worldwide. The Lagrangian approach provides an integral overview of the regional water cycle, evaporation from the oceans and consequent moisture uptake along the transport pathways of air masses from the oceanic sources to the adjacent land areas. Figure 7.10 shows the seasonally averaged low level wind field.

From the seasonal patterns of the wind vector, it follows that the low level winds play a major role in the transport of moisture. In the case of the Caribbean Sea and NSAS, the strong easterly flow is fundamental (as pointed out *Durán-Quesada et al., 2010*). During winter, the easterly winds are curved south-westward so that wind is able to carry moisture into southernmost Central America. Note that the conditions of the wind flow imply a reduction of the intensity of the wind between the northern Caribbean and the Gulf of Mexico. Moisture from upper levels is able to descend and air is able to penetrate into the continent where it can leave moisture over the northernmost portion of Central America. This explains the increase of the contributions from the Gulf of Mexico that are of importance during winter and early spring. During winter, the moisture content and the air temperature are less which may be partly responsible for the observed reduction in precipitation over Central America. But it is important to highlight that the amount of air parcels (which are drier compared to other seasons) that precipitates over Central America is reduced. This decrease in the amount of particles associated with precipitation over Central America is a result of the intensification of the low-level wind flow. The intense easterlies (which are mostly zonal during winter) transport the air to the ETPac region and as air is drier precipitation over Central America is very limited. In addition, the easterly flow acts as a barrier for air with origin in other locations, mainly from the ETPS. Note from figure 7.11.a, that during late winter the contributions from the Caribbean are reduced and they start to increase again after April. As the CLLJ secondary peak intensifies (during summer), more moisture is transported towards Central America. However, due to the width of Central America and moreover to the presence of topographic gaps, the intensified wind flow is funneled through the topographic gaps between cordilleras and penetrates far into the Pacific.

As the CLLJ starts to decrease in intensity, the moisture transported from the east is not able to cross to the Pacific (note that the wind flow over the topographic gaps of Tehuatepec and Papagayo decrease considerably). Moisture is available to precipitate over Central America if the instability conditions are favourable, especially on the windward (Caribbean) side where moist air is uplifted by the terrain. This marks the spring peak of precipitation over Central America. Over the ETPac, during winter and spring (even when the ITCZ is not as strong) the wind flow is southwesterly and moreover, the intensity of the easterly flow of the CLLJ, through the Papagayo gap, reduces it even more. This results in few chances for moisture from the Pacific to reach Central America, making that the amount of moisture transported from the Pacific to Central America be almost zero. Again in spring, when the easterlies are reduced, the flow from the NSAS coast can impact some parts of Central America, where it can contribute to local precipitation.

During summer, two key features of the regional climate are present: a) the MSD and b) the CLLJ. The main peak of the CLLJ (July) differs from the secondary (February) in the intensity but more importantly in the orientation of the flow. During summer, the CLLJ develops a northward branch, moisture from the Caribbean Sea is then transported in the direction of North America and does not point to southern Central America. Instead it points to northern Central America and follows the coastline toward the Gulf of Mexico. The direct result is the inhibition of wind flow from the Gulf of Mexico to travel to northern Central America by the same mechanism that previously inhibite wind from the Pacific to travel towards Central America. The reduction of wind flow to southern Central America results in a decrease of transport of moisture to this region. The magnitude of the wind is almost completely zonal toward northern Central America and has a similar effect to that of the topographic gaps. Then moisture transported in this direction reaches the Pacific instead of accounting for precipitation over northern Central America. The strengthening of the 'Tehuantepecers' and the Papagayos induces the moist easterly flow to go west into the Pacific (see figure 7.11.c). The moisture form the Caribbean being transported to the Gulf of Mexico, the Great Plains and the Pacific reduces the availability of moisture to precipitate over Central America. This causes a generalised decrease of precipitation over Central America during the MSD. The wind conditions favour the transport of moisture from NSA to southern Central America. In the case of the ETPac, southwestward flow is less zonally west and the gradient allows the wind low near the coast to become more meridional and point north, turning south-east and favouring the transport from

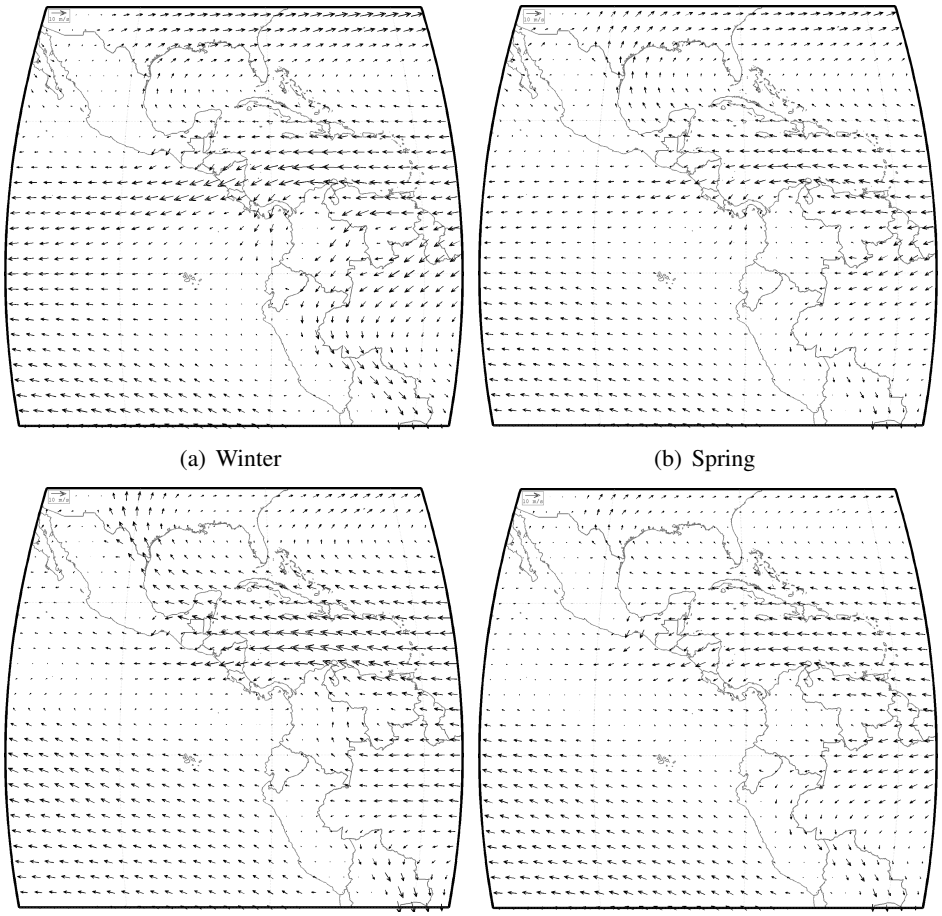

(a) Winter (b) Spring

(c) Summer (d) Autumn

Figure 7.12: Climatological seasonal wind at 850hPa for the 1980-1999 period from ERA-40 Reanalysis. The wind vector shows the direction of the wind flow in the lower levels.

the ETPac. In addition, evaporation increases over this the ETPac during summer, increasing the availability of moisture to be transported from this region. During summer, the ITCZ is at its northernmost position so moisture from the ETPac does not have to overpass this obstacle and is free to make its way to Central America without raining out of the ITCZ. As the CLLJ decreases considerably during autumn, wind transports moisture more efficiently to Central America, the wind flow does not favour more the transport of moisture from the NSA and the Gulf of Mexico, as for the latter the NAM is drawing air flow into a warm North America. whereas in winter the flow to Central America is favoured due to the thermal contrast, but the contributions are small as air is drier as shown in chapter 6. The contributions

from the Caribbean Sea are increased while those from NSA and the Gulf of Mexico reduced. Contributions from the ETPac are maintained until the ITCZ moves southward and inhibits the passage of moist air to Central America from the southwest by inducing it to precipitate over the ocean before reaching the continental region. As a response of the latent heat, during summer North America is a low pressure region and moisture flows to it while the opposite occurs for South America.

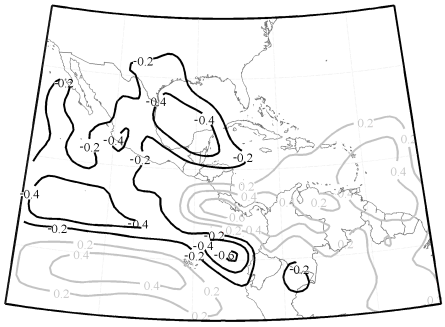

Figure 7.13: Correlation pattern between the intensity of the $(E-P)-6$ field for Central America and the surface wind field (significance at the 95% is plotted).

The importance of low level winds is not only associated with the transport of moisture but also with the increase of evaporation and the corresponding intensification of the evaporative sources of moisture over the ocean, as described by equation 1.2. This influence of the wind field is summarised in the spatial correlation pattern shown in figure 7.13. As wind speed increases the $(E-P)^{-6}$ increases too as indicated by the correlation between the $(E-P)^{-6}$ and the wind fields. In agreement with *Wang et al., (2008)* the strengthening of the CLLJ is associated with the increase of the $E-P$ and the transport of moisture to the west. An important aspect to highlight here is the existence of different precipitation regimes in Central America (as indicated in chapter 2). More intense moist easterlies may imply an intensification of precipitation over the Caribbean side of Central America as moisture is lifted orographically whereas on the leeward (Pacific) side of CA there would be less rain, this is in fact what we observe as two different precipitation regimes. This point is important and further work is still needed in order to provide more conclusive results, one interesting problem for further study may be the analysis of the interaction of moist air flow with local topography using the three dimensional structure of the trajectories.

A conceptual model for the modulation of moisture transport

The information provided by the trajectories is very valuable as it allows the identification of transport structures. By tracking the moisture content the regions were moisture of air is increased can be assessed. Within this framework we are now able to discuss how the moisture transport takes place.

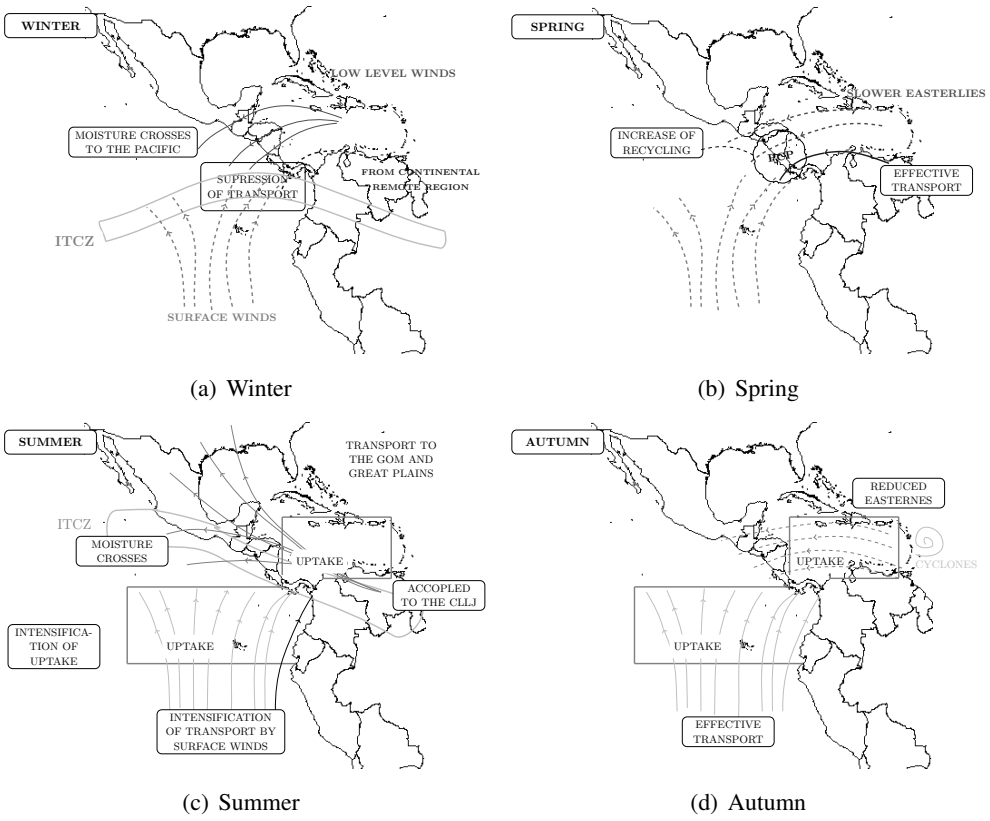

(a) Winter (b) Spring

(c) Summer (d) Autumn

Figure 7.14: Schematic representation of the main mechanisms related to the transport of moisture associated with precipitation over Central America for the each season. Continuous lines indicate strong wind flow while dashed lines indicate is used to indicate slower winds.

The structure of the trajectories reveals that low level winds are the main moisture conveyors for the moisture that reaches Central America. In addition, the evaluation of the moisture content along the trajectories shows that moisture uptake is important in the regions where winds are strong but also that moisture is lost under the ITCZ. Following diagrams shown in figure 7.14 , we see that the transport of moisture from the Caribbean (associated with the CS)

is mainly driven by the CLLJ component of the easterlies, during winter for the secondary maximum of the CLLJ which in this period is turned south-west under the influence of the South American Monsoon. As the intensity of the wind strengthens, part of the moisture is able to reach to the Pacific following the structure of the airflow. The southwesterly flow over the ETPac has a modest intensity that is even more reduced by the presence of the easterlies. The interaction between this two fluxes results in the inhibition of moisture from the ETPS reaching Central America. Moreover, the region where the wind converges is under the ITCZ, which at this moment is at its southernmost position and becomes a sink of the southwesterly moisture transport. Moisture being transported from the ETPS has then two barriers, the easterly flow from the Caribbean and the ITCZ. Most of the moisture transported from NSAS precipitates on the way to Central America and when the air reaches Central America the contribution is small since air is drier as has left moisture over the ocean. During spring, the reduction of the easterlies causes the moist air from the CS to stagnate over Central America and go no further, while the ITCZ moves northward and the CLLJ is no longer a barrier for the low level flow from the ETPS. The intensity of the easterly flow is such that moisture from NSAS is also transported and southern Central America becomes the region over which moisture flux from several directions. This increases the probability of precipitation and with it the recycling of moisture which is also an additional source of moisture and the increase of precipitation during spring is observed.

During winter, the results from chapter 5 indicate that the intensity of the CS is decreased while the ETPS is increased significantly compared to the previous months. The trajectories show an important increased in the uptake of moisture over the ETPS which results in moister low level winds. Uptake of moisture also increases over the Caribbean despite the reduction observed for CS. During summer, the ITCZ is at its northernmost position (reduced or no influence over the ETPS), the CLLJ is at its maximum intensity and the northward branch of the CLLJ is developed. As the winds turn north, moisture from the Caribbean moves with the wind away from southern Central America, reducing the contributions to precipitation. Moreover, the air flow from NSAS is coupled with the CLLJ and transport to Central America is reduced from this source. The results suggest the decrease of moisture transport from the Caribbean and for instance of the contributions to precipitation. It is important to remark that the intensified winds are associated with the increase of evaporative cooling which lowers the SST causing a

decrease of convective activity. Since the winds are turned in the opposite direction, the interaction between the easterly flow and the southwesterly flow does not occur and the intensified wind from the Pacific is able to transport the moist air (notice uptake has increased) to Central America. The structure of the CLLJ during summer indicates that over southern Central American Caribbean coast a region of low level convergence is developed. This convergence pattern and the effective transport from the ETPS explain why southern Central America is less affected by the MSD. Precipitation during summer is basically constrained to the small contributions from the CS and the larger contributions from the ETPS, so that the ETPS leads summer precipitation. In autumn, the easterly flow is a minimum, moisture transport from the ETPS account for big part of precipitation since winds are still strong. During this period the tropical cyclonesis has increased and those systems control a large part of the observed precipitation. Transport from the inner Caribbean is suppressed but increased from the outer Caribbean, as this moisture is transported quickly by the cyclonic systems. It is also important to highlight that the activity of the ITCZ is strongly connected to the SST distribution. Notice that heat fluxes modulate the supply of moist static energy to the tropopause then lead low level convergence (see e.g *Neelin and Held, 1987*) and surface heat fluxes are intensified by warmer SSTs. The forcing of an atmospheric response to SSTs anomalies has been studied in terms of the surface wind, evaporation and SST feedback (see e.g *Liu and Xie, 1994; Chang et al., 2000; Vimont, 2010*.)

7.5 Chapter highlights

The 'origin' of the air masses that provide moisture for Central America was determined, with most of the moisture flow coming from the Caribbean Sea. The application of the clustering algorithm described in chapter 4 enables us to reduce a huge amount of data into sets of clusters containing the mean information of the trajectory followed by the air particles. The structure of the transport was analysed on a climatological basis by means of the clusters of trajectories followed by the air parcels. This structure reveals a dominant component of the low levels winds as moisture conveyors. The efficiency of transport is associated with the intensity of the winds but also with the increases of moisture along the trajectories via uptake. The complex process of moisture transport and interaction among the components of regional climate is presented

in a simple conceptual model that contains the most relevant details on the transport of moisture. In addition, the response of the contributions to precipitation from modes of variability was analysed taking into account the effect of the variations in the amount of air transported from the evaporative sources as well to the effect of a key moisture modulator, the CLLJ. The results suggest that in some cases the variations of the relative contributions to precipitation are strongly related to the variability in the amount of air transported whereas in some other cases the variability in the content of moisture is more important. The interpretation of the interannual variability of the precipitation associated with the transport of moisture is quite complex as the same mechanism may be able to modulate both the transport and the moisture content of air particles. As feedback between the mechanisms becomes more active, the system becomes more complex. Despite the high non-linearity, some direct linear relationships were found to be useful in the simplification of the problem. The latter may allow us to focus on certain processes that dominate the variability of the regional water cycle. This can be used to identify particular structures that need the major improvement in climate modelling to obtain a better representation of the precipitation in the IAS region. Furthermore, these results encourage the use of the applied methodology for other complex regions within the tropics such as the convergence zones and the monsoon-like circulations. In the particular case of Central America, the mechanisms described enable us to pinpoint the key elements that need further study. The CLLJ has become an important element of study in the region, but the results suggests that there is a lot more of interactions within this structure that affect the region in multiple ways. The following chapter will focus on providing more detail about the role this structure plays in modulate regional precipitation patterns. The analysis presented provides information that is very useful as provides new insights that can be useful for improving our understanding of the transport of moisture in the IAS region. From the results, at least three important problems are highlighted to be considered: a) the analysis of how the AMS influence modifications in the trajectories that follow the air parcels that carry moisture towards Central America will require more attention. Understanding the response of this interaction to the climate modes will lead to a valuable improvement of our comprehension of the Americas climate as an integral system. Such analysis may provide us with interesting information of the effect of the regional monsoon-like circulations in the variability of precipitatio over Central America and how the CLLJ is an important element of the AMS. b) convection over South America as a modulator of precipitation in Central America via changes in the activity of the NSAS. This

moisture source located over northern South America has been just mentioned and there is a lot of work to be done. The results of this work encourage a detailed analysis of this source and further questions open new problems. One may think of the importance of the SAMS for the availability of moisture for the NSAS and also how does the extreme precipitation regimes of the Northeast of Brazil may exhert a remote influence over precipitation in Central America via this source. c) The problem of orographycally triggered precipitation over Central America and the study of the observed different precipitation patterns. With the information that the Lagrangian approach provide for the three dimensional structure of the moist air flow, we can analyse in detail how moist air from the east interact with the Central American mountain range and provide more information of the Caribbean and Pacific precipitation regimes beyond merely indicating that is caused by the effect of local topography.

8

The CLLJ and the modulation of the moisture transport

At the end of chapter two, among the main features of the climate in the IAS region, the CLLJ was introduced. Later, in chapter seven, the importance of low level winds for the regional transport of moisture was highlighted based on the average pattern of the trajectories followed by air parcels that precipitate over different regions of Central America. The presence of the CLLJ was used to explain the predominant features of the spatial distribution of the Caribbean Sea evaporative source of moisture. Moreover, it was indicated the simple process through which precipitation is inhibited in the presence of the CLLJ maximum winds. How this structure inhibits the transport of moisture from other sources (in agreement with results from previous studies) was also mentioned. Herein we are interested in a more detailed Lagrangian overview of the transport of moisture. Despite the importance of the five sources, we are now particularly interested in the transport of moisture from the Caribbean Sea and the role of the CLLJ on its modulation.

8.1 Mean structure of the transport of moisture from the Caribbean

From the vertical structure of the transport of moisture from the 'Atlantic regime', the presence of well defined low level air streams was identified. we notice how the influence of these air

streams becomes more important (in terms of amount of air particles and moisture) when the receptor (sink) is located to the north. The latter is basically a result of the presence of the CLLJ, which is responsible for the modulation of the transport of moisture over the Caribbean. A first point to asses is how do the air streams related to precipitation over Central America react to the presence of the CLLJ. Figure 8.1 presents the monthly mean clusters of air streams associated with precipitation over each subregion of Central America with the contours of mean zonal wind at 850hPa. The vertical structure of the clusters (air streams) is shown for the first 96 hours previous to the arrival of the air to the target (where it precipitates). This corresponds to the time in which the air particles undergo larger moisture changes. During winter the flow is relatively dry and the distribution of air particles that accounts for precipitation over Central America is quite uniform. During spring, moisture increases along the trajectory of the air over the easternmost Caribbean and the intensification of the moisture uptake is noticed. The moisture uptake increases so that in May reaches a maximum approximately over 75W, which is actually the location of the CLLJ core (in good agreement with the forcing of the winds on oceanic evaporation as indicated in chapter 1). Note that after the February maximum of the CLLJ, winds are decreased at the end of spring and a new intensification of the easterlies occurs towards the summer maximum. Moisture uptake is increased by the intensification of the winds and the speed of the wind flow is such that air can travel to the west but not as strong as to force most of the airmass to cross to the Pacific. This enhances the moisture losses over Central America. The wind flow from the east does not yet have a completely developed northward branch. At this point the wind still has an important southwestward component that favours precipitation over Central America.

In summer, as the CLLJ intensifies and the northward branch is developed, the distribution of the amount of air particles related to precipitation decreases considerably over the southern target regions compared to the increase observed for those over the northern receptor locations. A moisture uptake maximum is still enclosed by the CLLJ core and we also notice changes in the vertical structure of the trajectories followed by the precipitating air particles. For spring the moister jet-linked trajectories are below 1500 m, while in summer the air has been lifted and is located above this level.

This is an interesting difference when compared to the flux during the February maximum. The reason for this differences in the vertical structure has to do with the structure of the CLLJ itself. An important detail is that, depending on both the wind speed and altitude of the flow, due to to

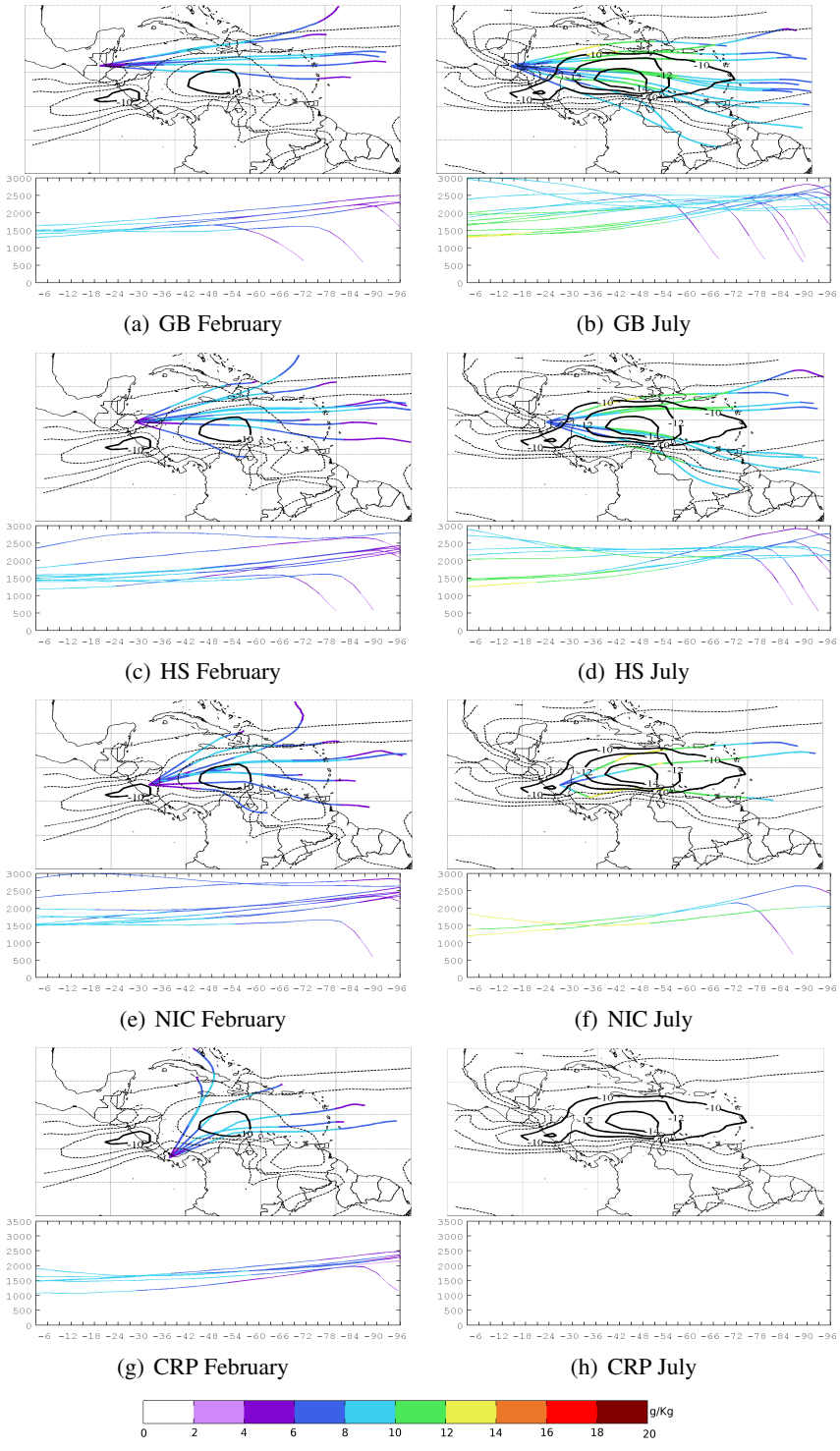

(a) GB February (b) GB July

(c) HS February (d) HS July

(e) NIC February (f) NIC July

(g) CRP February (h) CRP July

Figure 8.1: Zonal and vertical structure of the moisture transport associated with the CLLJ for each subregion (GB upper panel, HS upper middle panel, NIC lower middle panel and CRP bottom panel). February for left panels and July for right panels and October for bottom panels. Colors represent the average moisture content in g/Kg and the zonal wind at 850 mb is contoured with the black lines for the horizontal structure of the trajectories. The plots show the twenty years averaged clusters associated with the CLLJ that were found to precipitate over each subregion.

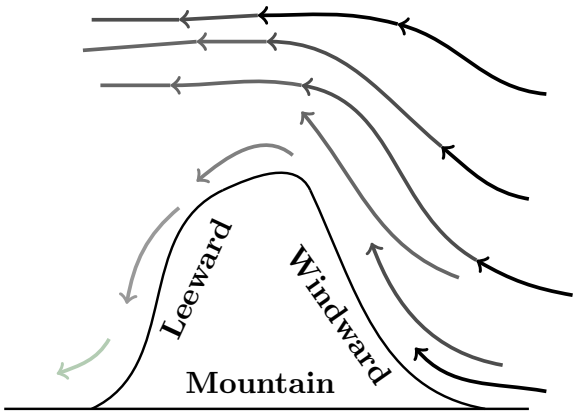

Figure 8.2: Schematic representation of orographic precipitation process. The intensity of the gray indicates the moisture content (black for moist and light gray for dry). Moist air (easterly flow in this case) is lifted due to the presence of a mountain, precipitation occurs and the air (dry because of the moisture loss due to rainout) descends over the leeward side of the mountain.

the presence of the mountain range in Central America, topographic convection can be forced which implies losses of moisture on the leeward of the mountains when part of the rainout occurs on the windward side (see diagram in figure 8.2). This is associated with the increase in the contributions from the CS. This will correspond to a more intensified magnitude of the $(E-P)^{-6}$ in the inner Caribbean. This occurs during the February maximum of the CLLJ, with strong very low-level winds. On the contrary, during the summer maximum, as was pointed out in previous chapter, the vertical structure of the CLLJ indicates the jet to be located at a higher altitude. This means that the strong winds can pass through to the Pacific with minimum interaction with the mountain system so that topographic precipitation is not enhanced as it is when the air flow is lower. As indicated in chapter 2 and depicted in figure 2.8.b, during the July maximum the CLLJ penetrates higher in the troposphere. This is important since it may be related to an additional influence of the CLLJ in triggering precipitation. The CLLJ is then related to precipitation not only by transporting moisture between regions but also by forcing variations in the instabilities that lead to the formation of precipitation. Moist air particles that go higher in the atmosphere do so because of reduced moist static stability and greater convection. When the level of moist air is higher the layer enhancing convection becomes more unstable favouring precipitation in a sub-saturated environment. This may account for

the differences observed in the contributions to precipitation during the two CLLJ maxima, for which even when precipitation is reduced it is still larger for summer compared to winter.

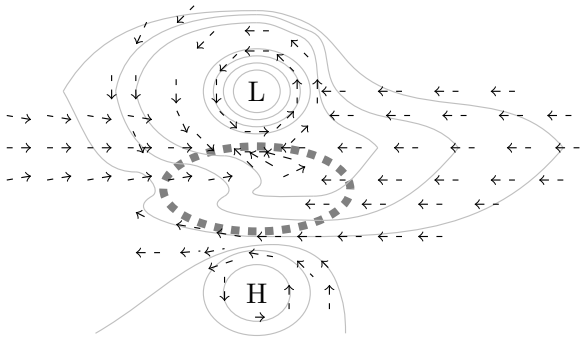

Figure 8.3: Schematic representation of the Gill-type heat induced response (horizontal view of the field) with the center of the SST heating anomaly indicated with a dashed oval

During autumn, more air particles are transported to Central America from the Caribbean and moisture uptake occurs over the Caribbean Sea. Moreover, the air flows at higher altitudes for the northern Central America regions compared to the southern, for which a very strong flow is observed at lower altitudes. This wind flow carries important amounts of moisture and we observe that the separation of the streams becomes smaller and that the moisture content is greater when the receptor/sink is located in the south. This indeed, may not be associated with the CLLJ but rather with the SST gradient between the Caribbean Sea and the ETPac, which exhibits a maximum during October due to the seasonal cycle of the WHWP as mentioned in chapter 2. The effect of warmer Caribbean SST induces Gill-type heat-induced response *(Gill, 1988)* (see diagram in figure 8.3). As part of the anomalous cyclonic circulation response at low-levels, the easterly flow weakens to balance the SST gradient, thus reducing the intensity of the flow from the Caribbean that enables most of the moisture content carried by the easterlies to precipitate over Central America (see figure 6.2.d chapter 6) (note that low level wind convergence may be enhanced for very strong gradients). This heat-induced response is therefore strongly linked with the sharp decrease of the easterlies that feature the absolute minimum of the CLLJ during October. Note that this thermally driven response of the flow provides a mechanism through which the role of the WHWP can be explained.

8.2 The role of the CLLJ as a modulating structure

A fundamental point here is the position of the analysis region. As the CLLJ develops nearby the equator the geostrophic approximation may not be suitable to describe very local features of climate. From the structure of the CLLJ, it follows that a south(equator)-ward component is developed which highlights the importance of considering the problem of the non geostrophic component of the flow. The two components of the non geostrophic wind play a role for determining the locations over which divergence (convergence) is enhanced or not. The basic dynamic assumptions lead to an approximate representation of the patterns of convergence and divergence produced by the variations in the intensity of the wind for low level jets. Those patterns are produced by the cross stream component of the non geostrophic wind as a result of the accelerations (decelerations) of the wind flow at the jet entrance (exit) region. Upper level divergence is enhanced by strong along-stream variations in the flow since the along-stream component has an effect on the convergence and divergence patterns due to curvature. The combined effect is the enhancement of the upper level divergence in the right entrance and left exit regions. This is discussed in *Amador (1998)*, and implies a pattern of convergence (divergence) in the rear/entry (front/exit) to the left of the jet axis and the opposite pattern to the right of the jet axis, as summarised in figure 8.4. In the case of the CLLJ this relationships provide an explanation of the differences observed in the distribution of precipitation over Central America between the northern and southern regions. This is the reasoning proposed by *Amador (1998)*, following the representation of the cross circulations. The importance of this lies in that it provides a dynamical framework that can be used to explain the role the CLLJ has for moisture transport as potential modulator of precipitation along with the activity of the neighboring sources of moisture.

By analysing the mean wind fields, SST, mean clusters of trajectories and their corresponding changes in moisture and vertical velocity within the CLLJ, we propose a simple model to describe the main features of moisture transport to Central America. The idea of this simplification we propose is to provide a general notion of the most important mechanisms that interact to determine whether the moisture transport via the CLLJ results in increases or decreases of precipitation over the region. For the months in which the CLLJ is more intense, several scenarios can occur: a) winds can be very strong, the structure of the CLLJ is well defined and most of the moisture goes directly to the Pacific side, b) CLLJ intensity is not so

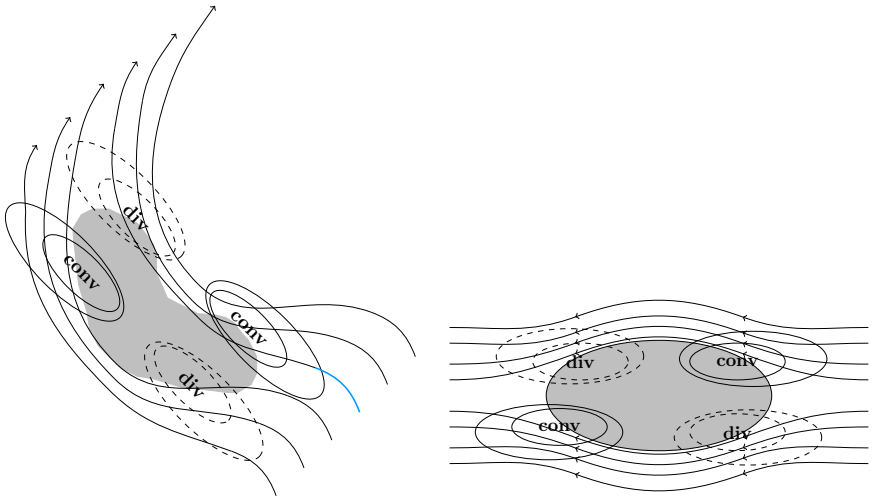

(a) Summer (b) Winter

Figure 8.4: Schematic representation of divergence and convergence pattern associated with the CLLJ. Panel a shows the development of the north component of the CLLJ and panel b represents the mostly zonal flow characteristic of winter.

strong and moisture can be lost over Central America (similar to what occurs when the wind flow interacts with local topography), c) easterlies are very weak and moisture is not even able to reach the Caribbean coast of Central America before raining out over the Caribbean. For the first two cases, an additional mechanism must be taken into account, the SST gradient between the Caribbean and Pacific. And a generalisation can be proposed that: a) A very strong CLLJ, with winds higher than 15 m/s (regardless of the direction of the SST gradient between the Caribbean and Pacific) results in most of the moisture being transported directly towards the Pacific (fig 8.5.a), b) CLLJ is intense and the SST gradient points to the Pacific, thus resulting in an even stronger CLLJ with most of the moisture passing through the Pacific (fig 8.5.b), c) The CLLJ is strong and the gradient between the two ocean basins is almost nil, some of the moisture transported from the Caribbean Sea can contribute to precipitation over Central America (fig 8.5.c), d) the CLLJ is intense and the Caribbean Sea is warmer than the Pacific, thus resulting in a decrease of the winds that then enhances the moisture transport to Central America, where precipitation due to contributions form the CS are increased (fig 8.5.d), e) the easterly flow is not strong and the SST gradient indicates a warmer Pacific, a thermal forcing accelerates the easterly flow moderately and transport of moisture to Central America from the Caribbean is enhanced (fig 8.5.e), f) As in e but for somewhat more intense winds, wherein

moisture transport is enhanced and if the conditions for triggering convection are favourable, the contributions to precipitation from the CS are increased (fig 8.5.f), g), the easterly flow is slower and no significant gradient between the Caribbean and Pacific SST is observed, this situation implies that no thermal forcing accelerates the winds and moisture transport will depend solely on the wind speed so that if it is between 8 and 12 m/s the transport is enhanced (fig 8.5.h), i) wind speed is between 8 and 12 m/s and the SST gradient points towards the Caribbean, a decrease of the easterlies is thereby responsible for a decrease in the transport of moisture. It is important to point out that whether the intensity of the easterly flow is very strong or not is determined by a threshold wind speed that according to the mean fields for the analysis periods can be set to approximately 12 m/s.

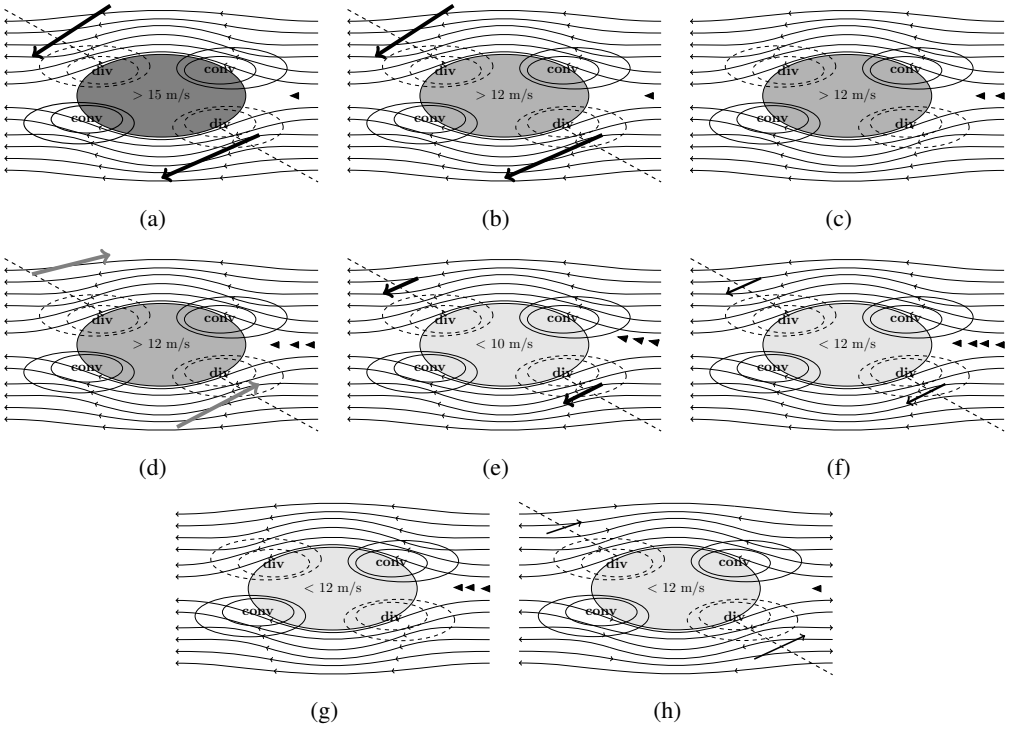

Figure 8.5: Sketch providing a summary of the conditions of the intensity of the CLLJ and the SST gradient between the Caribbean and ETPac that trigger the major changes in the transport of moisture from the Caribbean and associated precipitation. The direction of the temperature gradient is indicated with arrows (the size of the arrow is an indicative of the intensity of the gradient), black triangles are used to indicate the direction and intensity of the CLLJ (more triangles indicate stronger CLLJ).

Note that even when this is not a realistic model of the regional processes and does not account for all the scales of transport, it provides a good approximation for evaluating both the mean

state of the sources of moisture, transport and associated precipitation. Moreover, it may be useful to determine how changes in the wind and SST conditions can influence the components of the regional cycle.

8.3 The CLLJ as moisture transport and precipitation patterns modulator

Now that the mean structure of the transport of moisture from the Caribbean Sea (and even from the NSAS) has been presented and the mean structure of transport due to the CLLJ under the influence of the variability modes introduced, we are interested in analysing further details in regard to the role that the CLLJ may play. At the end of previous section, a simplified model of the transport of moisture in the region was presented which shows the interaction between some of the regional climate structures. In the present chapter the CLLJ has been determined to be associated with the efficiency of the transport and moreover with the spatial structure and the intensity of moisture uptake. These results derived from the trajectories suggests that the structure and the intensity of the CLLJ play a major role in the transport of moisture. Here we present an analysis of the mean features of the CLLJ combined with the results on the sources of moisture in order to identify if there are any reliable variability patterns that may match between the two spatial structures. The analysis of the mean fields for both parameters do not provide the information needed to evaluate the relation from a dynamical point of view. Since we are more interested in how variations in both may be associated we use composites for the positive and negative phases of the analysed signals. This provides a further explanation of the results described at the end of chapter 5 in terms of the dynamics of transport just discussed. The $(E-P)^{-6}$ fields, zonal wind speed and vertical velocity at 850hPa are used for this analysis. Composites are computed as described in chapter 4. Vertical velocity is used to identify the convergence/divergence patterns associated with the structure of the CLLJ and evaluate how they are associated with the evaporative sources by modification of the divergence/convergence regions.

In the case of ENSO, we notice that a positive phase weakens the February maximum (fig 8.6.a) and the convergence associated with the left of the jet core does not develop. This may result in the absence of precipitation on the Caribbean coast of Central America since divergence is increased (and thus, convection suppressed). This pattern continues during the

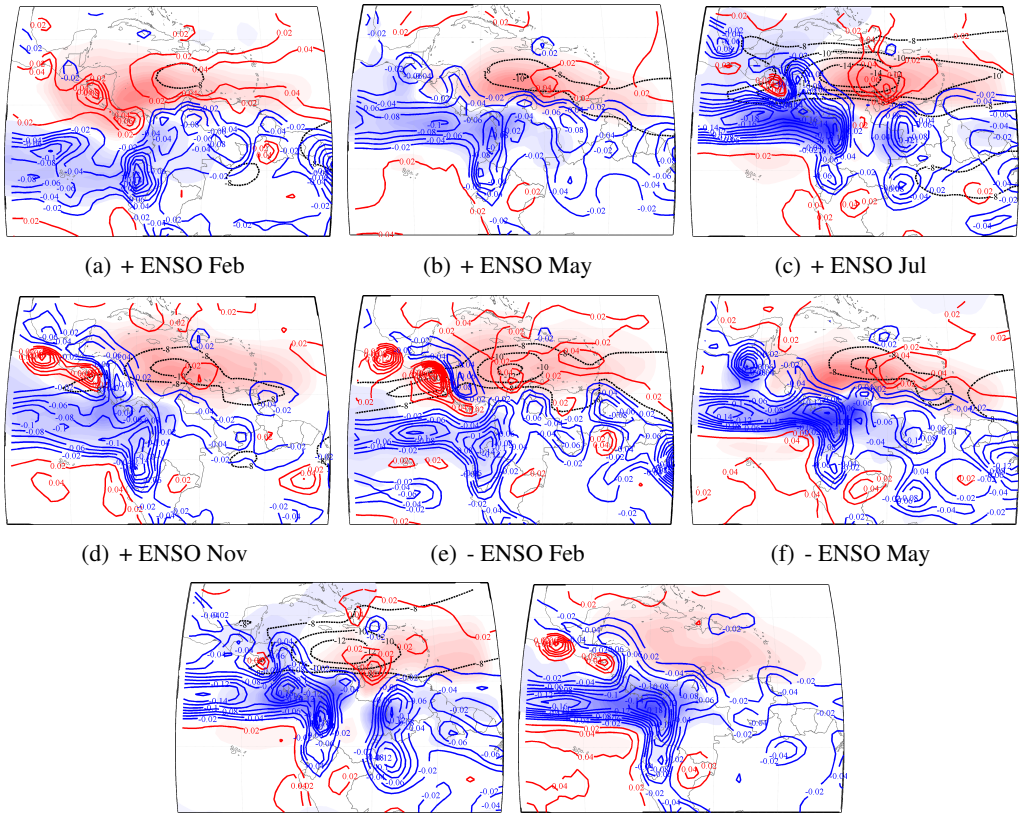

(a) + ENSO Feb (b) + ENSO May (c) + ENSO Jul

(d) + ENSO Nov (e) - ENSO Feb (f) - ENSO May

(g) - ENSO Jul (h) - ENSO Nov

Figure 8.6: Composites of $(E-P)^{-6}$ (shaded contours), zonal wind speed (black contours) and vertical velocity at 850hPa (red and blue contours) for ENSO.

rest of winter and part of spring. The latter is in good agreement with the known effect of the CLLJ to decrease the rainfall maximum of May during positive ENSO (fig 8.6.b). This pattern is reversed during negative ENSO such that the convergence occurs as a result of the intensification of the jet (fig 8.6.c). Note that in May the evaporative source in the CS is decreased in the positive compared to the negative phase of ENSO (fig 8.6.f). This results from the decrease of the jet intensity and the small SST gradient between the CS and the ETPac. During July (fig 8.6.c) the situation is reversed to that of February, due to the development of the northward branch, the divergence/convergence structures are also curved and during the negative phase the intensification of the jet increases the convergence, probably as a result of the westwards bifurcation.

Under the influence of NAO a weaker CLLJ is observed during February for the negative

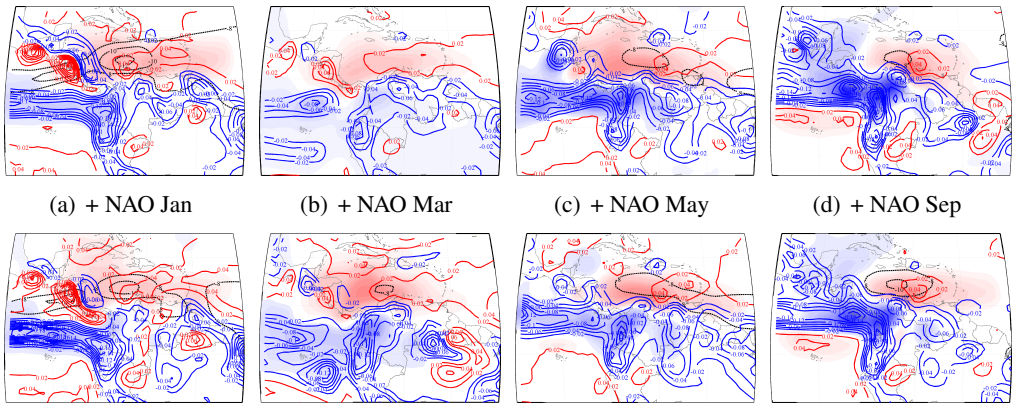

(a) + NAO Jan (b) + NAO Mar (c) + NAO May (d) + NAO Sep

(e) - NAO Jan (f) - NAO Mar (g) - NAO May (h) - NAO Sep

Figure 8.7: Composites of $(E-P)^{-6}$ (shaded contours), zonal wind speed (black contours) and vertical velocity at 850hPa (red and blue contours) for NAO.

phase (fig 8.7.a) while a strengthening occurs for the positive phase (fig 8.7.e). As with ENSO, a stronger jet is related to well defined convergence/divergence patterns associated with the presence of the strong CLLJ. From this, the convergence indicates (as is also observed and known from observations) that precipitation increases over this region. The intensification of the easterly flow during spring, linked to the negative phase, favours the intensification of the CS.

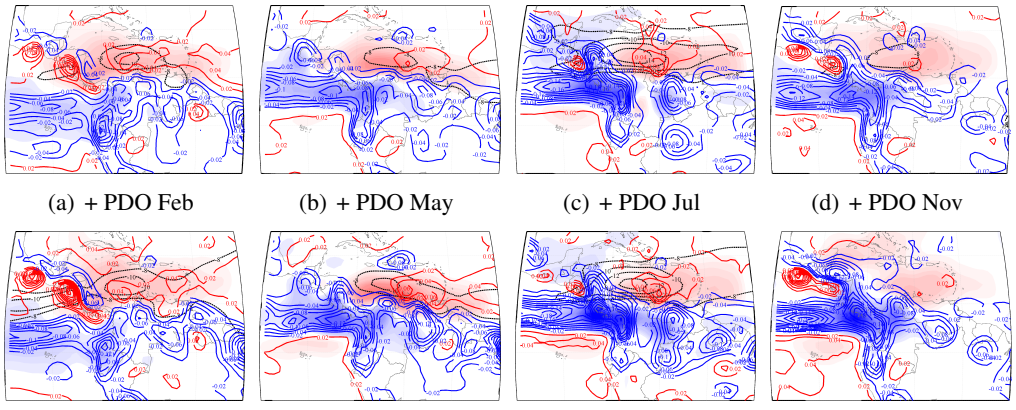

(a) + PDO Feb (b) + PDO May (c) + PDO Jul (d) + PDO Nov

(e) - PDO Feb (f) - PDO May (g) - PDO Jul (h) - PDO Nov

Figure 8.8: Composites of $(E-P)^{-6}$ (shaded contours), zonal wind speed (black contours) and vertical velocity at 850hPa (red and blue contours) for PDO.

The case for the PDO shows little evidences of variations, the Caribbean seems to be not very sensitive to this mode as does the SST in the adjacent tropical Pacific. However, it can be noticed in figures 8.8 that the positive phase of the PDO is associated with divergence over Central America (particularly over the Pacific coast) and more convergence during the negative phase. This is in agreement with the findings shown in chapter 5, where we find that the contributions from the ETPS experience a significant decrease during the first part of the 1980s, a period characterised by a positive PDO.

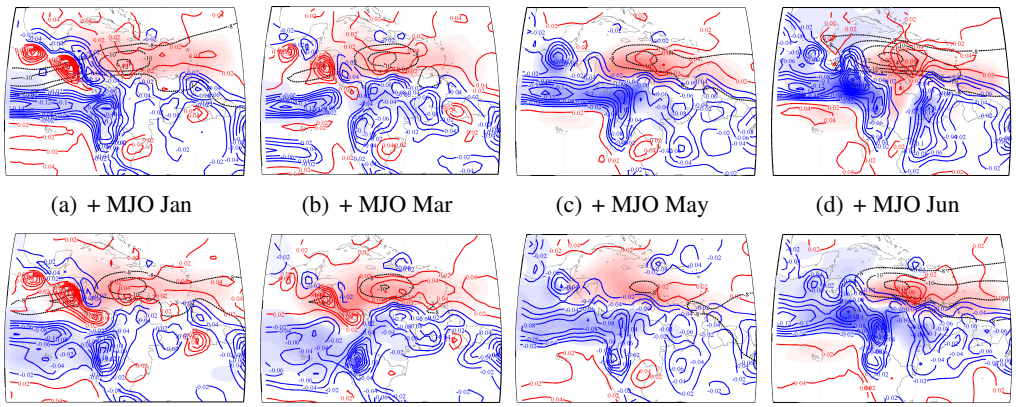

(a) + MJO Jan (b) + MJO Mar (c) + MJO May (d) + MJO Jun

(e) - MJO Jan (f) - MJO Mar (g) - MJO May (h) - MJO Jun

Figure 8.9: Composites of $(E-P)^{-6}$ (shaded contours), zonal wind speed (black contours) and vertical velocity at 850hPa (red and blue contours) for MJO.

During February when the MJO is in a positive phase, the jet is increased and as a result the convergence pattern, with a similar pattern for negative phase during July in which the bifurcation of the jet occurs and seems to have an effect joint with the increase of the flux from the ETPac due to the ascent to the GoM. The negative phase is associated with the intensification of the mentioned patterns as the the wind flow that characterises the jet is more confined. This implies that the presence of the CLLJ and associated convergence over the Caribbean coasts of Central America is useful to explain heterogeneity of the regional precipitation patterns.

In general terms it can be said that a strengthened CLLJ intensifies the convergence over the eastern Central American coast. This is associated with the increase of precipitation to which moisture transported from the central Caribbean contributes. Note that what defines the convergence/divergence patterns in the Caribbean and Central America is basically the structure of the CLLJ as given by the simple dynamic considerations of the cross circulations (represented

in the graphics by the vertical velocity at 850hPa). The superposition of the CLLJ intensity and vertical velocity altogether with the E-P field illustrates quite well how the CLLJ influences the structure and intensity of the evaporative source of moisture in the Caribbean and the relation this has with the cross circulation pattern. As noticed from the cases described before, there are some cases, especially during spring, when the presence of intensified easterlies do not set the complete background for describing the intensity and extension of the source, as well as the efficiency of transport. It was mentioned that the SST gradient between the Caribbean and the ETPac region is a key determinant in those cases. Moreover, the gradient is in part a measure of the activity of the WHWP. Based on the results obtained and the discussions, a conceptual model is proposed for the distribution of the evaporative source of moisture over the CS as it accounts for precipitation in Central America.

One definition of the CLLJ intensity through an index as defined in chapter 4, the SST gradient between the Pacific and the Caribbean Sea and the total integral of the backward conditional $(E-P)^{-6}$ for the Caribbean Sea for the neutral years as well as for the positive and negative phases of the variability modes is used to identify the pattern that defines the transport of moisture from the Caribbean Sea and Central America. Composite seasonal cycles of the monthly indices are shown in figure 8.10, left panels for the CLLJ index, middle panels for SST gradient and right panels for conditional (E-P)-6. It has been shown how the major changes occur as expected during the months when precipitation over Central America presents both maximum and minimum values. During the periods in which the CLLJ is a maximum, the transport is directly driven by the jet. Convergence and divergence patterns associated with the jet axis are key to define the horizontal extension of the regions that may contribute as sources and of those in which low level convergence is enhanced and associated with precipitation. During those periods in which the CLLJ is not the dominant feature, variations in the transport of moisture are triggered by the SST gradient between the Caribbean and the ETPac. As the difference between SST in the Caribbean and the Pacific becomes more positive, the contributions from the CS drop while the fall of this gradient in favour of a warmer ETPac enhance the increase of the transport. More importantly, a CLLJ intensity of the order of 12 m/s seems to be the threshold to determine when the CLLJ allows moisture to be transported to Central America. For larger values of the CLLJ intensity, moisture from the Caribbean is transported to the Pacific side (or northward to the Gulf of Mexico). This reduces the direct delivery of moisture to Central America. Conversely, below this value the role of the SST gradient becomes important

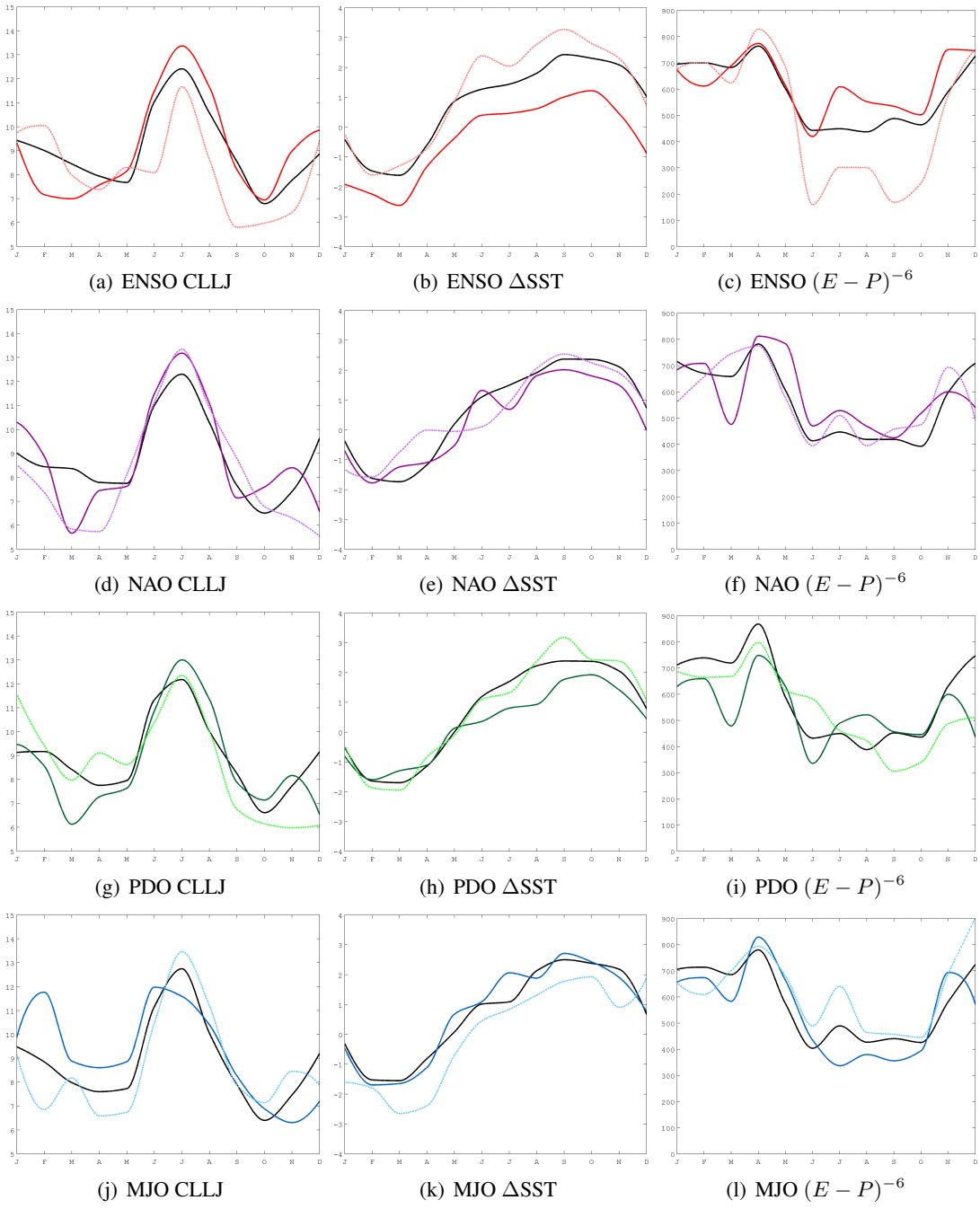

(a) ENSO CLLJ (b) ENSO ΔSST (c) ENSO $(E-P)^{-6}$

(d) NAO CLLJ (e) NAO ΔSST (f) NAO $(E-P)^{-6}$

(g) PDO CLLJ (h) PDO ΔSST (i) PDO $(E-P)^{-6}$

(j) MJO CLLJ (k) MJO ΔSST (l) MJO $(E-P)^{-6}$

Figure 8.10: Composite seasonal cycle of the monthly indices for the intensity of the CLLJ, SST gradient and conditional (E-P)-6 over the Caribbean Sea for the positive and negative phases of ENSO, NAO, PDO and MJO. Note that darker colours represent the positive phases while lighter colours the negative phases, mean neutral conditions are indicated with a black line.

in determining the features of transport. The interaction among mechanisms is quite complex as many processes are acting at the same time and interactions are rich in feedbacks.

8.4 Moisture transport, CLLJ and variability modes

In chapter 5, the effect of ENSO, NAO, PDO and MJO on the spatial distribution and intensity of the sources of moisture was described. In general, the largest variations were observed for the CS which suggests a large variability of this source of moisture. It is important to mention that since we are interested in the complete representation of the response of the backward trajectories, instead of computing composites, the most extreme phase of each considered variability modes were selected. We want to make clear that this is not directly comparable to the anomalies presented in chapter 5, even when the main structures of the changes forced by the modes is. Those months with most extreme values for each correspondent phase were selected for the comparison, this in order to compare a strong negative with a strong positive phase for each mode to show the contrast . Instead of using clustering to reduce the dataset for the cases, we preferred to make a selection of the particles to isolate a particular transport associated structure. The easterly flow was selected as moisture conveyor structure, with special attention to the CLLJ. For this reason, from the total of particles, those that lost moisture over the receptor/sink subregions in which Central America was divided were selected. Those associated to the clusters that circulate from the Caribbean and along the time their trajectories were below 2500m were extracted. After this, another selecting condition was imposed, those particle that have circulated at any time over the region of influence of the CLLJ were considered as associated to the main easterly flow that features the CLLJ (as indicated in chapter 4). After the selection process, the particles that were at any time associated with the CLLJ when active or with its influence region when inactive were retained for the analysis. The results are presented for the months in which the CLLJ is maximum (February and July), minimum (October) and dor the spring (May), the selected events were selected as the months with the maximum/minimum value for the corresponding climate index as shown in table 8.1.

ENSO

We are interested in the months were precipitation becomes more important as well as the transport associated structures. Since larger variations were found to occur for February, May,

		Feb	May	Jul	Oct
ENSO	+	1983 (2.18)	1992 (2.04)	1997 (1.97)	1997 (2.28)
	-	1989 (-1.62)	1988 (-0.47)	1988 (-1.38)	1988 (-2.33)
NAO	+	1989 (2.00)	1992 (2.63)	1994 (1.31)	1986 (1.55)
	-	1986 (-1.00)	1990 (-1.53)	1993 (-3.18)	1980 (-1.77)
PDO	+	1987 (1.75)	1996 (2.18)	1983 (3.51)	1997 (1.61)
	-	1991 (-1.19)	1999 (-0.68)	1999 (-0.66)	1999 (-2.23)
MJO	+	1985 (1.69)	1990 (0.92)	1981 (1.09)	1999 (1.28)
	-	1980 (-1.06)	1983 (-0.85)	1987 (-1.19)	1997 (-1.39)

Table 8.1: List of the months selected (February, May, July and October) as extreme events of ENSO, NAO, PDO and MJO based on the climate indices time series, the index is indicated.

July and October, the discussion will be focused on these months. In order to consider the variables of geopotential height, SST differences and the intensity of the CLLJ, the indices defined in chapter 4 are summarised in figure 8.10 . For the case of ENSO, during the warm phase of February 1983, a reduction of the winds is noticeable that enhances the efficiency in the transport of moisture to Central America. Due to the structure of the February maxima, the major transport occur towards CRP and decreases as the sink is located north (8.11.c). During the negative phase (1989), the CLLJ is intensified so that less moisture is transported to Central America. The identification of two air streams at different heights implies that stronger winds during this month enhances the downward transport of drier air. The positive phase is associated with an increase in the geopotencial gradient while the opposite occurs for the negative phase at the same time that SST is warmer over the ETPac. During May, the results suggests an intensified moisture flow from the Caribbean to CRP for the positive phase of 1992 (fig 8.11.g) for which the uptake region is located over the complete Caribbean basin opposite to the negative phase of 1988 when the amount of transported trajectories is smaller. The pattern is similar to February and the transport decreases northward (figs 8.11.c, 8.11.f). During the strong warm ENSO, July (1997) the CLLJ is significantly intensified by the raise of positive SST anomalies over the ETPac that induce a strengthen of the easterlies, therefore, of the CLLJ. This result in a marked decrease of moisture transport from the Caribbean Sea that is particularly sharped for Nicaragua (fig 8.11.k). This results is remarkable since this decrease may be related with the presence of drought conditions for this period over Central America as

indicated by the mean PDSI, which is higher for Nicaragua (see figure 8.12) During the cold event of 1988, the decrease of the intensity of the CLLJ is associated with the intensification of the transport. During October, ENSO seems to be an important influence in the variations of precipitation between the different regions of Central America. Warm ENSO favours the transport of moist air to the north while the cold phase does for the south. As the intensity of the CLLJ is more reduced that normal for the cold phase, the transport is enhanced and moreover the uptake of moisture occurs over a more extended are of the Caribbean and beyond the Lesser Antilles, as suggested by the anomalies composites of the E-P field for cold ENSO during summer.

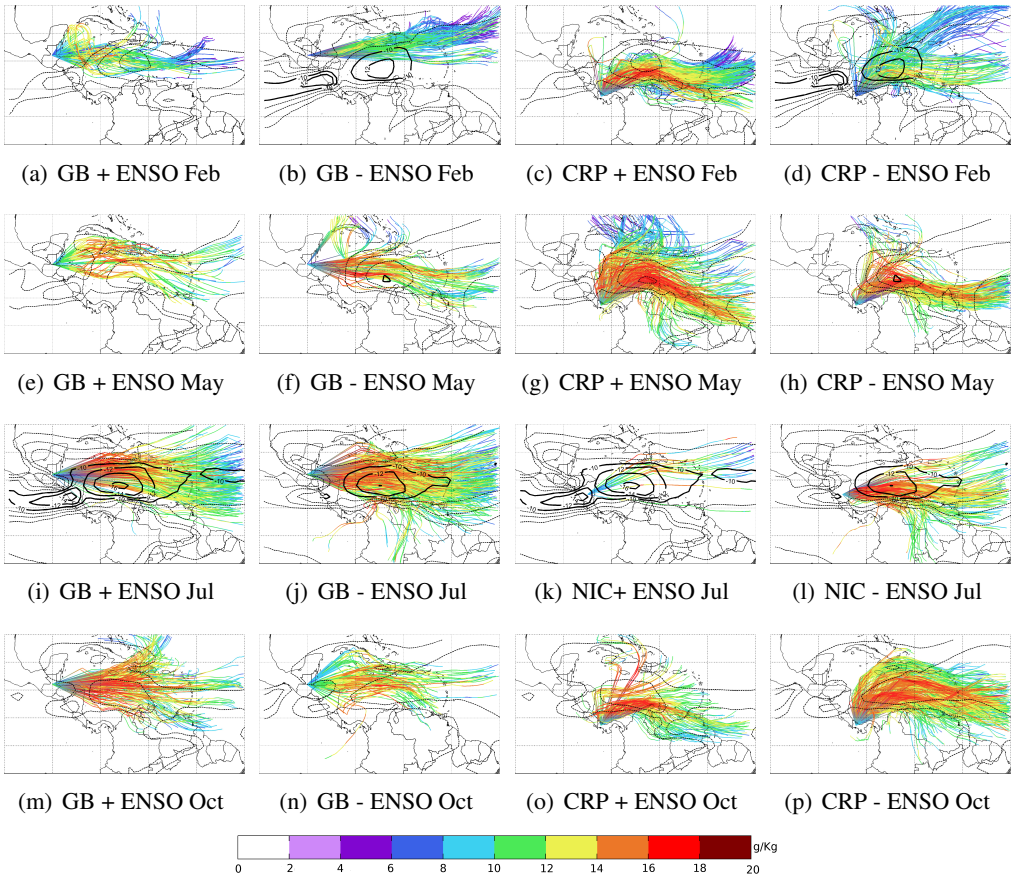

Figure 8.11: Mean trajectories analysis of transport of moisture for selected extreme ENSO events, upper panel February, upper middle panel May, lower middle panel July and bottom panel October for the indicated regions.

NAO

The influence of NAO is more related to the structure of the flow rather than the amount of moisture transported for February, even when the air is drier during the negative phase (1986) (fig 8.12.d). An interesting observation is that for the positive phase of 1989, the flow that reaches Nicaragua presents a well separated structure of drier upper level flow and moist low level flow (fig 8.12.c). A strong intensification of the transport of moisture is noticed with strong uptake over the Caribbean (more intense as southward) and with an increase of the moist flow from NSAS being transported by the easterlies associated with the CLLJ core location (fig 8.12.g, 8.12.h). For the negative phase the decrease of the transport efficiency that lead precipitation over Central America is associated with the intensification of the easterlies. During July, the results suggests that few influence of the NAO is exerted to the wind flow (as expected since the major variations may be associated to winter since is a winter time structure). Transport is slightly larger for the negative phase. In October, a small intensification of the easterly flow is associated with the reduction of the moist flow contributions to precipitation over Central America (fig 8.12.o).

PDO

The influence of the PDO alter both the moisture content transported and the direction from which the flow is travelling. During the positive phase of February 1987, dry air from the Caribbean and the Gulf of Mexico rise its moisture content in from of Central America coast to precipitate in the following 24 hours over Central America (fig 8.13.a, 8.13.c). Whereas during the negative phase of 1991, the CLLJ was intensified and transport decreased (fig 8.13.b, 8.13.d). During May, for the positive phase of 1996 the transport is increased and the structure of an early CLLJ is noticed. As the intensity increases but is not as large as to force all the air to pass to the Pacific, the transport of large amounts of moisture is very efficient, particularly to CRP (fig 8.13.g) compared to the situation of the negative phase of 1999. Beyond the earlier development of the CLLJ, a southward branch is well defined and moisture uptake takes place along the southernmost Caribbean. During July, an enhanced CLLJ is noticed for the positive phase (fig 8.13.j). A bit larger transport for the positive phase of 1983 for the northernmost part of Central America and for CRP with less transport for the HS region and particularly reduced transport to Nicaragua, which is actually almost null. This may be associated with the 'bands' that divided Central America into very dry and moister regions. The case of the

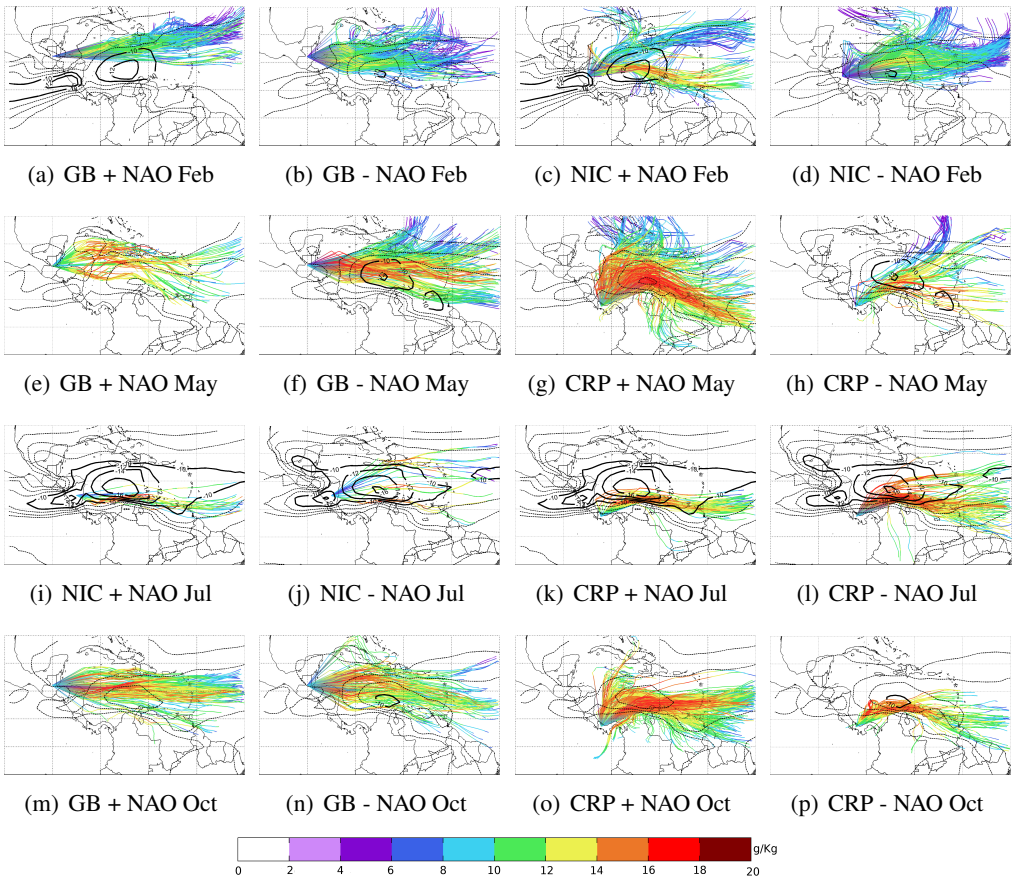

Figure 8.12: Mean trajectories analysis of transport of moisture for selected extreme NAO events, upper panel February, upper middle panel May, lower middle panel July and bottom panel October for the indicated regions.

dramatic reduction of the transport to Nicaragua corresponds again to a severe drought event. It can be concluded in this case, that drought conditions over Nicaragua are strongly forced by the decrease of the transport of moisture from the CS . Finally, during October, the positive phase of 1997 presents stronger transport of Central America (fig 8.13.m) and reduced for CRP (fig 8.13.o) while the negative phase of 1999 presents the opposite pattern and the transport to CRP is stronger compared to the positive phase when is very small (fig 8.13.o, 8.13.p).

MJO

The structure of the sources of moisture suggests that for positive (negative) MJO phase, there is a decrease (increase) on the intensity of the inner Caribbean as a source of moisture for

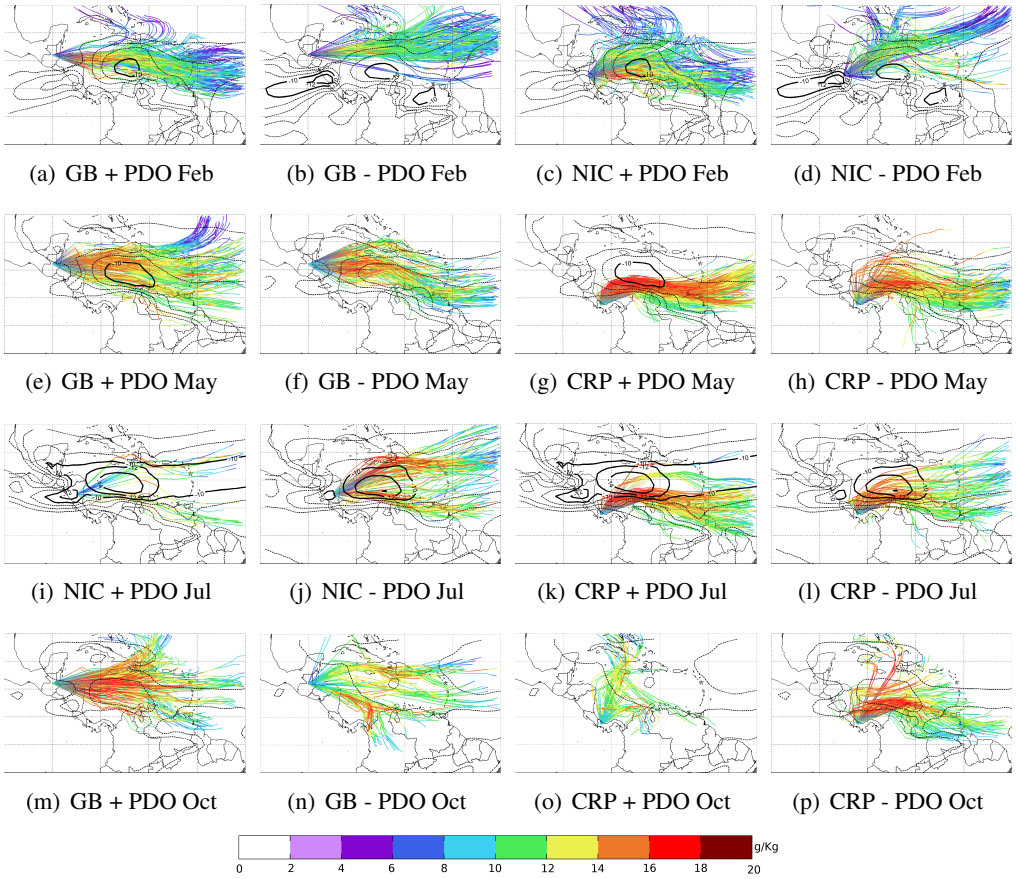

Figure 8.13: Mean trajectories analysis of transport of moisture for selected extreme PDO events, upper panel February, upper middle panel May, lower middle panel July and bottom panel October for the indicated regions.

Central America, as is observed from the structure of the flow for February. This is associated with the strengthen of the CLLJ during positive MJO (1985) that lead to stronger winds and less contributions to precipitation (fig 8.14.a, 8.14.c). In comparison the CLLJ is decreased during negative MJO of 1980 and moisture transport if intensified towards Central America, with an important southward component that increases the transport to CRP (fig 8.14.d). The positive MJO of May 1990 is associated with an intense earlier development of the CLLJ. The earlier developed northward branch results in the reduction of the transport of moisture to southernmost Central America (fig 8.14.g). Conversely, the transport in greatly intensified during the negative phase of 1983, for which moist air comes outside the Caribbean (the source

is extended to the tropical Atlantic[1]. This phase event was characterised by the presence of an anomalous cold tropical Atlantic. During July, for the negative MJO of 1987, a very strong intensification of the flow undergoes, however, its effect is not the suppression of transport to Central America completely but the funneling of the winds. Note that intense moisture increases are observed below the axis of the jet in agreement with the enhancement of divergence to the left of the axis of the jet in the front. Meanwhile a relatively uniform distribution of the transport is noticed for the 1981 positive phase (figs 8.14.i-l). During October, the positive phase of 1999 is featured by small transport of moisture from the Caribbean Sea by the easterlies with an even more reduced transport to CRP (fig 8.14.o). This results in a more reduced than normal easterly flow during October. On the other hand, for the negative event of 1997 an increased transport is observed, note that this corresponds to a warm ENSO related event, which implies winds intensification. Since winds during October are very reduced, the intensification due to the warm phase of ENSO may help to favour the transport to Central America. It is also important to note that under the positive phase, the flow from NSAS is able to reach northernmost Central America after gaining moisture over the Caribbean Sea.

The results shown in figure 8.11 allows to compare directly if the simplified model proposed in previous section is able to reproduce the mean response of the intensity of the moisture source to variations in the intensity of the CLLJ [2] and the SST gradient between the Caribbean and Pacific. It can be followed that in most of the cases, the results provided in figure 8.11 can be predicted by the simplified model. Which suggest that the performance of the model for evaluating mean conditions under determined circumstances is reasonably good. However, there are some cases in which the expected response of the source is found to be delayed compared to the observed. This differences, which are too few, are normally associated to those cases in which the intensity of the CLLJ is stronger than 14 m/s. Here we detect that when the CLLJ is very strong additional interactions need to be considered. Our proposal is that the response may be found in the vertical structure of the CLLJ. Indeed, those cases in which winds are stronger than $14 - 15m/s$ and the results observed in the average do not agree with those predicted from the model correspond to cases in which the vertical structure is modified. For very strong easterlies (larger than $14-15m/s$) in which the flow is confined to the lowest levels (below 1500m) the contributions from the source to precipitation are increased. This because

[1] the importance of anomalous SST over the tropical Atlantic has been studied by *Kucharsky et al., 2010*

[2] Easterlies over the same region of the CLLJ for those months in which the CLLJ is not active.

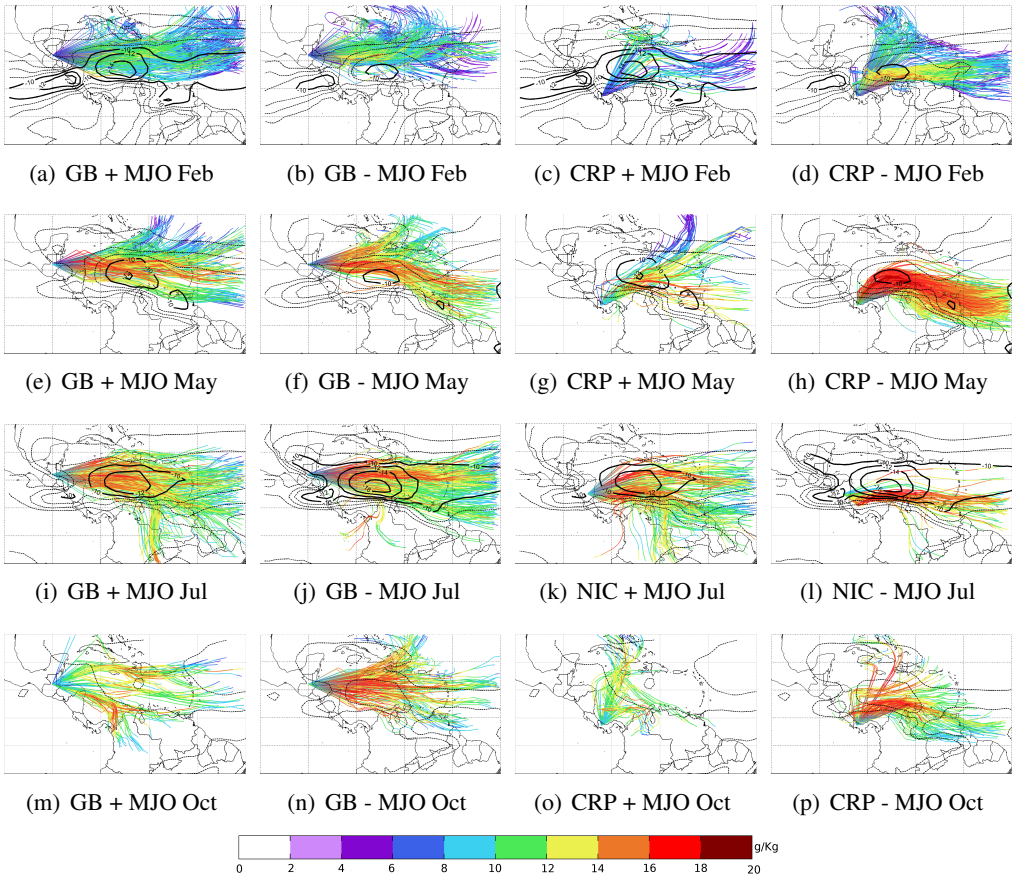

Figure 8.14: Mean trajectories analysis of transport of moisture for selected extreme MJO events, upper panel February, upper middle panel May, lower middle panel July and bottom panel October for the indicated regions.

topographic convection (fig 8.2) in enhanced so moisture transported from the Caribbean is more able to precipitate over Central America.

One can consider the role of the CLLJ by thinking on the structure of the jet as shown in figure 8.15 . The influence of the CLLJ in the transport of moisture and associated precipitation acts also via barotropic instability mechanisms as well as because of the vertical shear. The role that the CLLJ plays can be expressed as composed of two terms, one due to the presence of the divergence patterns in the rear and front of the jet and to the transport of moisture as follows from the decomposition of the divergence of the moisture flux (see equations 8.1 and 8.2). First term in equation 8.2 is key as it influences the distribution of precipitation whereas the second term is of importance for the modulation of the regional transport of moisture.

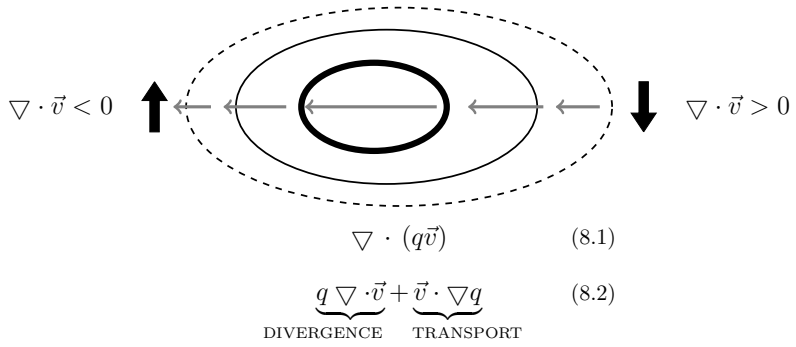

Figure 8.15: Schematical representation of a low level jet, gray arrows represent the mean wind flow which is stronger along the jet core with ascending motion in the exit and descending motion in the entrance of the jet.

The computation of these two terms may be useful to provide information on how the wind field modifies the divergence patterns and the transport. As a result, the sources of moisture associated with precipitation are modulated as a result of the variations of the trajectories and moisture content of the air masses that precipitates over Central America. As an example consider the case of the extreme positive and negative February ENSO events shown in figure 8.16 for which the terms in equation 8.2 are calculated and plotted.

Precipitation associated to the transport of moisture, role of the CLLJ and response to variability modes

The complexity of the interactions that take place in the IAS region are clear at this stage of the work. Despite the non-linearity of the climate system, determining the most direct linear relationship between different parameters may allow the identification of key connections between processes that may help to understand more complex interactions. Along this chapter, the role that the CLLJ plays as a moisture transport modulator structure, as well as its importance by increasing evaporation and convergence in the region have been discussed. To finally try to close the picture of the relationships between evaporative sources of moisture, transport and precipitation at different time scales, we would like to present a final discussion on the response of precipitation associated with the transport of moisture from the remote moisture sources. On the value of the work performed and as an additional contribution, we would like to establish a linkage between precipitation due to transport of moisture and the role of the CLLJ analysed from the perspective of the response of these three components (precipitation,

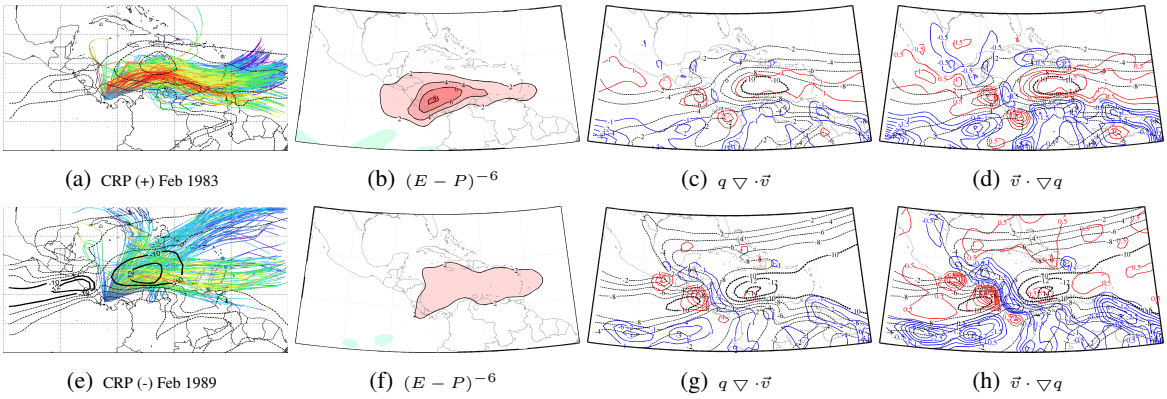

(a) CRP (+) Feb 1983 (b) $(E-P)^{-6}$ (c) $q \bigtriangledown \cdot \vec{v}$ (d) $\vec{v} \cdot \bigtriangledown q$

(e) CRP (-) Feb 1989 (f) $(E-P)^{-6}$ (g) $q \bigtriangledown \cdot \vec{v}$ (h) $\vec{v} \cdot \bigtriangledown q$

Figure 8.16:
Mean trajectories analysis of moisture transport, conditional positive $(E-P)^{-6}$, $q \bigtriangledown \cdot \vec{v}$ and $\vec{v} \cdot \bigtriangledown q$ for selected extreme ENSO events. Figures a and e show the trajectories of the air masses that precipitated over Central America with the colors showing the moisture content, b and f the positive values of the six days integrated net freshwater flux, c and g the divergence associated term and d and h the term associated with transport, both fields computed from the ECMWF ERA40 Analysis data integrated in the vertical.

moisture transport and the CLLJ) to the variability modes. Scatter plots were constructed for these three parameters in the same way as indicated in chapter 6, in order to make as clear as possible the picture of how the parameters respond to ENSO, MJO, NAO, PDO and the WHWP. In addition, slices of the zonal component of the wind and relative humidity along the CLLJ core position (75W, 12N) were obtained from the composite averages for positive, neutral and negative phase of each variability mode, in order to also show how the response of the structure of the CLLJ may have an impact on the other parameters.

Under the effect of the ENSO mode, the transport of moisture to CRP from the CS has the largest impact during late Spring, with the amount of air particles increasing as the easterly wind flow intensifies for warm ENSO (fig 8.17.a) corresponding the increase of air transported from the source with the intensification of the contributions to precipitation from this source. In this case, an increase of the contributions to precipitation from CS to CRP results from the increase of air transported. During April, the result found is different, in this case the largest response if noticed for the transport from the GoMS (fig 8.17.b). The easterly flow decreases this month for warm ENSO and increases strongly during the cold phase, when its vertical structure denotes an intensification of the flow at higher altitudes compared to the neutral and

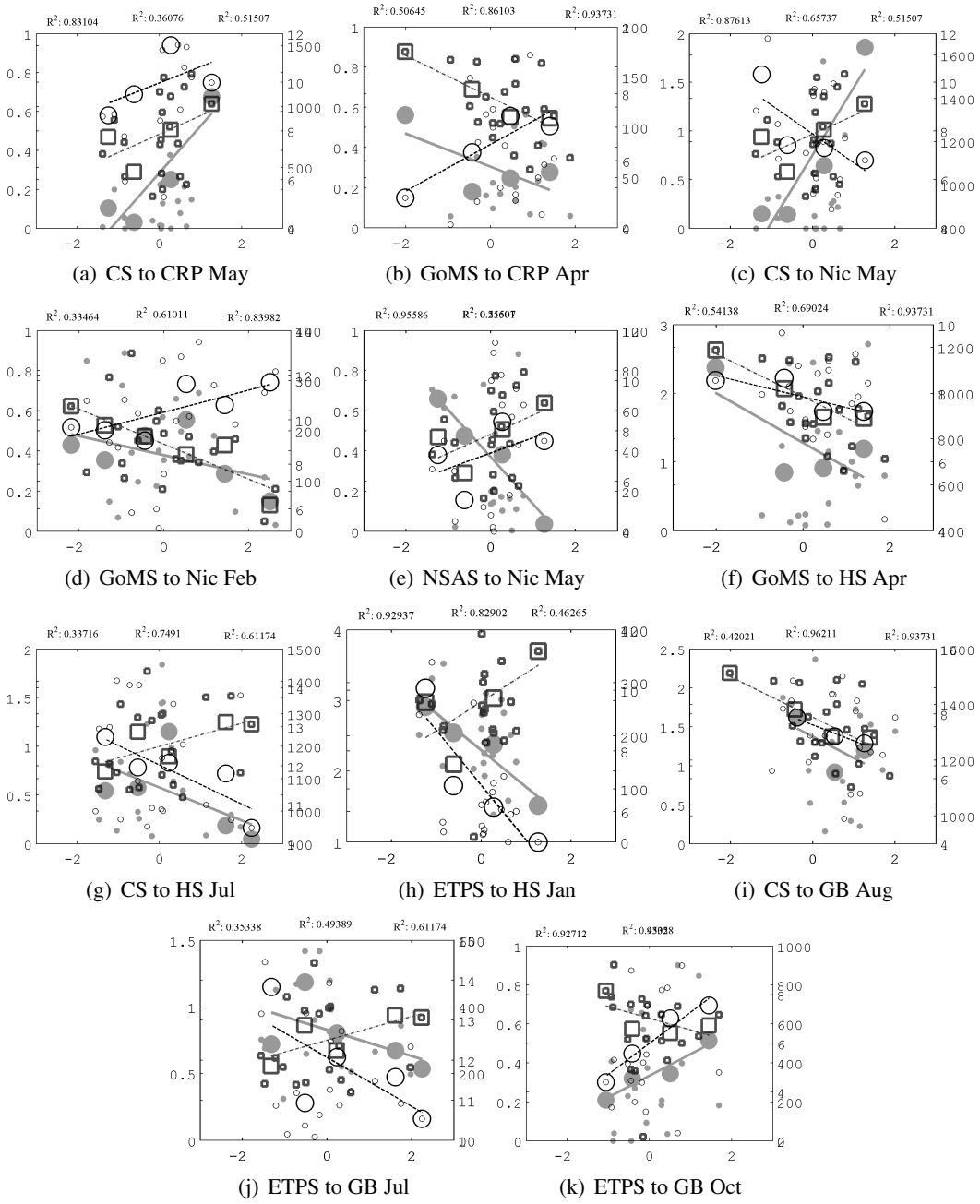

(a) CS to CRP May (b) GoMS to CRP Apr (c) CS to Nic May

(d) GoMS to Nic Feb (e) NSAS to Nic May (f) GoMS to HS Apr

(g) CS to HS Jul (h) ETPS to HS Jan (i) CS to GB Aug

(j) ETPS to GB Jul (k) ETPS to GB Oct

Figure 8.17: Scatter plots for the amount of air particles transported from each remote evaporative source to the target region (open circles), for the relative contributions to precipitation from the source to the target (filled gray circles) and the CLLJ index (open squares).

warm phases. For the transport from the GoMS, the role of the trade wind is to reduce the flow towards the south, so that the amount of air particles travelling from the GoMS is reduced (increased) for warm (cold) ENSO. However, there is no net increase of associated precipitation to this source as the amount of air transported increases, on the contrary, contributions to precipitation are reduced for warm ENSO. This result implies that the air particles transported during the cold phase are in average drier than for the warm ENSO phase and that convection may not be favoured. For Nicaragua, the decrease of the CLLJ during February for the warm phase of ENSO induces an increase in the transport from GoMS (fig 8.17.c) but with similar results to those found for CRP during April, this is, a reduction of contributions to precipitation associated to GoMS. During May however, as the intensity of the easterlies is intensified during warm ENSO, the transport from the CS associated with precipitation over Nicaragua is reduced but contributions to precipitation from the source increase, as the moisture content is intensified (fig 8.17.d). For the HS region, the reduction of the intensity of the easterly wind during warm ENSO is directly related with the decrease in the transport of air and the consequent reduction of contributions to precipitation from the ETPS during January (fig 8.17.e), indicating that for this source the amount of air particles is associated with precipitation which are increased for cold ENSO, showing how increased easterlies are able to modulate the transport from the ETPS. During April, a direct response to the intensity of the wind is associated with the transport and contributions to precipitation from the CS (fig 8.17.f) as the three decrease (increase) for warm (cold) ENSO. For the same source, the pattern reverse in Summer (fig 8.17.g) when intensified CLLJ during warm ENSO is associated with the reduction of the transport of air that precipitates over CRP and the contributions to precipitation from this source. With the further implication that warm ENSO inhibits the transport from the CS to HS as the more intense winds moves moist air toward the ETPac, as has been previously discussed. Air flow from the ETPS that moves towards GB is also influenced by the easterly flow as the increased CLLJ during summer (fig 8.17.h). The opposite is found for Autumn (fig 8.17.i) with the reduction of the easterly flow during this month is associated with the increase of both transport and associated contributions to precipitation from the ETPS.

For CRP, the main influence of the MJO seems to occur during summer as the airflow from the ETPS is reduced as the CLLJ is intensified during positive MJO (fig 8.18.a), despite the decrease of the transport and increase in the contributions to precipitation are noticed. Meanwhile, transport of air masses from the NSAS is increased with the intensified CLLJ but with

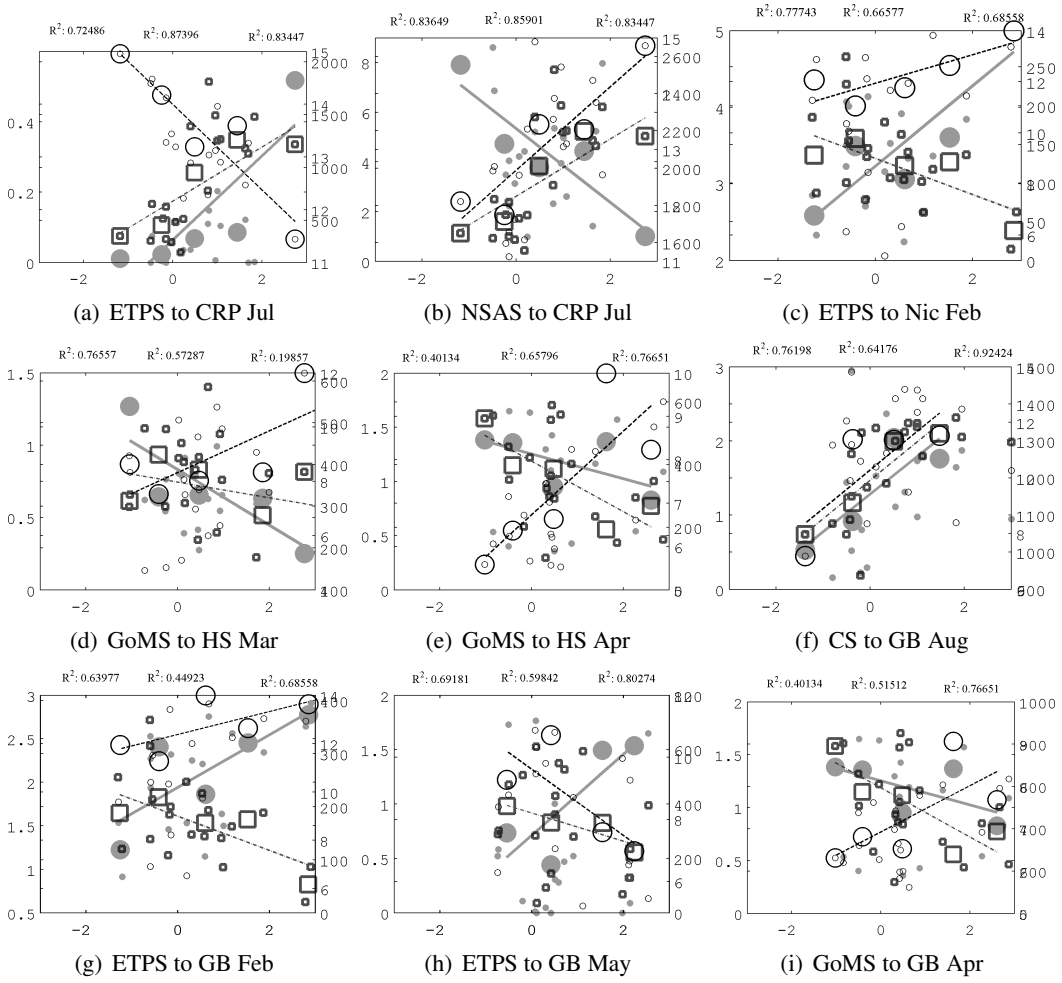

(a) ETPS to CRP Jul (b) NSAS to CRP Jul (c) ETPS to Nic Feb

(d) GoMS to HS Mar (e) GoMS to HS Apr (f) CS to GB Aug

(g) ETPS to GB Feb (h) ETPS to GB May (i) GoMS to GB Apr

Figure 8.18: Scatter plots for the amount of air particles transported from each remote evaporative source to the target region (open circles), for the relative contributions to precipitation from the source to the target (filled gray circles) and the CLLJ index (open squares).

a reduction in the contributions to precipitation associated with the source (fig 8.18.b). The CLLJ decrease (increase) found for positive (negative) MJO is found to trigger the intensification of both the transport of air masses from the ETPS and the contributions to precipitation over Nic form this source. For the HS region, significant linear relationship between the CLLJ, transport of moisture and contributions to precipitation was found only during April for the transport from the GoMS. decreased easterly flow associated with the increase of the transport of air masses but with the resulting decrease of contributions to precipitation from the source

(fig 8.18.c). The intensification of the CLLJ during August is related with the increase of air particles transported from the CS to GB and also with the increase of the contributions from this source with precipitation over GB during positive MJO (fig 8.18.d). During January, a decrease in the transport from the ETPS (and contributions to precipitation) is found to occur for positive MJO, however no relation is found with the easterly wind flow. In February, as the CLLJ decreases for the positive MJO phase, transport of air from the ETPS is enhanced, increasing the contributions from this source to precipitation (fig 8.18.e). In Spring, even when the decrease occurs for the transport of air particles occurs for the positive phase, the contributions to precipitation increase (decrease) for positive (negative) MJO. Note that the intensity of the flow is also reduced, opening the question of what may cause the marked increase of contributions to precipitation apart from the more or less obvious increase of the moisture content of the air travelling from this source.

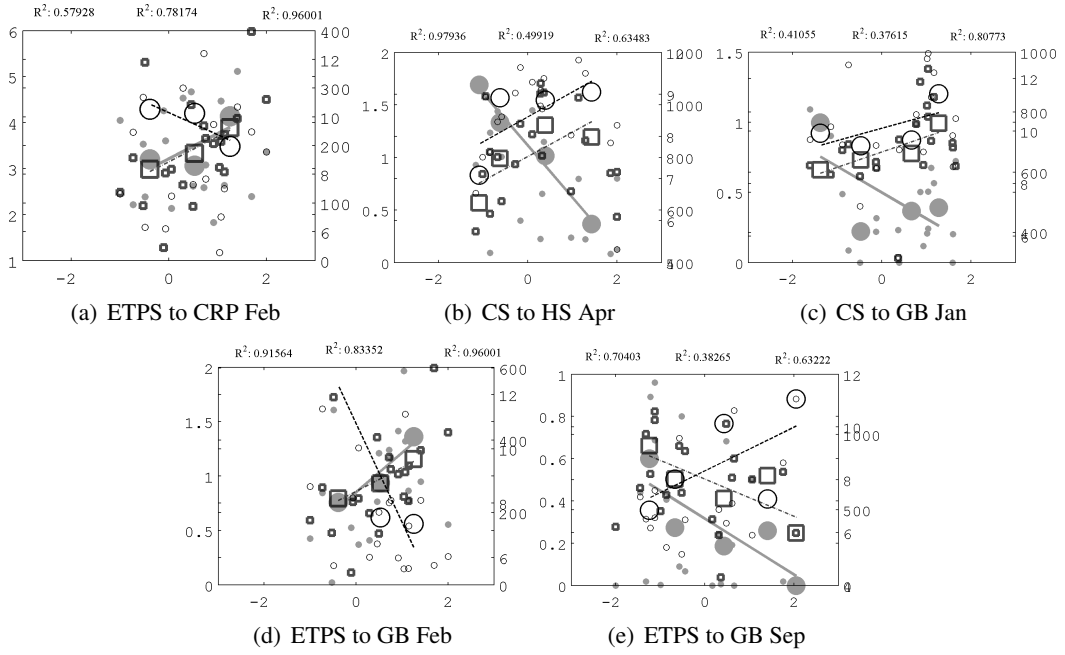

(a) ETPS to CRP Feb (b) CS to HS Apr (c) CS to GB Jan

(d) ETPS to GB Feb (e) ETPS to GB Sep

Figure 8.19: Scatter plots for the amount of air particles transported from each remote evaporative source to the target region (open circles), for the relative contributions to precipitation from the source to the target (filled gray circles) and the CLLJ index (open squares).

The reduction (intensification) of the transport of moist air from the ETPS to CRP during February for the positive (negative) phase of the NAO seems to be related with the increase

of the intensity of the CLLJ, however the decrease of the transport do not cause a fall in the contributions from this source to precipitation over CRP but an increase (fig 8.19.a). No significant linear relationship between moisture transport, the CLLJ and contributions from the sources to precipitation is found for the Nic region. The increase of the wind flow is suggested by the results shown in figure (8.19.b) to be related with the intensification of the amount of air particles transported to the HS region from the CS for positive NAO during April. However, no increase in the contributions to precipitation from this source is noticed but the decrease. During January, positive NAO triggers the increase of the intensity of the easterly flow, increasing also the amount of air particles transported from the CS to GB, with an associated reduction in the contributions to precipitation (fig 8.19.c). During February, the increase of the intensity of the CLLJ results in a reduction of the transport of air particles from the ETPS, conversely to what may be expected, a increase of precipitation associated with the transport from this source is found (fig 8.19.d). For the same source (ETPS), the decrease of the intensity of the easterly flow noticed in September (fig 8.19.e) favours the increase of the amount of air particles transported whereas contributions to precipitation are reduced for positive NAO.

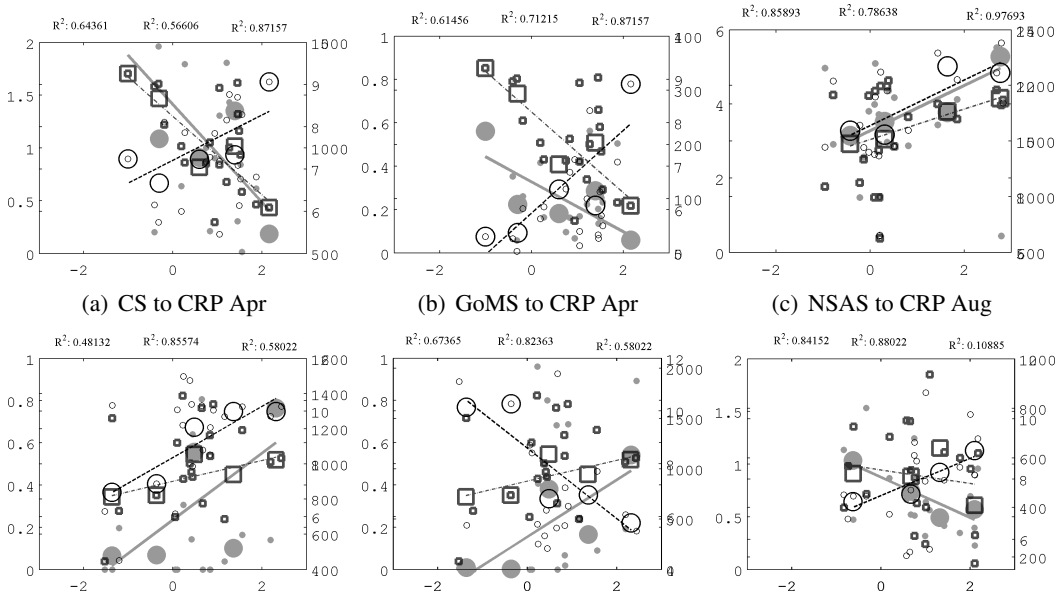

(a) CS to CRP Apr (b) GoMS to CRP Apr (c) NSAS to CRP Aug

(d) CS to GB Sep (e) ETPS to GB Sep (f) GoMS to GB Mar

Figure 8.20: Scatter plots for the amount of air particles transported from each remote evaporative source to the target region (open circles), for the relative contributions to precipitation from the source to the target (filled gray circles) and the CLLJ index (open squares).

The response noticed for the PDO indicates that for CRP the decrease of the easterly flow for positive PDO is related with the increase of the transport of air from CS during April but that a reduction in the contributions to precipitation form this source occurs (fig 8.20.a) and the same result is found for the transport and contributions from the GoMS (fig 8.20.b). During September, an interesting result is found for the transport from the NSAS, it is increased for the positive PDO phase as the easterlies are intensified resulting in the intensification of the contributions from this source to precipitation over CRP (fig 8.20.c). For the same month, a similar result is found for the transport of moisture from the CS to GB which is also associated with the intensification of the contributions to precipitation (fig 8.20.d) whereas the increase of contributions to precipitation from the ETPS occurs despite the transport is reduced for positive PDO (fig 8.20.e). No significant linear trends were found for the transport of moisture and associated precipitation for Nic and HS under the influence of NAO.

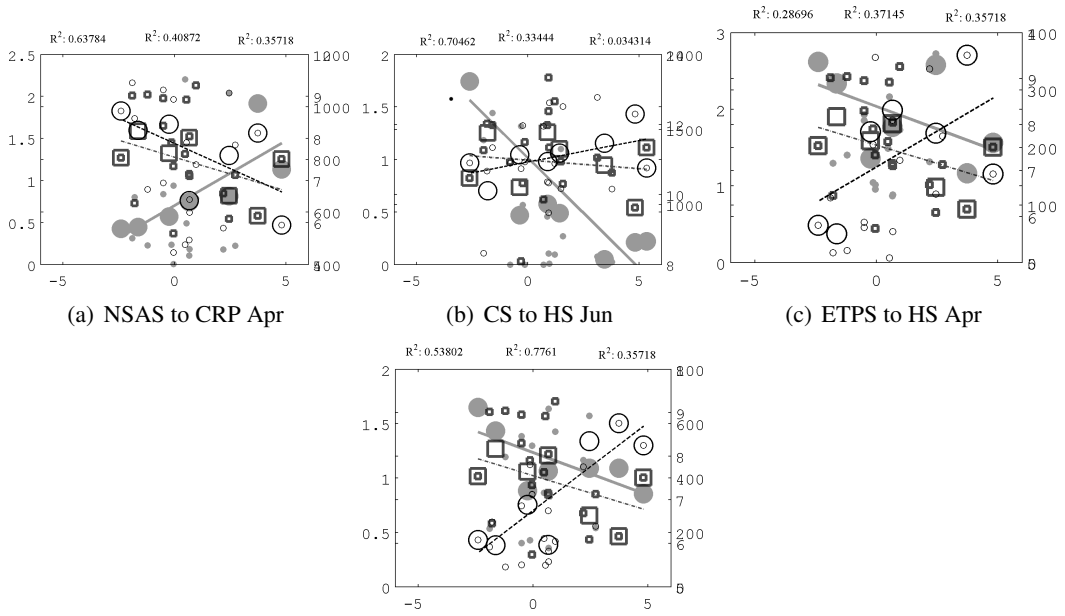

(a) NSAS to CRP Apr (b) CS to HS Jun (c) ETPS to HS Apr

(d) GoMS to HS Apr

Figure 8.21: Scatter plots for the amount of air particles transported from each remote evaporative source to the target region (open circles), for the relative contributions to precipitation from the source to the target (filled gray circles) and the CLLJ index (open squares).

In the case of the WHWP, the wind flow is found to be decreased during Spring for the positive phase and the transport of air particles from NSAS is found to be reduced whereas contribu-

tions to precipitation from this source are found to increase (fig 8.21.a), suggesting uptake of moisture to be enhanced. However, no simple linear relationship between moisture transport, precipitation and easterly wind flow was found for Nic and GB, the HS region exhibits a varied response to the forcing of the WHWP. For April, transport of moisture from the ETPS is increased as the easterly flow is reduced however, contributions to precipitation are decreased (figure 8.21.b). Meanwhile the transport from the GoMS is increased as a result of the reduction of the easterlies at the same time that contributions to precipitation from this source are reduced (fig 8.21.c).

8.5 Chapter highlights

In the present chapter the role of the CLLJ as an structure of particular importance for moisture transport and modulation associated with precipitation has been analysed. Due to the local features, the CLLJ interacts with different systems so that its role for regional modulation of precipitations ranges from evaporation enhancement over the ocean to forcing of topographic precipitation. A simplified conceptual model of the conditions that enhance/inhibit the moisture from the CS to account for precipitation was proposed with the aim of improving the understanding on how the different regional mechanisms interact to favour determined conditions of transport, therefore associated precipitation. The objective is to consider this simplification as start point for considering more complex interactions and build up a more integral view of climate processes that affect Central America, but that can be also of importance for other regions[3]. The Lagrangian analysis allowed not only a good identification of the three dimensional structure of the CLLJ but also of the moisture it transports. The agreement between the core where the peaks of intensity occur and the major uptake of moisture shows that besides of transporting moisture, the CLLJ is important for the enhancement of evaporation. Moreover the accuracy of the trajectories method for capturing both the seasonal cycle of the CLLJ and its variability allows us to consider this methodology for more complex studies in which the information extracted from mean fields is not good enough.

The CLLJ has been found to be extremely important in the modulation of the transport of moisture from the Caribbean to Central America and therefore of the precipitation over the

[3] a discussion of the importance of the CS as a source of moisture for the NAMS is included in appendix C.

region. Moreover, the CLLJ is indicated as the most important feature of the regional hydrological cycle, since it is involved in the complete cycle at different levels. The intensification of the easterly flow associated to the maximum of the CLLJ is related to the increase of evaporation due to the drag exerted by the wind over the ocean surface. In addition, the convergence/divergence patterns forced by the jet structure at the right and left of the core of the jet modulate the regional distribution of precipitation over the Caribbean Isles and the Caribbean coast of Central America where the main centers of convergence/divergence are located when the CLLJ is active. Finally, the intense easterly flow modulates the transport of the moisture from the Caribbean to Central America. Part if the moisture from the Caribbean reaches the Pacific side, while some other precipitates over Central America when the strength of the wind is favourable. Moreover, the CLLJ interacts with local topography to enhance orographic precipitation and at the same time, the interaction between the Caribbean and ETPac via SST gradients results in the modulation of the intensity of the CLLJ and therefore of the regional transport of moisture.

Part III

Final remarks

9 Conclusions

Through this work different aspects of the problem of moisture availability, transport of moisture and precipitation in a component of the IAS region to be Central America have been addressed. Being Central America a region poorly studied in comparison to other locations in the tropics, this kind of study was a need in order to provide further details on processes that even when can be considered as simple are of great importance for the region. The assessment of estimating precipitation in Central America presents the issue of the scarcity of data to calibrate the estimates. Whereas numerical models developed for tropical studies fail in the estimation of precipitation by large biases. The study presented was based on a Lagrangian methodology which is far a good alternative to the traditional Eulerian treatment for studying processes within the water cycle. Using this approach, the identification of the main sources of moisture for a region poorly studied was possible. Moreover, an integral analysis of the regional hydrological cycle was performed, providing useful information on the process of the transport of moisture in the region in terms of the key regional climate features.

9.1 Lagrangian approach

The skills of the method applied were found to be fairly good in the representation of the processes that occur in the IAS region, which is not always easy to obtain with numerical models

even when have being designed for tropical studies. Considering that the FLEXPART model has a simple set up and parametrisations compared to different numerical models used for climate modelling, its ability to capture the most important features of climate in the IAS is good. It is important to mention that the ERA40 analysis used as input may have some part of the credits of FLEXPART representing the mean climate conditions with an excellent accuracy. As the model was used for a preliminar study in which it captured the mean patterns, the time span used was too short to determine if the model could be able to handle variability. The simplicity of the model in terms of processes and parametrisations can be considered as a constraint, however it also has the advantage of not introducing noise due to parametrisations that may be not well suited. Here we are not exactly interested in using a model that copes well with every single process but in using a model that represents well the main climate features (which will depend on the input data) and represented with good accuracy the changes in moisture along the trajectory of air parcels as we are interested in precipitation. The conclusion on the performance of the model and dataset used is that the setup used enabled the representation of the main features of climate in the IAS which was essential for the study that was proposed. The further incorporation of different datasets to generate the backward trajectories can be now considered and using regional climate model outputs from numerical downscaling studies offers new possibilities for numerical experiments.

9.2 Sources of moisture and contributions to precipitation

In agreement with previous studies, two oceanic regions were found to be of importance as the major sources of moisture for precipitation over Central America. The Caribbean Sea (CS) is the main source of moisture, it provides the basis of the seasonal cycle of precipitation and is associated with the larger high frequency variability. The ETPS, was found to be important for providing moisture mainly to the west coast of Central America and was associated with a region of strong evaporation in the ETPac. Three sources that were not considered in the exploratory analysis were considered in the present work, the Gulf of Mexico even when is not featured as a very important source in terms of contributions, the sum of small contributions was found to be considerably important. The latter mainly for northern Central America and was found to be a important link between the transport of moisture from the Caribbean and the activity of the NAMS. Local recycling, on the other hand, was found to be of importance

during the rainy season as expected and to account for precipitation in a short temporal scale but also to have a lagged effect on precipitation by surface processes due to soil and vegetation. A remarkable result in terms of innovation compared to other studies is the identification of a source of moisture over northern South America which provided evidence on the coupling between precipitation over northern South America, low level winds and precipitation over Central America, which was found to be of importance for determining the seasonal cycle of precipitation. The NSAS can be from now considered from the point of view of the convective anomalies over South America as a new interesting analysis problem. The variability of the sources of moisture was also analysed and an important response of the main variability modes in terms of intensity and horizontal extension of the sources was found, being particularly important ENSO. A relationship between the sources and the easterly wind flow over the Caribbean suggested the the variability of the sources may be somehow related with the variability of this wind flow. Up to a 70% of the variability of the sources can be explained using 5 modes of an EOF pattern, from which three of the modes are related with the easterly flow. Being the first mode associated with the 'ground' signal of the easterlies that defined the mean state of the sources and an additional mode which accounts for the anomalies associated to the strengthen of the easterlies (the CLLJ). A third mode was associated with the horizontal extent and variations of the CS. Implying the importance of the zonal wind in determining the availability of moisture and the scale of transport. The analysis of the response of the $(E-P)^{-6}$ field to the variability modes provides valuable information about how ENSO, NAO, PDO and MJO affect the moisture sources for Central America and therefore associated precipitation. The ENSO mode was found to have the most important influence as a modulator of the sources of moisture because its direct influence was found to occur for longer time periods. In the particular case of winter and summer, the relationship between ENSO and the moisture sources was found to be extremely important. One interesting question that can be considered is to study with more detail the effect of an evolving ENSO event for the sources of moisture. In the case of the effect of NAO, a strong relationship was found for spring between the NAO index and the sources of moisture associated with the 'Atlantic regime' (CS, CAS and GoMS). This implies that the NAO exherts an influence via modifications over the Atlantic as expected from this mode. The role of the NASH merges as a possible explanation of the meachanisms involved and more analysis is required in order to provide a proper answer to the problem as we need first to explain the dynamical problem of how the NAO modifies the NASH and how

this modification affects the moisture sources. A large sensitivity of the NSAS to the PDO was found for spring and a linear relationship was also found between the other sources and PDO for autumn. The case of the NSAS calls particularly our attention as the presence of convective anomalies due to the PDO may explain this result, introducing the problem of the remote connection between convection over South America and precipitation in Central America. Similar for the case of the MJO, for which a relationship was found with the sources of moisture for winter and early spring. However, the problem of the modulation of the sources of moisture by the presence of the MJO will require a bigger effort of studying the effect of convection associated with MJO for precipitation over Central America.

Using a simple method that considers the rate change of specific humidity previous to the arrival of an air particle to a target region as an estimate of precipitation, estimates of precipitation due to the contribution from the identifies sources were computed. These estimates provide a quantitative basis for the analysis of the importance of the sources of moisture. By adding the relative contributions from each source, an estimate of the relative contribution from the sources of moisture to the total precipitation over the region was computed. Using a set of stations, quality control was performed to the data and a fraction of the total of stations was determined to be adequate to be used. However, as it corresponded to individual countries, a proper evaluation over Central America could not be performed and the correlation between the precipitation averaged for the stations and the estimated from the Lagrangian model was used instead. Even when this may not me considered as a complete evaluation of the method, is provides at list information on how reliable is the information obtained. The bias between estimated and observed precipitation ranges between 23 and 46%, which was considered to be reasonable[1]. The underestimation of precipitation that features the estimated from the Lagrangian approach is 'normal' considering that the approximation does not consider microphysical processes which account for part of the observed precipitation. The estimates were then considered as relative contributions to precipitation and not the total precipitation to be correct. The analysis of the estimates revealed that the contributions from the sources accounts for the major part of observed precipitation (up to an 80%). This result suggests that most of the precipitation that falls over Central America comes from remote sources, which implies that the external export of moisture is determinant for precipitation over the region. This results suggest the usage of the method for identifying the sources responsible for important deficits

[1] this compared to the biases of several numerical models

of precipitation under particular conditions, which may be useful to identify important analysis cases. More interesting is the time series for the contributions to precipitation from individual sources, which shows the different behaviour of each source. The contributions from the CS can be decomposed in two parts, a signal of the mean background signal of precipitation and a component of the variability of the Caribbean. Conversely, the ETPS does not have that background component and is more associated with a seasonal component of the observed precipitation and low frequency variability. The analysis of the time series revealed that the major variability occurs for the 2-8 years band which is actually ENSO band. However, the variability of the ETPS was found to be also probably linked to the effect of a lower frequency variability to be the PDO. Unfortunately, the series are not long enough to prove this result despite the analysis performed reveals some influence of the PDO on the signal of the contributions from the ETPS (accounting for that low frequency variability mentioned). In general, the oceanic sources were found to be more sensitive to the interannual forcing of the variability modes analysed. Moreover, the effect of the variability modes was found to trigger a lagged response from precipitation. This result is importance since the earlier/delayed begin of a dry or wet season is determinant for hydroelectricity and agricultural planning. Which is of great importance in the region since most of the electricity is generated by hydropower and the former countries of Central America have a historical economic dependence on agriculture, both for exportation and local consume. A better understanding on the response of precipitation to the variability modes can provides useful information to improve the planning of different economic activities.

9.3 Moisture transport and associated mechanisms

From the results and discussions presented in chapter 7, the most important result is the interaction between the mechanisms involved in the transport of moisture. The use of the backward trajectories enabled the reconstruction of the mean history of the air parcels prior to their arrival to Central America where they 'precipitated'. The applied method allowed us to obtain the complete three-dimensional structure of the transport of moisture. From which was determined that the main component of the transport is not only constrained to the troposphere but also below the boundary layer, as predicted from the theory (more than the 90% of the air particles that contribute to precipitation over Central America have travelled below 2000m).

This allowed us to obtain an accurate representation, by using clustering, of the features of the mean climatological flow that is responsible for part of the precipitation observed over Central America. In addition, the clustering algorithm used provided a good and efficient tool for reducing the large datasets into representative smaller amounts of air parcels, with the advantage that the clusters contain the main signature of the properties in which the study is focused. The method also allowed the identification of those regions where the most significant changes in the moisture content of the air parcels occurred. The latter is important since the identification of the uptake locations can be considered as a correction term of the location of the source of moisture. This means that even when air can be identified to come from a determined location, it can be dry air that increases its moisture content over other region. Therefore the contribution of moisture to precipitation from that trajectory is more realistic to be considered to come from the region where the uptake occurred rather than from the region when the air parcel 'started' to move towards the receptor region. Uptake locations were found to be associated with increases of evaporation due to local heating (mainly over the ETPac). But the forcing of low level winds over the Caribbean when the CLLJ is active was also important for the enhancement of evaporation. This result suggests the importance of studying the air-sea interaction that lays beneath the marine boundary layer under the CLLJ, since the forcing for uptake was found to be large and to increase in phase with the strengthen of the jet. Two structures were determined to exert the main influence in the modulation of the transport of moisture, the low level winds (both the easterly and the southeasterly flows from the Caribbean and the ETPac respectively) and the seasonal movement of the ITCZ which modulates the arrival of moisture from the ETPS to Central America. These two structures explain completely the seasonal cycle of the transport of moisture. As indicated in chapter 5, the first EOF pattern of the sources of moisture, that corresponds basically to the CS is strongly related with the forcing of the easterly flow. The variations in the extension and intensity of the CS described by the third EOF pattern (shown in figure number) are related with the variability in the scale of the transport from the Caribbean. In which long (short) range transport is associated with contributions from the outern (inner) Caribbean. The low level convergence of the winds that transport moisture during spring explains not only the intensification of precipitation but also remarks the importance of the interaction between the Caribbean and ETPac through Central America. As a summary of the mechanisms involved in the transport of moisture, the diagrams of figures provides a good schematic representation of the regional transport of moisture. The application

of the Lagrangian approach was satisfying, however we are concerned of the importance of improving the representation of the estimation of precipitation as has been also stated by Sodemann (2008). This because the Lagrangian approach used present a big potential to be used for analysis in specific region, for which the estimates of precipitation may be more accurate. Despite the issue of the uncertainties in the estimation of precipitation, the method provides a good tool jointly with the generated dataset for this analysis to be applied in the study of case analysis, from which we are particularly interested in severe drought conditions in determined locations of Central America.

9.4 Role of the CLLJ in moisture transport and distribution of precipitation

The importance of the CLLJ was introduced in the second chapter and the first evidence of its role on the modulation of the intensity of the sources of moisture was given, in terms of our results, in chapter 5. Where the influence of the easterly flow was found to be present in three of the main modes of the EOF of the (E-P)-6 field. Accounting up to a 30% of the variability of the field. The analysis of the backward trajectories, as already mentioned, enable the reconstruction of the path followed by the air particles and the changes in the properties they undergo. This is extremely useful in the identification of specific structures, which using basic dynamic assumptions can be isolated for individual analysis. In the case of the CLLJ, the flow is as confined in the period of activity of the jet, that its structure is isolated by basically constraining the mean height of the flow to be below 3000 m. After applying the second condition, which was based on the geopotencial height gradient between the trajectories, few variations in the amount of air particles attributed to the CLLJ during the two peaks (February and July). In average, after the second condition was applied to the particles with origin to the east of the targets, variations smaller than 5% in the number of air particles were found compared to those obtained after only constraining the height. This implies a strong coherence of the easterly flow in presence of the CLLJ, which during its activity lead all the processes in the Caribbean Sea. The typical jet-like structure of the CLLJ, in which the convergence pattern is located to the west of the core is related with the increase of precipitation over Central American Caribbean coast. This accounts for the seasonal differences observed in precipitation between southern and northern Central America. This is important since these patterns also modulate

precipitation over the Caribbean Isles. In addition, the development of a divergence wind to the right of the core along the axis of the jet is related with the horizontal distribution of the CS.[2] A well developed jet, with the correspondent convergence/divergence patterns is related with the result that during spring the recycling of moisture over Central America is a feature of the sources of moisture as shown by the (E-P)-6 field. Meanwhile during the period in which the jet is active in summer over the east coast of southern Central America there is low level convergence (and associated precipitation) instead. However, during winter the pattern is not the same and the (E-P)-6 field suggests the presence of divergence over the region which may be considered as different from expected following the latter discussion. The reason of this difference is that during winter the convergence pattern is different from that observed during summer. Then, during summer a strong pattern of low level convergence is located all over Central America while during winter divergence is observed over northern Central America, left to the convergence pattern. The reason for this lies on the features of the wind flow, being this divergence pattern observed during winter associated with the pass of the easterly flow trough Central American enclosed by the Yucatan peninsula since the mostly zonal structure remains. This does not occur during summer since the axis of the jet is dislocated to the north as the CLLJ develops its northward branch. A description of the intensity of the contributions from the CS was given in terms of the properties of the intensity of the CLLJ and the SST gradient between the Caribbean and the Pacific. The proposed conceptual model of the intensity of the contributions aimed to show how these two variables were enough to explain the modulation of the moisture transport from the Caribbean Sea to Central America. The CLLJ index was found to be useful as a measure of the intensity of the jet as described by Wang (2007) but the SST gradient was also found to be useful for analysing the probability of the difference of SST to induce a thermal response from the easterlies. The latter was found to be even more important as it supports the role of the WHWP as a modulator of the transport of moisture, as the ΔSST accounts as a measure of the importance of the WHWP. Using composites and analysis the trajectories for selected events (associated with the larger variations of the main variability modes) the model proposed was tested, under the assumption that the selected composites represented the mean variations and the selected cases variations in the sources due to specific conditions. The result was found to be that the model of variations in the intensity

[2] note that this implies that the second mode of the EOF pattern of the (E-P)-6 field is also related with the CLLJ

of the CLLJ and the SST gradient explain very well the patterns described by the CS (for the composites) and the transport of moisture (for the selected cases). Suggesting that in order to improve the knowledge on the regional patterns of precipitation and the assessment of forecast (and numerical models evaluation), the focus must be put on the interaction between the CLLJ and the AWP. As the model is too simple, it does not account for explaining all the patterns, however it was found that for those cases in which the pattern did not represent the expected result, the vertical structure of the easterly flow provided a partial explanation for the observed differences. This implies that the three dimensional structure of the CLLJ is more important in terms of analysing precipitation than rather just evaluate the horizontal mean fields. The analysis presented enabled a complete study of the regional hydrological cycle of Central America in terms of its components as described in the first chapter. The Lagrangian methodology was found to fulfill the gaps of information that are often present in the analysis of climate when Eulerian type analysis applied, since the reconstruction of the history of the air particle allows the study of the complete structure of transport and not just only of the mean state. The application of this approach to the case of Central America allowed us to provide an answer to the questions proposed so that the main objective of the work was accomplished. But more importantly, the results obtained encouraged the further study of specific aspects that were found to be of importance, some of which are of common interest with different groups as is the case of the extratropical moisture export and the contributions of the moisture transported from the Caribbean Sea to the NAMS. As well as to other that have not been study up to now as the vertical structure of the moisture of transport and the eventual coupling with the moisture transport through the tropopause, the forcing of evaporation due to the drag of the CLLJ over the ocean surface as well as the response of the CLLJ to forcing from the Atlantic and correspondent influence on the modulation of regional moisture transport and precipitation. Finally, this study provides a complete and detail analysis of the main components of the regional water cycle in the heart of tropical Americas. The main mechanisms involved in the transport of moisture and the modulation of precipitation over Central America have been assessed. The objectives of the proposed work were satisfactorily accomplished and the obtained results provided the input for the proposal of future studies in which some aspects of the regional climate need to be explored.

As a general conclusion, we can say that the two major results of the work presented are: a) In general we can indicate that this Lagrangian approach is very useful as it provides many

valuable insights for further studies, but its potential is not limited to the problems discussed in this work as the approach provides information that can be used to analyse several problems. New considerations for numerical modelling experiments and a wide variety of possibilities indicate that the Lagrangian based analysis is becoming a very powerful tool for climate analysis and that the increasing computing capabilities are encouraging its use for both scientific and practical applications. b) The exploration of the components of the regional hydrological cycle in Central America, the study of the sources of moisture and the moisture transport process associated with precipitation in Central America allowed the analysis of the problem of precipitation from different perspectives and for different time scales. With this we were able to provide answers to the questions proposed for the analysis and in addition we provided new information that is important for further detauled analysis. Beyond answering some questions, the results obtained suggest more directions to be considered for the analysis of indivifual problems and more importantly new questions came out to be considered as further work.

10
Further research lines

This work constitutes a detailed analysis of the sources of moisture for precipitation over Central America, a region poorly studied and of a great importance for several reasons. Beyond the identification of the sources that provide moisture to the region, a quantification of the relative contributions from the sources was presented. The variability of the sources of moisture and related effect on regional precipitation estimates was also considered. Even when the role of some of the sources was at least supposed, this work demonstrates their existence in a quantitative basis rather than a qualitative overview. Which is of importance since also allowed the identification of an additional continental remote source. The structures involved in the transport of moisture and how do they interact as part of a complex regional water cycle were used to explain part of the dynamics of moisture transport in the region. Finally, the role of the CLLJ as the main moisture transport (and precipitation) modulator was analysed in terms of the results obtained from the Lagrangian analysis and the basic concepts of atmospheric balance. It can be said that even when one must think that a bunch of questions were properly answered, much more came out from the work developed. This is how this work has opened different associated research lines that may be considered for further work (some which are already being explored):

10.1 Transport of moisture to and from additional structures

Monsoon-like circulations

The methodology applied needs a review and improvement in order to be adapted for further applications in the study of the transport of moisture associated with the global monsoon-like circulations. In the case of this structures the main interest is to explain in detail how the development of the monsoon is fed by the moisture inflow and at the same time the moisture within the system contributes with intense heavy rainfall when the monsoon is in the active phase. This would allow a deep analysis on the moist structure of the monsoon system from the seasonal to the interannual time scales. Note that a first attempt to show the advantages of the methodology for this problem has been included. Moreover, it would be interesting to study how does the transport of moisture change in a region when the monsoon shifts as is the case of the Asian monsoon. In the very specific case of the NAMS (which is of great importance for improving the understading of the dynamics of moisture transport for Central America), the Lagrangian trajectories analysis may help in the improvement of conceptual models for the understanding of the interaction between regional low level jets and the life cycle of the monsoon circulation. Moreover such an analysis must consider the effect of the NAMS for precipitation over other locations as found for the case of Central America. In order to make use of the campaign fields in the NAMS, a new set of backward trajectories for the periods in which the campaigns were held is being prepared using ERA-Interim Reanalysis data. The latter with the aim of providing a detailed analysis using the backward trajectories method that may be contrasted with in situ observations, for which the NAME and MESA experiments provide a great research and method validation opportunity.

Moisture transport processes related with the South Pacific Convergence Zone

The convergence regions in the tropics are also of interested in terms of the transport of moisture and other tracers. The study of the moisture imports and exports from the South Pacific Convergence is in progress. In this case, a backward trajectories dataset based on ERA Interim Reanalysis data for an extended tropical channel has been prepared. The aim is this joint research activity is to provide a novel interpretation of the processes take take place in the SPCZ, not only regarding precipitation but the transport of different atmospheric tracers. The first exploring analysis have consisted of studying the trajectories features for different

configurations of the SPCZ, by considering the high frequency displacements of the SPCZ. Based on the results obtained in the work herein presented, an improved clustering algorithm is being prepared for computing the average clusters of air particles associated with the SPCZ in order to evaluate its structure under variable magnitude low level wind flow. The next steps are the analysis of the variability of the SPCZ structure under ENSO and the establishment of a relationship between trajectories characteristics and vertical moisture variability statistics. Additional, we are also interested and looking forward to study the tracer constituent transport nearby the SPCZ for which additional backward datasets have been generated using several tracers rather than water vapour.

Transport of moisture associated to cyclonic structures

Based on a previous work developed with M.Reboita and A.M. Ramos, in which the moisture export associated to selected extra-tropical cyclones in the southern hemisphere, an study of the moisture transport processes related with heavy rainfall events in Portugal has been prepared. In the case of the southern hemisphere cyclones a tracking method can be used to track the cyclones. Once the position of the cyclone was determined, the evaporative sources of moisture were identified centred in the position of the best track of the cyclone. This allowed us to know where the moisture that feed the cyclone is coming from, then the origin of moist air that contributed to precipitation over Lisbon was determined in order to establish the link between the inflow of moisture into the cyclone and the moisture export to the Iberian Peninsula for the selected case.

Moisture and energetics for extreme hurricanes

Following an analogue reasoning to that of the study of the extra-tropical cyclones, the moisture inflow into selected severe tropical hurricanes is under study. In this case backward Lagrangian trajectories with three hours resolution data were used to explore the moisture import of the hurricanes. As the extension of the hurricanes is very variable, the identification of the associated sources of moisture was carried out by considering the extension of the section between the eyewall and the border where moisture content was maximum. These two limits were based on the position of the best track of the hurricanes, the eyewall and maximum relative humidity radii were estimated using ERA-Interim Reanalysis data. The moisture imports and exports for each stage of the life cycle of the hurricanes selected was studied in order to analyse the net

moisture conversions inside the hurricane and how they modulate the internal energetics of the cyclone. In addition, forward in time trajectories from the 'hurricane domain' were then computed so the export of moisture could be analysed. Moisture losses from the forward in time trajectories are useful to identify the regions to where the hurricane contributed with heavy rainfall which allows to validate the estimations based on the Lagrangian approach when in situ precipitation observations when available.

10.2 Vertical structure of the transport of moisture

Following the results presented in the analysis, the potential of the Lagrangian approach for exploring in more detail the vertical structure of the transport of moisture comes out. The reconstruction of the trajectories air reaching determined receptor regions with information on several variables allows the study of the processes that lead precipitation over the receptor location. What is more important about this application is that this Lagrangian methodology is useful for studying the properties of transport at different spatial scales.

Short range transport and orographic convection

As mentioned in chapter 8, the easterly flow, due to the presence of a mountainous range system over Central America, presents an important interaction with local topography. The latter is of importance since the lifting of the moist air particles which come from the Caribbean Sea (and even Northern South America) enhance the orographic precipitation over the windward side (as shown in fig 8.2). This has an important implication: vertical structure of the transport of moisture is responsible by the different precipitation regimes in Central America, from which a wetter Caribbean is well known. This reasoning has been several times used to justify the differences in observed precipitation over the Caribbean and Pacific slopes of Central America. However most of the results have been based on the solely assumption while a detailed analysis on the vertical structure of the transport may improve the understanding on the interaction between moist wind flow and topography. Particularly in the cases in which the transport of moisture present important height variations, such an study might be useful to determine how structures like the CLLJ can modify precipitation in other locations rather than the coastal regions. In addition, it could provide further evidences on the impact the transport

of moisture towards the Pacific has on precipitation over inner land regions. Finally, a comprehensive analysis on the features of the wind flow (mainly velocity and height) can be useful for identifying locations that might be considered as ideal regions for wind farm development.

Long range transport and the extra-tropical connection

It has been found that the transport of moisture from the Caribbean Sea may have a role in the transport of moisture to extra-tropical regions. A brief evaluation of the sources of moisture for the NAMS (appendix C) show that the Caribbean can contribute with moisture directly to the core of the monsoon as well as transport to the Gulf of Mexico. However, as shown in figure 6.2 the Caribbean Sea also has an important connection with precipitation falling over the US Great Plains. The study of the extra-tropical transport of moisture from the Caribbean would be an interesting problem to solve, because in the transport towards the Great Plains via the Gulf of Mexico, moisture from the Caribbean can be separated into two types of flow: a) one going northward to the Great Plains region where it can account for precipitation over e.g the Mississippi basin and b) moist air flow that travels eastward to contribute to the development of synoptic systems in the North Atlantic. For this second type of flow, the regional features of climate may have a remarkable importance, mainly the seasonality that features the WHWP.

Vertical transport of moisture to higher altitudes

Besides the importance of the horizontal transport of moisture due to its role in the forcing of precipitation. An interesting problem for which the use of Lagrangian trajectories can be considered as potentially useful is the vertical transport of moisture in the atmosphere. According to the results of *Fueglistaler et al., 2005*, a region of irreversible transport of moisture across the tropopause is located in the west Pacific Ocean. However, during summer this crossing through the tropopause extends to the east with an important maximum over the ETPac and Central America. The vertical structure of the wind field during summer averaged in the 10-20 latitude band suggests that the structure of the CLLJ (which reaches upper altitudes during summer) may be associated with the intensification of the vertical transport. This may provide the conditions to create a bridge of transport that links the ETPac with the western Caribbean. This problem is quite interesting since up to know, the potentials of the vertical structure of the CLLJ have not been studied.

10.3 Response of the sources of moisture to conditional forcing

With the results of this study, in which details on the regional hydrological cycle are given, some additional aspects may be considered of importance.

Warming

Which may be the response of the sources of moisture to warming? Since the CLLJ is our proposed main moisture conveyor and regional precipitation modulator and some evidence has been found on the circulation being modified under warming, which may be the response of precipitation over Central America to these future conditions. How warming could intensify the marked precipitation patches over Central America. According to the results presented by *Trenberth et al., (2005)*, there is a linear trend in the increase of water vapour over the oceans which suggests an increment of 1.2% per decade for the 1988-2004 period. As suggested by their results, changes in the runoff may lead to a decrease in regions like Central America. Therefore it might be of importance to consider the results proposed in this study to think ahead on the possible effect of warming on the regional distribution of precipitation.

Atlantic SST forcing

Finally, a problem that may be of interest and is a potential application of numerical modeling is the influence of variations of SST in the Atlantic in the modulation of the CLLJ. It has been shown that an anomalous heating in the tropical Atlantic presents the typical structure of a Gill-Matsuno-type quadrupole, whose signal is transported by Rossby waves to Central America and the ETPac through the Caribbean (*Kucharski et al., 2009*). As known, the CLLJ is sensitive to these systems and more important it modulates precipitations patterns. Which means that any system that may force an anomalous behaviour of the CLLJ can trigger the precipitation patterns over the Caribbean Isles and Central America. How does the CLLJ respond to the signal of this heating and which is the impact it may have on the transport of moisture and associated precipitation?

Extreme events

Under the premise of the importance of the transport of moisture from the identified sources for precipitation in Central America, and with knowledge on the occurrence of mild to se-

vere drought episodes in the region, a detailed study of the transport of moisture during these episodes is important. Such study may improve the understanding of the mechanisms causing drought in the region, but also in other nearby locations. Evidence on the decreases of moisture effective moisture transport were found to be associated with dry events (particularly in Nicaragua). Moreover, as the NSAS was found to have a significant contribution to precipitation, understanding how precipitation variability over northern South America may affect precipitation over Central America is important. An study on this direction may require a longer analysis period because the frequency of sustained extreme dry events (that drive dry conditions up to six months) that affect the region were found to be more important outside the analysed period. In addition, a preliminar review of extended drought in Central America has highlighted the importance of the heterogeneity of precipitation.

10.4 CLLJ related aspects

Besides the problems related with the regional distribution of precipitation, the problem of the CLLJ and its interactions have not been totally exploited. Several aspects of this structure still need to be analysed in detail. Because of the features of this jet, the processes within the boundary layer in which is involved is of interest.

Air-sea interaction

In the case of the interaction of the CLLJ with the ocean surface, two problems are proposed for further analysis:

Associated increase of evaporation

An important region of moisture uptake was found to be located in the vicinity of the CLLJ core, a quantification of the moisture advected to the atmosphere due to the strengthen of the low level winds that provide the other component of the water cycle to which the CLLJ may be related. A quantification of the evaporation forced by the drag of the CLLJ is of interest because it provides further information on the importance the CLLJ has for increasing atmospheric moisture.

Associated Langmuir circulation

The intensification of the easterly flow in presence of the peaks of the CLLJ may be associated with a forcing of Langmuir type circulations. This is important because it may have an impact on the mixing in the ocean, therefore on the air-sea fluxes of heat, momentum and also mass. Moreover, the interaction of the intensified easterly flow and local topography may be related with the forcing of SST variations over the ETPac (*Fiedler et al., 2006*). Those variations are of biological importance because of their link to the production nutrients, as has been already indicated in the case of the Costa Rica Dome (CRD).

A

Brief introduction to FLEXPART

The advantage of using Lagrangian trajectories analysis in atmospheric studies relies on the possibility of following the air parcels and knowing its properties at each time. A variety of models that enable the computation of such trajectories is available by now e.g HYSPLIT, LAGRANTO and FLEXPART. Due to the requirements of the particular research the Lagrangian model FLEXPART was used. This model was originally developed by Dr. Andreas Stohl during the early nineties as part of his military service in the Austrian Forces. Since then, the model has been improved, new parameterizations have been added and others optimized. Latest updates of the model have derived in an important tool for studying the problems of transport and dispersion of tracers and have been validated during different intercontinental air pollution studies. The FLEXPART model is a freely available Fortran 77 standard code that can be implemented using several compilers and operating systems. This section provides a brief description on some aspects of the version 6.2 of the model as described in the model technical note *(Stohl et al., 2005)*, extra information on aspects of interest for the presented research (specific parameterizations) is added, more information can be found in the FLEXPART homepage (http://transport.nilu.no/flexpart).

A.1 Computing

The FLEXPART model written as a Fortran 77 standard code is a sequential structure in which a list of subroutines are called from a main program. With the previous definition of the configuration of the model for a particular run in the configuration files, data is load and read. A check to determine all required data and paths are correctly set is performed and then the start of the run proceeds with the assignment of the data according to the specific set up. Later on, the set of subroutines containing the physics of the model are implemented to finally generated the output files according to the information asked to be saved. The model was design in a way that each physical parameterization is performed by a single routine that acquires the information from the results of individual smaller subroutines. Similar to the structure followed by the start of a single run of the model in which individual subroutines load the information from the configuration files and then build up the set up of the model in order to proceed with the input data reading and the execution of the model itself.

A.2 Input data

Data initially in a hybrid coordinate system as retrieved from the ECMWF model is converted to pressure coordinates. Furthermore, vertical wind is calculated to be mass-consistently from the spectral data through a pre-processor. The model requires a set of fields as indicated in the table:

1. Three dimensional fields: horizontal wind components, temperature and specific humidity.
2. Two dimensional fields: surface pressure, total cloud cover, 10 m horizontal wind components, 2m temperature and dew point temperature, large scale and convective precipitation, sensible heat flux, east/west and north/south surface stress, topography, land-sea mask and subgrid standard deviation of topography.

Table A.1: Input data required to execute the FLEXPART model

A.3 Physics of the model

A Lagrangian model compute the trajectories for a set of particles in backward or forward mode depending on the specific analysis. The utility of this kind of models is based on the advantage that Lagrangian models are independent of the computational grid, have infinitesimally resolution and unlike the Eulerian methods there is no numerical diffusion *(Stohl et al., 2005)*.

Parameterizations

Boundary Layer

Boundary Layer parameterization is based on the surface stresses and sensible heat fluxes retrieved from the ECMWF to compute the frictional velocity term as indicated in B.1, in the case data is not available, the computation is performed applying the profile method *(Berkowickz & Prahm, 1982)*.

$$u_* = \sqrt{\frac{\tau}{\rho}} \tag{A.1}$$

in order to obtain the the heat flux term,

$$(\overline{w'\Theta'})_0 = -\rho c_p u_* \Theta_* \tag{A.2}$$

the next set of equations are iteratively solved

$$u_* = \frac{\kappa \Delta u}{ln(\frac{z_l}{10}) - \Psi_m(\frac{z_l}{L}) + \Psi_m(\frac{10}{L})} \tag{A.3}$$

$$\Theta_* = \frac{\kappa \Delta \Theta}{0.74[ln(\frac{z_l}{2}) - \Psi_h(\frac{z_l}{L}) + \Psi_h(\frac{2}{L})]} \tag{A.4}$$

$$L = \frac{\overline{T} u_*^2}{g \kappa \Theta_*} \tag{A.5}$$

Note that ABL heights are computed following the critical Richardson number criteria, being Ri defined as the ratio of buoyancy to shear production of turbulence that provides a measure of the dynamic stability of the flow. The critical Ri threshold has been set to be 0.25 as defined by *Taylor, 1931* using perturbation theory. Thus, the ABL height h_{mix} is set to the height of the first model level l for Ri exceeding this value, being R_{il} defined as

$$R_{il} = \frac{(\frac{g}{\Theta_{v1}})(\Theta_{vl} - \Theta_{vl})(z_l - z_1)}{(u_l - u_1)^2 + (v_l - v_1)^2 + 100 u_*^2} \tag{A.6}$$

For convective situations, a correction term can be added so that Θ_{vl} can be replaced with Θ'_{vl} for an improvement of the parameterization.

$$\Theta'_{vl} = \Theta_{vl} + 8.5\frac{\overline{(w'\Theta'_v)_0}}{w_* cp} \tag{A.7}$$

where

$$w_* = \left[\frac{(\overline{w'\Theta'_v})_0 g h_{mix}}{\Theta_{vl} c_p}\right]^{1/3} \tag{A.8}$$

Moist convection

Convection processes are greatly important moreover dealing with tropical climate issues since significant convection takes place all year round over the region in the form of intense convective systems. Convective transport due to updrafts in convective clouds are not represented by the ECMWF vertical velocity since the transport is grid-scale in the vertical but sub-grid scale horizontally. A redistribution of the particles is the needed to represent this transport and the *Emanuel and Živković-Rothman, 1999*, convection parameterization scheme (hereafter E-ZR scheme) is applied by the model. The current E-ZR scheme is based on a previous parametreization by Emanuel *(Emanuel, 1991)* with the advantage of offering a good performance in comparison to other schemes in regional modelling. On FLEXPART, the E-ZR scheme has been used in a way that convection is triggered when the virtual temperature of an air parcel lifted to the level above the lifting condensation level (LCL) exceeds a threshold:

$$T_{vp}^{LCL+1} \geq T^{LCL} + 1_v + 0.9K \tag{A.9}$$

Then the net mass flux is determined by using (1) the mixing hypothesis for which increasing buoyancy with height might enhance detrainment and allows an adjustment between the cloud mass fluxes and buoyancy and (2) buoyancy-sorting hypothesis. In FLEXPART, a matrix of unsaturated upward and downward mass fluxes within the clouds is calculated based on the buoyancy-sorting hypothesis by accounting for entrainment and detrainment. The mass fluxes matrix described is used to redistribute the particles in the convective active boxes which fulfilled the criteria given by B.9. The method has the advantages of eliminating numerical diffusion by calculating subsidence velocity as well as fulfilling the well mixed criterion.

Wind fluctuations

Wind fluctuations are parametrized following the parametrization scheme proposed by *Hanna, 1982*, based on the boundary layer parameters with a modification applied by *Ryall et al., 1997*. Turbulence components are estimated taking into consideration the stability following criteria similar to *Panofsky et al., 1977*, and *Hicks, 1985*. Constant vertical diffusivity is used as described by *Legras et al., 2003*, in the stratosphere ($D_z = 0.1m^2s^-1$) while a horizontal diffusivity is used in the free troposphere ($D_h = 50m^2s^-1$). Distinction between troposphere and stratosphere are based on a threshold of 2 pvu and diffusivities are converted into velocity scales using $\sigma_{vi} = \sqrt{\frac{D_i}{dt}}$. Being u , v and w the along-wind, cross-and vertical components of turbulent velocity the equations for computing the turbulence terms as indicated by *Stohl et al., 2005*, for each stability case are:

Neutral conditions

$$\frac{\sigma_u}{u_*} = 2.0\exp(-3f\frac{z}{u_*}) \tag{A.10}$$

$$\frac{\sigma_v}{u_*} = \frac{\sigma_w}{u_*} = 1.3\exp(-2f\frac{z}{u_*}) \tag{A.11}$$

$$\tau_{L_u} = \tau_{L_v} = \tau_{L_w} = \frac{0.5\frac{z}{\sigma_w}}{1 + 15f\frac{z}{u_*}} \tag{A.12}$$

Stable conditions

$$\frac{\sigma_u}{u_*} = 2.0\left(1 - \frac{z}{h}\right) \tag{A.13}$$

$$\frac{\sigma_v}{u_*} = \frac{\sigma_w}{u_*} = 1.3\left(1 - \frac{z}{h}\right) \tag{A.14}$$

$$\tau_{L_{u,v,w}} = 0.15\frac{h}{\sigma_{u,v,w}}\left(\frac{z}{g}\right)^{0.5} \tag{A.15}$$

Unstable conditions

$$\frac{\sigma_u}{u_*} = \frac{\sigma_v}{u_*} = \left(12 + \frac{h}{2|L|}\right)^{1/3} \tag{A.16}$$

$$\tau_{L_u} = \tau_{L_v} = 0.15\frac{h}{\sigma_u} \tag{A.17}$$

$$\frac{\sigma_u}{w_*} = \left[1.2\left(1 - 0.9\frac{z}{h}\right)\left(\frac{z}{h}\right)^{2/3} + \left(1.8 - 1.4\frac{z}{h}\right)u_*^2\right]^{1/2} \tag{A.18}$$

$$\tau_{L_w} = \begin{cases} 0.1\frac{z}{\sigma_w[0.55-0.38(z-z_0)/L]} & \text{if } z/h < 0.1 \text{ and } z - z_0 > -L \\ 0.59\frac{z}{\sigma_w} & \text{if } z/h < 0.1 \text{ and } z - z_0 < -L \\ 0.15\frac{h}{\sigma_w}\left[1 - \exp\left(\frac{-5z}{h}\right)\right] & \text{if } z/h > 0.1 \end{cases} \tag{A.19}$$

Particle transport and diffusion

FLEXPART uses the 'zero acceleration scheme' (B.20) with first order accuracy implementing also a one iteration of the Peterson scheme (1940) for the grid-scale winds as a correction term to the position computed through the 'zero acceleration' under certain conditions (see FLEXPART technical notes for more details).

$$X(t + \Delta t) = X(t) + v(X, t)\Delta t \tag{A.20}$$

A Markov process based on the Langevin equation *(Thomson, 1987)* was used to parametrize the turbulent motions for the wind components. For long time steps the Langevin equation is considered as in *Legg and Raupach, 1982*, with an additional term for the decrease of air intensity with height from *Stohl and Thomson, 1999*, leading to

$$dw = -w\frac{dt}{\tau_{L_w}} + \frac{\partial\sigma_w^2}{\partial z}dt + \frac{\sigma_w^2}{\rho}\frac{\partial\rho}{\partial z}dt + \left(\frac{2}{\tau_{L_w}}\right)^{1/2}\sigma_w dW \tag{A.21}$$

Otherwise, for short time steps the Langevin equation is considered in terms of $\frac{w}{\sigma_w}$ following Wilson et al, (1983)

$$d\left(\frac{w}{\sigma_w}\right) = -\frac{w}{\sigma_w}\frac{dt}{\tau_{L_w}} + \frac{\partial\sigma_w}{\partial z}dt + \frac{\sigma_w}{\rho}\frac{\partial\rho}{\delta z}dt + \left(\frac{2}{\tau_{L_w}}\right)^{1/2}dW \tag{A.22}$$

The difference between formulations described by B.21 and B.22 is the fulfillment of the well mixed criterion. Even when B.21 does not meet the criterion for strongly inhomogeneous turbulence the method has been shown to be more robust with increasing integration time step. Discretization of both formulations uses two methods in order to optimize the computational resources usage.

$$\left(\frac{w}{\sigma_w}\right)_{k+a} = \begin{cases} r_w\left(\frac{w}{\sigma_w}\right)_k + \Lambda\frac{\partial\sigma_w}{\partial z}\tau_{L_w} + \Lambda\frac{\sigma_w}{\rho}\frac{\partial\rho}{\partial z}\tau_{L_w} + [\Lambda(1+r_w)]^{1/2}\zeta & \text{if } \frac{\Delta t}{\tau_{L_w}} \geq 0.5 \\ \left(1-\frac{\Delta t}{\tau_{L_w}}\right)\left(\frac{w}{\sigma_w}\right)_k + \frac{\partial\sigma_w}{\partial z}\Delta t + \frac{\sigma_w}{\rho}\frac{\partial\rho}{\partial z}\Delta t + \left(\frac{2\Delta t}{\tau_{L_w}}\right)^{1/2}\zeta & \text{if } \frac{\Delta t}{\tau_{L_w}} < 0.5 \end{cases} \tag{A.23}$$

where Λ is $(1 - r_w)$ for $r_w = \exp(-\Delta t/\tau_{L_w})$, the correlation for the vertical wind. A normally distributed random number with mean zero and unit standard deviation is represented by ζ and Δt is the time step between k and $k + 1$.

More useful information

FLEXPART model can run both forward or backward in time, for the first mode the particles are released from the source(s) and concentrations are determined downwind on a grid while for the latter mode the particles are released from a receptor location, being this mode more suitable for studying source-receptor relationships. A plume trajectories method based on *Dorling et al., 1992*, cluster analysis is also available in the model. Radioactive decay as well as wet and dry deposition are also considered explicitly in the model.

The model strictly linearity allows the segmentation of a problem into several runs and later combination of the results which optimizes the run-time performance instead of the usage of a parallel code. The design of the code in calculation routines and subroutines containing the parametrizations and control files with the configuration facilitates the use of the model and offers the possibility of modifying single parametrizations if needed. Output is gridded and files are written as compressed binary files in order to optimize the use of space and avoid extremely large output files. The model provides a particle dump option useful for long range runs, in case of FLEXPART terminates the run can be continued with the information of the last run provided by the files header and partposit_end.

B

Brief introduction to FLEXPART

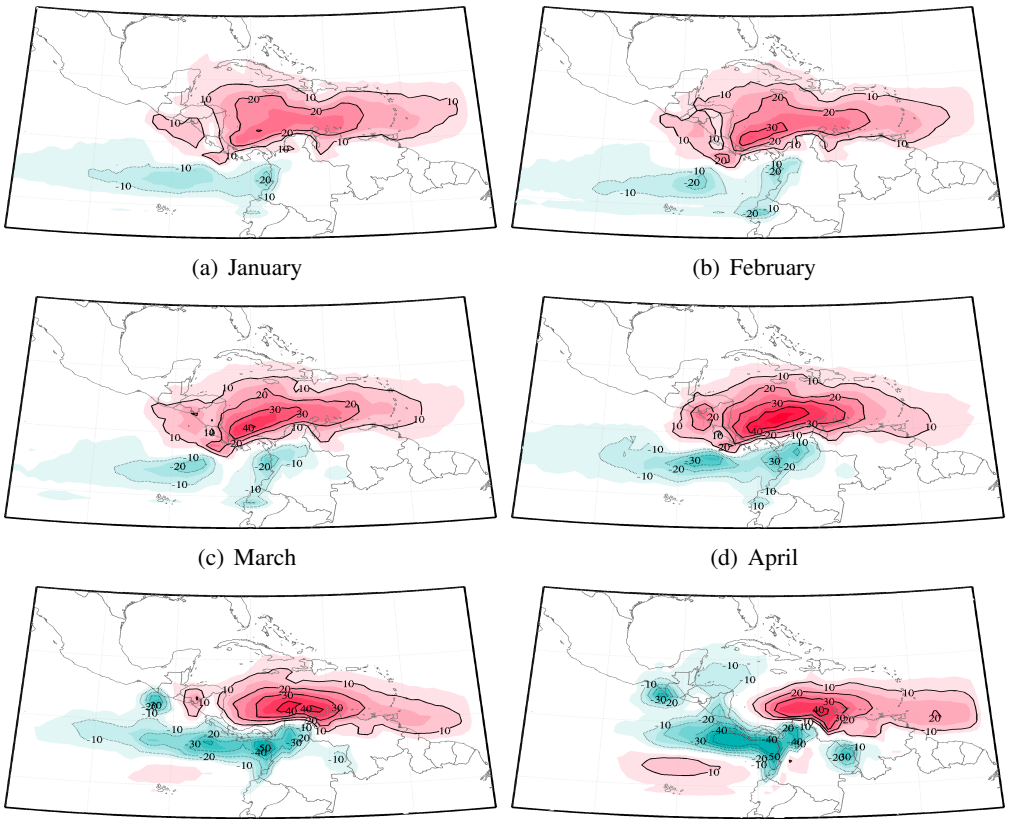

(a) January (b) February

(c) March (d) April

(e) May (f) June

Figure B.1: Monthly march of $(E-P)^{-6}$ integrates, positive values indicate the sources of moisture associated with precipitation over continental Central America .

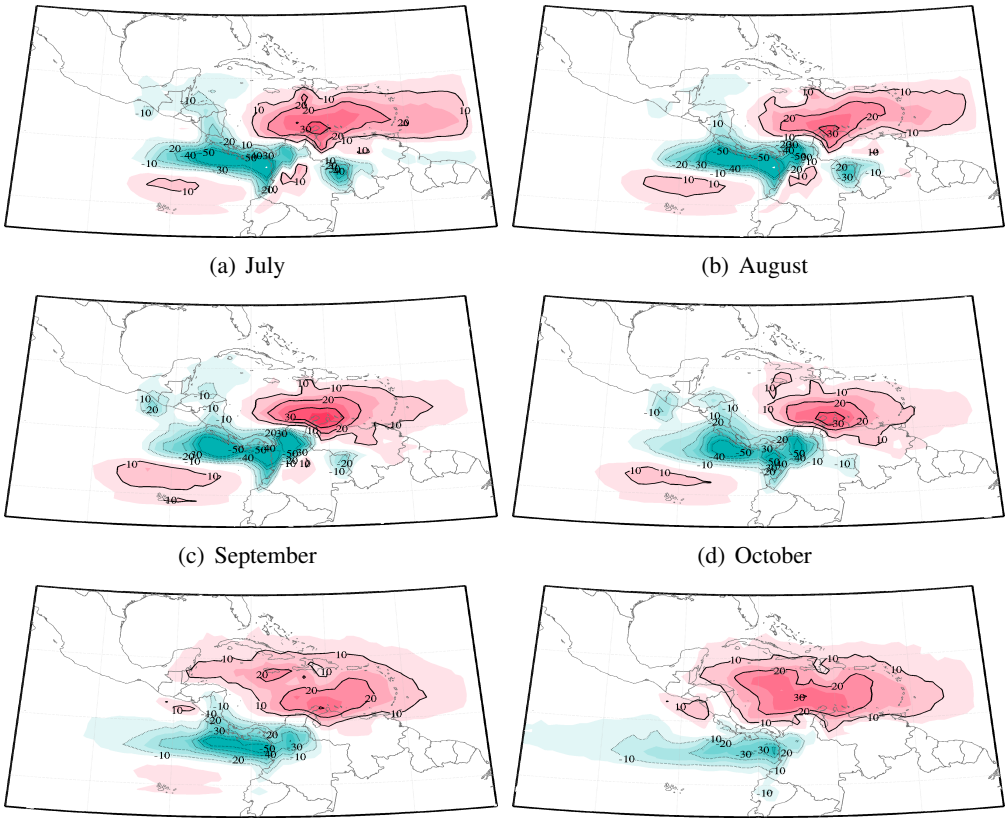

(a) July (b) August

(c) September (d) October

(e) November (f) December

Figure B.2: Monthly march of $(E-P)^{-6}$ integrates, positive values indicate the sources of moisture associated with precipitation over continental Central America .

C

Sources of moisture for the NAMS

A monsoon-like anticyclone development near the south of Mexico (at 200hPa) starts at the end of the spring and migrates northward during summer *(Ropelewsky et al., 2004)*. This structure is associated with the intense precipitation observed over north-western Mexico (NWM) and south-western United States of America (SWUS). The seasonal feature, known as the North American Monsoon (NAM) accounts for approximately 40% of the summer local rainfall and even up to 70% in some regions of Mexico *(Douglas et al., 1996)*. The NAM system has an oceanic component (Gulf of California, eastern Pacific Ocean and the Gulf of Mexico) and an overland counterpart (Sierra Madre Mountain Range). Several works have been performed on the dynamics of the NAM, which is under study since a century ago approximately. Several attempts to identify the sources of moisture for the NAM system have been done. Most of those works are based on traditional Eulerian approximations or WVTs (Water Vapour Tracer) *(Bosilovich and Schubert, 2001)* . Local continental evaporation and transport from adjacent oceanic regions are highlighted as dominant sources of moisture *(Castro et al., 2001)*. *Dominguez et al., 2008*, show evidence on the importance of local recycling for the supply of moisture to the monsoon. Previous studies (e.g *Higgins et al., 1997*) suggest that the source of moisture to the NAMS is located eastward, highlighting the Gulf of Mexico as an important source. Recently, *Knippertz & Wernli, 2010*, indicate the link between the NAMS and the inflow of air masses from the Gulf of Mexico. Furthermore, the regions affected by the

NAM are very sensitive to the forcing of different inter-annual signals. There is an increasing interest in understanding the variability of the monsoon precipitation from seasonal to inter-annual scales (see e.g *Liang et al., 2008*). This information is valuable not only as a scientific achievement but also for monitoring and forecasting. El Niño-Southern Oscillation (ENSO), the North Atlantic Oscillation (NAO), the Madden-Julian Oscillation (MJO) and the Pacific Decadal Oscillation (PDO) are known to exert an influence over the NAMS and for instance are herein considered. Herein, we provide a study of the summer transport of moist air masses based on backward Lagrangian trajectories. Sources of moisture for a defined NAM core influence region are identified. The evolution of the sources of moisture from the onset to the end of the monsoon is studied. The response of the contribution from the sources of moisture to precipitation over the monsoon core is evaluated for leading signals. The main variations are discussed considering previous results on the analysis of the NAM and key features of the regional circulation.

C.1 Moisture sources analysed from backward trajectories

A region of moisture flux divergence in the vicinity of the Gulf of Mexico and eastern North Mexico is a signature of the field for southern North America and over the Gulf of California, in contrast with the convergence observed in western Mexico (fig C.1). The moisture flux vector indicates transport of moisture from the IAS (shown by red arrows). From this average fields is not easy to determine with accuracy which region provides most of the moisture for the NAMS. Using the methodology described in chapter 4, an evaluation of the main sources of moisture for the NAM core was performed. Results for summer, when the NAM is active, are provided in figure C.2. Potential sources of moisture were found to present a maximum intensity during the first six backward days. Climatological monthly mean values of the six days integrated net freshwater flux $(E - P)^{-6}$ from May through September are contoured in figure C.2. Only positive values are shown to highlight the representative evaporative sources of moisture. For NWM a strong excess of evaporation over precipitation is noted to start in May with a higher intensity in the western coast (GoC) . As the time passes by, the presence of a second source over north-eastern Mexico (NEM) merges. During July, when the monsoon reaches its highest intensity, the source of the Gulf of California and the Baja Peninsula (GoC) has decreased considerably. Meanwhile, the source over NEM has increased three times its intensity for

the previous month. In addition, the influence of a third source becomes noticeable over the Caribbean Sea region (Caribbean) and the Gulf of Mexico (GoC).

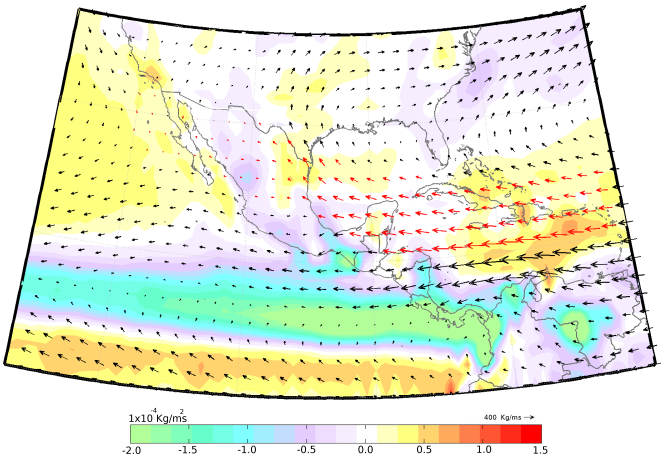

Figure C.1: Long term mean of vertically integrated moisture flux divergence (shaded contours) and vertically integrated moisture flux (vector). Positive colours indicate the regions associated with evaporative sources of moisture whereas the negative the regions associated with moisture sinks (regions of dominance of precipitation). The moisture flux associated with the CLLJ is highlighted in red to show the mean northward branch of the Caribbean flow.

The intensification of the availability of moisture presents the same temporal structure of the precipitation in the monsoon core region (figure C.2). Magnitude of the potential sources of moisture starts to decrease as the end of Summer approaches. While the monsoon season reaches the end, the intensity of the GoC and NEM has decreased. Moreover, the light source in the Caribbean is vanished. The results suggests that the moisture available during the initial stages of the development of the monsoon comes primarily from the GoC. As the monsoon becomes a mature structure, the role of continental sources of moisture strengthens. The role of a remote source of moisture, represented by the Caribbean, is also important during July (fig C.2.c). The pattern described by this latter source, follows the path of the northward branch developed by low level winds during the maximum intensity of the Caribbean Low level Jet (CLLJ). This result provides additional evidence on the direct role of the CLLJ transporting moisture from the Caribbean Sea to the NAM system. The strong intensification of the NEM source during the active phase of the NAM suggests the intensification of local evaporation and further interaction with the NAM system. Notice that the NEM region is also influenced by an increase in precipitation due to the monsoon (even when the monsoon core is located west-

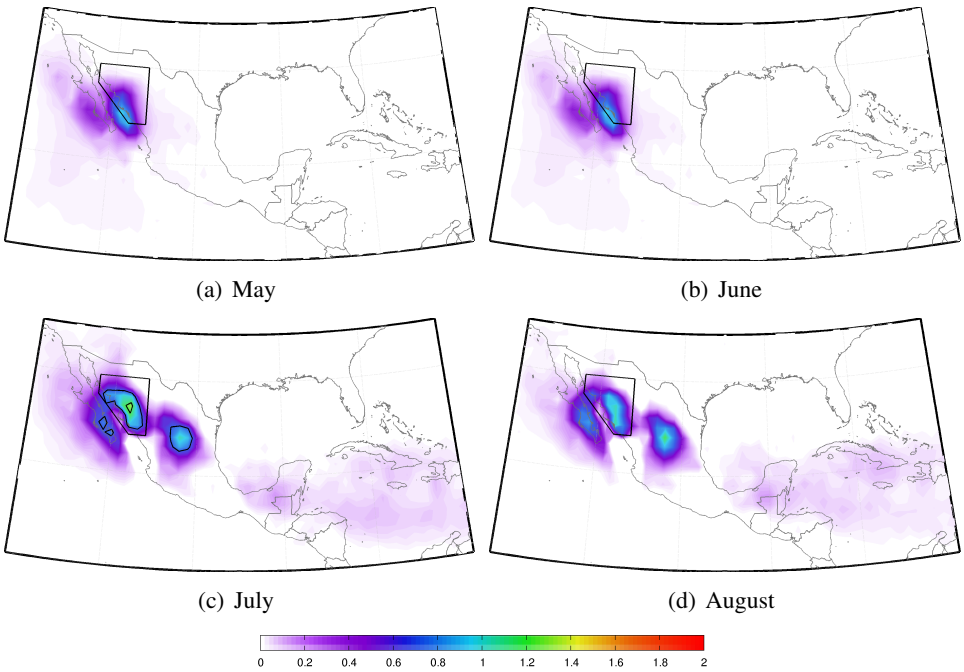

Figure C.2: Long term seasonal means of the the conditional $(E-P)^{-6}$ field in mm/day estimated for the six backward days prior to precipitation over the NAM core defined by the polygon indicated with black lines.

ward). Therefore, local evaporation over the NEM becomes very active during the monsoon, which implies an increase of the local recycling of moisture. This result has been analysed by *Domínguez et al., (2006)* on the importance of continental recycling of moisture during the monsoon. Notice also that the intensification of evaporation over precipitation for NEM during summer is a feature of the presence of the MSD (*Magaña et al., 1999)*. It is important to notice that the role of the GoM is not completely direct, since moisture from this source can reach the NAM core in two ways: a) from direct winds and b) by providing moisture to NEM which is then transported from the NEM.

Estimates of the contributions ti precipitation from each source were computed as for the case of Central America (chapter 5) with the result of an important increase of the contributions between May and August. This in agreement with the intensification of precipitation during the monsoon. The annual cycle has been widely explored, and here we are more interested in the variations of the intensity of the monsoon that may be associated with the variability of the transport of moisture. Composites of the contributions were computed in a monthly basis for the positive and negative phases of ENSO, NAO, PDO and MJO (using the table from chapter

4) as well as for the neutral conditions. An 'artificial' annual cycle for each phase was created in order to evaluate the variations that may occur between the active period of the NAM and the rest of the months. Anomalies of the contributions were computed extracting the neutral annual cycle from each phase and signal. Figure C.3 shows the annual cycle of anomalies from which it can be noticed that the larger variations are still observed when the NAM is active. In interesting observation is that it seems that the PDO can be related with the variation of the development of the monsoon, as the peak of contributions to precipitation is shifted to the right for positive PDO.

To study with more detail the contributions to precipitation during summer, the comparison between the composites for positive and negative phases of each signal are presented for June-September in figure C.4 . Notice that here we only account for 'direct' contributions, this is, moisture that has been transported directly towards the NAM core and not by any intermediate process, so the contributions from the GoM only consider when moisture has been directly transferred to the NAM core and contributions from the NEM contain, therefore, an important signature of the moisture from the GoM.

An immediate result is that the GoC and the region of NEM (plus SWUS) are the main sources of the moisture foe the NAM. As a result of local circulation, The GoM, the nearest portion of the ETPac and the Caribbean Sea also contribute as sources of moisture. However their role is no strictly direct since due to the transport scales. Their importance is more related to transporting moisture to the main source regions. The ETPac contributes strongly advecting moisture to the GoC and the GoM to eastern Mexico. The Caribbean Sea advects moisture mainly to the GoM and in minor quantities directly to the NAMS core.

Most of the changes in the direction from which low level air masses come to the NAM core region are triggered by changes in the circulation patterns. Mainly variations in the wind field mostly enhanced by changes in the pressure gradient signature. The approximate origin of moisture is explored. The latter provides an overview of the conditions of low level transport, since air masses can be dry or wet, these results may be analysed with caution (more air does not necessarily imply more moisture). Notice that the intrusion of dry air masses affects importantly the transport of moisture and the development of deep convection which is essential for the development and maintenance of the monsoon. In average, air flow coming from all sources during May is relatively dry. By June, moisture content of air flow from the Caribbean increases when travelling over the GoM while air from the GoM experiences an increase of

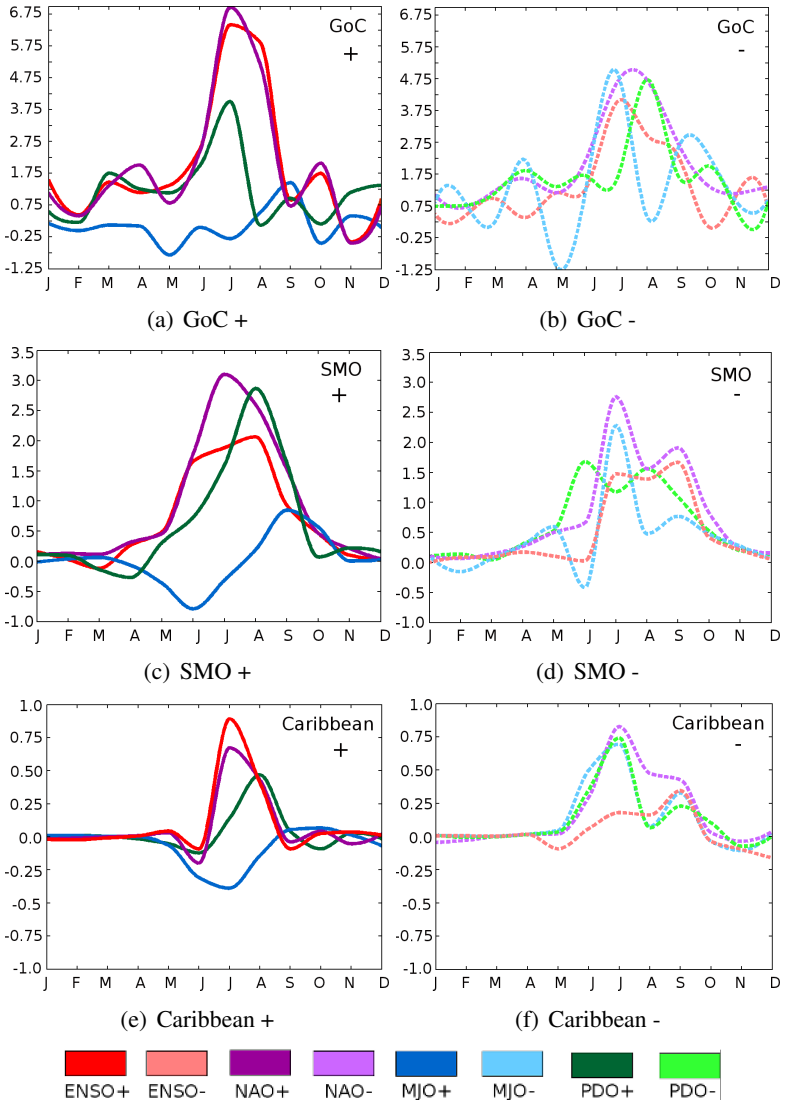

(a) GoC + (b) GoC -

(c) SMO + (d) SMO -

(e) Caribbean + (f) Caribbean -

Figure C.3: Annual cycle of the anomalies of the contributions from selected source of moisture (in mm/day) for the composites computed to precipitation in the area defined as NAM domain (following previous studies on the moisture sources for the NAM). The composites were computed for each positive and negative phases pf each climate mode based on the 0.75 STD criteria.

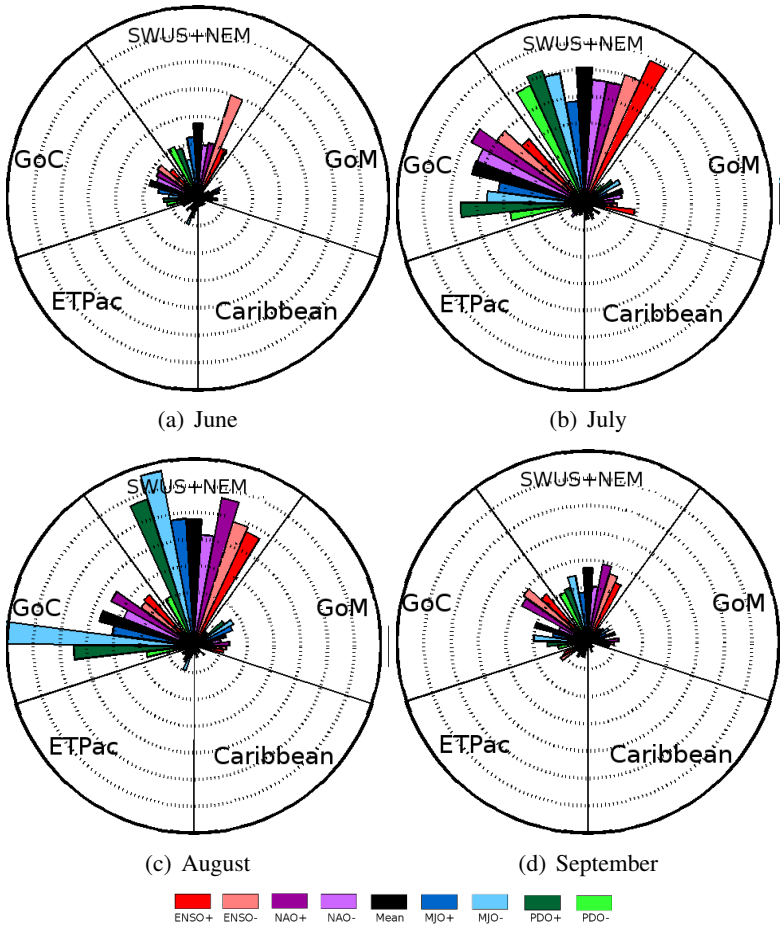

Figure C.4: Mean contributions from each source of moisture (in mm/day) for the composites computed, black presents the mean of the neutral composites.

moist content over eastern Mexico. During the monsoon peak, air from the west coast of southern Mexico and the GoC is extremely moist. In the same period (July) air is relatively dry over the outer Caribbean, for this airflow moisture content increases over the western Caribbean and the southern edge of the GoM. Correspondent air stream reaches a peak of moisture over the NEM region and then losses moisture over the NAM core. Conversely for July, air from the SWUS is dry whereas air from northern Mexico is enriched in moist content. For August the situation is similar to July, with the difference that during this month the influence from the Caribbean has decreased and air flow from the GoM is dry until it enters the continental region. In September air masses are dry in general, except for the air from the west coast of Mexico.

Mean relative contributions from the identified sources to precipitation falling over NAM core region were computed in a monthly basis. Composites were computed as already described foe positive and negative phases of ENSO, NAO, MJO and PDO. Anomalies reveal important variations under warm ENSO for the GoM and all positive phases for the Caribbean. Negative phases of NAO affect contributions from all sources while negative of PDO does for SUWS-NEM. Negative MJO triggers variations mainly for the contributions from the SWUS-NEM, GoC and Caribbean. A wide variety of studies have been performed regarding the forcing of the NAMS by ENSO (see e.g *Yu and Wallace, 2001*; *Gutzler, 2002*; *Brito-Castillo et al., 2002* among others). Composites of monthly relative contributions to precipitation are shown in figure 2 (lower panel, contributions every 2 mm/day from 0 in the origin to 14 in the outer circle) in comparison with the patterns of the percentage of 'air particles' from each source region.

In the case of ENSO, for June, the increase of flow from the SWUS-NEM during the cold phase is followed by a large intensification of the contributions from this region to precipitation over the NAM core. During the peak of the NAM influence of the cold phase is small in comparison to the mean climatology (black) but larger contributions are found during cold (warm) ENSO from the GoC (SWUS-NEM and GoM). During August this pattern is reversed and contributions from the GoM are very small. Contributions decrease in September with larger values for cold ENSO for both main sources. The increase of contributions from the GoC region for cold ENSO (La Niña) is related with wetter conditions associated with the dislocation of the eastern Pacific ITCZ to the north *(see Cavazos & Hastenrath, 1990)*. The results suggest that the total of contributions to precipitation increases during warm ENSO in good agreement with the increase of precipitation during July. Notice a reduced contribution from the GoC and increased contributions from SWUS-NEM and GoM during warm ENSO. The differences between ENSO phases may be associated with the fact that warm (cold) ENSO is characterised by a reduction (increase) of easterly wave activity. Tropical cyclones increase during warm ENSO, which implies an increase of moisture from the GoM, NEM and a little the CS. On the other hand, surges intensify during cold ENSO, enhancing the increase of contribution of moisture from the GoC. The results are in good agreement with the study of *Brito-Castillo et al., 2003*, which found wet (dry) monsoons association with ENSO warm (cold) phases. A generalised decrease of contributions from the main sources of moisture occurs during the negative phase of the NAO. Contributions from the GoC increase during positive NAO for July while for August the increase is noticed for the contributions from the

GoC and SWUS-NEM region. Positive NAO is known to be related with stronger westerlies favouring the transport of moisture from the GoC into the NAM.

Variations of the contributions triggered by the phases of the MJO are also marked. *Higging & Shi, 2001* point out that the importance of the MJO to the NAM is related with the meridional adjustments in precipitation patterns in the ETPac. Their results suggest a strong relation between the MJO and precipitation over western Mexico. For notation, positive (negative) MJO represents the suppression (enhancement) of convection. Then a positive (negative) MJO is associated with an easterly (westerly) phase. Differences are stronger during August rather than July, since for the latter the value of composites for both phases does not exceed the climatological mean values. During August, a strong intensification of the contributions from the main sources is associated with negative MJO. The increment of the contributions to precipitation over the NAM core from the SWUS-NEM and particularly larger from the GoC is in agreement with the observed intensification of precipitation over the NAM during the westerly phase of the MJO. *Lorenz & Hartmann, 2006*, suggest that this intensification of precipitation is triggered by the intensification of easterly waves and the subsequent effect on the ETPac cyclone activity. Both are known to account for the enhancement of gulf surges. Then, if transport of moisture from the GoC is correlated with the surges, negative MJO must be associated with an increase of the contributions to precipitation from this source. The result shown by light blue for July and August confirms this relation, notice also the increase in the contributions from the GoM for negative MJO. Increase from the SWUS-NEM region during August during negative MJO is also related with the enhancement of Mesoscale convective systems (MCSs) in the NAM as pointed by *Lorenz & Hartmann, 2006*.

Brito-Castillo et al., 2003, indicate that the PDO is a modulator of precipitation in western Mexico so that PDO is a good indicator of low frequency variability of the NAM core. The patterns for the phases of the PDO presents a reversed relationship for the NAM peak between the percentage of 'air particles' arriving to the NAM core and the contribution to precipitation. The first implication of this result is that even when there are more air masses being transported to the NAM core region, their moisture content is quite small during negative PDO (suggesting the circulation of dry air). Positive PDO seems to be influenced by a marked increase of the contributions from the GoC during July and even larger for August. Meanwhile, the contributions from the SWUS-NEM region for this phase are just slightly larger for July compared to the negative PDO and much more intense during August. The latter suggest positive

(negative) PDO to be linked with wetter (drier) monsoon conditions. For positive PDO, the increase of contributions to precipitation from the SWUS-NEM source region is mainly due to the intensification of the contributions from NEM which are associated with the enhancement of convection over the Sierra Madre Oriental produced by the moist air inflow from the GoM (notice that also direct contributions from the GoM increase for positive PDO). This excess of moisture availability is confirmed by the results of *Englehart and Douglas, 2001* which show an increase of rainfall over north western Mexico associated with tropical cyclones during positive PDO. Similar, increase of the contributions from the GoC are related also with stronger tropical cyclone activity and more with the warm SST that characterised the ETPac region during positive PDO that influences the intensification of surges in the GoC.

The Lagrangian approach applied results to be very useful for the representation of the variability of the NAM in terms of the contributions to precipitation from the main sources of moisture. The good agreement between the results derived from the Lagrangian estimates and the various studies performed on the variability of the NAM is very encouraging on the application of these methods since the results of the variability of the NAM are supported by a large amount of studies not only based on mean fields and numerical modelling but also on a relative good long term network observations. The next objective regarding Lagrangian based analysis and the NAM is to study the relationship between the transport of moisture form the Caribbean Sea in order to study how does the CLLJ is coupled during the NAM due to the development of its northward branch. Moreover, it is also important to analyse the transport of moisture from the Caribbean to the Gulf of Mexico and to the Great Plains, in order to study the importance of the CLLJ for the extra-tropics.

Year	GB				HS				NIC				CRP			
	CAR	**GoM**	**ETPS**	**NSAS**	**CAR**	**GoM**	**ETPS**	**NSAS**	**CAR**	**GoM**	**ETPS**	**NSAS**	**CAR**	**GoM**	**ETPS**	**NSAS**
1980	30.8	1.4	67.2	0.6	52.1	1.7	45.0	1.1	72.2	0.6	25.4	1.9	62.9	1.6	7.8	27.7
1981	52.3	0.0	47.7	0.0	69.3	0.0	29.3	1.5	69.8	1.0	15.9	13.3	37.4	2.6	1.5	58.5
1982	63.3	0.0	36.7	0.0	81.8	0.0	17.9	0.2	84.5	0.2	9.0	6.3	40.5	20.5	1.9	37.1
1983	8.7	10.2	80.5	0.7	32.6	5.3	61.0	1.1	52.4	4.8	33.3	9.5	31.9	8.0	7.0	53.0
1984	48.6	0.0	51.2	0.2	70.0	0.0	22.8	7.2	70.8	0.5	9.9	18.8	28.6	5.3	1.2	64.8
1985	62.0	0.0	35.1	2.9	75.5	0.0	19.2	5.2	73.2	0.0	14.0	12.8	28.7	0.0	0.2	71.1
1986	38.2	0.0	61.8	0.1	59.9	0.2	31.5	8.4	64.9	1.0	21.6	12.4	54.8	3.7	9.8	31.6
1987	39.8	0.4	57.3	2.4	47.2	2.3	36.7	13.8	40.1	3.2	23.2	33.4	16.4	1.9	8.7	73.0
1988	43.2	0.0	55.7	1.1	70.4	0.0	26.8	2.8	78.6	0.0	11.3	10.1	46.8	1.8	1.5	49.9
1989	64.7	0.0	34.8	0.5	76.5	0.4	22.3	0.8	75.3	1.2	18.8	4.7	48.8	5.2	10.2	35.8
1990	47.4	1.4	50.5	0.6	69.7	1.5	26.9	1.9	74.5	6.7	10.1	8.7	56.3	13.0	2.7	28.0
1991	51.9	0.0	47.8	0.4	65.6	0.0	32.2	2.2	68.7	0.0	20.3	11.1	43.8	0.2	6.4	49.6
1992	26.1	2.4	70.4	1.1	43.9	0.0	54.4	1.7	62.7	0.8	27.6	8.8	41.9	2.7	5.5	49.9
1993	18.2	0.0	81.4	0.4	39.7	0.0	60.1	0.3	65.4	1.3	30.3	3.0	63.0	3.7	2.6	30.6
1994	67.6	0.0	32.4	0.0	89.2	0.0	10.8	0.0	92.3	1.4	1.8	4.5	36.1	19.2	4.0	40.7
1995	32.7	0.0	66.7	0.6	51.8	0.1	46.0	2.1	66.1	0.0	28.8	5.1	47.1	4.2	8.1	40.6
1996	26.9	0.0	73.1	0.0	50.6	0.1	48.3	1.0	68.6	0.3	25.0	6.1	53.7	1.7	5.9	38.8
1997	68.9	0.0	28.9	2.2	80.4	0.0	10.5	9.1	66.8	0.3	2.8	30.1	28.9	3.8	0.7	66.6
1998	9.7	5.1	83.1	2.0	27.0	1.8	63.4	7.8	33.9	10.4	40.2	15.5	13.7	13.2	16.9	56.3
1999	33.7	0.0	66.0	0.3	52.3	0.0	47.7	0.0	71.4	1.3	25.	1.7	56.6	10.0	5.1	28.3
Avg	**41.7**	**1.0**	**56.4**	**0.8**	**60.3**	**0.7**	**35.6**	**3.4**	**67.6**	**1.8**	**19.7**	**10.9**	**41.9**	**6.1**	**5.4**	**46.6**

Table C.1: February Month

Year	GB				HS				NIC				CRP			
	CAR	GoM	ETPS	NSAS	CAR	GoM	ETPS	NSAS	CAR	GoM	ETPS	NSAS	CAR	GoM	ETPS	NSAS
1980	36.6	1.7	58.5	3.1	46.6	2.0	31.9	19.5	37.1	4.0	12.5	46.4	6.6	14.6	1.7	77.1
1981	34.5	3.8	61.6	0.1	47.5	12.4	34.3	5.9	36.4	26.3	22.3	15.0	6.3	43.6	7.3	42.7
1982	30.1	4.7	63.4	1.8	38.5	11.2	46.2	4.1	34.0	25.2	34.4	6.3	12.5	43.6	12.9	31.0
1983	63.4	3.3	33.0	0.2	77.3	0.5	7.3	14.9	65.0	2.0	1.7	31.4	14.5	16.6	1.2	67.7
1984	40.8	12.0	41.1	6.0	50.7	7.8	12.4	29.2	36.9	5.2	2.6	55.4	15.3	22.3	3.7	58.7
1985	47.6	0.4	51.8	0.2	65.4	0.0	24.9	9.7	54.3	0.9	12.4	32.4	16.8	17.9	5.8	59.4
1986	32.8	1.2	62.2	3.8	37.4	4.8	44.7	13.1	33.9	16.4	30.6	19.1	15.1	38.5	10.0	36.3
1987	44.7	2.3	53.0	0.0	68.7	0.4	26.9	3.9	61.1	9.1	11.5	18.3	26.5	17.4	4.1	52.0
1988	23.4	5.8	69.7	1.1	34.0	9.8	49.3	6.9	40.1	17.3	29.3	13.3	12.9	31.5	8.3	47.3
1989	41.5	2.5	48.1	7.8	53.5	2.6	27.7	16.2	54.0	7.6	11.8	26.6	16.1	26.2	2.6	55.1
1990	40.0	4.4	51.6	4.0	39.7	15.5	27.6	17.2	28.1	27.3	16.5	28.1	10.9	27.3	5.3	56.5
1991	42.0	7.3	48.0	2.8	41.8	17.9	28.7	11.6	26.2	33.7	17.9	22.2	7.2	40.9	2.6	49.3
1992	30.4	0.1	69.5	0.0	49.2	0.0	50.0	0.8	62.2	1.0	30.5	6.4	38.2	9.7	5.4	46.7
1993	28.5	6.5	65.0	0.0	43.0	12.9	41.8	2.3	38.2	31.4	25.9	4.5	16.8	42.7	10.0	30.5
1994	44.1	1.0	50.7	4.2	54.5	0.1	30.3	15.2	37.2	4.6	17.4	40.8	6.0	28.9	5.7	59.5
1995	39.5	4.7	53.3	2.6	45.6	11.2	23.1	20.1	24.2	17.2	12.3	46.3	6.2	33.0	4.3	56.4
1996	31.0	9.0	53.9	6.1	37.5	15.4	26.4	20.8	26.9	22.2	11.1	39.7	5.7	40.2	4.5	49.6
1997	67.4	0.0	29.5	3.2	77.7	0.0	8.8	13.5	46.4	1.9	0.6	51.0	6.6	0.1	0.0	93.3
1998	35.9	0.0	62.3	1.8	48.8	0.1	36.1	14.1	53.5	2.2	21.7	22.6	21.4	20.6	5.8	52.2
1999	51.2	0.0	45.5	2.4	58.8	0.0	24.8	16.4	38.5	7.2	14.0	40.3	8.0	34.6	6.3	51.1
Avg	**40.3**	**3.5**	**53.6**	**2.6**	**50.8**	**6.3**	**30.1**	**12.8**	**41.7**	**13.1**	**16.9**	**28.3**	**13.5**	**27.5**	**5.4**	**53.6**

Table C.2: May Month

Year	GB				HS				NIC				CRP			
	CAR	**GoM**	**ETPS**	**NSAS**	**CAR**	**GoM**	**ETPS**	**NSAS**	**CAR**	**GoM**	**ETPS**	**NSAS**	**CAR**	**GoM**	**ETPS**	**NSAS**
1980	72.4	1.0	8.7	17.9	55.2	0.0	1.7	43.1	22.0	1.1	0.1	76.8	3.1	12.8	0.6	83.5
1981	71.5	0.5	7.1	20.9	55.8	0.4	0.2	43.6	29.2	1.0	0.5	69.4	7.0	22.2	1.8	68.9
1982	71.6	0.1	0.1	28.2	50.0	0.9	0.0	49.1	14.1	1.5	0.0	84.4	2.4	10.8	0.1	86.6
1983	64.2	0.2	0.8	34.8	34.8	0.0	0.1	65.1	10.2	1.5	0.0	88.3	3.1	19.9	1.2	75.8
1984	61.0	7.2	11.8	20.0	46.3	6.2	1.2	46.3	19.0	6.1	0.5	74.4	5.5	27.1	0.9	66.5
1985	66.5	0.8	5.1	27.5	50.2	1.9	0.3	47.6	26.2	2.4	0.2	71.2	8.1	20.0	0.9	70.9
1986	63.7	0.3	0.2	35.9	44.9	1.4	0.0	53.7	13.2	5.1	1.1	80.6	2.1	16.4	0.8	80.7
1987	58.2	2.7	2.3	36.8	41.0	3.9	1.5	53.5	12.9	7.9	2.1	77.0	2.9	32.1	1.9	63.1
1988	64.0	3.6	12.9	19.5	52.4	5.5	4.6	37.4	27.4	7.5	2.3	62.9	4.3	31.7	3.3	60.8
1989	61.9	11.6	10.7	15.8	49.3	12.6	3.0	35.1	20.2	11.6	2.9	65.2	3.8	26.0	1.3	68.8
1990	70.4	0.8	5.9	22.9	59.8	0.5	0.1	39.6	35.5	1.7	0.3	62.5	7.2	18.5	0.7	73.6
1991	59.4	8.8	18.8	12.9	57.7	4.1	3.8	34.4	30.7	2.9	0.9	65.5	3.9	23.5	1.6	71.0
1992	67.0	1.4	17.	29.9	48.6	0.6	0.0	50.8	16.0	1.6	0.0	82.4	2.3	18.1	0.6	79.0
1993	63.6	8.0	2.9	25.6	51.7	6.0	1.1	41.2	31.3	3.7	0.1	64.9	5.6	17.1	0.5	76.9
1994	72.1	0.0	8.9	18.9	57.5	0.0	1.7	40.7	19.9	0.7	0.1	79.3	3.2	16.5	0.8	79.5
1995	71.8	2.2	2.3	23.7	55.7	2.2	1.1	41.0	27.2	5.4	1.0	66.4	6.9	34.8	3.4	55.0
1996	47.5	10.7	25.2	16.6	37.7	15.5	14.7	32.1	20.8	21.4	12.2	45.6	7.2	32.4	5.0	55.5
1997	68.8	0.3	1.6	29.2	50.9	0.3	0.7	48.2	14.7	1.3	0.3	83.8	1.4	5.7	0.0	92.9
1998	63.9	6.4	7.5	22.2	58.2	5.8	1.4	34.6	32.9	8.4	0.2	58.6	7.1	11.2	0.4	81.3
1999	54.0	11.3	20.4	14.3	52.0	10.3	10.0	27.7	35.7	8.2	4.9	51.2	5.9	25.8	3.8	64.4
Avg	**64.7**	**3.9**	**7.7**	**23.7**	**50.5**	**3.9**	**2.4**	**43.2**	**23.0**	**5.1**	**1.5**	**70.5**	**4.7**	**21.1**	**1.5**	**72.7**

Table C.3: July Month

Year	GB				HS				NIC				CRP			
	CAR	GoM	ETPS	NSAS	CAR	GoM	ETPS	NSAS	CAR	GoM	ETPS	NSAS	CAR	GoM	ETPS	NSAS
1980	52.1	2.4	39.2	6.2	55.4	10.5	20.6	13.5	25.8	29.3	16.2	28.8	4.1	44.5	4.7	46.7
1981	64.3	2.8	22.5	10.5	62.6	2.9	8.1	26.4	48.2	8.7	2.8	40.2	15.2	40.9	2.5	41.5
1982	36.5	1.6	55.6	6.3	44.1	8.5	33.0	14.3	34.2	17.3	18.4	30.0	15.9	38.7	5.3	40.1
1983	58.2	4.0	28.3	9.5	60.0	2.5	13.3	24.2	31.7	6.7	5.3	56.3	7.8	41.9	5.8	44.5
1984	80.9	0.0	17.6	1.4	88.0	0.0	1.7	10.3	63.2	1.2	1.7	33.9	19.3	37.3	3.0	40.4
1985	46.2	3.0	44.9	6.0	45.4	4.9	31.1	18.7	31.6	11.3	22.9	34.2	12.7	32.6	5.6	49.2
1986	48.6	0.2	40.6	10.5	56.4	2.2	16.6	24.8	42.0	8.8	8.5	40.7	16.7	38.1	5.8	39.4
1987	21.1	2.6	76.3	0.0	52.2	1.9	44.7	1.1	53.0	7.8	33.0	6.2	23.6	44.6	13.7	18.1
1988	50.3	12.8	34.1	2.8	75.7	9.0	8.8	6.4	64.9	13.2	2.4	19.6	22.9	46.9	6.5	23.6
1989	33.1	8.7	52.6	5.6	44.5	11.6	24.8	19.1	48.6	12.1	9.2	30.2	15.9	35.5	2.6	46.0
1990	24.1	11.1	64.6	0.2	39.9	6.1	50.1	3.8	32.0	22.8	37.0	8.3	10.6	54.2	16.2	19.0
1991	54.8	1.6	37.1	6.6	53.2	0.2	26.8	19.8	39.5	9.6	18.2	32.7	9.9	43.3	6.6	40.2
1992	44.8	6.0	42.5	6.7	54.9	5.1	21.3	18.7	44.3	8.6	6.6	40.5	11.5	32.6	3.9	52.1
1993	47.6	4.3	37.1	11.0	52.7	3.9	7.9	35.5	38.7	7.3	1.5	52.5	10.0	37.1	2.7	50.2
1994	32.5	8.4	52.4	6.7	40.0	12.0	29.1	18.9	37.3	18.3	13.6	30.8	10.2	48.1	6.0	35.7
1995	19.9	9.8	70.1	0.3	24.6	10.1	59.2	6.1	17.0	26.9	43.3	12.7	3.8	59.8	14.4	22.0
1996	28.3	5.4	62.9	3.5	41.4	5.4	37.5	15.6	27.4	28.1	25.1	19.4	8.3	45.9	8.3	37.5
1997	30.7	12.1	53.6	3.5	33.8	12.6	41.3	12.3	31.7	15.4	34.9	17.9	11.1	29.6	19.4	39.9
1998	43.6	14.2	29.1	13.0	40.9	15.0	21.1	23.0	27.6	23.3	20.6	28.5	6.4	43.2	10.6	39.9
1999	27.3	4.6	62.1	5.9	20.6	9.5	49.5	20.5	12.1	28.6	34.0	25.3	4.9	59.3	15.6	20.2
Avg	**42.2**	**5.8**	**46.2**	**5.8**	**49.3**	**6.7**	**27.3**	**16.7**	**37.5**	**15.3**	**17.8**	**29.4**	**12.0**	**42.7**	**8.0**	**37.3**

Table C.4: October Month

D

Vertical structure of the CLLJ for the variability modes

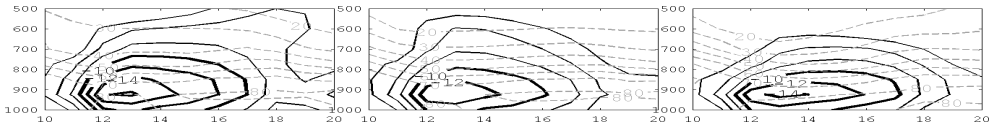

(a) Meridional structure Jan

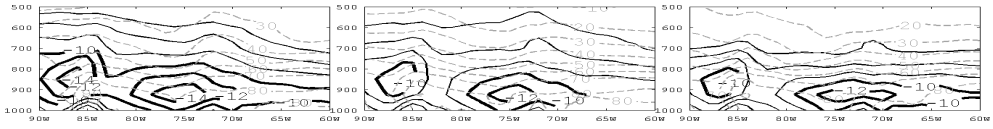

(b) Zonal structure Jan

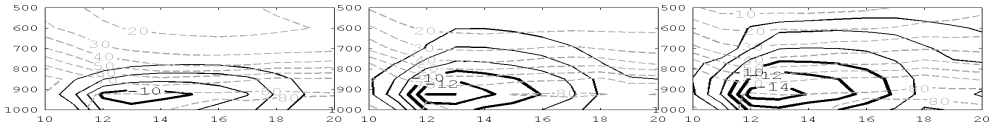

(c) Meridional structure Feb

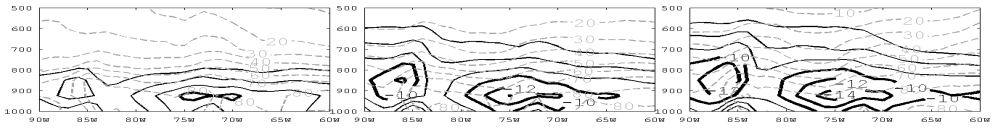

(d) Zonal structure Feb

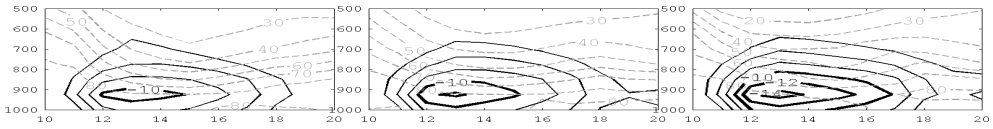

(e) Meridional structure Apr

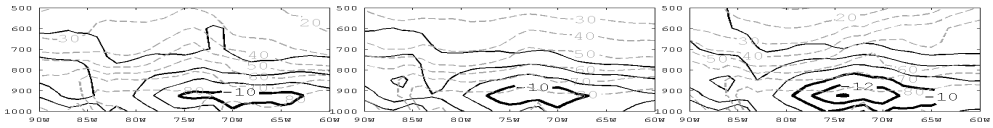

(f) Zonal structure Apr

Figure D.1: Climatological meridional and zonal averaged vertical structure of the CLLJ for ENSO composites. Zonal wind speed is shown with black contours (winds stronger than 10 m/s are highlighted with thicker lines) and relative humidity with gray dashed lines.

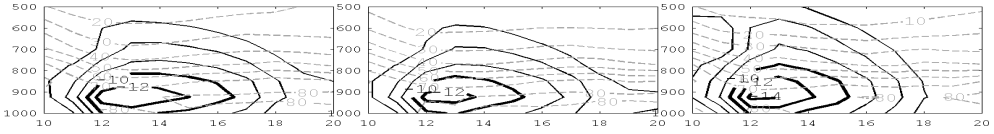

(a) Meridional structure Jan

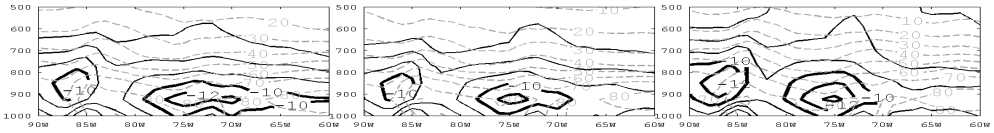

(b) Zonal structure Jan

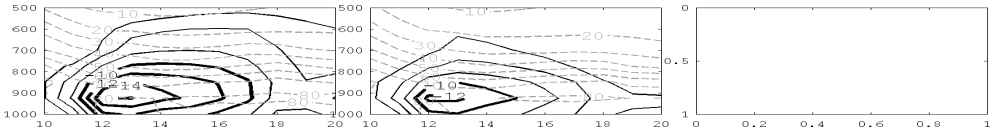

(c) Meridional structure Feb

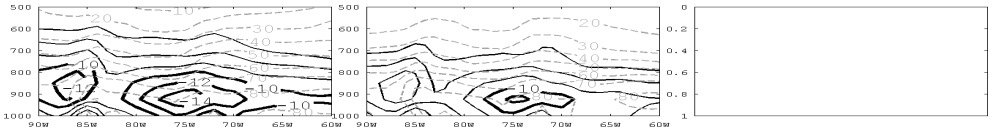

(d) Zonal structure Feb

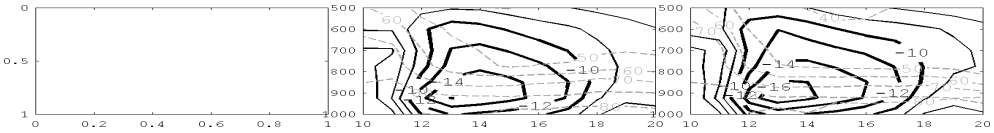

(e) Meridional structure Jul

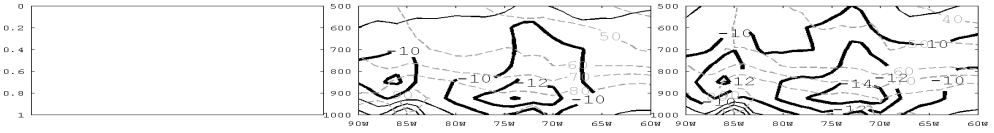

(f) Zonal structure Jul

Figure D.2: Climatological meridional and zonal averaged vertical structure of the CLLJ for NAO composites. Zonal wind speed is shown with black contours (winds stronger than 10 m/s are highlighted with thicker lines) and relative humidity with gray dashed lines.

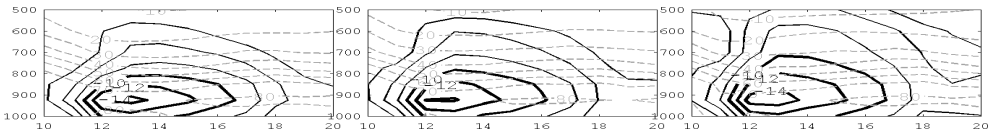

(a) Meridional structure Jan

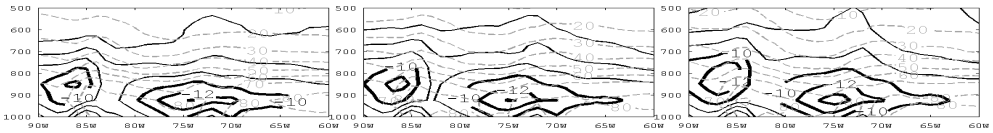

(b) Zonal structure Jan

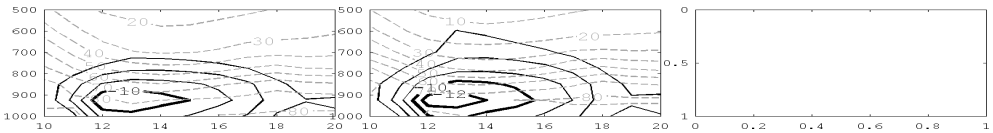

(c) Meridional structure Mar

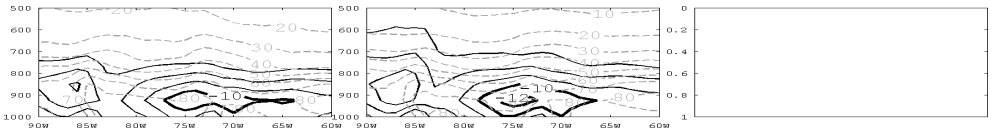

(d) Zonal structure Mar

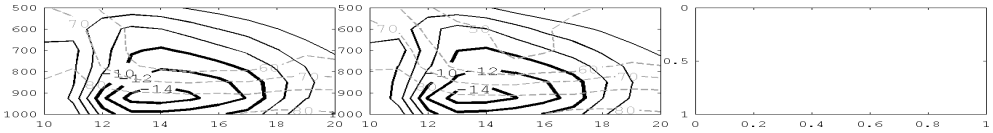

(e) Meridional structure Jun

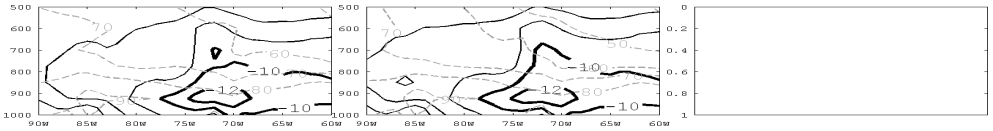

(f) Zonal structure Jun

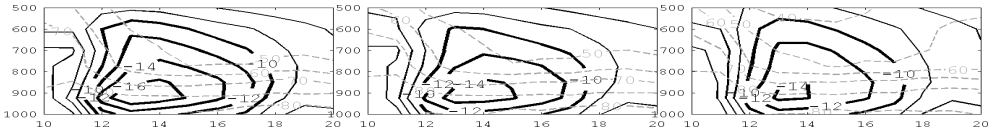

(g) Meridional structure Jul

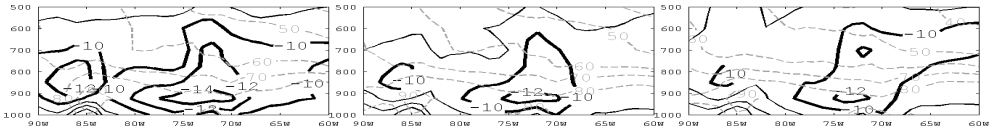

(h) Zonal structure Jul

Figure D.3: Climatological meridional and zonal averaged vertical structure of the CLLJ for MJO composites. Zonal wind speed is shown with black contours (winds stronger than 10 m/s are highlighted with thicker lines) and relative humidity with gray dashed lines.

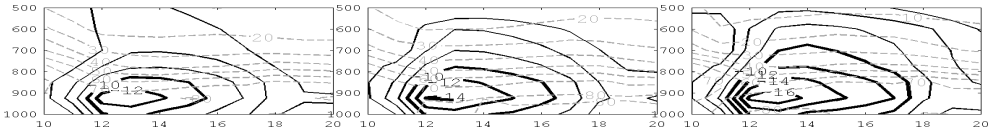

(a) Meridional structure Jan

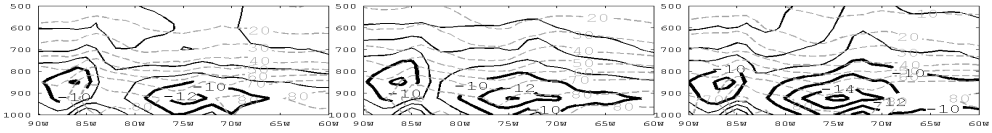

(b) Zonal structure Jan

Figure D.4: Climatological meridional and zonal averaged vertical structure of the CLLJ for PDO composites. Zonal wind speed is shown with black contours (winds stronger than 10 m/s are highlighted with thicker lines) and relative humidity with gray dashed lines.

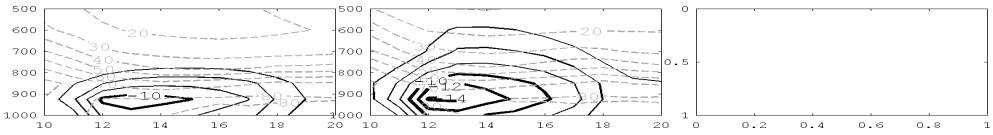

(a) Meridional structure Feb

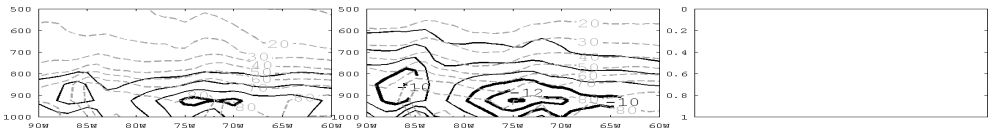

(b) Zonal structure Feb

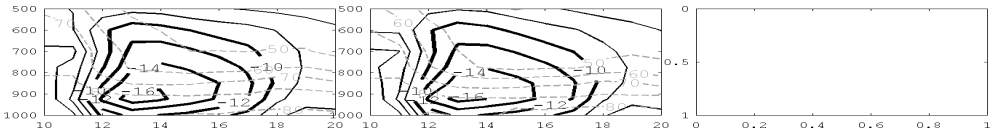

(c) Meridional structure Jul

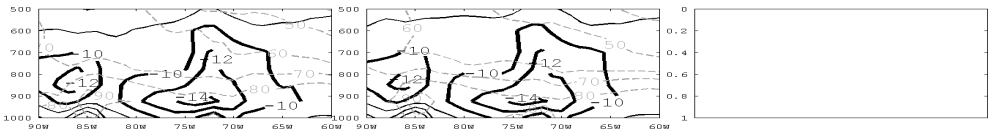

(d) Zonal structure Jul

Figure D.5: Climatological meridional and zonal averaged vertical structure of the CLLJ for WHWP composites. Zonal wind speed is shown with black contours (winds stronger than 10 m/s are highlighted with thicker lines) and relative humidity with gray dashed lines.

E

List of acronyms

ABL Atmospheric Boundary Layer

AEW African Easterly Wave

AMO Atlantic Multi-decadal Oscillation

AMS American Monsoon System

AWP Atlantic Warm Pool

CAS Central America Source

CLLJ Caribbean Low Level Jet

CMAP Climate Prediction Center Merged Analysis of Precipitation

COLA Center for Ocean-Land-Atmosphere Studies

CPC Climate Prediction Center

CRD Costa Rica Dome

CRP Costa Rica- Panama

CRU Climate Research Unit

CS Caribbean Source

DIV Divergence

EAf East Africa

ECMWF European Centre for Medium-Range Weather Foreccast

EEEV Eastern Eurasia Evapotranspiration

ENP Eastern North Pacfic

ENSO El Nino-Southern Oscillation

EOF Empirical Orthogonal Function

ETPac Eastern Tropical Pacific

ETPS Eastern Tropical Pacific Source

GB Guatemala-Belize

GCM General Circulation model

GoC Gulf of California

GoMS Gulf of Mexico Source

GPLLJ Great Plain Low Level Jet

GPS Global Positioning System

HS Honduras- El Salvador

IAS Intra Americas Seas

ITCZ Inter Tropical Convergence Zone

IO Indian Ocean

LDM Lagrangian Dispersion Model

LPDM Lagrangian Particle Dispersion Model

MCS Meso-scale Convective System

MES Monsoon Experiment South America

MJO Madden-Julian Oscillation

MS Mediterranean Sea

MSD Mid Summer Drought

MSLP Mean Sea Level Pressure

NAM North American Monsoon

NAME North American Monsoon Experiment

NAMS North American Monsoon System

NAO North Atlantic Oscillation

NASH North Atlantic Subtropical High

Natl North Atlantic

NCEP National Centers for Environmental Prediction

NEM North Eastern Mexico

NIC Nicaragua

NP North Pacific

NSAS Northern South America Source

NWM North Western Mexico

OAFlux Objectively Analyzed air-sea Heat Fluxes

PBL Planetary Boundary Layer

PDO Pacific Decadal Oscillation

PDSI Palmer Drought Severity Index

PDV Pacific Decadal Variability

RS Red Sea

SA South America

SACZ South American Convergence Zone

Saf South Africa

SALLJ South American Low Level Jet

SALLJEX South American Low Level Jet Experiment

SAMS South American Monsoon System

SCA Southern Central America

SLP Sea Level Pressure

SP South Pacific

SPCZ South Pacific Convergence Zone

SST Sea Surface Temperature

SWUS South Western United States

TCWV Total Column Water Vapour

TNA Tropical North Atlantic

USEV United States of America Evapotranspiration

USGS United States Geological Survey

VIDMF Vertical Integral of divergence of moisture flux

VITCWV Vertical Integral of Total Column Water Vapour

WAf West Africa

WCR Water Cycle Research

WHWP Western Hemisphere Warm Pool

WVT Water Vapour Tracer

References

[1] D. K. Adams and A. C. Comrie. The North American Monsoon. *Bulletin of the American Meteorological Society*, 78:2197–2213, October 1997.

[2] H. Alexandersson. A homogeneity test applied to precipitation data. *J. Climatol.*, pages 661–675, 1986.

[3] E.J. Alfaro. Some characteristics of the annual precipitation cycle in central america and their relationships with its surrounding tropical oceans. *Top. Meteorol. Oceanogr.*, 9:88–103, 2002.

[4] J. Amador. A climatic feature of tropical americas: The trade wind easterly jet. *Top. Meteor. Ocean.*, pages 91–102, 1998.

[5] J. Amador and V. Magana. Dynamics of the low level jet over the caribbean sea. *In Preprints of 23th Conference on Hurricanes and Tropical Meteorology, American Meteorological Society*, pages 868–869, January 1999.

[6] J. A. Amador. The Intra-Americas Sea Low-level Jet. *Annals of the New York Academy of Sciences*, 1146:153–188, December 2008.

[7] J.A. Amador, R. Chacon, and S. Laporte. Climate and climate variability in the arenal river basin of costa rica. *Klewer Academic Publishers B.V.*, pages 317–350, 2003.

[8] Jorge A. Amador, Eric J. Alfaro, Omar G. Lizano, and Victor O. Magaña. Atmospheric forcing of the eastern tropical pacific: A review. *Progress In Oceanography*, 69(2D4):101 – 142, 2006. A Review of Eastern Tropical Pacific Oceanography.

[9] M.E. Angeles, J.E. Gonzalez, N.D. Ramirez-Beltran, C.A. Tepley, and D.E. Comarazamy. Origins of the caribbean rainfall bimodal behavior. *J. Geophys. Res.*, 1996.

[10] S.A. Ashby, M.A. Taylor, and A.A. Chen. Statistical models for predicting rainfall in the Caribbean. *Theoretical and Applied Climatology*, 82:65–80, August 2005.

[11] M. Barlow and D. Salstein. Summertime influence of the Madden-Julian Oscillation on daily rainfall over Mexico and Central America. *Geophys. Res. Lett*, 33:21708, November 2006.

[12] A.G. Barnston and R.E. Livezey. Classification, Seasonality and Persistence of Low-Frequency Atmospheric Circulation Patterns. *Monthly Weather Review*, 115:1083, 1987.

[13] G.D. Bell and M. Chelliah. Leading Tropical Modes Associated with Interannual and Multidecadal Fluctuations in North Atlantic Hurricane Activity. *Journal of Climate*, 19:590, 2006.

[14] R. Berkowicz and L. P. Prahm. Sensible Heat Flux Estimated from Routine Meteorological Data by the Resistance Method. *"Journal of Applied Meteorology"*, 21:1845–1864, December 1982.

[15] M. Biasutti, A.H. Sobel, and Y. Kushnir. Agcm precipitation biases in the tropical atlantic. *Journal of Climate*, 19:935, 2006.

[16] B. Bisselink and A.J. Dolman. Precipitation recycling: Moisture sources over europe using era-40 data. *Journal of Hydrometeorology*, 9:1073, 2008.

[17] J .Bjerknes. A possible response of the atmospheric hadley circulation to equatorial anomalies of ocean temperature. *Tellus*, 18:820, May 1966.

[18] J. Bjerknes. Atmospheric teleconnections from the equatorial pacific1. *Monthly Weather Review*, 97:163, 1969.

[19] W. D. Bonner. Climatology of the Low Level Jet. *Monthly Weather Review*, 96:833, 1968.

[20] M.G. Bosilovich, Y.C. Sud, S.D. Schubert, and G.K. Walker. Numerical simulation of the large-scale north american monsoon water sources. *J. Geophys. Res.*, D16, 2003.

[21] L. Brito-Castillo, A. V. Douglas, A. Leyva-Contreras, and D. Lluch-Belda. The effect of large-scale circulation on precipitation and streamflow in the Gulf of California continental watershed. *International Journal of Climatology*, 23:751–768, June 2003.

[22] M. Budyko and A. Drozdov. Zakonomernosti vlagooborota v atmosfere (regularities of the hydrologic cycle in the atmosphere). *Izv. Akad. Nauk SSSR*, 4:5–14, 1953.

[23] Mikhail Budyko. *Climate an Life*. Academic Press Inc.l, London, UK, 1974.

[24] M.A. Cane, S.E. Zebiak, and S.C. Dolan. Experimental forecasts of el nino. *Nature*, 321:827–832, June 1986.

[25] C.L. Castro, T.B. McKee, and R.A. Pielke. The relationship of the north american monsoon to tropical and north pacific sea surface temperatures as revealed by observational analyses. *Journal of Climate*, 14:4449–4473, December 2001.

[26] C.-P. Chang, Y. Zhang, and T. Li. Interannual and Interdecadal Variations of the East Asian Summer Monsoon and Tropical Pacific SSTs. Part I: Roles of the Subtropical Ridge. *Journal of Climate*, 13:4310–4325, December 2000.

[27] A.A. Chen and M.A. Taylor. Investigating the link between early season caribbean rainfall and the el niño + 1 year. *International Journal of Climatology*, 22:87–106, January 2002.

[28] K.H. Cook and E.K. Vizy. Hydrodynamics of the Caribbean Low-Level Jet and Its Relationship to Precipitation. *Journal of Climate*, 23:1477, 2010.

[29] S. Curtis and D.W. Gamble. Regional Variations of the Caribbean Mid-Summer Drought. *AGU Spring Meeting Abstracts*, page C2, May 2007.

[30] M. J. Czikowsky and D. R. Fitzjarrald. Detecting rainfall interception in an Amazonian rain forest with eddy flux measurements. *Journal of Hydrology*, 377:92–105, October 2009.

[31] M.J. Czikowsky and D.R. Fitzjarrald. Detecting rainfall interception in an Amazonian rain forest with eddy flux measurements. *Journal of Hydrology*, 377:92–105, oct 2009.

[32] A. Dai and T.M.L. Wigley. Global Patterns of ENSO-induced Precipitation. *Geophys. Res. Lett*, 27:1283, May 2000.

[33] I. Daubechies. *Ten Lectures on Wavelets*. SIAM, New York, USA, 1992.

[34] T. Delworth, S. Manabe, and R. J. Stouffer. Interdecadal Variations of the Thermohaline Circulation in a Coupled Ocean-Atmosphere Model. *Journal of Climate*, 6:1993–2011, November 1993.

[35] T. L. Delworth and R. J. Greatbatch. Multidecadal Thermohaline Circulation Variability Driven by Atmospheric Surface Flux Forcing. *Journal of Climate*, 13:1481–1495, May 2000.

[36] T. L. Delworth and M. E. Mann. Observed and simulated multidecadal variability in the northern hemisphere. *Climate Dynamics*, 16:661–676, 2000. 10.1007/s003820000075.

[37] M.D. Dettinger, D.S. Battisti, R.D. Garreaud, G.J. McCabe, and C.M. Bitz. *Interhemispheric effects of interannual and decadal ENSO-like climate variations on the Americas, in Inter-hemispheric Climate Linkages*. Cambridge University Press, Cambridge, UK, 2001.

[38] P.A. Dirmeyer and K.L. Brubaker. Evidence for trends in the northern hemisphere water cycle. *Atmos. Environ.*, 2006.

[39] P.A. Dirmeyer and K.L. Brubaker. Characterization of the Global Hydrologic Cycle from a Back-Trajectory Analysis of Atmospheric Water Vapor. *Journal of Hydrometeorology*, 8:20, 2007.

[40] F. Dominguez and P. Kumar. Precipitation recycling variability and ecoclimatological stability -a study using narr data. part i: Central u.s. plains ecoregion. *Journal of climate*, 21(20):5165–5186, 2008. eng.

[41] F. Dominguez, P. Kumar, X.Z. Liang, and M. Ting. Impact of Atmospheric Moisture Storage on Precipitation Recycling. *Journal of Climate*, 19:1513, 2006.

[42] S.R. Dorling, T.D. Davies, and C.E. Pierce. Cluster analysis a technique for estimating the synoptic meteorological controls on air and precipitation chemistry - method and applications. *Atmospheric environment. Part A, General topics*, 26(14):2575–2581, 1992. eng.

[43] M.W. Douglas, R.A. Maddox, K. Howard, and S. Reyes. The Mexican Monsoon. *Journal of Climate*, 6:1665–1678, August 1993.

[44] A.M. Durán-Quesada, L. Gimeno, J.A. Amador, and R. Nieto. Moisture sources for Central America: Identification of moisture sources using a Lagrangian analysis technique. *Journal of Geophysical Research (Atmospheres)*, 115:5103, March 2010.

[45] A.M. Durán-Quesada, M. Reboita, and L. Gimeno. Precipitation in tropical america and the associated sources of moisture: a short review. *Hydrological Sciences Journal*, 57(4):612–624, 2012.

[46] E.A.B. Eltahir and R.L. Bras. Precipitation recycling. *Reviews of geophysics (1985)*, 34(3):367–378, 1996. eng.

[47] E.A.B. Eltahir and C. Gong. Dynamics of Wet and Dry Years in West Africa. *Journal of Climate*, 9:1030–1042, may 1996.

[48] K. Emanuel and R.T. Pierrehumbert. *Microphysical and dynamical control of tropospheric water vapor in Clouds, Chemistry and Climate, Nato ASI Series 35*. Springer, Berlin, Germany, 1995.

[49] K.A. Emanuel and M. Ivkovi-Rothman. Development and Evaluation of a Convection Scheme for Use in Climate Models. *Journal of Atmospheric Sciences*, 56:1766–1782, jun 1999.

[50] D.B. Enfield, A.M. Mestas-Nunez, and P.J. Trimble. The atlantic multidecadal oscillation and its relation to rainfall and river flows in the continental u.s. *Geophys. Res. Lett.*, 10:2077–2080, 2001.

[51] M.N. Evans, M.A. Cane, D.P. Schrag, A. Kaplan, B.K. Linsley, R. Villalba, and G.M. Wellington. Support for tropically-driven Pacific decadal variability based on paleoproxy evidence. *Geophys. Res. Lett.*, 28:3689–3692, oct 2001.

[52] B. Everitt. *Cluster analysis*. Heinemann, London, UK, 1 edition, 1980.

[53] C. W. Fairall, E. F. Bradley, J. E. Hare, A. A. Grachev, and J. B. Edson. Bulk Parameterization of Air Sea Fluxes: Updates and Verification for the COARE Algorithm. *Journal of Climate*, 16:571–591, February 2003.

[54] M. Falvey and R.D. Garreaud. Moisture variability over the South American Altiplano during the South American Low Level Jet Experiment (SALLJEX) observing season. *Journal of Geophysical Research (Atmospheres)*, 110(D9):22105, nov 2005.

[55] L. Feng, D. Wu, X. Lin, and X. Meng. The effect of regional ocean-atmosphere coupling on the long-term variability in the Pacific Ocean. *Advances in Atmospheric Sciences*, 27:393–402, mar 2010.

[56] B. Fontaine and S. Janicot. Sea Surface Temperature Fields Associated with West African Rainfall Anomaly Types. *Journal of Climate*, 9:2935–2940, November 1996.

[57] S. Fueglistaler, M. Bonazzola, P. H. Haynes, and T. Peter. Stratospheric water vapor predicted from the Lagrangian temperature history of air entering the stratosphere in the tropics. *Journal of Geophysical Research (Atmospheres)*, 110:8107, April 2005.

[58] D. J. Gaffen, T. P. Barnett, and W. P. Elliott. Space and Time Scales of Global Tropospheric Moisture. *Journal of Climate*, 4:989–1008, October 1991.

[59] J. Galewsky, A. Sobel, and I. Held. Diagnosis of Subtropical Humidity Dynamics Using Tracers of Last Saturation. *Journal of Atmospheric Sciences*, 62:3353–3367, September 2005.

[60] D.W. Gamble, D.B. Parnell, and S. Curtis. Spatial variability of the Caribbean mid-summer drought and relation to north Atlantic high circulation. *International Journal of Climatology*, 28:343–350, mar 2008.

[61] A. Giannini, J. C. H. Chiang, M. A. Cane, Y. Kushnir, and R. Seager. The ENSO Teleconnection to the Tropical Atlantic Ocean: Contributions of the Remote and Local SSTs to Rainfall Variability in the Tropical Americas(. *Journal of Climate*, 14:4530–4544, December 2001.

[62] A. Giannini, Y. Kushnir, and M.A. Cane. Interannual Variability of Caribbean Rainfall, ENSO, and the Atlantic Ocean*. *Journal of Climate*, 13:297–311, jan 2000.

[63] A. Giannini, R. Saravanan, and P. Chang. Oceanic Forcing of Sahel Rainfall on Interannual to Interdecadal Time Scales. *Science*, 302:1027–1030, November 2003.

[64] L. Gimeno, A. Drumond, R. Nieto, R.M. Trigo, and A. Stohl. On the origin of continental precipitation. *Geophys. Res. Lett.*, 37:13804, jul 2010.

[65] L. Gimeno, R. Nieto, A. Drumond, A.M. Durán-Quesada, A. Stohl, H. Sodemann, and R.M. Trigo. A close look at oceanic sources of continental precipitation. *EOS Transactions*, 92:193–194, jun 2011.

[66] S. B. Goldenberg, C. W. Landsea, A. M. Mestas-Nuñez, and W. M. Gray. The Recent Increase in Atlantic Hurricane Activity: Causes and Implications. *Science*, 293:474–479, July 2001.

[67] S.B. Goldenberg and L.J. Shapiro. Physical Mechanisms for the Association of El Niño and West African Rainfall with Atlantic Major Hurricane Activity. *Journal of Climate*, 9:1169–1187, jun 1996.

[68] W. W. Grabowski and M. W. Moncrieff. Moisture-convection feedback in the tropics. *Quarterly Journal of the Royal Meteorological Society*, 130(604):3081–3104, 2004.

[69] William M. Gray. Strong association between west african rainfall and u.s. landfall of intense hurricanes. *Science*, 249(4974):1251–1256, 1990.

[70] A.M. Grimm. The El Niño Impact on the Summer Monsoon in Brazil: Regional Processes versus Remote Influences. *Journal of Climate*, 16:263–280, jan 2003.

[71] C.E. Hane, , C.L. Ziegler, and H.B. Bluestein. Investigation of the Dryline and Convective Storms Initiated along the Dryline: Field Experiments during COPS-91. *Bulletin of the American Meteorological Society*, 74:2133–2145, nov 1993.

[72] S.R. Hanna. *Applications in Air Pollution Modeling, in F. T. M. Nieuwstadt and H. van Dop (eds.), Atmospheric Turbulence and Air Pollution Modelling*. D. Reidel Publishing Company, Dordrecht, 1982.

[73] D.L. Hartmann. *Global Physical Climatology*. Academic Press, 1994.

[74] S. Hastenrath. Circulation and teleconnection mechanisms of Northeast Brazil droughts. *Progress in Oceanography*, 70:407–415, aug 2006.

[75] S. L. Hastenrath. On General Circulation and Energy Budget in the Area of the Central American Seas. *"Journal of Atmospheric Sciences"*, 23:694–711, November 1966.

[76] S. L. Hastenrath. Diurnal Fluctuations of the Atmospheric Moisture Flux in the Caribbean and Gulf of Mexico Area. *"journal of geophysical research"*, 72:4119, August 1967.

[77] S.L. Hastenrath. Rainfall distribution and regime in central america. *Archiv fur Meteorologie, Geophysik, and Bioklimatologie, Series B*, 15:201–241, 1967.

[78] S.L. Hastenrath. Fourier analysis of central american rainfall. *Archiv fur Meteorologie, Geophysik und Bioklimatologie, Series B*, 16:81–94, 1968.

[79] B. B. Hicks. Behavior of Turbulence Statistics in the Convective Boundary Layer. *Journal of Applied Meteorology*, 24:607–616, June 1985.

[80] R.W. Higgins, Y. Yao, and X.L. Wang. Influence of the North American Monsoon System on the U.S. Summer Precipitation Regime. *Journal of Climate*, 10:2600–2622, oct 1997.

[81] B. J. Hoskins and M. J. Rodwell. A Model of the Asian Summer Monsoon. Part I: The Global Scale. *Journal of Atmospheric Sciences*, 52:1329–1340, May 1995.

[82] R.A. Houze and A.K. Betts. Convection in GATE. *Reviews of Geophysics and Space Physics*, 19:541–576, nov 1981.

[83] Q. Hu and S. Feng. Interannual Rainfall Variations in the North American Summer Monsoon Region: 1900-98*. *Journal of Climate*, 15:1189–1202, May 2002.

[84] J.W. Hurrel. Influence of variations in extratropical wintertime teleconnections on northern hemisphere temperature. *Geophysical research letters*, 23(6):665–668, 1996. eng.

[85] S. Janicot, F. Mounier, N. M. J. Hall, S. Leroux, B. Sultan, and G. N. Kiladis. Dynamics of the West African Monsoon. Part IV: Analysis of 25-90-Day Variability of Convection and the Role of the Indian Monsoon. *Journal of Climate*, 22:1541, 2009.

[86] B. Joseph and M. Moustaoui. Transport, Moisture, and Rain in a Simple Monsoonlike Flow. *Journal of Atmospheric Sciences*, 57:1817–1838, June 2000.

[87] I.S. Kang, C.H. Ho, Y.K. Lim, and K.M. Lau. Principal Modes of Climatological Seasonal and Intraseasonal Variations of the Asian Summer Monsoon. *Monthly Weather Review*, 127:322, 1999.

[88] B.D. Katsoulis and D.M. Whelpdale. A climatological analysis of four-day back trajectories from aliartos, Greece. *Theoretical and Applied Climatology*, 47:93–103, jun 1993.

[89] A. Keats, E. Yee, and L. Fue-Sang. Bayesian inference for source determination with applications to a complex urban environment. *Atmospheric environment (1994)*, 41(3):465–479, 2007. eng.

[90] R.A. Kerr. A north atlantic climate pacemaker for the centuries. *Science*, 288:1984–1986, 2000.

[91] P. Knippertz and W. Heini. A lagrangian climatology of tropical moisture exports to the northern hemispheric extratropics. *Journal of climate*, 23(4):987–1003, 2010. eng.

[92] P. Knippertz and J.E. Martin. Tropical plumes and extreme precipitation in subtropical and tropical West Africa. *Quarterly Journal of the Royal Meteorological Society*, 131:2337–2365, jul 2005.

[93] Y. Kodama. Large-scale common features of subtropical precipitation zones (the baiu frontal zone, the spcz, and the sacz). i : Characteristics of subtropical frontal zones. *Journal of the Meteorological Society of Japan*, 70(4):813–836, 1992. eng.

[94] V. Krishnamurthy and J. Shukla. Intraseasonal and Interannual Variability of Rainfall over India. *Journal of Climate*, 13:4366–4377, dec 2000.

[95] N. Kurita, N. Yoshida, G. Inoue, and E.A. Chayanova. Modern isotope climatology of Russia: A first assessment. *Journal of Geophysical Research (Atmospheres)*, 109(D18):3102, feb 2004.

[96] M.S. Lachniet, W.P. Patterson, S.J. Burns, Y. Asmerom, and V.J. Polyak. Caribbean and pacific moisture sources on the isthmus of panama revealed from stalagmite and surface water d18o gradients. *Geophys. Res. Lett.*, 2007.

[97] Christopher W. Landsea, Roger A. Pielke, Alberto M. Mestas-Nuñez, and John A. Knaff. Atlantic basin hurricanes: Indices of climatic changes. *Climatic Change*, 42:89–129, 1999. 10.1023/A:1005416332322.

[98] M. Latif, E. Roeckner, M. Botzet, M. Esch, H. Haak, S. Hagemann, J. Jungclaus, S. Legutke, S. Marsland, U. Mikolajewicz, and J. Mitchell. Reconstructing, Monitoring, and Predicting Multidecadal-Scale Changes in the North Atlantic Thermohaline Circulation with Sea Surface Temperature. *Journal of Climate*, 17:1605–1614, April 2004.

[99] K.M. Lau and H.Y. Weng. Climate signal detection using wavelet transform: How to make a time series sing. *Bull. Amer. Meteor. Soc.*, pages 2391–2402, 1995.

[100] G. Leduc, L. Vidal, K. Tachikawa, F. Rostek, C. Sonzogni, L. Beaufort, and E. Bard. Moisture transport across central america as a positive feedback on abrupt climatic changes. *Nature*, 445:908–911, 2007.

[101] J.D. Lenters and K.H. Cook. Summertime Precipitation Variability over South America: Role of the Large-Scale Circulation. *Monthly Weather Review*, 127:409, 1999.

[102] R.S. Lindzen and S. Nigam. On the Role of Sea Surface Temperature Gradients in Forcing Low-Level Winds and Convergence in the Tropics. *Journal of Atmospheric Sciences*, 44:2418–2436, sep 1987.

[103] B. R. Lintner and J. C. H. Chiang. Adjustment of the Remote Tropical Climate to El Niño Conditions. *Journal of Climate*, 20:2544, 2007.

[104] W. T. Liu, K. B. Katsaros, and J. A. Businger. Bulk Parameterization of Air-Sea Exchanges of Heat and Water Vapor Including the Molecular Constraints at the Interface. *Journal of Atmospheric Sciences*, 36:1722–1735, September 1979.

[105] Z. Liu and S. Xie. Equatorward Propagation of Coupled Air-Sea Disturbances with Application to the Annual Cycle of the Eastern Tropical Pacific. *Journal of Atmospheric Sciences*, 51:3807–3822, December 1994.

[106] D.J. Lorenz and D.L. Hartmann. The Effect of the MJO on the North American Monsoon*. *Journal of Climate*, 19:333, 2006.

[107] R.A. Madden and P.R. Julian. Observations of the 40 50-Day Tropical Oscillation A Review. *Monthly Weather Review*, 122:814, 1994.

[108] R. A. Maddox, D. M. McCollum, and K. W. Howard. Large-Scale Patterns Associated with Severe Summertime Thunderstorms over Central Arizona. *Weather and Forecasting*, 10:763–778, December 1995.

[109] V. Magaña, J.A. Amador, and S. Medina. The Midsummer Drought over Mexico and Central America. *Journal of Climate*, 12:1577–1588, jun 1999.

[110] V. Magaña, J.A. Amador, and S. Medina. The Midsummer Drought over Mexico and Central America. *Journal of Climate*, 12:1577–1588, jun 1999.

[111] B.A. Malmgren, A. Winter, and D. Chen. El Niño-Southern Oscillation and North Atlantic Oscillation Control of Climate in Puerto Rico. *Journal of Climate*, 11:2713–2718, oct 1998.

[112] E.D. Maloney and S.K. Esbensen. The Amplification of East Pacific Madden-Julian Oscillation Convection and Wind Anomalies during June-November. *Journal of Climate*, 16:3482–3497, nov 2003.

[113] H.B. Mann and D.R. Whitney. On a test of whether one of two random variables is stochastically larger than the other. *The Annals of Mathematical Statistics*, pages 50–60, 1947.

[114] N.J. Mantua and S.R. Hare. 2002 review the pacific decadal oscillation. *Journal of Oceanography*, 58:35–44, 2002.

[115] N.J. Mantua, S.R. Hare, Y. Zhang, J.M. Wallace, and R.C. Francis. A Pacific Interdecadal Climate Oscillation with Impacts on Salmon Production. *Bulletin of the American Meteorological Society*, 78:1069–1079, jun 1997.

[116] B.E. Mapes, P. Liu, and N. Buenning. Indian Monsoon Onset and the Americas Midsummer Drought: Out-of-Equilibrium Responses to Smooth Seasonal Forcing. *Journal of Climate*, 18:1109–1115, apr 2005.

[117] J.A. Marengo. Interannual variability of surface climate in the Amazon basin. *International Journal of Climatology*, 12:853–863, dec 1992.

[118] J.A. Marengo, B. Liebmann, V.E. Kousky, N.P. Filizola, and I.C. Wainer. Onset and End of the Rainy Season in the Brazilian Amazon Basin. *Journal of Climate*, 14:833–852, mar 2001.

[119] E.R. Martin and C. Schumacher. Modulation of Caribbean Precipitation by the Madden-Julian Oscillation. *Journal of Climate*, 24:813–824, feb 2011.

[120] D. Martínez-Castro, R. Porfirio da Rocha, A. Bezanilla-Morlot, L. Alvarez-Escudero, J.P. Reyes-Fernández, Y. Silva-Vidal, and R.W. Arritt. Sensitivity studies of the RegCM3 simulation of summer precipitation, temperature and local wind field in the Caribbean Region. *Theoretical and Applied Climatology*, 86:5–22, sep 2006.

[121] C.R. Mechoso, A.W. Robertson, C.F. Ropelewski, and A.M. Grimm. 2005: The american monsoon systems: An introduction. *WMO Tech. Doc. 1266*, pages 197–206, 2005.

[122] M. Méndez and V. Magaña. Regional Aspects of Prolonged Meteorological Droughts over Mexico and Central America. *Journal of Climate*, 23:1175, 2010.

[123] F. Mesinger, G. Dimego, E. Kalnay, K. Mitchell, P.C. Shafran, W. Ebisuzaki, D. Jovi, J. Wollen, E. Rogers, E.H. Berbery, M.B. Ek, Y. Fan, R. Grumbine, W. Higgins, H. Li, Y. Lin, G. Manikin, D. Parrish, and W. Shi. North American Regional Reanalysis. *Bulletin of the American Meteorological Society*, 87:343–360, mar 2006.

[124] A. M. Mestas-Nuñez and D. B. Enfield. Eastern Equatorial Pacific SST Variability: ENSO and Non-ENSO Components and Their Climatic Associations. *Journal of Climate*, 14:391–402, February 2001.

[125] A. M. Mestas-Nunez, D. B. Enfield, and C. Zhang. Water Vapor Fluxes over the Intra-Americas Sea: Seasonal and Interannual Variability and Associations with Rainfall. *AGU Spring Meeting Abstracts*, page A3, May 2007.

[126] A.M. Mestas-Nuñez, C. Zhang, and D.B. Enfield. Uncertainties in Estimating Moisture Fluxes over the Intra-Americas Sea. *Journal of Hydrometeorology*, 6:696, 2005.

[127] J.-Y. Moon, B. Wang, and K.-J. Ha. ENSO regulation of MJO teleconnection. *Climate Dynamics*, 37:1133–1149, September 2011.

[128] E. Muñoz, A. J. Busalacchi, S. Nigam, and A. Ruiz-Barradas. Winter and Summer Structure of the Caribbean Low-Level Jet. *Journal of Climate*, 21:1260, 2008.

[129] R. E. Newell, N. E. Newell, and C. Scott. Tropospheric rivers?-A pilot study. *Geophysical research letters*, 19:2401–2404, December 1992.

[130] A. Numaguti. Origin and recycling processes of precipitating water over the Eurasian continent: Experiments using an atmospheric general circulation model. *"Journal of geophysical Research"*, 104:1957–1972, 1999.

[131] H. A. Panofsky, H. Tennekes, D. H. Lenschow, and J. C. Wyngaard. The characteristics of turbulent velocity components in the surface layer under convective conditions. *Boundary-Layer Meteorology*, 11:355–361, May 1977.

[132] José P. Peixóto and Abraham H. Oort. Physics of climate. *Rev. Mod. Phys.*, 56:365–429, Jul 1984.

[133] W.A. Petersen, S.W. Nesbitt, R.J. Blakeslee, R. Cifelli, P. Hein, and S.A. Rutledge. TRMM Observations of Intraseasonal Variability in Convective Regimes over the Amazon. *Journal of Climate*, 15:1278–1294, jun 2002.

[134] R.T. Pierrehumbert, H. Brogniez, and R. Roca. Chapter 6 on the relative humidity of the atmosphere. 2008.

[135] W. Portig. Central american rainfall. *Geography*, pages 68–90, 1965.

[136] V.B. Rao, I.F.A. Cavalcanti, and K. Hada. Annual variation of rainfall over brazil and water vapor characteristics over south america. *J. Geophys. Res.*, 101:539–551, 1996.

[137] M.R. Raupach. Applying lagrangian fluid mechanics to infer scalar source distributions from concentration profiles in plant canopies. *Agricultural and forest meteorology*, 47(2-4):85–108, 1989. eng.

[138] M.S. Reboita, R. Nieto, L. Gimeno, R.P.da Rocha, T. Ambrizzi, R. Garreaud, and L.F. Krüger. Climatological features of cutoff low systems in the Southern Hemisphere. *Journal of Geophysical Research (Atmospheres)*, 115(D14):17104, sep 2010.

[139] J. D. Restrepo, B. Kjerfve, M. Hermelin, and J. C. Restrepo. Factors controlling sediment yield in a major South American drainage basin: the Magdalena River, Colombia. *Journal of Hydrology*, 316:213–232, January 2006.

[140] M. J. Rodwell, D. P. Rowell, and C. K. Folland. Oceanic forcing of the wintertime North Atlantic Oscillation and European climate. *"Nature"*, 398:320–323, March 1999.

[141] J.C. Rogers. The Association between the North Atlantic Oscillation and the Southern Oscillation in the Northern Hemisphere. *Monthly Weather Review*, 112:1999, 1984.

[142] R.D. Rosen, D.A. Salstein, and J.P. Peixoto. Variability in the Annual Fields of Large-Scale Atmospheric Water Vapor Transport. *Monthly Weather Review*, 107:26, 1979.

[143] S. Saha, S. Moorthi, H.L. Pan, X. Wu, J. Wang, S. Nadiga, P. Tripp, R. Kistler, J. Woollen, D. Behringer, H. Liu, D. Stokes, R. Grumbine, G. Gayno, J. Wang, Y.T. Hou, H.Y. Chuang, H.M.H Juang, J. Sela, M. Iredell, R. Treadon, D. Kleist, P. van Delst, D. Keyser, J. Derber, M. Ek, J. Meng, H. Wei, R. Yang, S. Lord, H. van den Dool, A. Kumar, W. Wang, C. Long, M. Chelliah, Y. Xue, B. Huang, J.K. Schemm, W. Ebisuzaki, R. Lin, P. Xie, M. Chen, S. Zhou, W. Higgins, C.Z. Zou, Q. Liu, Y. Chen, Y. Han, L. Cucurull, R.W. Reynolds, G. Rutledge, and M. Goldberg. The NCEP Climate Forecast System Reanalysis. *Bulletin of the American Meteorological Society*, 91:1015–1057, aug 2010.

[144] E.P. Salathé and D.L. Hartmann. A Trajectory Analysis of Tropical Upper-Tropospheric Moisture and Convection. *Journal of Climate*, 10:2533–2547, oct 1997.

[145] H. Savenije. New definitions for moisture recycling and the relationship with land-use changes in the Sahel. *Journal of Hydrology*, 167:57–78, may 1995.

[146] M. E. Schlesinger and N. Ramankutty. An oscillation in the global climate system of period 65-70 years. *"Nature"*, 367:723–726, February 1994.

[147] C. A. Schlosser and P. R. Houser. Assessing a Satellite-Era Perspective of the Global Water Cycle. *Journal of Climate*, 20:1316, 2007.

[148] M.W. Schmidt, H.J. Spero, and D.W. Lea. Links between salinity variation in the caribbean and north atlantic thermohaline circulation. *Nature*, 428:160–163, 2004.

[149] J. T. Schmitz and S. L. Mullen. Water Vapor Transport Associated with the Summertime North American Monsoon as Depicted by ECMWF Analyses. *Journal of Climate*, 9:1621–1634, July 1996.

[150] E.K. Schneider, B.P. Kirtman, and R.S. Lindzen. Tropospheric Water Vapor and Climate Sensitivity. *Journal of Atmospheric Sciences*, 56:1649–1658, jun 1999.

[151] N. Schneider and B.D. Cornuelle. The Forcing of the Pacific Decadal Oscillation(. *Journal of Climate*, 18:4355–4373, nov 2005.

[152] P. Seibert and A. Frank. Source-receptor matrix calculation with a Source-receptor matrix calculation with a backward mode. *Atmospheric Chemistry & Physics Discussions*, 3:4515–4548, August 2003.

[153] S.C. Sherwood. Maintenance of the Free-Tropospheric Tropical Water Vapor Distribution. Part II: Simulation by Large-Scale Advection. *Journal of Climate*, 9:2919–2934, nov 1996.

[154] S.C. Sherwood, R. Roca, T.M. Weckwerth, and N.G. Andronova. Tropospheric water vapor, convection, and climate. *Reviews of Geophysics*, 48:2001, apr 2010.

[155] S.C. Sherwood, R. Roca, T.M. Weckwerth, and N.G. Andronova. Tropospheric water vapor, convection, and climate. *Rev. Geophys.*, 48, 2010.

[156] R. J. O. Small, S. P. de Szoeke, and S.-P. Xie. The Central American Midsummer Drought: Regional Aspects and Large-Scale Forcing*. *Journal of Climate*, 20:4853, 2007.

[157] H. Sodemann, C. Schwierz, and H. Wernli. Interannual variability of Greenland winter precipitation sources: Lagrangian moisture diagnostic and North Atlantic Oscillation influence. *Journal of Geophysical Research (Atmospheres)*, 113(D12):3107, feb 2008.

[158] H. Sodemann and A. Stohl. Asymmetries in the moisture origin of Antarctic precipitation. *Geophysical research letters*, 36:22803, nov 2009.

[159] D. J. Stensrud. Importance of Low-Level Jets to Climate: A Review. *Journal of Climate*, 9:1698–1711, August 1996.

[160] A. Stohl. Trajectory statistics - a new method to establish source-receptor relationships of air pollutants and its application to the transport of particulate sulfate in europe. *Atmos. Environ.*, 30:579–587, 1996.

[161] A. Stohl and P. James. A Lagrangian Analysis of the Atmospheric Branch of the Global Water Cycle. Part I: Method Description, Validation, and Demonstration for the August 2002 Flooding in Central Europe. *Journal of Hydrometeorology*, 5:656, 2004.

[162] A. Stohl and P. James. A Lagrangian Analysis of the Atmospheric Branch of the Global Water Cycle. Part II: Moisture Transports between Earth's Ocean Basins and River Catchments. *Journal of Hydrometeorology*, 6:961, 2005.

[163] Youmin Tang and Bin Yu. An analysis of nonlinear relationship between the mjo and enso. *Journal of the Meteorological Society of Japan*, 86:867–881, 2008.

[164] A.S. Taschetto, R.J. Haarsma, A.S. Gupta, C.C. Ummenhofer, K.J. Hill, and M.H. England. Australian Monsoon Variability Driven by a Gill-Matsuno-Type Response to Central West Pacific Warming. *Journal of Climate*, 23:4717–4736, sep 2010.

[165] M.A. Taylor, D.B. Enfield, and A.A. Chen. Influence of the tropical Atlantic versus the tropical Pacific on Caribbean rainfall. *Journal of Geophysical Research (Oceans)*, 107:3127, sep 2002.

[166] A. Timmerman, S-I. An, U. Krebs, and H. Goosse. Enso suppression due to weakening of the north atlantic thermohaline circulation. *J. Climate*, pages 3122–3139, 2005.

[167] C. Torrence and G. P. Compo. A Practical Guide to Wavelet Analysis. *Bulletin of the American Meteorological Society*, 79:61–78, January 1998.

[168] K.E. Trenberth. Atmospheric Moisture Recycling: Role of Advection and Local Evaporation. *Journal of Climate*, 12:1368–1381, may 1999.

[169] K.E. Trenberth, J.T. Fasullo, and J. Mackaro. Atmospheric Moisture Transports from Ocean to Land and Global Energy Flows in Reanalyses. *Journal of Climate*, 24:4907–4924, sep 2011.

[170] Kevin E. Trenberth. Atmospheric moisture residence times and cycling: Implications for rainfall rates and climate change. *Climatic Change*.

[171] S. M. Uppala, P. W. KAllberg, A. J. Simmons, U. Andrae, V. Da Costa Bechtold, M. Fiorino, J. K. Gibson, J. Haseler, A. Hernandez, G. A. Kelly, X. Li, K. Onogi, S. Saarinen, N. Sokka, R. P. Allan, E. Andersson, K. Arpe, M. A. Balmaseda, A. C. M. Beljaars, L. Van De Berg, J. Bidlot, N. Bormann, S. Caires, F. Chevallier, A. Dethof, M. Dragosavac, M. Fisher, M. Fuentes, S. Hagemann, E. HAlm, B. J. Hoskins, L. Isaksen, P. A. E. M. Janssen, R. Jenne, A. P. Mcnally, J.-F. Mahfouf, J.-J. Morcrette, N. A. Rayner, R. W. Saunders, P. Simon, A. Sterl, K. E. Trenberth, A. Untch, D. Vasiljevic, P. Viterbo, and J. Woollen. The era-40 re-analysis. *Quarterly Journal of the Royal Meteorological Society*, 131(612):2961–3012, 2005.

[172] J. Van der Ent Rudi, H.G. Savenije, S. Bettina, and S.C. Steete-Dunne. Origin and fate of atmospheric moisture over continents. *Water resources research*, 46(9), 2010. eng.

[173] C. Vera, W. Higgins, J. Amador, T. Ambrizzi, R. Garreaud, D. Gochis, d. Gutzler, D. Lettenmaier, J. Marengo, C.R. Mechoso, J. Nogues-Paegle, P.L.S. Dias, and C. Zhang. Toward a Unified View of the American Monsoon Systems. *Journal of Climate*, 19:4977, 2006.

[174] D. J. Vimont. Transient Growth of Thermodynamically Coupled Variations in the Tropics under an Equatorially Symmetric Mean State*. *Journal of Climate*, 23:5771–5789, November 2010.

[175] G.T. Walker and E.W. Bliss. 1932: World weather v. mem. *Roy. Meteor. Soc.*, 4:53–84, 1932.

[176] G.T. Walker and E.W. Bliss. 1937: World weather vi. mem. *Roy. Meteor. Soc.*, 4:119–139, 1937.

[177] C. Wang. Variability of the Caribbean Low-Level Jet and its relations to climate. *Climate Dynamics*, 29:411–422, sep 2007.

[178] C. Wang and D.B. Enfield. The Tropical Western Hemisphere Warm Pool. *AGU Fall Meeting Abstracts*, page C2, dec 2002.

[179] C. Wang and D.B. Enfield. A Further Study of the Tropical Western Hemisphere Warm Pool. *Journal of Climate*, 16:1476–1493, may 2003.

[180] C. Wang, D.B. Enfield, S.K. Lee, and C.W. Landsea. Influences of the Atlantic Warm Pool on Western Hemisphere Summer Rainfall and Atlantic Hurricanes. *Journal of Climate*, 19:3011, 2006.

[181] C. Wang, S.-K. Lee, and D. B. Enfield. Climate Response to Anomalously Large and Small Atlantic Warm Pools during the Summer. *Journal of Climate*, 21:2437, 2008.

[182] C. Wang, S.K. Lee, and D.B. Enfield. Climate Response to Anomalously Large and Small Atlantic Warm Pools during the Summer. *Journal of Climate*, 21:2437, 2008.

[183] Chunzai Wang and Lee Sang-Ki. *Geophysical research letters*, 34(2), 2007. eng.

[184] G.M. Webber Benjamin, A.J. Matthews, and K.J. Heywood. A dynamical ocean feedback mechanism for the madden-julian oscillation. *Quarterly Journal of the Royal Meteorological Society*, 136(648A):740–754, 2010. eng.

[185] F. J. Wentz, L. Ricciardulli, K. Hilburn, and C. Mears. How much more rain will global warming bring? *Science*, 317, 2007.

[186] F.S. Whyte, M.A. Taylor, T.S. Stephenson, and J.D. Campbell. Features of the Caribbean Low Level Jet. *AGU Spring Meeting Abstracts*, page G8, may 2007.

[187] H. M. Worden, J. A. Logan, J. R. Worden, R. Beer, K. Bowman, S. A. Clough, A. Eldering, B. M. Fisher, M. R. Gunson, R. L. Herman, S. S. Kulawik, M. C. Lampel, M. Luo, I. A. Megretskaia, G. B. Osterman, and M. W. Shephard. Comparisons of Tropospheric Emission Spectrometer (TES) ozone profiles to ozonesondes: Methods and initial results. *Journal of Geophysical Research (Atmospheres)*, 112:3309, February 2007.

[188] K. Wyrtki. Equatorial currents in the pacific 1950 to 1970 and their relations to the trade winds. *J. Phys. Oceanogr.*, pages 372–380, 1974.

[189] K. Wyrtki. El niño: The dynamic response of the equatorial pacific ocean to atmospheric forcing. *J. Phys. Oceanogr.*, pages 572–584, 1975.

[190] P. Xie and P. A. Arkin. Global Precipitation: A 17-Year Monthly Analysis Based on Gauge Observations, Satellite Estimates, and Numerical Model Outputs. *Bulletin of the American Meteorological Society*, 78:2539–2558, November 1997.

[191] J.H. Yoon and N. Zeng. An Atlantic influence on Amazon rainfall. *Climate Dynamics*, 34:249–264, feb 2010.

[192] L. Yu and R.A. Weller. Objectively Analyzed Air Sea Heat Fluxes for the Global Ice-Free Oceans (1981 2005). *Bulletin of the American Meteorological Society*, 88:527, 2007.

[193] C. Zhang. Madden-Julian Oscillation. *Reviews of Geophysics*, 43:2003, jun 2005.

[194] R. Zhang and T.L. Delworth. Impact of atlantic multidecadal oscillations on india/sahel rainfall and atlantic hurricanes. *Geophys. Res. Lett.*, 2006.

[195] Y. Zhang, J. M. Wallace, and D. S. Battisti. ENSO-like Interdecadal Variability: 1900-93. *Journal of Climate*, 10:1004–1020, May 1997.

[196] J. Zhou and K.M. Lau. Does a Monsoon Climate Exist over South America?. *Journal of Climate*, 11:1020–1040, may 1998.

[197] Y. Zhu and R.E. Newell. Atmospheric rivers and bombs. *Geophys. Res. Lett*, 21:1999–2002, sep 1994.

[198] Y. Zhu and R.E. Newell. A Proposed Algorithm for Moisture Fluxes from Atmospheric Rivers. *Monthly Weather Review*, 126:725, 1998.